1987

Late Pleistocene Stratigraphy And Events In The Asbestos-valcourt Region, Southeastern Quebec

Michel Parent

LATE PLEISTOCENE STRATIGRAPHY AND EVENTS IN THE ASBESTOS-VALCOURT REGION, SOUTHEASTERN QUEBEC

by

Michel Parent

Department of Geology

Submitted in partial fulfillment
of the requirements for the degree of
Doctor of Philosophy

Faculty of Graduate Studies
The University of Western Ontario
London, Ontario

April 1987

ISBN 0-315-36585-4

THE UNIVERSITY OF WESTERN ONTARIO
FACULTY OF GRADUATE STUDIES

CERTIFICATE OF EXAMINATION

Chief Advisor

A. Occhietti

Advisory Committee

Examining Board

P. J. Karrow

C.

B. H. Luckman

The thesis by
Michel Parent

entitled
Late Pleistocene stratigraphy and events
in the Asbestos-Valcourt region,
southeastern Québec

is accepted in partial fulfillment of the
requirements of the degree of
Doctor of Philosophy

Date 3 Sept. 1987

Chairman of Examining Board

ABSTRACT

The stratigraphic record of the Asbestos-Valcourt region indicates that glacial sediments deposited during at least two regional glacial advances (drift units A and C) underlie ice-contact and glaciolacustrine sediments deposited during the last deglaciation (Late Wisconsinan); glaciolacustrine sediments of unit B which were deposited during a rather short-lived interstade underlie till deposited during the Late Wisconsinan glacial maximum (drift unit C).

Till deposited in the Appalachian Uplands during the earlier glacial advance (drift unit A) contains only rare Precambrian (Shield-type) erratics and has a distinctive Appalachian provenance. Till geochemistry as well as till clast lithology and fabrics indicate that drift unit A was deposited by a glacier that was advancing westward from Appalachian outflow centers. However, the presence of some northwest-derived clasts in till of drift unit A provides evidence for an earlier phase of southeastward ice-flow. This glacial unit is believed to be a correlative of Chaudière Till. The upper part of drift unit A contains no record of an influx of northwest-derived debris that should be expected from a long episode of coalescence with the Laurentide Ice Sheet, such as that proposed by earlier workers. Instead, ice-flow sequences recorded in drift unit A suggest that a shift of outflow centers within an Appalachian-based glacier took place toward the close of glacial phase A; it is during this part of glacial phase A that a northward ice-flow episode occurred in uplands of the Asbestos region.

Glaciolacustrine sediments of unit B were deposited in a glacial lake (or a series of glacial lakes) that was impounded in front of the glacier which subsequently deposited drift unit C. The age of these mainly proximal glacial-lake sediments remains poorly known; unit B is a probable correlative of the Gayhurst Formation (Middle Wisconsinan).

Till deposited during the last regional ice advance (drift unit C) commonly contains Precambrian erratics as well as abundant northwest-derived local debris. Glacial dispersal trains, subtill glacitectonic deformations and till clast fabrics consistently indicate that drift unit C and its equivalent, Lennoxville Till, were deposited by ice that advanced southeastward from a Laurentide outflow center and that this ice-flow pattern was maintained until final ice-retreat.

During northward ice-retreat that followed glacial phase C, a series of recessional end-moraines (Cherry River / East-Angus, Mont Ham and Ulverton-Tingwick Moraines, in order of decreasing age) were deposited and glacial lakes were impounded south of the ice front. The Mont Ham Moraine is coeval with the maximum extent of the Sherbrooke phase of Glacial Lake Memphremagog while the Ulverton-Tingwick Moraine was built after glacial-lake level had fallen to that of the Fort Ann phase of Glacial Lake Vermont. Subsequent glacial retreat along the edge of the Appalachian uplands together with deglaciation of the Québec City narrows allowed marine waters to invade the isostatically depressed Central St. Lawrence Lowland, thus forming the Champlain Sea about 12 000 years BP. Patterns and gradients of marine-limit isolines closely resemble those of previous glacial-lake isobases, thus providing additional support to the proposed deglacial history.

Absence of Lake Vermont strandlines in valleys northeast of Warwick together with regional deglacial patterns suggest that a large mass of residual Laurentide ice may have been isolated in uplands of the Thetford-Mines area as a result of marine incursion. A late-glacial northward ice-flow reversal may have taken place in that region as a result of drawdown toward a calving bay that retrograded up the St. Lawrence River estuary. However, this ice-flow reversal apparently did not produce the northward- and westward-trending striations recorded in the Asbestos-Valcourt region; the latter are best interpreted as residual features that were formed during glacial phase A.

ACKNOWLEDGEMENTS

I wish to express my deep gratitude to Dr. Aleksis Dreimanis who supervised this investigation; his encouragement and his thoughtful comments through all phases of this study were greatly appreciated.

Sincere thanks are also extended to Drs. Jean-Marie M. Dubois (Université de Sherbrooke) and William W. Shilts (Geological Survey of Canada) who contributed several discussions during the course of this investigation and critically read the near-final draft of this manuscript. Dr. Stephen R. Hicock kindly reviewed and commented on an earlier draft of this thesis. Drs. Gordon G. Winder and William R. Church reviewed the chapter on bedrock geology and physiography.

This thesis has been financially supported through NSERC grant A-4215 (Canada) to A. Dreimanis and through FCAR grant EQ-2057 (Québec) to J.M.M. Dubois. This support was essential and is strongly acknowledged.

Several colleagues and friends discussed facts and interpretations presented in this thesis: Michel Lamothe, Robert A. Stewart, Bruce E. Broster, Guy Lortie, R. Claude Gauthier, Q. Hugh J. Gwyn, Serge Occhietti, Gilbert Prichonnet and Pierre Clément. Michel and Bob shared my office room in London and are particularly thanked for numerous memorable discussions on the infinitudes of glacial geology, till genesis and Quaternary stratigraphy.

I also thank Manon Tétreault (U. de S.) for her competent word-processing as well as Marc Lacroix and François Charron (U. de S.) for their fine photographic work of my text-figure originals. Roger Lafontaine (U. de S.) prepared the photographic plates. Sincere thanks are also extended to Mrs. Karin Lootsma (UWO) for carrying out the granulometric and carbonate analyses, to Guy Bilodeau and Mariette Lambert (U. de S.) for assisting me with microfossil extraction and identifica-

tion and with other laboratory work, to John Forth (UWC) for preparing thin sections and to Luc St-Pierre (U. de S.) for computing some of the clast fabric statistics. I also thank W.W. Shilts for defraying the cost of most of the geochemical analyses.

Finally, I would like to thank my wife, Claire, for her patience and for encouragement throughout this study. To her and to my children, Daniel and Johanne, I apologize for my absences, both mental and physical.

TABLE OF CONTENTS

LIST OF PHOTOGRAPHIC PLATES

LIST OF TABLES

LIST OF FIGURES

CHAPTER 1

INTRODUCTION

1.1 Statement of project

The main objectives of this study are:

(1) to provide a stratigraphic framework for Pleistocene glacial and non-glacial events in the study area;

(2) to investigate relationships between till stratigraphy and ice-flow patterns, as revealed by glacial striations, glacitectonic deformations, till fabric and till provenance;

(3) to evolve a temporal framework for regional late-glacial events, particularly the formation of the Highland Front Morainic System and of other Late Wisconsinan end moraines, the development of proglacial lakes, the inception of the Champlain Sea and an inferred late-glacial ice-flow reversal.

1.2 The study area

The study area (Figure 1-I) extends over an area of about 5400 km^2 and lies entirely within the Appalachian uplands and piedmont of southeastern Quebec; its latitude is from 45°15'N to 46°15'N and its longitude, from 71°30'W to 72°30'W. The Asbestos-Valcourt region, as defined herein, includes the following NTS 1:50 000 topographic sheets: 21 E/12 (Dudswell), 21 E/13 (Warwick), 31 H/8 (Orford) and 31 H/9 (Richmond); it also includes parts of 21 E/5 (Sherbrooke), 21 L/4 (Arthabaska), 31 I/1 (Aston) and most of 31 H/16 (Drummondville).

On the basis of previous work (see section 1.3), the study area was delineated so as to include areas where a Late Wisconsinan ice-flow reversal had been recognized (Asbestos region) as well as areas where a

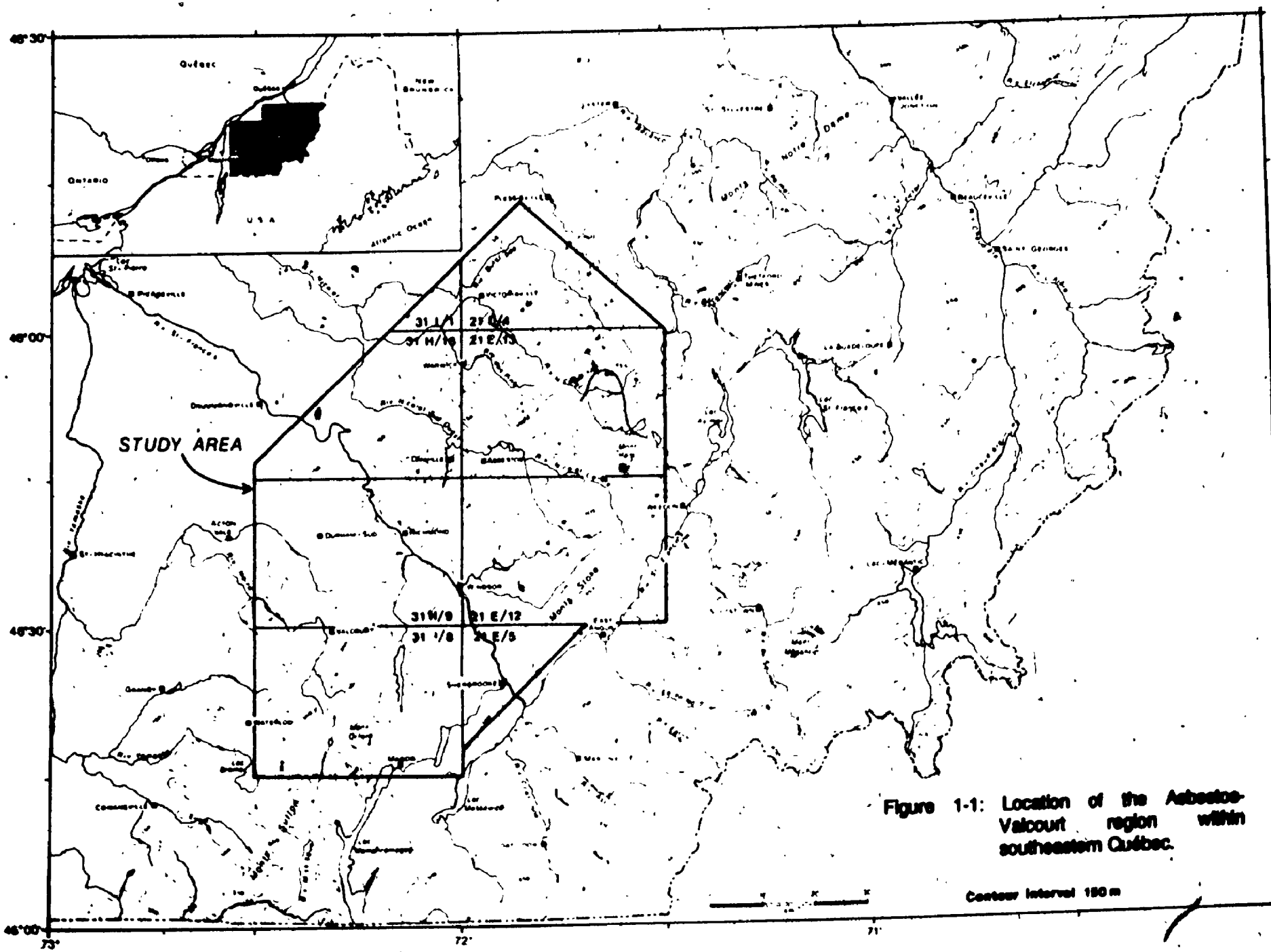

Figure 1-1: Location of the Asbestos-Valcourt region within southeastern Québec.

reversal event had not been recognized (Valcourt region); this was required because an important objective of this investigation is to clarify relationships between the inferred reversal event and the regional stratigraphic and deglacial record. Other reasons for selecting the study area were:

(1) preliminary investigations had revealed the presence of hitherto unrecognized morainic belts;

(2) it was expected that this investigation would uncover sections likely to supplement the regional Late Pleistocene stratigraphic record;

(3) the Asbestos-Valcourt region includes areas where surficial geology maps were available (21 E/5, 31 H/9, 31 H/16, 31 H/8 E) as well as areas in which, at the outset of this study, surficial geology mapping was by-and-large incomplete (21 E/12, 21 L/13, 21 L/4, 31 H/8 W);

(4) a fairly dense road network provides easy access to most of the area;

(5) the investigator had previous experience mapping Pleistocene deposits in the region (Parent, 1978).

1.3 Previous work

Prior to the 1960's, several authors had contributed occasional articles, reports or theses dealing with various aspects of the Quaternary record in the southeastern Quebec Appalachians. Most of these contributions were the result of dominantly local studies; a few others, including a report by Chalmers (1898), were more regional in scope but only dealt with a few aspects of the Quaternary record, and thus lacked some of the insight which is usually gained when multiple aspects of the geologic record are investigated. Several summaries of these early contributions are available (McDonald, 1967a; Shilts, 1970, 1981;

Lortie, 1976; La Salle et al., 1977a). For the above reasons and for the sake of brevity, this early work will not be reviewed in the present thesis.

1.3.1 Development of a regional stratigraphic framework (the Traditional Framework)

A fairly comprehensive assessment of the Quaternary record in the southern Quebec Appalachians evolved mainly from surficial geology mapping projects carried out in the Sherbrooke-Richmond region (McDonald, 1966, 1967a, 1967b, 1969) and later in the Lac-Mégantic region (Shilts, 1970, 1981). Stratigraphic aspects of this work are summarized by McDonald and Shilts (1971) while deglacial events and chronology are outlined by Gadd, McDonald and Shilts (1972a). For the purposes of this summary, their comprehensive framework may be conveniently termed "Traditional Framework". Stratigraphic and chronologic aspects of this Traditional Model are shown in Table 1-1. The "Revised Traditional Framework", that which is presented in Figure 1-2, upholds all of the stratigraphic relationships contained in the original framework, except those involving units or events which are presumably related to a proposed Late Wisconsinan ice-flow reversal. These aspects of the revised model will be discussed in section 1.3.2. Also shown in Figure 1-2 are stratigraphic units of the St. Lawrence Lowland (Gadd, 1971; Occhietti, 1980) as well as suggested correlations between the two regions (McDonald, 1971; Gadd et al., 1972b; Gadd, 1976; Shilts, 1981).

The Traditional Framework holds that, following the last interglacial, three separate glacial events of full glacial severity occurred in the southeastern Quebec Appalachians. These glacial events are represented, from oldest to youngest, by the Jonnville, Chaudière and Lennoxville Tills. The sedimentary record of pre-Johnville events consists of oxidized fluvial gravel beds exposed at two widely separated localities; these beds are believed to date back to the last interglacial (Sangamonian). Sub-till saprolites which have been uncovered at several localities in the southern Quebec Appalachians (Clément and de Kimpe, 1977; La Salle et al., 1985) are believed to be of Tertiary age.

Table 1-1: "Traditional Stratigraphic Framework" for Late Pleistocene units, southeastern Québec (from McDonald and Shilts, 1971: Table 1).

Time-Stratigraphic Unit		Rock-Stratigraphic Unit	Chronologic Control
WISCONSIN STAGE	LATE	post-Lennoxville sediments	12,640 ± 190 (GSC-312;peat)* 12,570 ± 220 (GSC-419;peat)** 12,000 ± 230 (GSC-936; marine shells) 11,500 ± 160 (GSC-475-2; marine shells)
	MIDDLE	Lennoxville Till	
		Gayhurst Formation	>20,000 B.P. (GSC-1137) ca. 4000 varves
		Chaudière Till	
	EARLY	Massawippi Formation	>54,000 B.P. (Y-1683) >41,000 B.P. (GSC-507) >40,000 B.P. (GSC-1084)
		Johnville Till	
pre-Wisconsin stage(s)		pre-Johnville sediments	

* GSC-312 comes from organic clay at the base of the Petit Lac Terrien core and is considered as probably anomalous due to contamination by old carbonates (Mott, 1977)

** GSC-419 comes from clay-containing "some plant detritus" and may also be anomalous (see discussion in Terasmae and Lasalle, 1968: p. 255-256)

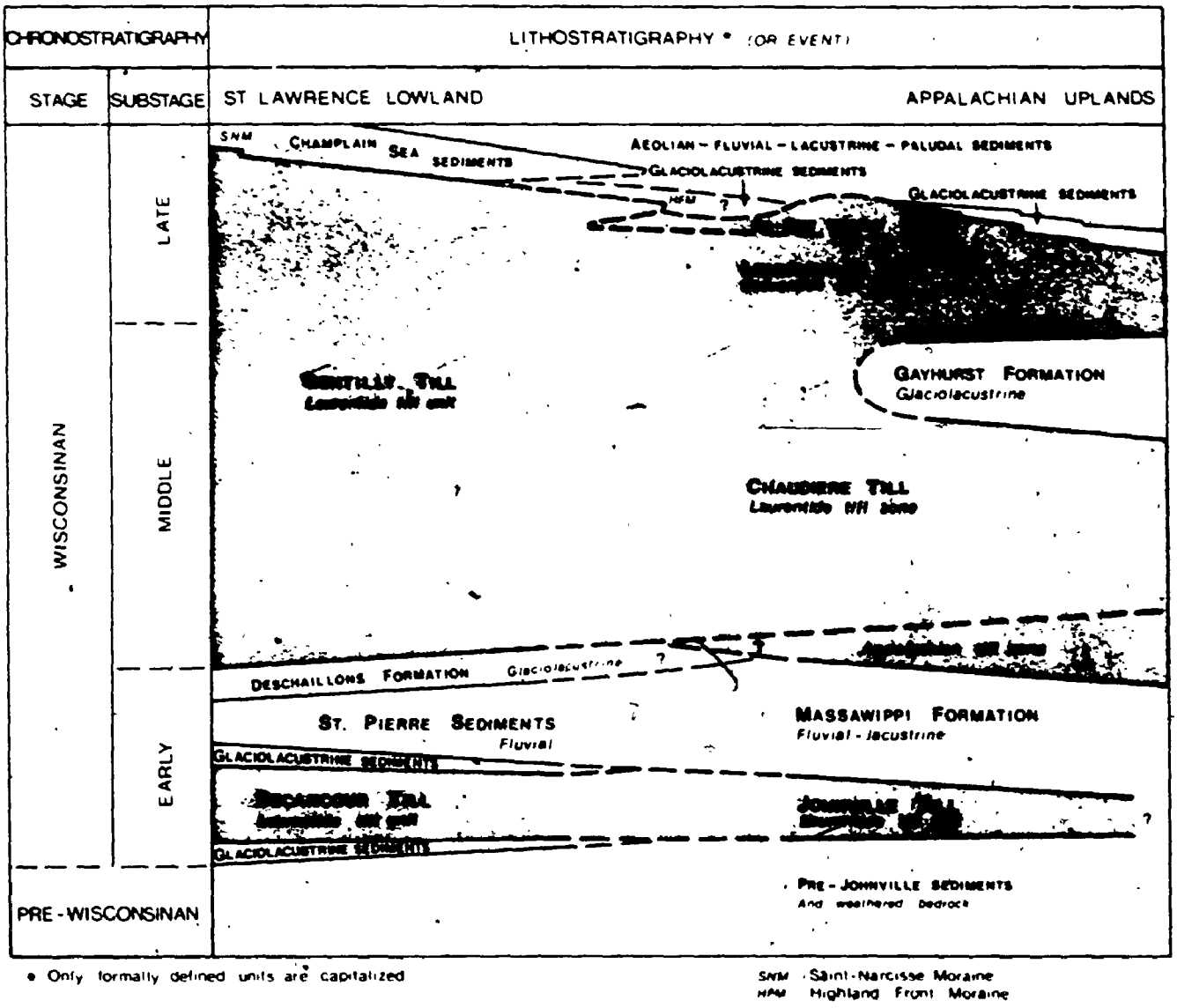

Figure 1-2 : Revised traditional stratigraphic framework for Late Pleistocene units of southern Québec, mainly after Gadd et al. (1972 b) and Shilts (1981). This revised framework includes a late-Lennoxville ice-flow reversal which brings into question the status of both pre-Champlain Sea glaciolacustrine sediments and the Highland Front Moraine.

Mostly on the basis of lithological and fabric data, McDonald and Shilts (1971) inferred that Johnville, Chaudière and Lennoxville Tills were deposited by glaciers originating from Precambrian Shield terrains and advancing southeastward across the southern Quebec Appalachian uplands and into the New England uplands. Thus they considered that all three units recorded separate advances of the Laurentide Ice Sheet. However, the Chaudière glaciation was recognized as a more complex event: during an early phase (Maritime Ice Cap of Shilts, 1981), glaciers advanced from the east and northeast and deposited a lower till member (Appalachian till zone in Figure 1-2); as Laurentide ice centers began to take over, glacial flow shifted from southwestward to southeastward, an event which is recorded by the deposition of a "Laurentide till zone".

Ice-retreat following Johnville glaciation was more extensive than that which followed Chaudière glaciation. During the earlier deglacial event, when the Massawippi Formation was deposited, it is believed that the Appalachian uplands were largely free of glacier ice, allowing streams to flow north toward the St.Lawrence River. Because of this and also because the Massawippi Formation contains organic detritus of infinite radiocarbon age (Y-1683: >54 000 BP; GSC-507: >41 500 BP; GSC-1084: >40 000 BP), as well as pollen suggesting a cool boreal forest environment, the Massawippi Formation has been correlated with the St. Pierre Sediments (Early Wisconsinan). Since high-level proglacial lakes remained impounded in Appalachian valleys throughout the next deglacial event (Gayhurst Formation), McDonald and Shilts (1971) inferred that the ice-front had only retreated to a position well within the uplands, and thus suggested that the Chaudière Till — Gayhurst Formation — Lennoxville Till succession in the Appalachian uplands represents a time span roughly equivalent to that of Gentilly Till in the Lowland. As sediments of the Gayhurst Formation are generally devoid of organics, the unit was assigned to a Middle Wisconsinan interstade on the basis of a single ^{14}C date of >20 000 years BP (GSC-1137). Subsequent ^{14}C dating of calcareous concretions (QC-508: 32 900 + 2300/ -1800 BP; QC-558: 20 640 $\pm$ 640 BP) from varves at the type section (Gayhurst dam), as re-

ported by Hillaire-Marcel (1979) and Occhietti (1982), is in apparent conflict with the reported 4500 years maximum duration of the Gayhurst episode (Shilts, 1981) and, partly because of the nature of the dated material, does not help to assess the true age of the unit.

According to the Traditional Framework (Gadd, McDonald and Shilts, 1972a: Figure 4), the retreat of the Lennoxville glacier started well before 13 000 years BP, perhaps as early as 14 000 years BP. As the margin of this last ice sheet retreated northwestward across the region, a series of discontinuous end-moraines was formed. Because the retreating ice margin blocked free drainage of northward-flowing streams, proglacial lakes were impounded in most valleys of the Appalachian uplands. Later, these lakes expanded onto the Appalachian piedmont as the ice margin retreated from the position of the Highland Front Morainic System to that of the Drummondville Moraine (Figure 1-3); shortly afterwards marine waters invaded the isostatically depressed St. Lawrence valley to form the Champlain Sea. In early Champlain Sea time (ca 11 500 BP), the retreating ice-front formed much of the northern shore of the marine water body while the southeastern Quebec Appalachians were largely free of glacial ice, except for a possible small remnant ice-cap centered in the vicinity of Thetford-Mines. This local exception had become necessary after Lamarche (1971) had uncovered several crag-and-tail striae indicating a late-glacial northward ice-flow episode in the Appalachian uplands around Thetford-Mines.

1.3.2 Regional extent of the northward ice-flow episode and the need for a revision of the Traditional Framework

Subsequent fieldwork (Lamarche, 1974; Gauthier, 1975; Lortie, 1976; La Salle et al., 1977a) revealed that crag-and-tail striations indicating northward ice-flow are common throughout a vast area of the southeastern Quebec Appalachians (Figure 1-3). Recognition of the considerable areal extent of these striations and of their persistant northward trend soon led most investigators to set aside the idea that they were produced by a remnant ice mass supporting radial outward flow.

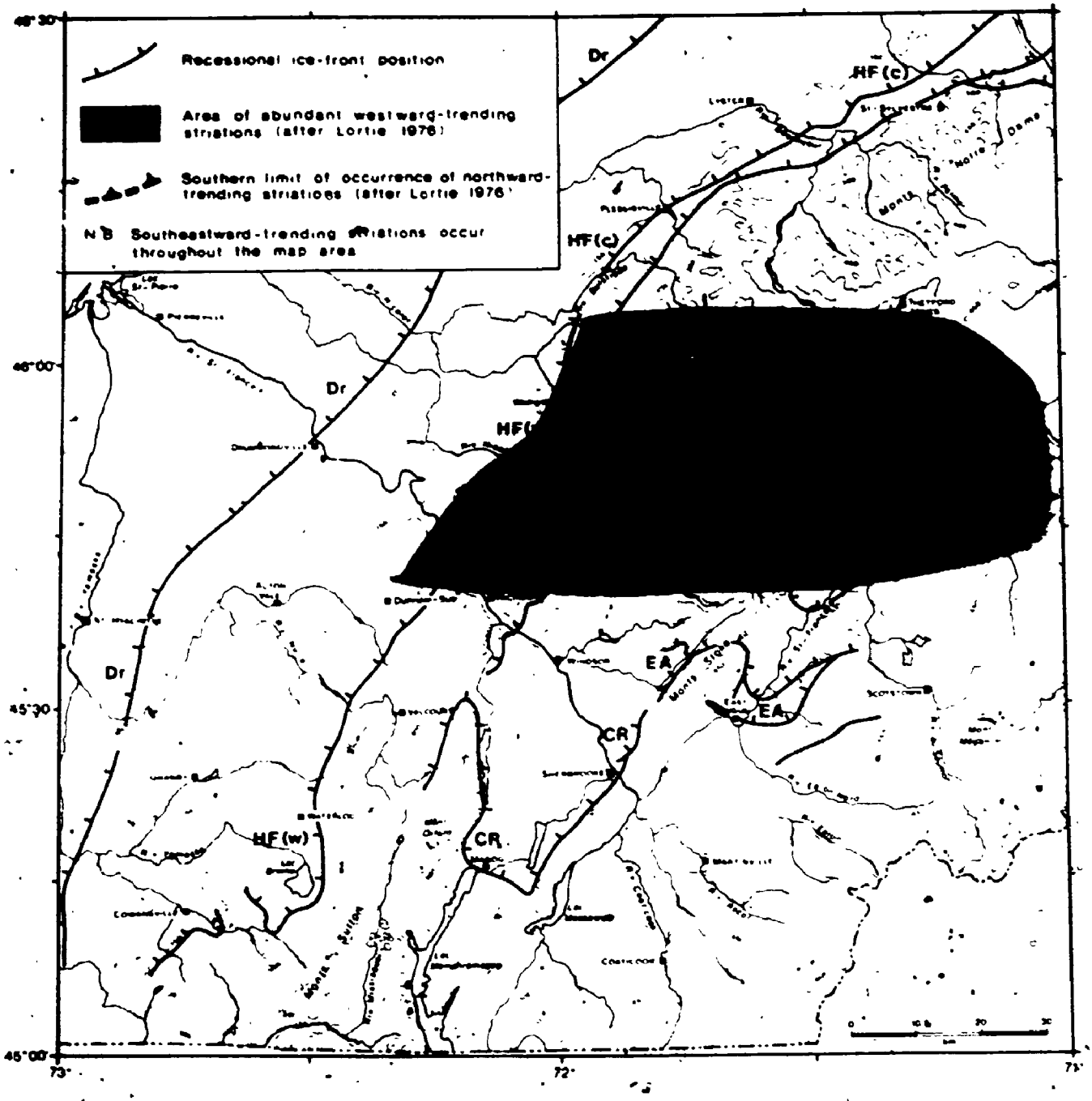

HF(w) Highland Front Moraine (western segment)*
HF(c) " " " (central segment)*
Dr Drummondville Moraine*
MH* Mont Ham Moraine**
EA East-Angus Moraine**
CR Cherry River Moraine***

* After Gadd et al. 1972a
** After Parent, 1978
*** After McDonald, 1967a

Figure 1-3 : Previously recognized morainic belts in the Asbestos-Valcourt region and adjacent areas. Also shown is the areal extent of northward- and westward-trending striations.

Rather these findings led them to infer that an ice-flow reversal occurred near the close of Late Wisconsinan (Lennoxville) glaciation along the northwestern margin of the southeastern Quebec Appalachian uplands (Lamarche, 1974; Gauthier, 1975; Lortie, 1976; Shilts, 1976b, 1981; Gadd, 1976; La Salle et al., 1977a). In the above interpretations, the regional ice-flow reversal was presumably caused by the development of a calving bay in the St. Lawrence Estuary. Ice being drawn preferentially toward the ice-sea interface at a time of globally rising sea level, a saddle was formed at the ice-sheet surface, and this regional reversal of the ice-surface gradient caused the ice-flow reversal. Reports of older-than-expected ^{14}C dates (GSC-1859: 12 800 ± 220 BP; GSC- 1646: 12 200 ± 160 BP) on marine shells from the Ottawa Valley (Richard, 1974, 1975) led to further suggestions that this calving bay may have retrograded rapidly into the central St. Lawrence Lowland (Gadd, 1976; Shilts, 1976b; Thomas, 1977), and perhaps into the Ottawa Valley as well (Gadd, 1980).

Regardless of the true extent of this marine incursion, it is implied that Appalachian ice, either in the form of a single large body or consisting of several more-or-less distinct masses, was cut off from its original Laurentide source. This hypothesis had been expressed earlier by Antevs (1925, p. 66) who proposed that: "... a large mass of ice was isolated southeast of the St. Lawrence".

The most interesting attempt to reconcile the northward ice-flow episode with the other aspects of the regional Quaternary record is perhaps that of Shilts (1976b, 1981). This hypothesis, which is a key part of the "Revised Traditional Framework", was aptly summarized in a schematic cross-section (Shilts, 1981: Figure 11) and was discussed more fully in a later paper (Shilts, 1982). Briefly stated, his thesis holds that a diachronous ice divide, which he named the Quebec Ice Divide, formed within Appalachian ice as it was being cut off from its Laurentide source. Thus, in regions lying north of the divide, ice was drawn toward a calving bay and northward ice-flow replaced the earlier southeasward flow; in regions lying south of the divide, southeastward ice-

flow persisted as the ice margin retreated northward during its wastage (Figure 1-2).

This revised framework has the advantage of encompassing much of the data that were available at the time:

(1) The inferred relative chronology (southeastward, then northward and westward) of glacial striations (Lamarche, 1971, 1974; Lortie, 1975, 1976; La Salle et al., 1977a) and their known areal distribution are, at least broadly, in agreement with the hypothesis.

(2) Most features of the prominent southeastward Thetford-Mines indicator train (Shilts, 1973a, 1975, 1976a) as well those indicating northward and westward glacial dispersal in the vicinity of Thetford-Mines (Lortie, 1976) can be accommodated.

(3) The more-or-less northward ice-retreat pattern and coeval ice-dammed lakes in the upper Chaudière valley (Shilts, 1970, 1981) and in southern tributary valleys of the upper Saint-François River (McDonald, 1967a: Figure 12; 1969: Figure 6; Clément et Parent, 1977: Figure 6) may then be associated with glacial retreat toward the Quebec Ice Divide rather than toward a Laurentide ice center.

(4) Sedimentary structures indicating paleocurrent toward the St.Lawrence Estuary within several ice-contact bodies (Dionne, 1972; Gadd et al., 1972b; La Salle et al., 1977a) forming the easternmost segments of the Highland Front Morainic System (St-Antonin Moraine of Lee, 1962) would accordingly result from meltwater activity at the seaward margin of the remnant Appalachian ice.

In spite of the above, several remaining key points must be adressed before this Revised Stratigraphic Framework becomes fully coherent:

(1) The central and western segments of the Highland Front Morainic System (those extending from the vicinity of Saint-Sylvestre to the Lac Brome area, as shown in Figure 1-3) were reportedly built at the margin of southeastward-flowing ice (McDonald, 1967a, 1968; Gadd, McDonald and Shilts, 1972a; Gadd, 1976, 1978; Prichonnet et al., 1982a, 1982b). Yet, several of these moraine segments lie within terrain where the latest glacial movements are reportedly toward north and west. In order to resolve this difficulty, Shilts (1981, 1982) postulated that, within terrains lying north of the moraine, southeastward- flowing ice replaced northward-flowing ice and that Laurentide ice may have readvanced across an early arm of the Champlain Sea to build the Highland Front Morainic System. However, no evidence supporting such a readvance could be found in the Québec City area (La Salle et al., 1977a: p. 54), a region in which deglacial events prior to and during the early Champlain Sea incursion have long been recognized as very significant elements of any regional deglaciation framework. Moreover, such a readvance would not really solve the problem as it would still imply a final southeastward ice-flow event within areas where the latest glacial striations indicate northward and westward ice-flow (see Figure 1-3).

(2) Some reconnaissance work by the author (Parent, 1977, 1978; Clément et Parent, 1977) in the Appalachian uplands east of Asbestos (a region where the last ice-flow events are reportedly toward north and west) revealed the presence of several recessional moraine segments which were clearly built at the margin of a glacier which was retreating toward northwest and which, conceivably, was still moving toward southeast at the close of the last glacial episode. Thus deglacial features similar to those which have led to postulate a readvance were known to extend into the area east of Asbestos as well.

(3) The proposed readvance also aimed to resolve some of the difficulties pertaining to the history of proglacial lakes in the

Saint-François River valley (Shilts, 1982). In this region, high-level proglacial lakes, such as the Sherbrooke phase of Glacial Lake Memphrémagog, can be impounded only if the ice-front stands at a position several kilometers south of the Highland Front Morainic System (McDonald, 1967a, 1968). This is apparently what led Shilts (1982, p. 50) to suggest "... a surge-like readvance... with deep lobes extending up the major valleys (Champlain, St.François, Chaudière)..." Because such an extensive readvance had not been recognized during previous work in the Saint-François River valley and adjacent areas north of Sherbrooke (McDonald, 1967a, 1968; Parent, 1978), it became necessary not only to investigate this possibility but also to further assess the paleogeographic and stratigraphic record of glaciolacustrine water bodies relative to regional glacial and deglacial events, including the Champlain Sea incursion.

CHAPTER 2

GEOLOGIC AND PHYSIOGRAPHIC SETTING

The study area lies entirely within the Appalachian geologic province and, except for small areas near Lake Memphrémagog and around the Stoke Mountains, it is underlain by rocks of Cambrian and Ordovician age (Figure 2-1). In the southeastern Québec Appalachians, strongly deformed Paleozoic strata generally strike northeast with steep, near-vertical dips; this tectonic alignment imparts a strong northeast-trending topographic grain which stands out at all scales, from that of regional physiographic units to that of most bedrock ridges or ledges.

2.1 Bedrock geology

The bedrock geology map (Figure 2-1) was compiled at a scale of 1:500 000 from several sources (Avramtchev et al., 1985; Avramtchev, 1985; St-Julien and Hubert, 1975; Harron, 1976; Cooke, 1950; St-Julien, 1970; Osberg, 1965; Lamarche, 1973; de Römer, 1980, 1981, 1984; Globensky, 1978; Clark, 1964a, 1964b, 1964c, 1977; Clark et Globensky, 1973, 1976; Charbonneau, 1980, 1981; Marleau, 1968; Caron, 1983a, 1983b; Hébert, 1982). Names of representative lithostratigraphic units listed in Table 2-1 were compiled from the same sources.

Although a compilation map at a scale of 1:500 000 became available recently (Avramtchev et al., 1985), reliable intermediate-scale (ca 1:50 000) geologic maps are not available for several areas within and outside the Asbestos-Valcourt region. As a result, the reliability of bedrock geology maps varies significantly from place to place. This evidently poses some problems for an investigation such as the present one which utilizes provenance as one of several criteria for deciphering a presumably complex glacial history. Bedrock units or contacts based on somewhat outdated reports had to be dropped, added or modified in several instances, because more reliable reports have been published since. For example, recent mapping by Caron (1983b) shows that basaltic

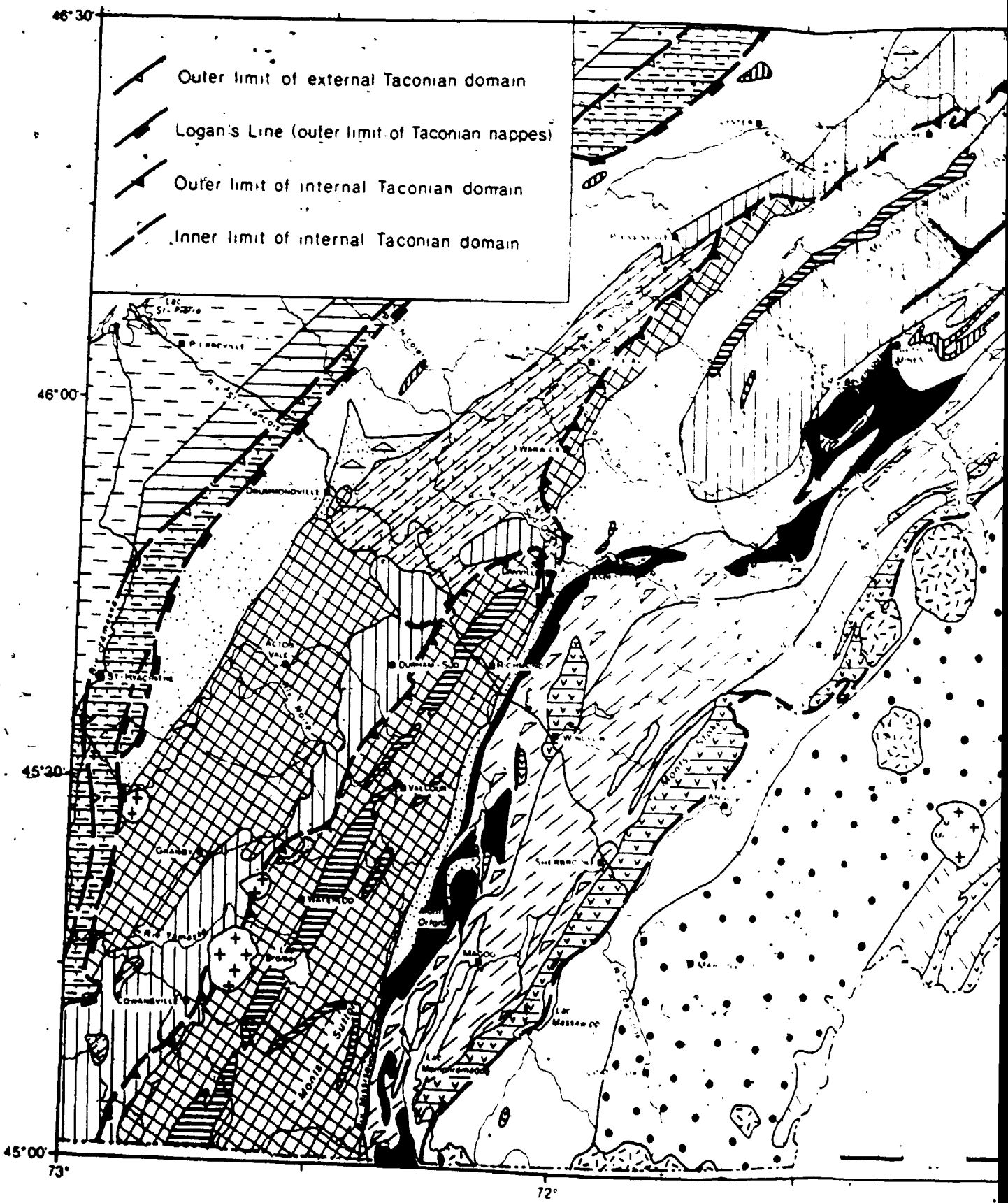

Figure 2-1: Generalized bedrock geology, southeastern Québec.

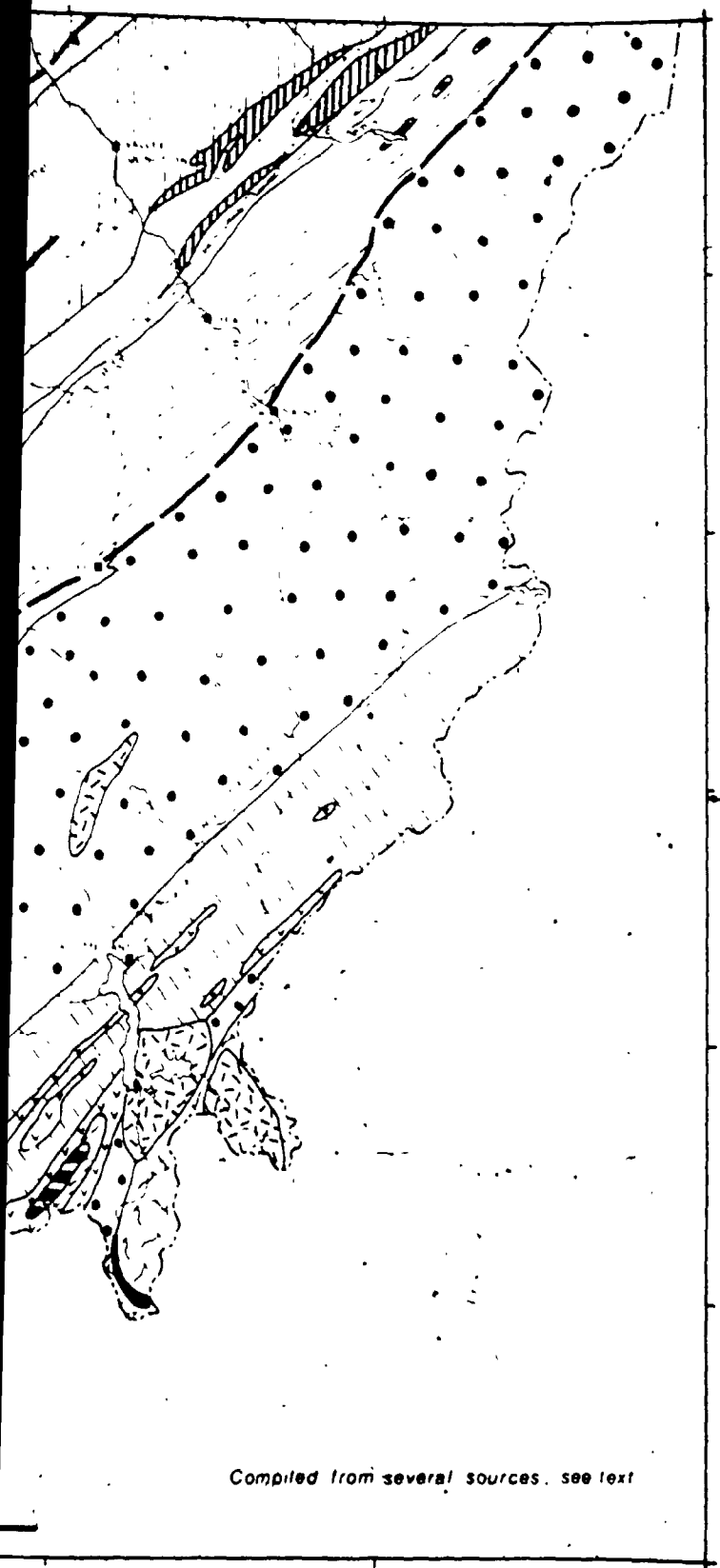

Compiled from several sources, see text

71

70°

24 Alkalic intrusive rocks (Monteregian)

ST LAWRENCE PLATFORM

23 [illegible] and sandstone

22 [illegible] and graywacke

21 Limestone, shale and graywacke

ACADIAN OROGEN

20 [illegible] intrusive rocks

19 [illegible] graywacke, conglomerate, limestone

18 [illegible] sandstone and shale

17 Diorite and gabbroic intrusive rocks

16 [illegible] and slate, some gabbroic sills

15 Mafic volcanic rocks

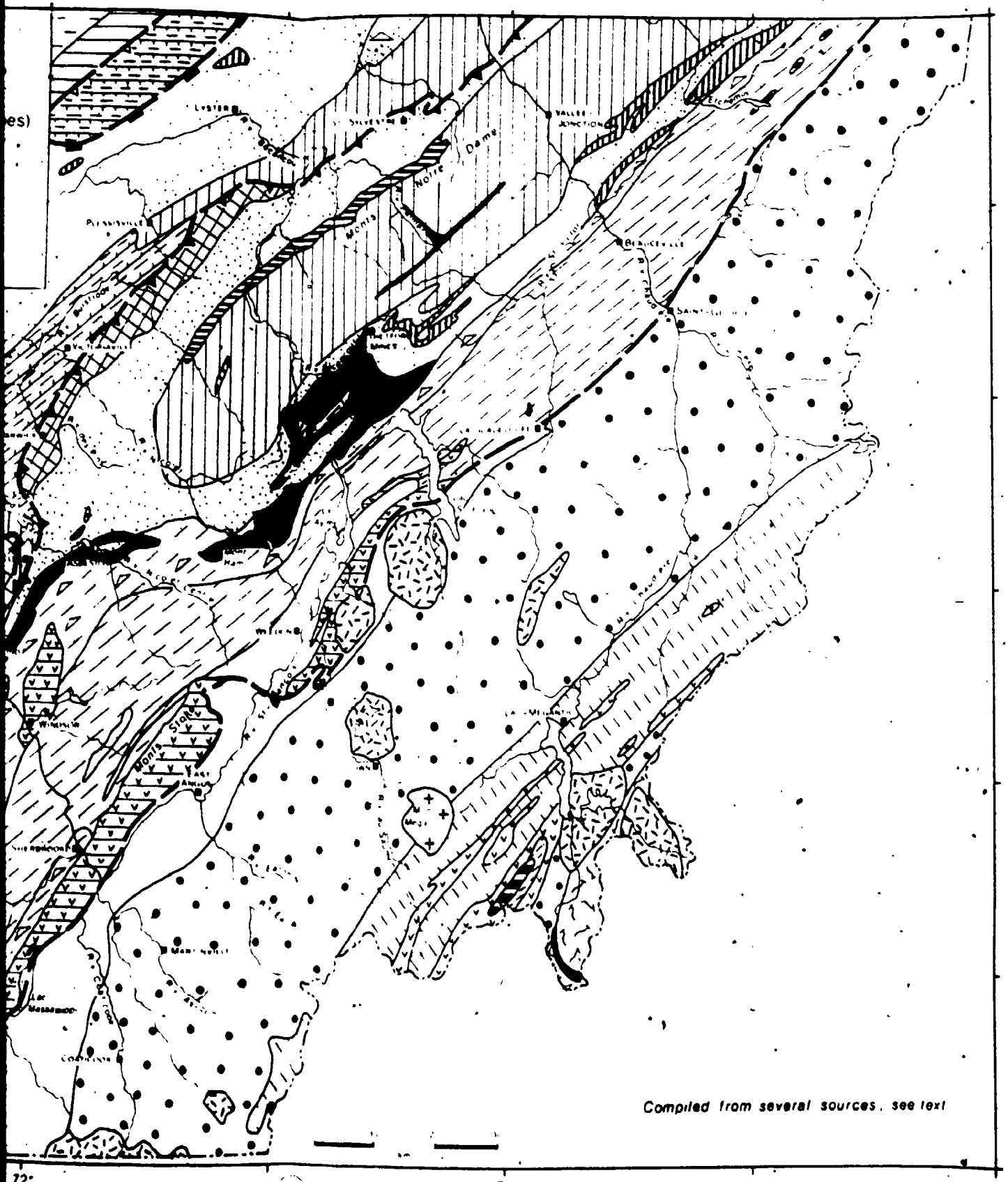
Notre Dame
Monts
Monts Sigo
Compiled from several sources, see text
72°
71
70°

TACONIAN OROGEN

- [illegible] intrusive rocks (Monteregian)

ST LAWRENCE PLATFORM

- Red shale and sandstone
- [illegible] shale and graywacke
- Limestone shale and graywacke

ACADIAN OROGEN

- Granitic intrusive rocks
- Shale graywacke conglomerate limestone
- Calcareous sandstone and shale
- Dioritic and gabbroic intrusive rocks
- Sandstone and slate some gabbroic sills
- Mafic volcanic rocks

14 Slate quartzite felsic tuff

13 Wildflysch

12 Calcareous shale and argillaceous limestone

11 Black slate and graywacke minor felsic tuff

10 Felsic to mafic pyroclastic rocks minor rhyolite and granite

9 Melange and slate

8 Metabasalt

7 Feldspathic sandstone and slate (green red gray)

6 Ophiolite complex and ultramafic rocks

5 Amphibolite

4 Phyllite slate quartz-albite-muscovite schist (local interbeds of conglomerate limestone orthoquartzite and feldspathic sandstone)

3 Quartz-albite-muscovite schist, phyllite, slate, graywacke, quartzite dolostone, limestone

2 Chlorite-albite-epidote schist (metabasalt)

1 Crystalline metasandstone (Chain Lakes massif)

Table 2-1: Main lithostratigraphic units corresponding fully or partly to bedrock geology map-units

MAP UNIT #	LITHOSTRATIGRAPHIC UNITS	
24	* Monteregian (Cretaceous) intrusives	
A) ST. LAWRENCE PLATFORM (Cambrian and Ordovician system)		
23	Richmond Group (Bécancour and Pontgravé Formations)	
22	Lorraine Group (Nicolet Formation)	
21	Les Fonds Formation and Saint-Germain Complex	
B) ACADIAN OROGEN (Silurian and Devonian system)		
20	* Devonian granites	
19	St. Francis Group and Compton Formation	
18	Lake Aylmer Formation, Glenbrooke Group, and correlatives	
17	* Saddle Hill intrusives	
16	Frontenac Formation (sedimentary member)	
15	Frontenac Formation (volcanic member)	
C) TACONIAN OROGEN (Cambrian and Ordovician system)		
	INTERNAL DOMAIN	EXTERNAL DOMAIN
14	Chesham Formation	
13		Drummondville Wildflysch
12		Bulstrode and Saint-Sabine Formations
11	Magog Group (Saint-Victor and Beauceville Formations)	
10	Ascot and Weedon Formations, and correlatives	
9	Saint-Daniel Formation	
8	Caldwell and Armagh Groups (volcanic members)	Saint-Flavien Formation
7	Mansonville and Bromptonville Formations; Caldwell and Armagh Groups (sedimentary members)	Granby and Sillery Groups
6	* Mont Orford, Asbestos and Thetford-Mines ophiolite complexes	
5	* Vianney amphibolite	
4	Rosaire Group	Stanbridge Group
3	Oak Hill Group	Shefford Group
2	Tibbit Hill Formation	
1	Arnold River Formation (Precambrian)	

* These are listed as useful terms; they are not formal lithostratigraphic units.

rocks of the Tibbit Hill Formation (map-unit #2) crop out only over a small area at the southwest end of Monts Notre-Dame, instead of the much larger area which had been shown on previous geological maps (e.g. Harron, 1976). Another example is the addition of a 5 km-long outcrop of amphibolite (map-unit #5) located about 25 km east of Victoriaville (Caron, 1983a), a rock unit which had gone unreported in previous geological reports and maps. Other examples could be pointed out. Every effort was made to utilize what appeared to be the most reliable sources.

Comprehensive summaries of the bedrock geology of the southeastern Quebec Appalachians are provided by Cooke (1937, 1950), Cady (1960, 1969), St-Julien et al. (1972) and, more particularly, St-Julien and Hubert (1975). Thus, only those concepts and observations which will be utilized herein will be reviewed.

Clastic-dominated Cambro-Ordovician strata of the southeastern Quebec Appalachians were deformed mainly during the Taconian orogen, forming a foldbelt which lies southeast of the relatively undeformed sedimentary cover of the St. Lawrence Platform (Figure 2-1). A belt of younger Siluro-Devonian strata, which are also clastic-dominated and which were deformed during the Acadian orogen, lies southeast of the Taconian foldbelt and runs parallel to it; this belt is commonly designated as the Connecticut Valley-Gaspé Synclinorium (Cady, 1969; St-Julien and Hubert, 1975). The regional metamorphic grade for both Taconian and Acadian foldbelts is greenschist.

St-Julien and Hubert (1975) recognized two main tectonic domains within the Taconian foldbelt: an internal domain (map-units #2 through #11) and an external domain which in turn comprises an outer belt of thrust-imbricated structures (map-unit #21) and an inner belt of nappes (map-units #3, 4, 7, 8, 12, 13). These two belts are separated by a major regional thrust fault (Logan's Line), as are the internal and external domains. Because the external domain includes a belt of gravity nappes derived from the internal domain (St-Julien and Hubert, 1975;

fig. 6), several map-units (#3, 4, 7, 8) of the internal domain are repeated in the external domain.

Much of the Asbestos-Valcourt region is underlain by rocks of the internal Taconian domain. St-Julien and Hubert (1975) subdivided these rocks into two regional sequences: (1) a continental rise sequence (map-units #2, 3, 4, 5, 7, 8) which has been deformed into two anticlinoria, the Sutton Anticlinorium and the Notre-Dame Anticlinorium, and (2) an oceanic crust sequence (map-units #6, 9, 10, 11). The proposed boundary between these two lithologic sequences, the Baie Verte-Brompton Line, is the northwest limit of the ophiolite suite (map-unit #6) in the study area and has been recognized throughout the Canadian Appalachians (Williams and St-Julien, 1982).

Strata of both the internal and external Taconian domains predominantly consist of slate (or shale) ± sandstone assemblages (Figure 2-1). Because lithologic assemblages within several of the map-units closely resemble those of other map-units and also because several map-units are repeated as separate near-parallel belts, most hand-size rock fragments, hence till clasts, cannot be readily assigned to specific outcrop belts. In spite of this somewhat monotonous bedrock lithology, a few additional observations are warranted:

(1) Schistose rocks, which are very common within the continental rise sequence of the internal Taconian domain, are quite uncommon within the oceanic crust sequence and are conspicuously absent in nappes of the external Taconian domain.

(2) Strata which make up the oceanic crust sequence of the internal Taconian domain are generally more pelite-dominated than those of the continental rise sequence.

(3) Because most of the Taconian foldbelt strata are non-calcareous, calcareous shales and argillaceous limestones of the Bulstrode Formation (map-unit #12) as well as calcareous sandstones and shales of the St. Francis Group and of the Lake Aylmer Formation

(map-unit #18) constitute fairly distinctive lithologic assemblages.

Ultramafic rocks (map-unit #6) consisting mainly of serpentized peridotite, dunite and pyroxenite (Lamarche, 1973; Laurent, 1980; Hébert, 1982) are the most distinctive rock units of the Asbestos-Valcourt region. They constitute the basal units of ophiolite suites which have been labelled as (1) Mont Orford, (2) Asbestos and (3) Thetford-Mines ophiolite complexes. The Asbestos ophiolite complex is the smallest of the three and it lies entirely within the study area where it crops out as a generally narrow 55 km-long belt.

Metabasalts of the Tibbit Hill Formation (map-unit #2) are also distinctive rocks. However, mafic volcanic rocks are present in other rock units such as the ophiolite complexes and the Ascot-Weedon Formations (map-units #6 ans #10). Since all three units extend across the study area as separate outcrop belts, the usefulness of these volcanic rocks as provenance indicators is hindered.

2.2 Physiography

Physiographic divisions and subdivisions within, and adjacent to, the study area are delineated in Figure 2-2 and listed in Table 2-2. Much of this work represents an original contribution; its main purpose is to provide a physiographic framework so as to ease description and discussion of Late Pleistocene stratigraphy and events in their regional context. The units proposed herein differ somewhat from previous suggestions (Bostock, 1970; Dubois, 1974), mainly because of differing purpose and work-scale, and also because significant insights into the regional bedrock geology were made since the time of the earlier proposals.

Tectono-stratigraphic domains, as defined by St-Julien and Hubert (1975), together with major topographic features, provide an excellent basis for characterizing and delineating distinctive physiographic divisions and subdivisions. Thus the present assessment of the physiography

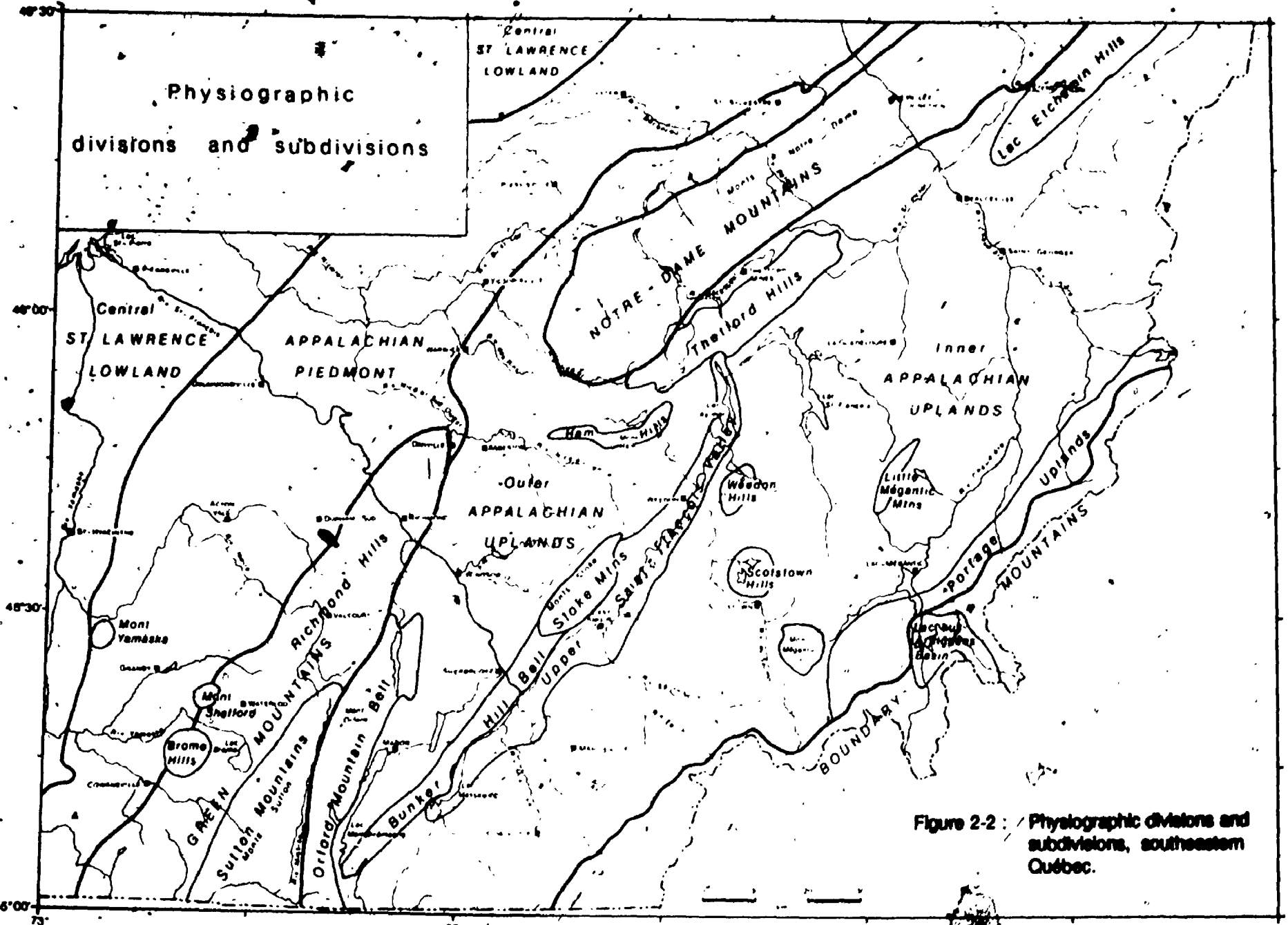

Figure 2-2 : Physiographic divisions and subdivisions, southeastern Québec.

Table 2-2: Physiographic divisions and subdivisions, southeastern Québec

Divisions	Subdivisions
St. Lawrence Lowland	Central St. Lawrence Lowland
Appalachian Piedmont	
Green Mountains	Sutton Mountains Richmond Hills
Notre-Dame Mountains	
Appalachian Uplands	Outer Appalachian Uplands Inner Appalachian Uplands Orford Mountain Belt Ham Hills Thetford Hills Lac Etchemin Hills Stoke Mountains Bunker Hill Belt Upper Saint-François Valley Portage Uplands Weedon Hills Scotstown Hills Little Mégantic Mountains
Boundary Mountains	(Boundary Mountains) Lac aux Araignées Basin
Monteregian Hills	Mont Yamaska Mont Shefford Brome Hills Mont Mégantic

of the southeastern Quebec Appalachians is derived from an updated geologic data base and from major landscape features.

2.2.1 St. Lawrence Lowland

The St. Lawrence Lowland, whose elevation ranges from 10 m to about 90 m ASL, is a plain underlain by horizontal strata of the St. Lawrence Platform. Within the area covered by Figure 2-2, bedrock topography of the Lowlands is concealed underneath a thick cover of Late Quaternary sediments, most commonly by Champlain Sea deposits. The landscape consists of extensive level surfaces into which the main rivers are cut to depths of 10 to 30 m. Terraces are quite common along major streams, particularly at lower elevations along the St. Lawrence River. Gullying occurs mainly along river banks and less commonly along terrace scarps.

Except for the Monteregian Hills (see Table 2-2 and section 2.2.6) which are prominent summits isolated within several physiographic units, the remaining physiographic divisions and subdivisions shown in Figure 2-2 are part of the Appalachian region.

2.2.2 Appalachian Piedmont

The Appalachian Piedmont is a slightly inclined surface consisting of low and broad strike ridges underlain by folded strata of the external Taconian domain. Bedrock control on topography is less evident here than elsewhere in the Appalachian region. This is due in part to the low relief of the drift-mantled Piedmont, where elevations gently rise southeastward from about 90 m to about 175 m ASL. This is also due to the fact that, as the inner limit of the Piedmont coincides quite closely with the upper limit of the Champlain Sea incursion, extensive areas adjacent to the main rivers are covered by deltaic sediment bodies (see Figure 3-1).

2.2.3 Green Mountains and Notre-Dame Mountains

Both the Green Mountains and the Notre-Dame Mountains are the topographic expression of northeast-trending anticlinoria belonging to the internal Taconian domain. Although they are underlain by strata of similar lithology and age, they may be considered as distinct physiographic divisions. The main reason is that they are separated, in the vicinity of Asbestos, by a 30 km-wide gap which results from the northeastward plunge of the Sutton Anticlinorium as well as from the southwestward plunge of the Notre-Dame Anticlinorium.

The Green Mountains are subdivided into two units, the Sutton Mountains and the Richmond Hills. The Sutton Mountains, where summit elevations commonly exceed 600 m ASL, reaching as much as 872 m (Roundtop), are the northern part of a mountain range, extending from Vermont into southern Quebec. Although altitudes range from about 150 m to as much as 709 m (Pinnacle Mountain), the Richmond Hills form a belt of hilly terrain whose altitude averages only about 225 m and where local relief rarely exceeds 100 m. Strike ridges, which are typically steep-sided when underlain by more resistant strata (e.g. metabasalt, quartzite), are quite prominent features of the Richmond Hills landscape; yet, their summits only occasionally attain altitudes of 300 m.

The Notre-Dame Mountains are a low mountain range where most summits rise to altitudes of about 600 m, thus standing 200 to 300 m above the general level of the surrounding uplands. A few through-valleys, such as the Palmer River and Osgood River valleys, extend across this range which is otherwise characterized by a mature fluvial dissection landscape, a rather unique feature among physiographic divisions of southeastern Quebec.

2.2.4 Appalachian Uplands

The Appalachian Uplands are by far the most extensive physiographic division of southeastern Quebec. In addition to the many bedrock knobs and knolls, and the numerous strike ridges standing above the general

level of the upland surface, there are several well-defined groups and belts of hills or mountains whose description as distinct physiographic subdivisions is warranted.

Inner and Outer Appalachian Uplands

The Inner and Outer Appalachian Uplands form a low-relief hilly surface whose general level rises southeastward from about 250 m ASL near the Piedmont to about 450 m ASL near the Boundary Mountains. The general slope of the Uplands is thus only on the order of 0,25%. The Inner and Outer Uplands share characteristics of gentle slopes and wide valleys, with local relief generally less than 100 m. Within both subdivisions, slopes in the lower half of valley sides tend to be steeper than in the upper half. As it has been shown previously (Clément et Poulin, 1975; Shilts, 1981), Quaternary sediments tend to form a thicker cover in valleys than on interfluves where bedrock is usually veneered by a thin layer (less than 1 or 2 m) of till. As will be seen later (see sections 4.1 and 4.2), there are several exceptions to this rule.

Admittedly, the distinction between the Inner and Outer Appalachian Uplands is introduced chiefly for convenience. Yet, there are good reasons to do so:

(1) the two subdivisions are neatly separated by the broad, parallel-to-strike, Upper Saint-François Valley in the vicinity of the study area and, north of it, by the Notre-Dame Mountains;

(2) the Outer Uplands are underlain by Cambro-Ordovician rocks that were deformed mainly during the Taconian orogen while the Inner Uplands are chiefly underlain by Siluro-Devonian strata that were deformed mainly during the Acadian orogen;

(3) general altitude within the Outer Uplands varies between 250 and 350 m and is thus lower than within the Inner Uplands where it varies between 350 and 450 m.

Other subdivisions of the Uplands consist of series of hills or mountains, except of course for the Upper Saint-François Valley, which owe several of their characteristics to underlying bedrock types.

Orford Mountain Belt, Ham Hills and Thetford Hills

Three subdivisions, the Orford Mountain Belt, the Ham Hills and the Thetford Hills, are associated with ophiolite complexes. Their main landscape features, that is the location and form of mountains, hills and knobs, are apparently controlled (1) by tectonic structures within the ophiolite complexes and (2) by variations of resistance to chemical and mechanical weathering within and between the rock types of the ophiolite suites. Most summits are, for instance, underlain by gabbroic or mafic volcanic rocks rather than by ultramafic rocks.

The Orford Mountain Belt consists of a series of small and large mountains which are dominated by the Mont Orford Massif (876 m); this belt extends from the international boundary to the vicinity of Brompton Lake and includes such summits as Owl Head (762 m), Sugar Loaf (671 m), Mont Chagnon (610 m), Mont Chauve (594 m) and Mont des Trois-Lacs (472 m). Contact zones with the adjacent Sutton Mountains and Appalachian Uplands coincide respectively with the Missisquoi River Valley and the Lac Memphrémagog basin.

The Ham Hills are a somewhat disconnected series of large hills and mountains whose summits attain altitudes of about 465 m, roughly 150 m above the surrounding uplands. They extend northeastward from Petit Mont Ham (457 m) to Mont Louise (488 m) near Lac Nicolet; the main summit of the series is Mont Ham (716 m).

The Thetford Hills are similarly characterized by a northeast-trending suite of large hills and mountains which are underlain by the Thetford-Mines ophiolite complex; their height relative to the uplands is usually in excess of 150 m. The belt extends from Colline Nadeau (450 m), across the upper Bécancour valley, and hence to Le Grand Morne (602 m). In addition to numerous steep-sided knobs and hills, the

Thetford Hills include summits such as Colline Belmina (495 m), Mont du Caribou (557 m), Quarry Hill (518 m) and Mont Adstock (712 m). Knobs and hills located near both the northeast and southwest extremities of these hills occur as large strike ridges underlain by resistant mafic rocks, while those of the core area occur mostly as aligments of near-circular masses underlain by ultramafic rocks.

Lac Etchemin Hills

The Lac Etchemin Hills are characterized by a series of prominent northeast-trending strike ridges stretching out along the southeastern flank of the Notre-Dame Mountains east of the Chaudière River valley. Summits generally reach altitudes of 520 m or more; their height above the adjacent Inner Uplands is thus on the order of 175 m. The Lac Etchemin Hills are underlain by strata of the St-Victor Synclinorium (upper part of the oceanic crust sequence of the internal Taconian domain; Fig. 2-1: map-unit #11) which were locally intruded by dioritic and gabbroic rocks during the Acadian orogen.

Stoke Mountains and Bunker Hill Belt

Both the Stoke Mountains and the Bunker Hill Belt are underlain by volcano-sedimentary strata of the Ascot Formation. Because it is flanked by deep valleys along much of its length, the Bunker Hill Belt appears as a rather prominent suite of hills, especially when viewed from the south. Summit elevation is about 400 m, which is in fact only about 125 m above the level of surrounding uplands.

The Stoke Mountains are the continuation of the Bunker Hill Belt. They consist of a closely spaced series of summits rising to about 550 m ASL, the highest being Chapman Peak (655 m); their height relative to the adjacent Uplands thus exceeds 250 m.

Weedon Hills, Scotstown Hills and Little Mégantic Mountains

The Weedon Hills, Scotstown Hills and Little Mégantic Mountains are isolated series of large hills and mountains commonly rising 150 to 200 m above the level of the Inner Uplands. All three subdivisions are underlain by Devonian granitic stocks. Summits of the Weedon Hills form a near-circular pattern; the main ones are Mont Aylmer (518 m) and an unnamed summit (556 m) northeast of Fontainebleau. The Scotstown Hills consist of a series of hills encircling rock basins occupied by Lake Magill and Lake Moffatt; the highest of these hills reaches an altitude of 541 m. The Little Mégantic Mountains consist of several aligned summits, the most prominent of which are Mont Sainte-Cécile (887 m) and Morne de Saint-Sébastien (831 m).

Portage Uplands

As for other physiographic units of the Lac-Mégantic region (Mont Mégantic, Little Mégantic Mountains, Lac aux Araignées Basin), the Portage Uplands are a physiographic subdivision which has been aptly characterized by Shilts (1981). This unit, like those listed above, lies well outside the study area and will therefore be described rather succinctly.

Because the Portage Uplands share a number of characteristics with the Appalachian Uplands division, it is herein considered as one of its subdivisions. It consists of a high, relatively level upland with altitudes ranging between 525 and 640 m; they are separated from the adjacent Inner Uplands by a prominent 100 m-high escarpment.

Upper Saint-François Valley

The Upper Saint-François Valley is a broad valley which stretches out, paralled to strike, over a distance of roughly 110 km. It is occupied by the upper Saint-François River and by a tributary stream, the Massawippi River. At the confluence of these two streams, near Lennoxville, the Saint-François River abruptly changes direction and thence

flows across strike toward the St. Lawrence Lowlands. Valley flanks are commonly 100 m-high and are typically asymetric, the southeast-facing slopes being almost everywhere higher and steeper than the opposite ones.

The valley is underlain mostly by calcareous sandstones and shales of the St. Francis Group and of the Lake Aylmer Formation. The formation of the valley is probably due, at least in part, to higher rates of weathering and erosion of the calcareous substrate. In the absence of adequate borehole data, the role and extent of glacial overdeepening relative to preglacial or interglacial weathering remains somewhat speculative. What is clear is that, at several localities in the valley, the bedrock floor lies well below the level of buried bedrock sills (Ascot Formation: map-unit #10 of Figure 2-1) near Sherbrooke (McDonald, 1967a; Clément et Poulin, 1975).

Between East-Angus and Lake Massawippi, the valley floor is covered by thick drift accumulations through which the modern Saint-François and Massawippi Rivers are entrenched down to an altitude of about 135 m ASL. Starting about 5 km upstream of the bedrock sill at East-Angus, postglacial downcutting is more moderate and the valley floor gently rises from 190 m ASL to about 250 m ASL around Lake Aylmer.

2.2.5 Boundary Mountains

The Boundary Mountains, a northeast extension of the White Mountains of New England, form a range whose summits stand at altitudes above 750 m; the highest is Mont Gosford (1219 m). The range owes its high altitudes to the underlying erosion-resistant Arnold River and Frontenac Formations (Shilts, 1981). Relative to the area originally defined by Shilts (1981), the unit has been extended southwestward so as to include an unnamed mountain range south of Martinville. This range includes Mont Hereford (876 m) and several other summits with altitudes of 600 m or more.

The crest of the range forms the divide between the Saint-François River and Chaudière River watersheds on one hand and, on the other, the Kennebec River and Connecticut River watersheds; this divide also serves to delineate the International Boundary over a distance of more than 130 km.

Lac aux Araignées Basin

The Lac aux Araignées Basin is herein considered as a subdivision of the Boundary Mountains; its floor (425 m ASL) is underlain by a Devonian intrusive body of granodiorite which erosion has "barely unroofed" (Lord, 1938; Shilts, 1981). The basin extends southeastward into northern Maine and includes the depression surrounding Arnold Pond.

2.2.6 Monteregian Hills

The hills and mountains of the Monteregian Hills are distinctive and isolated features which stand well above the level of the surrounding terrain. They are underlain by erosion-resistant Cretaceous intrusive rocks (mostly gabbroic rocks). The isolated hills are irregularly disposed along an east-west array extending from the vicinity of Montréal to Mont Mégantic. The circular outline of individual mountains or series of hills is a typical feature (see Figure 2-2), and so are their steep-sloped outer flanks.

Four of these hills lie within the area of Figure 2-2: these are Mont Yamaska (411 m), Mont Shefford (526 m), Brome Hills (including Mont Brome: 556 m) and Mont Mégantic (1150 m). Their relief is thus on the order of 300 m or more, 700 m in the case of Mont Mégantic.

CHAPTER 3

METHODS OF INVESTIGATION

In order to meet the objectives stated in the introduction (Chapter 1), several methods of investigation have been utilized in the field and in the laboratory. The majority of these methods were aimed at acquiring directional and compositional data (provenance, in particular) that were expected to contribute to establishing direct relationships between the stratigraphic record and former ice-flow patterns.

3.1 Field methods

Fieldwork was carried out mainly during the summers of 1979 and 1980 and intermittently during the 1981 and 1982 field seasons. Only occasional field visits have been made since.

3.1.1 Mapping glacial and deglacial landforms and deposits

Because surficial geology maps (McDonald, 1966, 1967b; Warren et Bouchard, 1976; Parent, 1978; Chauvin, 1979a) were available for about half the study area and because the author conducted fieldwork without the help of field assistants, this study did not include a surficial geology mapping project. However, aerial photographs at a scale of 1:40 000 along with field investigations were utilized not only to locate natural and artificial exposures but also to prepare a regional map of glacial and deglacial deposits and landforms (Figure 3-1). For obvious reasons, the emphasis was placed on areas that were not previously mapped, such as the northern and eastern parts of the Dudswell map-area (21 E/12), the whole of the Warwick map-area (21 E/13) and, to a lesser extent, the west half of the Orford map-area (31 H/8).

3.1.2 Section description and surface till sampling

Stratigraphic sections were described following standard methods of sedimentology. For instance, every effort was made to describe stratified sediments with terminology utilized in Blatt, Middleton and Murray (1980). However, since tills and related glacigenic sediments are important components of the stratigraphic record of this region (both in terms of volume and of significance), recognition of different varieties of till, when possible, was made following descriptions and criteria discussed mainly by Boulton (1968, 1970a, 1970b, 1971, 1978) and by Dreimanis (1969, 1976); the nomenclature that was "... tentatively adopted by the Till Work Group of the INQUA Commission on genesis and lithology of Quaternary deposits" (Dreimanis, 1983: p. 501) has been utilized during the write-up stage of this thesis. Locations of stratigraphic sections are given in Figure 3-1; descriptions are given in Appendix I where sections are listed according to their order of appearance in text.

In addition to about 150 samples (mainly till and other diamictons) that were collected in stratigraphic sections, a surface till sampling programme was also carried out; this was done in order to facilitate interpretations of compositional variations recorded in stratigraphic sections as well as to test these interpretations, much as suggested by Shilts (1978). Because ultramafic rocks of the Asbestos ophiolite complex (see Figure 2-1 for location) were expected to provide an excellent local provenance indicator, as in the nearby Thetford-Mines area (Shilts, 1973a, 1975, 1976a), a suite of about 200 surface till samples were collected in terrains lying both northwest and southeast of the ophiolite complex. This network of samples essentially covers the central half of the study area.

3.1.3 Glacial striations

Since glacial striations on bedrock have been measured by several authors (McDonald, 1966, 1967a, 1967b; Lamarche, 1974; Lortie, 1976; Warren et Bouchard, 1976; Parent, 1978) throughout much of the study

area, little emphasis was placed on further measurements of striae during the present study. However, because of conflicting interpretations in the area east of Asbestos (northwestward ice-retreat versus westward and northward "late-glacial" ice movements; see section 1.3.2), several outcrops were investigated in the vicinity of Asbestos. Following Lamarche (1971, 1974) and Lortie (1976), ice-flow direction was assigned only on the basis of crag-and-tail features. Other types of striations and ice-marks, such as nailhead striae, p-forms, lunate fractures, crescentic gouges and fractures, which may also yield fairly reliable directions of ice-flow, are much less common in this region; hence, there is no need to discuss their reliability as indicators of ice-flow direction. Glacial striations measured during this investigation are plotted in Figure 3-1.

Although crag-and-tail striations ("rat tails" in Flint, 1971) are regarded as "absolute" criteria of ice-flow direction by a number of authors, including Lamarche (1971, 1974) and Lortie (1976), some puzzling features were observed during this investigation. For instance, on a large outcrop located 3.7 km due south of Warwick, grooves that contain abundant SE-trending crag-and-tail striations were also found to contain a few NW-trending crag-and-tail striations; in one case, the two sets, rigorously parallel but facing one another, were obviously produced by the same ice-flow event. The criterion may therefore not always be definitive.

Moreover, determination of ice-flow direction, even on the basis of crag-and-tail striations, does involve some subjectivity; for instance, Lortie (1976: p. 68) reports that he (accompanied by McDonald and Shilts) assigned a southeastward ice-flow direction at two sites near Richmond where Lamarche (1974) had reported NW-trending crag-and-tail striations; in another such site near Kingsey-Falls, they could not assign a reliable direction. Doing so allowed them to dismiss Lamarche's contention that a late-glacial northwestward ice-flow event had taken place in the Saint-François River valley.

For these and other reasons, glacial striations have simply been considered as one of several directional criteria during this investigation. Since the interpretation of cross-cutting relationships is also a rather subjective matter, relative chronology of glacial striations at sites shown in Figure 3-1 is based on superimposition of one set of striations upon an older glacially abraded surface; in most cases, simple crosscutting relationships were not accepted as reliable evidence.

3.1.4 Till clast fabric measurements

Till clast fabrics were measured in stratigraphic sections distributed across much of the study area. Measurements were carried out in order to establish ice-flow directions (or sequences of ice-flow directions) recorded in exposed till units and in order to recognize ice-flow patterns associated with respective till sheets.

The orientation (azimuth and plunge) of the A-axis (long) of elongated till clasts was measured in addition to the length of the long (A), intermediate (B) and short (C) axes; sampling was restricted to prolate ($B/A < 0.67$; $C/B \geq 0.67$) and bladed (B/A and $C/B < 0.67$) pebbles between 16 and 64 mm in length. In order to help distinguish between transverse and parallel fabrics (Boulton, 1971), orientation of the B-axis of bladed pebbles (between about 70 and 85% of measured pebbles) was also determined; C-axis orientation (poles to clast A/B planes) can then be easily obtained on the stereonet. Most commonly, 50 elongated till stones were measured in freshly excavated, undisturbed exposures of matrix-dominated lodgement till; sampling area was restricted to about 50 cm vertically and about 75 cm laterally.

3.1.5 Paleocurrent measurements

Generalized direction of paleocurrent indicators was summarily investigated in a large number of ice-contact stratified drift exposures (mostly eskers and subaquatic outwash bodies). However, in a few instances, in order to meet specific needs, paleocurrent measurements were carried out in trough-cross-bedded sand or gravel and in ripple-drift

laminated sand. Most commonly, five (5) cross-bed measurements (direction of true dip) were obtained from each of several tabular or trough sets that were exposed at different levels or locations within the investigated sediment body or unit. In cross-laminated sands, a subhorizontal bench was excavated within ripple-drift cosets; again, the orientation of five (5) different ripple trains was measured in each of several cosets that were exposed at different levels and locations within the investigated unit.

3.1.6 Till clast lithology

The lithology of till clasts was carefully examined in stratigraphic sections and at over 200 surface till localities. Early investigations quickly revealed that distinctive indicator pebbles, consisting mainly of ultramafic and Precambrian (Shield-type) clasts, are commonly present, though in low percentages, in tills of the study area. Mainly because of these obviously low percentages, particularly in areas where provenance data was most needed (e.g., uplands east of Asbestos), pebble counts were not carried out, except in a few cases such as in tills and other diamictons of the Norbestos section (see Table 4-2).

However because ultramafic clasts constitute distinctive <u>local</u> provenance indicators while Precambrian clasts (mainly gneiss and several varieties of granitoid rocks) constitute distinctive <u>distant</u> provenance indicators, the relative abundance (or absence) of these two lithological groups in tills of the Asbestos-Valcourt region was systematically noted in the field. Given the large number of clasts that commonly lie at the surface of till outcrops in this region, this has at least the advantage that abundances as low as about one per thousand can be detected.

3.1.7 Altimetry

The altitude of about half of the strandline features which were recorded during this study was measured with a Paulin surveying altimeter (model M-1). The "Single Altimeter Method" described by Hodgson

(undated) was utilized; hence, altimeter traverses were made only during periods of presumably stable barometric conditions. All traverses were closed to a bench mark or spot elevation in less than one hour; readings were corrected for temperature and for barometric variations. Two duplicate traverses were carried out and results varied by 0.5 and 1.0 m, respectively; thus, measurement error should be within 4 m (± 2 m). Results are listed in Appendix IV, together with strandline features whose altitudes were read from topographic maps: measurement error is then considered to be equivalent to the contour interval of the map, that is 8 m or 25 feet (± 4 m) in the study area.

3.2 Laboratory methods

Laboratory analyses were carried out mainly in the Pleistocene Laboratory of the University of Western Ontario, and computer work was also done there.

3.2.1 Granulometric analysis

Grain size analysis of the <2 mm fraction was carried out on 100 g subsamples; 50 g subsamples were utilized for a few silt- or clay-rich samples. Granulometry of the silt-clay fraction (<0.063 mm) was determined by hydrometer analysis (ASTM, 1972); following wet sieving, granulometry of the sand fraction was determined by dry sieving. Percentages of sand (2.0 - 0.063 mm), silt (0.063 - 0.004 mm) and clay (<0.004 mm) were determined from cumulative curves drawn on probability paper. Standard grain size statistics (M_z: Graphic mean; σ_I: Inclusive graphic standard deviation, an index of sorting; Sk_I: Inclusive graphic skewness; K_G: Graphic kurtosis) were calculated using formulae given in Folk and Ward (1957). Results are listed in Tables A-2, A-3 and A-4. In order to avoid sample contamination for subsequent geochemical analyses, only stainless steel sieves were utilized during this study.

3.2.2 Carbonate analysis of the silt-clay fraction

Calcite and dolomite contents of the silt-clay fraction (<0.063 mm) were measured using Chittick apparatus (Dreimanis, 1962). Since Pleistocene sediments in the study area contain relatively small amounts of carbonates, 1.2 g samples were used; results are listed in Tables A-2, A-3 and A-4. Duplicate measurements were made on all samples and were found to be consistently similar to initial measurements.

3.2.3 Trace element analysis of the silt-clay fraction

The <0.063 mm fractions of most of the samples (mainly till) collected during this investigation were analyzed for Ni, Cr, Co, Cu, Pb and Zn concentrations. These were determined commercially (Bondar-Clegg and Co., Ltd) by atomic absorption techniques after a partial, two hour, hot mixed-acid (HCl-HNO_3) leach. This analytical procedure was followed mainly to ensure that results can be compared directly with large bodies of data acquired by Shilts (1973a, 1973b, 1976a, 1978, 1981) in the nearby Thetford-Mines and Lac-Mégantic regions; his work has convincingly shown that Ni and Cr concentrations in the <0.063 mm fraction of till can be excellent indicators of debris derived from ultramafic rock sources. Since the Asbestos ophiolite complex includes a belt of ultramafic rocks that runs SW-NE across much of the study area (see Figures 2-1 and 4-21), a situation which compares well with that of the Thetford-Mines region, it was expected that Ni and Cr concentrations in till would reveal glacial dispersal patterns of ultramafic rocks and would also provide provenance data for till units exposed in stratigraphic sections. Results are listed in Tables A-2 and A-3.

As a test of the applicability of the method in the study area, four samples of serpentinized peridotite (the most abundant ultramafic rock-type in this part of the ophiolite belt) that were collected at scattered sites along the ultramafic rock belt were crushed and submitted to the same analytical procedure as till samples; Ni concentrations varied between 710 and 7900 ppm ($\bar{x}$ = 4578 ppm) while Cr concentrations varied between 330 and 984 ppm ($\bar{x}$ = 630 ppm). This suggests

that ultramafic rocks of the Asbestos ophiolite complex are major local sources of Ni and Cr in till; for instance, a sample of gabbroic rock collected in the Mont Burbank quarry, near Asbestos, was found to contain only 4 ppm Ni and 6 ppm Cr.

Work by Shilts (1973a, 1975) also indicates that till samples richer in clay tend to contain higher amounts of Ni and Cr, especially in tills that have only background Ni and Cr concentrations. A scatter diagram of Ni content versus % clay in the silt-clay fraction was prepared for the surface till sample suite (Figure 3-2); the suite includes 204 samples of both unoxidized and oxidized till collected within or outside of ultramafic dispersal trains. Contrary to diagrams prepared by Shilts (1973a: fig. 14), Figure 3-2 shows no obvious relationships between Ni content and % clay in the silt-clay fraction. This is perhaps best explained by the fact that clay contents (relative to the total silt- clay fraction) are much lower (between about 10% and 40%; $\bar{x}$ = 25%) in tills of the Asbestos-Valcourt region than they are in tills of the Lac-Mégantic region (between about 30% and 70%).

3.2.4 Heavy mineral analysis

In this study, heavy minerals are defined as fine sand (0.250 - 0.125 mm) particles of specific gravity greater than 2.85. Separation of the heavy mineral fraction was accomplished by standard techniques (Carver, 1971), using bromoform (S.G. = 2.85) as a separating medium. Since 10 to 15 g of fine sand were used for separations, weight of the heavy mineral fraction was sufficiently high to be measured directly; heavy mineral weight of till samples varied between about 3 and 8%.

The magnetic fraction was subsequently removed from the heavy mineral fraction with a small hand magnet; weight of the non-magnetic fraction was used as a basis for computing the percentages of magnetic minerals. Weight of the magnetic fraction in till varied between about 6 and 16%; results are listed together with heavy mineral weight (%) in Table A-2. Following McDonald (1967a) and Shilts (1973a, 1975, 1981),

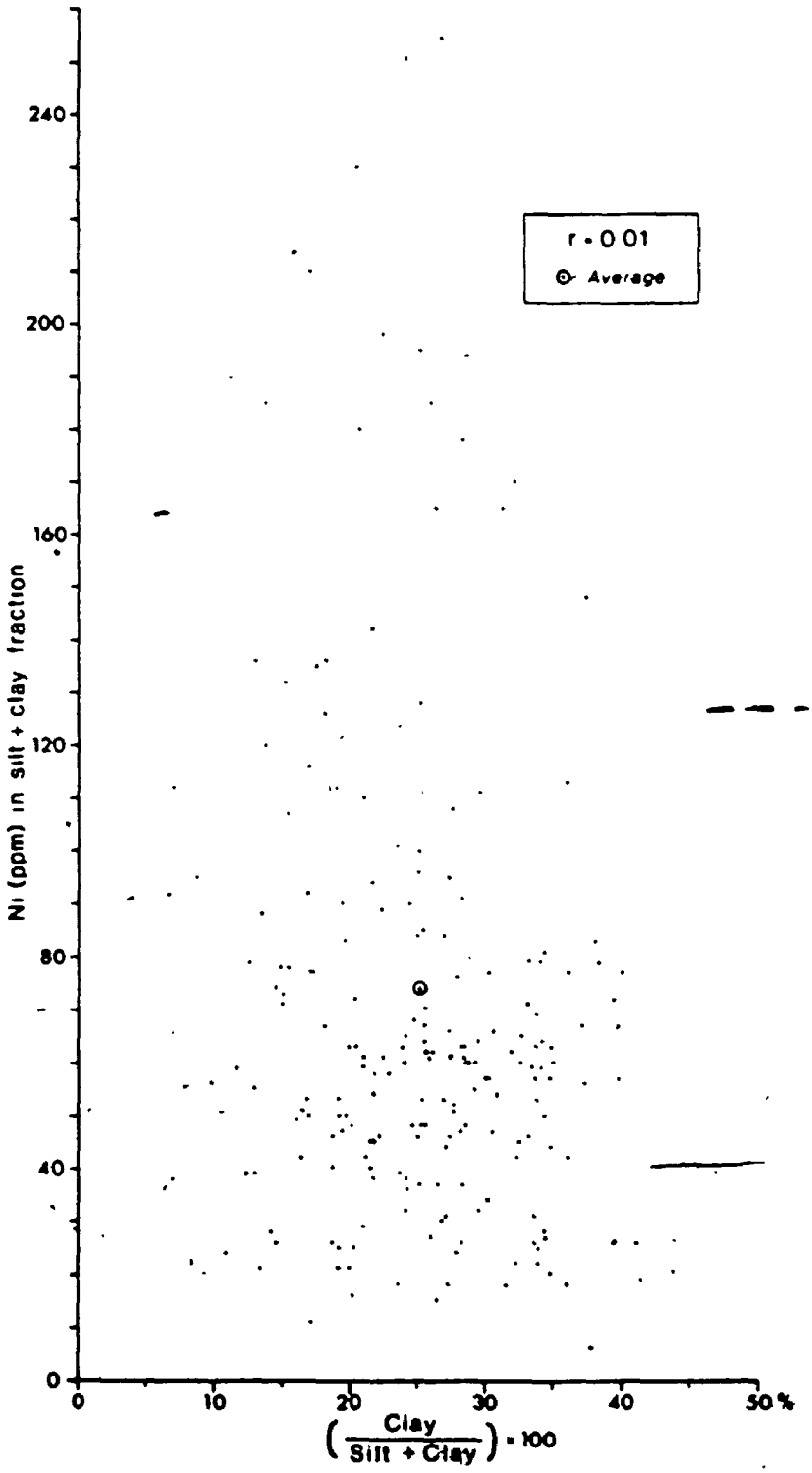

Figure 3-2 : Scatter diagram of Ni content versus clay content in the silt-clay fraction (<0.063 mm) of surface till samples. Only two of 204 samples have a Ni content (450 and 275 ppm) beyond the range of the diagram (see Table A-3 : samples #90-155 and #90-156).

it was expected that magnetic mineral content would provide additional information on glacial dispersal of ultramafic components.

3.2.5 Analysis and presentation of paleocurrent data

Paleocurrent data were grouped into 10° classes and their frequency distribution was plotted on conventional rose-diagrams. The data were analyzed statistically by the method of Curray (1956) in which the direction of preferred orientation is given by $\bar{X}_v$ (vector mean) and the degree of preferred orientation is given by L (% vector magnitude); using the Raleigh test of significance, L values are then tested against the probability that orientation data were drawn from a random distribution. All paleocurrent distributions are strongly non-random.

3.2.6 Analysis and presentation of till clast fabric data

Scatter and contoured diagrams of clast fabric data were plotted onto the lower hemisphere of the Lambert equal-area projection (so called Schmidt net) using a computer program written by Starkey (1970, 1977); in this program, the counting area for preparing contoured stereograms is (100/N) % of the area of the stereonet, where N is the number of observations. Contoured stereograms of A-axis and C-axis data are presented in Appendix II.

The eigenvalue method (Scheidegger, 1965; Mark, 1973, 1974) was used as a data reduction technique as well as to provide a statistical assessment of clast fabric data. The computer program written by Mark (1973) carries out a three-dimensional vector analysis in order to extract the eigenvectors and eigenvalues of a 3 x 3 matrix (A). This matrix is constructed by converting each measured axis to Cartesian coordinates and summing each resulting matrix and its transpose:

$$A = \sum_{j=1}^{N} X_j X_j^T \qquad (3\text{-}1)$$

where X_j is a unit vector paralleling the (j)th observation axis, (X_j^T is the transpose of X_j, and N is the number of observations. Eigenvalues ($\lambda_1 \geq \lambda_2 \geq \lambda_3$) and eigenvectors ($V_1$, V_2, V_3) of matrix A are then computed. The orientation (azimuth and plunge) of the largest eigenvector (V_1) indicates the direction of maximum clustering; the smallest eigenvector (V_3) refers to the direction of minimum clustering. Normalized eigenvalues, $S_1 \geq S_2 \geq S_3$, are also computed:

$$S_j = \lambda_j/N \qquad (3\text{-}2)$$

S_j values provide a measure of the degree of clustering about eigenvectors (V_j). Also computed is an angle,

$$\theta_j = \arccos (\lambda_j/N) \qquad (3\text{-}3)$$

which Scheidegger (1965) termed the "standard scattering angle". Results are listed in Table A-1.

Woodcock (1977) proposed a method of evaluating fabric shape and strength on the basis of the eigenvalue ratios; fabric strength (C) and shape (K) parameters are computed by the following formulae:

$$C = \ln (S_1/S_3) \qquad (3\text{-}4)$$

$$K = \frac{\ln (S_1/S_2)}{\ln (S_2/S_3)} \qquad (3\text{-}5)$$

The value of C is proportional to fabric strength, with C tending toward 0 for uniformly distributed data and reaching a maximum of about 6 or 7 in naturally occurring distributions (Woodcock, 1977). For $0 \leq K \leq 1$, fabric elements plot as girdles on the stereonet while they plot as clusters for $1 < K < \infty$. Eigenvalue ratios of clast fabric measurements from the Asbestos-Valcourt region are shown in Figure 3-3 and listed in Table 3-1. Figure 3-3 shows that A-axis fabric data plot mainly in the girdle/cluster transition zone (K = 1), with more than half of K values comprised between 0.5 and 1.0; C-axis data distinctly plot as clusters,

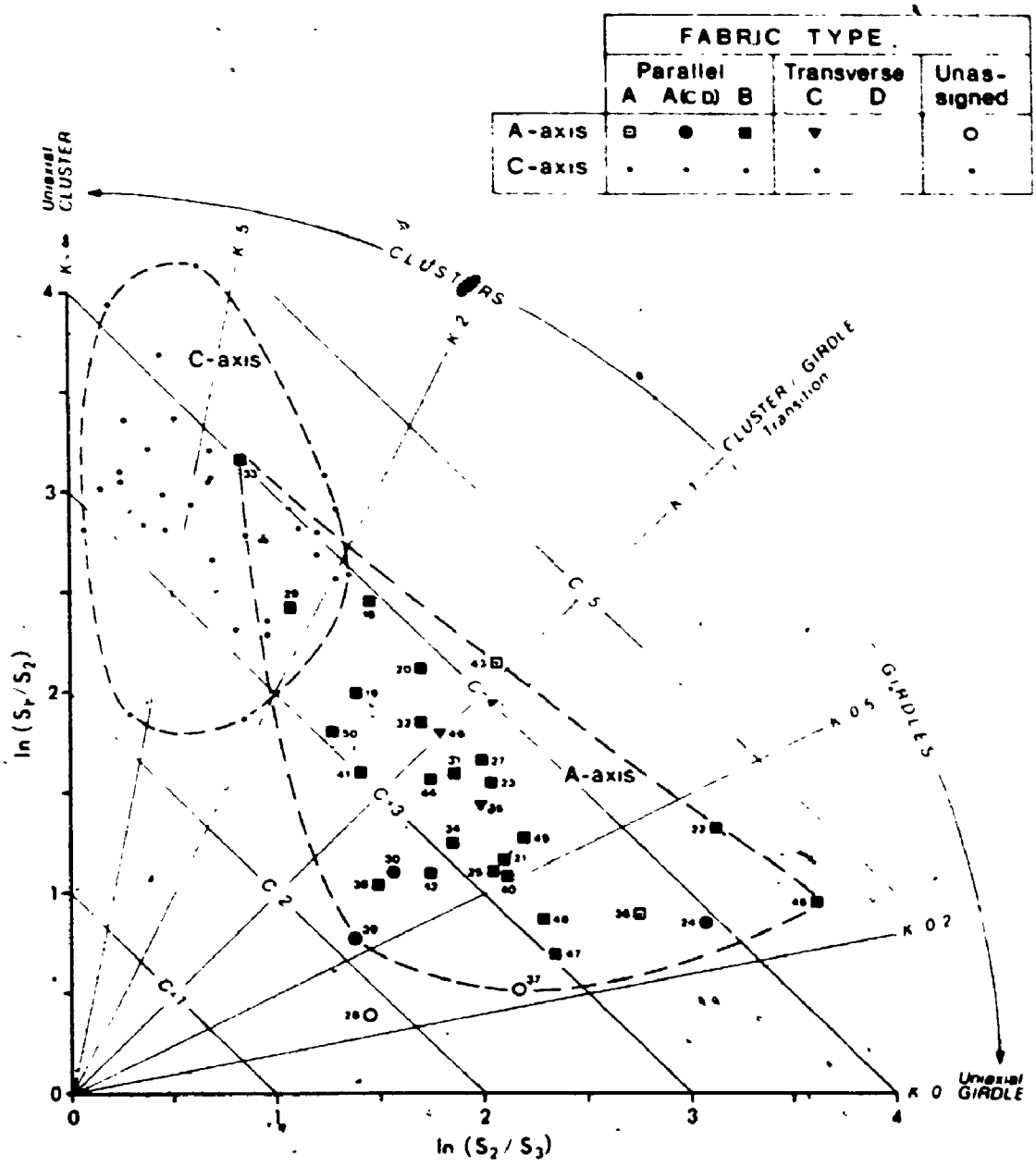

Figure 3-3 : Relationship between fabric strength (C) and fabric shape (K) for A-axis and C-axis data. C-axis fabrics plot as uniaxial clusters while A-axis fabrics plot in the cluster/girdle transition zone.

with K values most commonly above 2.0. Although fabric strength varies between about 2 and 5 for both A-axis and C-axis data, C-axis fabric strength is somewhat higher. The strength (C) of A-axis clast fabrics measured during this investigation is noticeably higher than that currently recorded in debris flows or flow tills (Stewart, 1982, Lawson, 1979).

Since the main objective of till clast fabric measurements in this study is to recognize ice-flow directions recorded in till, further statistical tests are required. Prior to this however, the orientation of V_1 is compared to contoured stereograms in order to check whether maximum eigenvectors fall within clast fabric modes or whether they fall between modes, as this may happen when fabric data are bimodal or multimodal. The only sample in which V_1 falls between A-axis fabric modes is FT-28, a sample which is rejected as a result of testing procedures outlined below.

Eigenvalue data were submitted to two additional tests prior to accepting preferred orientation as statistically significant:

1) As proposed by Anderson and Stephens (1972), S_1 must be sufficiently large to reject the null hypothesis that the data were randomly drawn from a uniform population. A table of significance points for S_1 is available in Anderson and Stephens (1972: table 1). The null hypothesis was rejected at the 99% confidence level for all samples (Table 3-1).

2) The estimate of precision parameter (k) must be greater than 3 (Andrews and Smith, 1970); for $0 < k < 3$, analysis ceases as the distribution under consideration is probably not spherically normal. Values of k, which may be calculated from S_1 values, were read from a table prepared by Watson (1966: table 2). Only two clast fabrics, FT-28 and FT-37, were rejected as a result of low k values for A-axis orientation data.

The next step consists of establishing a 95% zone of confidence about V_1 in order to verify:

- whether preferred A-axis orientation, $V_1(A)$, departs significantly from the horizontal (or from the depositional plane if this is known),

- whether preferred C-axis orientation, $V_1(C)$, departs significantly from the vertical (or from the pole to the depositional plane if this is known).

The zone of confidence is an ellipse whose major axis (ψ_2) is parallel to V_2 and whose minor axis (ψ_3) is parallel to V_3. By analogy with an equation given by Mark (1974), the angular distance (ψ) of the perimeter of the ellipse around V_1 is given by

$$\text{sine } (\psi j) = \left(\frac{\chi^2_\alpha}{k \cdot N \cdot (S_1 - S_j)} \right)^{\frac{1}{2}} \qquad (3\text{-}6)$$

where χ^2_α is the value of chi-square with two degrees of freedom at confidence level α(95%); the other variables were defined earlier. Computed values of ψ_2 and ψ_3 are listed in Table 3-1. Zones of confidence about $V_1(A)$ and $V_1(C)$ are then plotted on the stereonet in order to verify whether or not they intersect the reference plane or axis being tested; significant dip for preferred A-axis and C-axis orientation is acknowledged only when the zone of confidence does not intersect the horizontal and does not include the vertical, respectively. Results of the test are given in Table 3-1. The procedure is analogous to that suggested by Mark (1974), except that the dip of largest eigenvectors (S_1) is being tested directly rather than being tested on the unverified hypothesis that the smallest eigenvectors (S_3) of A-axis data provide a correct estimate of the preferred orientation of C-axis data.

The procedure outlined above is designed as an attempt to objectively distinguish transverse clast fabrics from parallel fabrics, hence to assign measured till clast fabrics to one of four fabric types which

commonly occur in lodgement and melt-out tills (Figure 3-4). Several studies of modern glacial sedimentation (Boulton, 1970b, 1971, 1976; Lindsay, 1970; Mills, 1977, 1978; Lawson, 1979) have indeed shown that:

1) clast A-axes may lie parallel or transverse to the direction of ice-flow; in parallel fabrics measured in basal ice or in subglacially deposited tills (basal melt-out and lodgement tills), clast A-axes commonly show preferred upglacier plunge (fabric type B); however clast A-axes may lie more-or-less subhorizontally in both parallel (fabric type A) and transverse (fabric type C and D) fabrics;

2) clast A/B planes (normals to C-axes) in basal ice and in subglacially deposited tills commonly show significant upglacier imbrication whether A-axes lie parallel (fabric type B) or transverse (fabric type C) to the direction of ice-flow.

Till clast fabrics measured during this investigation were assigned to fabric types A, B, C or D on the basis of internal fabric characteristics (Figure 3-4), and directions of former ice-flow were inferred only after fabric types have been determined:

Types A and D: In fabric types A and D, the zone of confidence about $V_1(A)$ intersects the horizontal plane and the zone of confidence about $V_1(C)$ does not depart from the vertical; type A fabrics cannot be usually distinguished from type D fabrics on the basis of internal characteristics. Yet, mainly because of greater C-axis orientation strength, the vertical sometimes falls outside of the zone of confidence about $V_1(C)$; if $V_1(A)$ and $V_1(C)$ lie in subparallel directions, fabric type A is inferred. Five type A fabrics were recognized.

Type B: In fabric type B, the zone of confidence about $V_1(A)$ does not intersect the horizontal plane and the zone of confidence about $V_1(C)$ departs from the vertical; $V_1(A)$ and $V_1(C)$ lie in

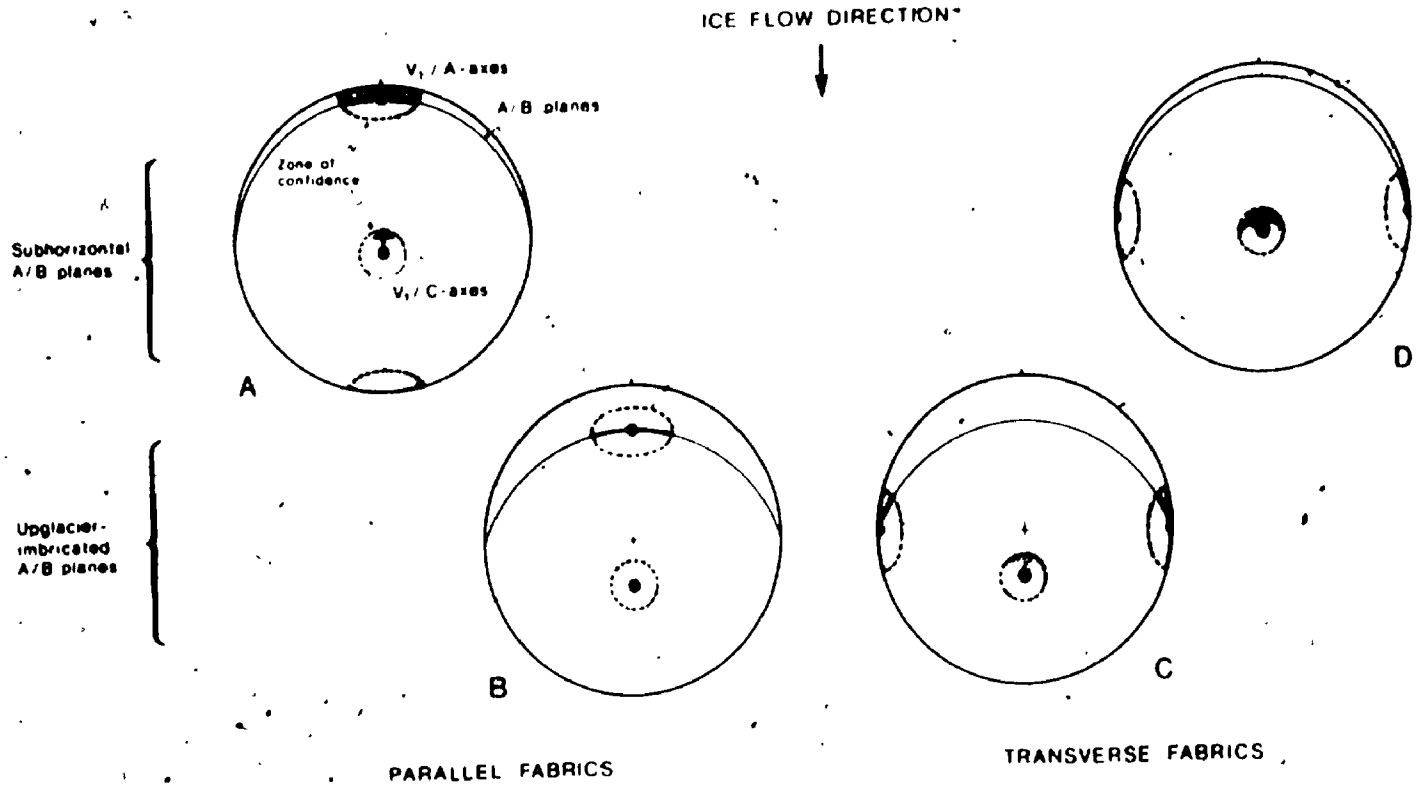

Figure 3-4 : Internal characteristics of till clast fabric types and relationships with inferred direction of ice movement. Fabric types A and B show preferred A-axis orientation parallel to ice movement, but only type B shows preferred upglacier imbrication (A/B planes). Fabric types C and D show preferred A-axis orientation transverse to ice movement, but only type C shows preferred upglacier imbrication (See text).

Table 3-1: Summary of statistics and interpretation of clast fabric analyses

Sample Number	Axis (N)	Maximum eigenvector (V_1)							Fabric shape parameters		Fabric type****	Inferred ice-flow direction
						Zone of confidence (95%)						
		Azimuth	Plunge	R_o***	k***	ψ_2	ψ_3	-DIP****	C	K		
FT-16	A (50)	345°	9°	+++	11.2	6.5°	6.3°	Yes(H)	3.94	1.68	B	165°
	C (38)	161°	81°	+++	12.1	7.1°	6.9°	Yes(V)	3.95	1.89		
FT-19	A (50)	347°	16°	+++	7.6	8.4°	8.0°	Yes(H)	3.37	1.43	B	167°
	C (47)	150°	74°	+++	12.6	6.2°	6.2°	Yes(V)	3.17	20.15		
FT-20	A (50)	343°	10°	+++	8.8	7.6°	7.2°	Yes(H)	3.83	1.25	B	163°
	C (41)	155°	80°	+++	20.0	5.1°	5.0°	Yes(V)	4.13	8.31		
FT-21	A (50)	332°	18°	+++	4.6	13.0°	11.0°	Yes(H)	3.27	0.56	B	152°
	C (33)	140°	74°	+++	13.0	7.3°	7.2°	Yes(V)	3.63	3.24		
FT-22	A (50)	170°	11°	+++	5.4	11.3°	9.7°	Yes(H)	4.45	0.42	B	350°
	C (38)	357°	80°	+++	18.3	5.6°	5.5°	Yes(V)	3.89	4.65		
FT-23	A (50)	162°	12°	+++	6.0	10.2°	9.2°	Yes(H)	3.58	0.77	B	342°
	C (37)	350°	79°	+++	13.0	6.9°	6.8°	Yes(V)	3.70	2.92		
FT-24	A (50)	116°	05°	+++	3.8	16.3°	12.4°	No (H)	3.93	0.28	A, (D)	296°
	C (34)	006°	84°	+++	18.3	5.9°	5.8°	No (V)	4.33	2.46		
FT-25	A (50)	008°	16°	+++	4.6	13.6°	11.4°	Yes(H)	3.16	0.54	B	188°
	C (29)	168°	80°	+++	11.9	8.3°	8.0°	Yes(V)	3.86	1.98		
FT-27	A (50)	162°	20°	+++	6.4	9.6°	8.8°	Yes(H)	3.66	0.84	B	342°
	C (35)	352°	69°	+++	11.6	7.5°	7.5°	Yes(V)	3.19	7.75		
FT-28	A (25)	255°	09°	+++	2.1	53.6°	30.0°	No (H)	1.84	0.27	Rejected (k < 3)	
	C (20)	038°	86°	+++	5.5	16.6°	16.2°	No (V)	2.17	6.37		
FT-29	A (50)	357°	13°	+++	11.2	6.6°	6.4°	Yes(H)	3.49	2.27	B	177°
	C (38)	189°	79°	+++	13.0	6.8°	6.7°	Yes(V)	3.89	2.22		

Table 3-1 (continued)

FT-30	A (50)	097°	05°	+++	4.1	14.4°	12.1°	No (H)	2.66	0.70	A, (D)	277°
	C (30)	250°	88°	+++	11.9	8.0°	8.0°	No (V)	3.28	5.97		
FT-31	A (50)	345°	19°	+++	6.0	10.1°	9.2°	Yes(H)	3.45	0.86	B	165°
	C (35)	162°	72°	+++	13.8	6.8°	6.8°	Yes(V)	3.45	6.50		
FT-32	A (50)	347°	09°	+++	7.2	8.8°	8.2°	Yes(H)	3.55	1.09	B	167°
	C (43)	165°	81°	+++	13.2	6.4°	6.2°	Yes(V)	3.72	2.89		
FT-33	A (50)	344°	13°	+++	18.3	4.9°	4.8°	Yes(H)	3.99	3.78	B	164°
	C (38)	142°	78°	+++	20.0	5.3°	5.3°	Yes(V)	3.90	6.43		
FT-34	A (50)	352°	21°	+++	4.8	12.5°	10.8°	Yes(H)	3.10	0.68	B	172°
	C (34)	160°	69°	+++	10.4	8.2°	8.1°	Yes(V)	2.88	37.56		
FT-35	A (50)	038°	05°	+++	5.5	11.0°	9.7°	No (H)	3.43	0.22	C	128°
	C (36)	167°	79°	+++	14.2	6.7°	6.5°	Yes(V)	4.00	2.30		
FT-36	A (50)	356°	11°	+++	3.9	15.9°	12.3°	No (H)	3.64	0.33	A	176°
	C (31)	161°	81°	+++	18.5	6.1°	6.1°	Yes(V)	3.66	12.36		
FT-37	A (50)	010°	12°	+++	2.7	25.2°	16.3°	No (H)	2.69	0.24	Rejected (k < 3)	
	C (36)	191°	79°	+++	8.8	8.9°	8.6°	Yes(V)	3.25	2.35		
FT-38	A (50)	015°	16°	+++	3.9	15.1°	12.6°	Yes(H)	2.53	0.69	B	195°
	C (35)	231°	75°	+++	8.7	9.1°	8.8°	Yes(V)	3.12	2.84		
FT-39	A (50)	359°	05°	+++	3.1	19.7°	15.2°	No (H)	2.15	0.56	A, (C)	179°
	C (48)	222°	78°	+++	6.3	10.7°	10.2°	Yes(V)	2.72	2.19		
FT-40	A (50)	010°	14°	+++	4.3	14.0°	11.6°	Yes(H)	3.19	0.51	B	190°
	C (37)	198°	77°	+++	16.3	6.0°	6.0°	Yes(V)	3.58	8.52		
FT-41	A (50)	326°	23°	+++	6.3	9.9°	9.1°	Yes(H)	3.02	1.14	B	146°
	C (32)	156°	69°	+++	9.4	9.1°	8.8°	Yes(V)	3.33	2.44		
FT-42	A (50)	070°	19°	+++	4.2	14.1°	11.8°	Yes(H)	2.84	0.63	B	250°
	C (44)	240°	71°	+++	13.8	6.1°	6.0°	Yes(V)	3.53	4.90		

Table 3-I (continued)

PT-43	A (50)	305°	06°	+++	9.4	7.3°	6.9°	No (H)	4.22	1.04	A	125°
	C (40)	161°	83°	+++	16.0	5.9°	5.8°	Yes(V)	3.77	4.40		
PT-44	A (50)	207°	12°	+++	5.9	10.3°	9.3°	Yes(H)	3.30	0.90	B	27°
	C (34)	009°	75°	+++	14.4	6.8°	6.7°	Yes(V)	3.94	2.52		
PT-45	A (50)	069°	13°	+++	4.2	14.7°	11.6°	Yes(H)	4.56	0.27	B	249°
	C (40)	249°	77°	+++	20.0	5.1°	5.0°	Yes(V)	4.75	6.57		
PT-46	A (50)	255°	03°	+++	7.0	9.0°	8.3°	No (H)	3.60	1.01	C	165°
	C (38)	158°	79°	+++	20.0	5.2°	5.2°	Yes(V)	4.14	19.54		
PT-47	A (50)	352°	17°	+++	3.3	19.4°	14.0°	Yes(H)	3.05	0.30	B	172°
	C (46)	173°	74°	+++	14.2	5.8°	5.8°	Yes(V)	3.45	12.49		
PT-48	A (50)	047°	19°	+++	3.7	16.6°	12.8°	Yes(H)	3.15	0.38	B	227°
	C (29)	267°	68°	+++	14.3	8.5°	8.3°	Yes(V)	3.36	3.80		
PT-49	A (50)	126°	21°	+++	5.0	12.1°	10.4°	Yes(H)	3.46	0.58	B	306°
	C (39)	294°	70°	+++	13.7	6.5°	6.4°	Yes(V)	3.31	12.02		
PT-50	A (40)	318°	24°	+++	6.5	10.5°	9.8°	Yes(H)	3.08	1.43	B	138°
	C (25)	144°	66°	+++	15.6	7.6°	7.5°	Yes(V)	3.73	4.51		

*: Hypothesis of isotropicity for preferred orientation (V_1) rejected at 99% confidence level (+++); 95% (++); 90% and lower (+).

**: If $k \geq 3$, distribution is spherically normal; if $k < 3$, distribution is probably not spherically normal and fabric is thus rejected.

***: Zone of confidence about V_1 does (Yes) or does not (No) depart from the horizontal (H) or the vertical (V) for A-axis or C-axis data, respectively.

****: Parallel (A or B) or transverse (C or D) fabrics according to internal fabric character (see Figure 3-4); when an alternative fabric type is also possible, the first of two letters indicates the most probable type, given the geological context.

subparallel directions. Type B fabrics are the most common of measured till clast fabrics (23 out of 32).

Type C: In fabric type C, the zone of confidence about $V_1(A)$ intersects the horizontal plane but the zone of confidence about $V_1(C)$ departs from the vertical; the direction of $V_1(C)$ is more-or-less perpendicular to that of $V_1(A)$. Only two type C fabrics have been recognized.

3.2.7 Organic matter content

Organic matter content of the <0.063 mm fraction was measured in a series of samples from the Rivière Landry section (MP-79-16). The analytical procedure (modified Walkley-Black method) described in McKeague (1978) was carried out on duplicate sample sets of 1.0 and 1.5 g; results of the two sets of measurements were almost identical and were thus averaged (Table A-4).

3.2.8 Extraction and identification of microfossils

Microfossils (foraminifers and ostracodes) were extracted from a series of 18 samples collected in the Rivière Landry section (MP-79-16). About 75-150 g of sediment, usually 100 g, were soaked overnight in a dispersing solution (sodium pyrophosphate, N/2.5) and washed through a 200 mesh sieve (0.074 mm). Ostracode valves were hand-picked from the sediment. Foraminifer tests were separated by flotation in carbon tetrachloride; sediment was re-examined after flotation and remaining tests were hand-picked. Samples typically yielded between 0 and 10 microfossil specimens; one sample contained about 150 ostracode valves but no foraminiferal tests.

Ostracodes were identified after photographic plates prepared by Cronin (1977a: plates III and IV). Foraminifers were identified only to genus level. Plates prepared by Cronin (1977a: plates I and II; 1979b: plates 1 through 6) were used during examination of foraminiferal tests.

CHAPTER 4

LATE PLEISTOCENE GLACIAL UNITS AND INTERCALATED NON-GLACIAL SEDIMENTS

4.1 Introduction

Investigation of stratigraphic sections of the Asbestos-Valcourt region reveals that glacial units are a prominent component of the Late Pleistocene stratigraphic record. Three superposed lithostratigraphic units underlie sediments associated with the last deglaciation (Late Wisconsinan). These three units, from top to bottom, are:

- Drift unit C, a unit which constitutes the regional "surface till" and which comprises a lodgement till, as its main constituent, and related glacigenic sediments;

- Unit B, a glaciolacustrine unit which includes muddy proximal deep-water sediments as well as sandy subaquatic outwash sediments;

- Drift unit A, a unit which includes the oldest sediments observed in the study area and which consists of lodgement till and related glacigenic sediments.

The locations of stratigraphic sections which will be discussed in the present chapter are shown in Figure 4-1. A more accurate location of these sections may be found in Figure 3-1 (in pocket).

Largely because of the fairly monotonous bedrock lithology, the physical characteristics (e.g., colour, texture, compactness) of equivalent facies of drift units A and C are similar and they are not useful for distinguishing the two units. Furthermore, several of the measured properties, such as grain-size parameters or heavy mineral and trace element content, show considerable overlap, even in a single section. The identification of units A and C in sections must therefore rely on

stratigraphic position, at least initially; this identification is then tested against appropriate area-specific or site-specific criteria. The most useful criteria were found to be those pertaining to provenance and to ice-flow direction, such as:

- nickel content of the silt-clay fraction of till,
- till clast fabric orientation,
- attitude of subtill glacitectonic deformations,
- till clast lithology.

Key stratigraphic relationships within and between sections are thus established not only on the basis of superposition but also on the basis of the characteristics of depositional (or erosional) events. Such a procedure is essential because stratigraphic units, particularly those underlying drift unit C (surface till), have only limited lateral continuity and thus cannot be visually traced from section to section. This procedure provides at least a partial check for the presence of significant stratigraphic hiatuses and pinch-outs and also for the possible repetition of units due to glaciotectonic overthrusting. In view of the fact that, in several of the investigated sections, stratigraphic units are exposed laterally over distances of only a few tens of meters, this procedure is seen as an essential precaution. Lastly, it must be added that the apparent absence of dateable organic material within drift units A and C as well as within the intervening glaciolacustrine sediments (unit B) precludes utilizing conventional geochronologic methods (such as radiocarbon or amino-acid dating) as stratigraphic tools.

The procedure outlined above indicates that distinctive provenance and ice-flow patterns are associated with each of the two drift units; this in turn suggests that only two main drift units are present in sections of the Asbestos-Valcourt region. When glacial or non-glacial sediments observed in sections are assigned to units A, B or C, it is done on the basis of inferred geologic events (which are similar in scope to stadials and interstadials) rather than on the basis of strictly lithostratigraphic criteria. There will thus be no attempt, at the

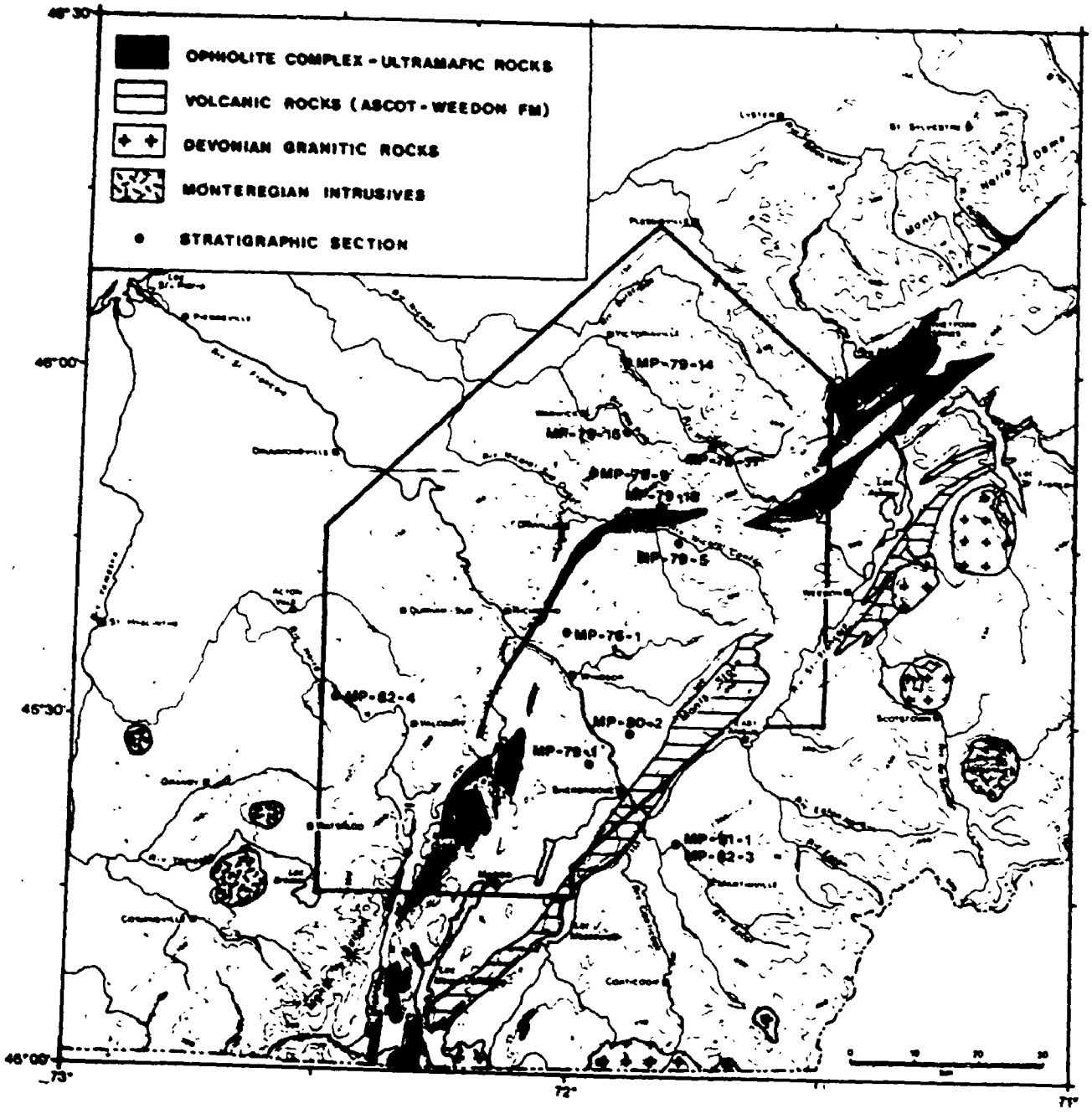

Figure 4-1: Location of stratigraphic sections described in this chapter. Also shown are the outcrop patterns of distinctive bedrock units and the location of the Ascot River sections (MP-81-1 and MP-82-3).

present time, to propose a formal lithostratigraphic nomenclature; not only would this not really serve the primary objectives of this thesis, but it would also contribute to undue lengthening of this text.

As will be shown in this chapter, provenance and ice-flow patterns for drift units A and C differ significantly from those which had been previously suggested or which could be deduced from work carried out in neighboring regions (McDonald, 1967a; McDonald and Shilts, 1971; Lortie, 1976; Shilts, 1981).

4.2 Drift unit A

Drift unit A is the oldest sedimentary unit exposed in four sections (MP-79-18, MP-79-9, MP-76-1 and MP-79-1). All four sections are located within the Outer Appalachian Uplands. A probable equivalent unit is exposed in a fifth section (MP-82-4) located witnin the Appalachian Piedmont. The possibility that Quaternary sediments older than drift unit A occur in the study area should not be ruled out; this investigation can only report a lack of direct evidence for earlier units. Furthermore, it must be kept in mind that the basal contact of drift unit A with bedrock is exposed in only two of these five sections.

4.2.1 Norbestos section (MP-79-18)

The Norbestos section is located on the north side of an abandoned open-pit asbestos mine. Except for a 500 to 600 m segment at the west end of the narrow east-trending pit, steep bedrock walls extend up to ground surface level. In the west half of the pit, the bedrock surface plunges westward to a depth of about 30 m, which is about the level reached by water now filling much of the pit, and is overlain by a thick sequence of Quaternary sediments. Except for a few places where small brooks flowing into the pit keep the section relatively clean, the sediments are concealed under a substantial slump cover.

Because the better exposed sediments showed considerable lateral variability in thickness and facies, three subsections (A, B and C) were measured and investigated in detail. Stratigraphic logs, along with clast fabric and other structural data, are shown in Figure 4-2. The Norbestos section is a most significant component of the regional stratigraphic record because:

1) essential characteristics of the three main regional units, particularly those of drift unit A and of unit B, can be established quite clearly;

2) the ENE-trending belt of ultramafic rocks (Asbestos ophiolite complex) which lies a few tens of meters south of the section provides an excellent opportunity to obtain unequivocal provenance data for both drift units.

The lower unit exposed in all three subsections is a very compact, matrix-dominated, fissile, gray, calcareous diamicton; it is interpreted, by its structures and fabric, to be a subglacial till, dominantly of lodgement origin. It is unoxidized and typical for the region. Pebble content, as indicated by the weight of the +2.0 mm fraction of 13 samples, is quite variable; it ranges from 7% to 46%, values of about 25% being most common. Boulders tend to be concentrated at discrete levels; such "boulder zones" occur at similar depths in subsections B and C (13.6 m and 11.5 m, respectively), but they do not appear to form true boulder pavements. The till shows distinct textural layering, similar to that reported by Shilts (1978) in the neighboring Lac-Mégantic region. Numerous shear planes are visible in exposures where the till is "etched out" by running water, as in subsection C; here, it is obvious that shearing and textural layering are coeval and were produced during subglacial deposition.

The till matrix (-2.0 mm) has an average content of 42% sand, 43% silt and 15% clay; its average grain size mean (M_z) and sorting (σ_I) are 4.8ϕ and 3.1ϕ, respectively. Observed range of granulometric data along with means and standard deviations are given in Table 4-1. As the ternary diagram (Figure 4-3) shows, the grain-size composition of drift unit A is quite variable, especially when compared to drift unit C.

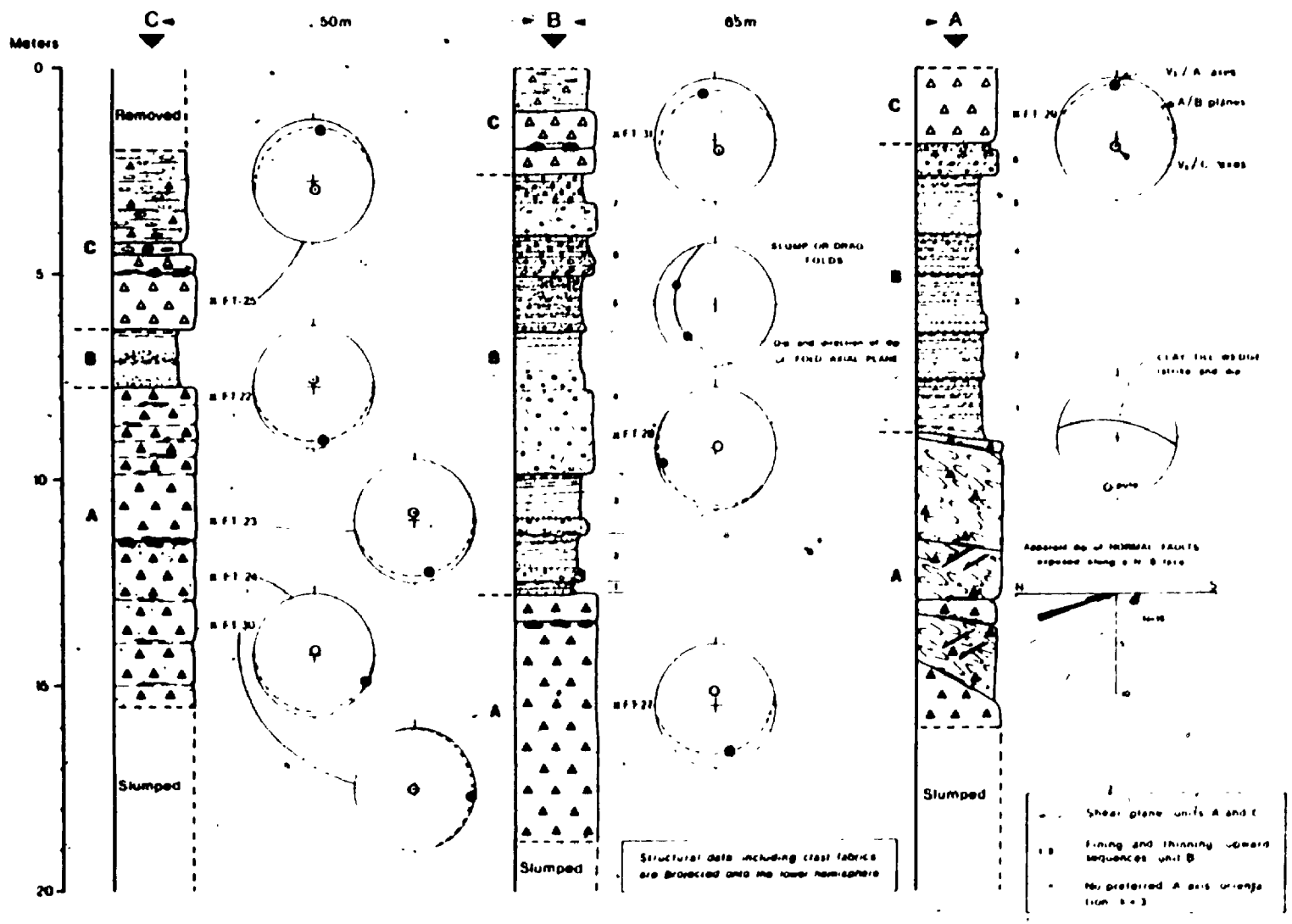

Figure 4-2 : Stratigraphic logs of subsections A, B and C at the Norbestos locality (MP-79-18), showing till clast fabrics and other structural data. (See legend in Figure 4-12)

Table 4-1: Comparative granulometric, heavy mineral, trace element and carbonate data for drift units A and C, Norbestos section

	DRIFT UNIT A (n=13)			DRIFT UNIT C (n=12)		
	$\bar{X}$	S.D.	Range	$\bar{X}$	S.D.	Range
GRAIN SIZE (-2.0 mm)						
$M_z(\varphi)$	4.8	0.5	3.9-5.8	4.0	0.4	3.6-4.7
$\sigma_I(\varphi)$	3.1	0.3	2.7-3.7	3.0	0.2	2.7-3.4
Sand (%)	42	6	30-52	55	6	45-61
Silt (%)	43	5	32-48	34	3	29-41
Clay (%)	15	5	8-24	11	3	8-18
HEAVY MINERALS (0.250-0.125 mm)						
% heavies/fine sand	5.7	0.5	5.0-6.6	4.7	0.7	4.1-6.30
% magnetic/heavies	7.4	1.2	5.9-10.1	9.4	1.4	6.3-11.0
TRACE ELEMENTS (-0.063 mm)						
Ni (ppm)	50	26	20-87	33	5	26-41
Cr (ppm)	24	8	14-38	18	4	14-26
*Clay ratio (%)	26	7	14-39	25	4	22-34
CARBONATES (-0.063 mm)						
Dolomite (%)	2	1	1-3	--	--	**0-2
Calcite (%)	4	1	2-6	--	--	0-5
Total (%)	6	3	3-9	--	--	0-7

* Calculated as $\left(\frac{\%\text{ clay}}{\%\text{clay}+\%\text{silt}}\right) \cdot 100$

** Only 3 samples were not completely leached of carbonates.

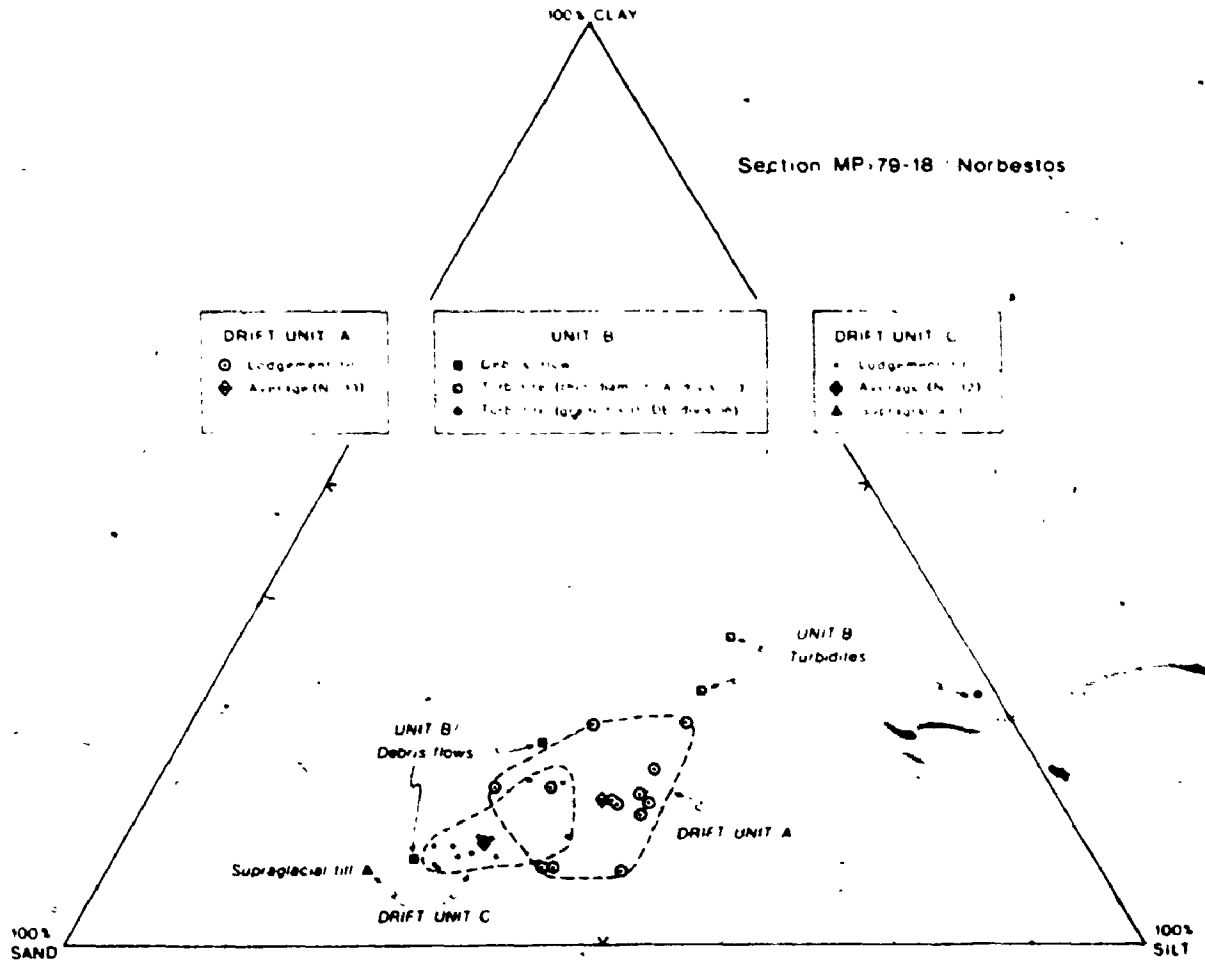

Figure 4-3 : Textural ternary diagram, Norbestos section.

This greater variability is largely due to an increased clay content in the upper part of the till (Figure 4-4: samples C-2, C-10, C-3 and B-4). This increase is interpreted as resulting from subglacial incorporation of fine-grained glaciolacustrine sediments by ice that readvanced toward north during the closing stages of this glacial episode.

Strong evidence to support this interpretation comes from a 6 m-thick unit of deformation till which overlies "normal" lodgement till in subsection A and is absent in subsections B and C (Figure 4-2). The deformation till consists of stacked thrust-slices of glaciolacustrine muds, which greatly resemble the overlying ones (unit B). Major shear planes dipping toward south are clearly visible between thrust slices (Plate 4-1A). Within the deformed muds, there are three additional sets of features which indicate not only a glacitectonic origin for the unit but also the general northward direction of the subglacial stresses. These are:

1) limbs and hinges of overturned and recumbent folds (metric to submetric amplitude) are strongly sheared toward north (upslope) while fold axial planes dip toward south (Plate 4-1B);

2) synthetic sets of small low-angle normal faults with northward throw and dip are interpreted as shear faults (Plate 4-1A);

3) 30 to 90 cm-thick lodgement till beds which occur between some of the thrust slices have sharp, erosional upper and lower contacts; the uppermost one contains a clay-till wedge which strikes N 100° and dips about 75° toward north (Figure 4-2).

Northward-flowing ice is further corroborated by clast fabrics measured in the upper part of drift unit A in adjacent subsections. Three type B fabrics (FT-22, FT-23 and FT-27; see section 3.2.6 and Table 3-1) show a significant A-axis plunge toward south; preferred A-axis orientations are N 170°, N 162° and N 162°, respectively. Because of the strong imbrication shown by A/B planes and because of the

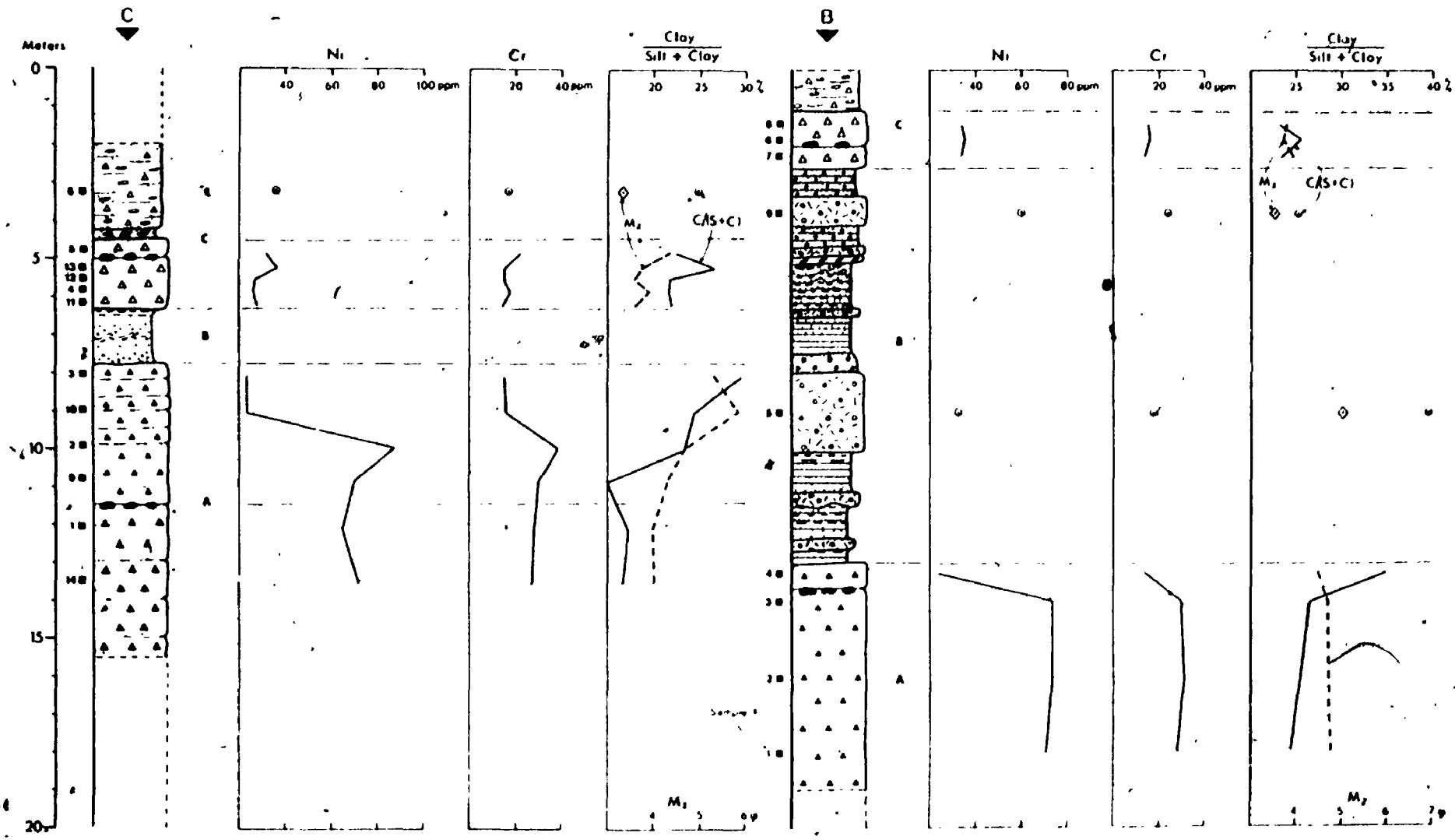

Figure 4-4 : Vertical variations of Ni and Cr contents in the silt-clay fraction (<0.063 mm) of tills and diamictons of the Norbestos section (subsections B and C). Variations of mean grain size (M_z) and of clay content of the silt-clay fraction are also shown. (See legend in Figure 4-12)

Plate 4-1

A) Stacked thrust-slices of the deformation till unit (drift unit A), Norbestos section (MP-79-18A). Thrust slices #1, #2 and #3 are bounded by south-dipping thrust faults (φ). Minor, north-dipping, low-angle normal faults which occur in thrust slice #2 are interpreted as shear faults that were also produced by northward-flowing ice. Photographed at a depth of 14 m. Intervals on staff are 30 cm-long.

B) Sheared limb and hinges of recumbent fold in deformation till unit (drift unit A), Norbestos section (MP-79-18A). The head of the hammer (33 cm-long) rests along the sheared upper limb of a syncline whose axial plane dips south (right). Photographed at a depth of 11 m.

Arrows indicate direction of subglacial shear (toward north).

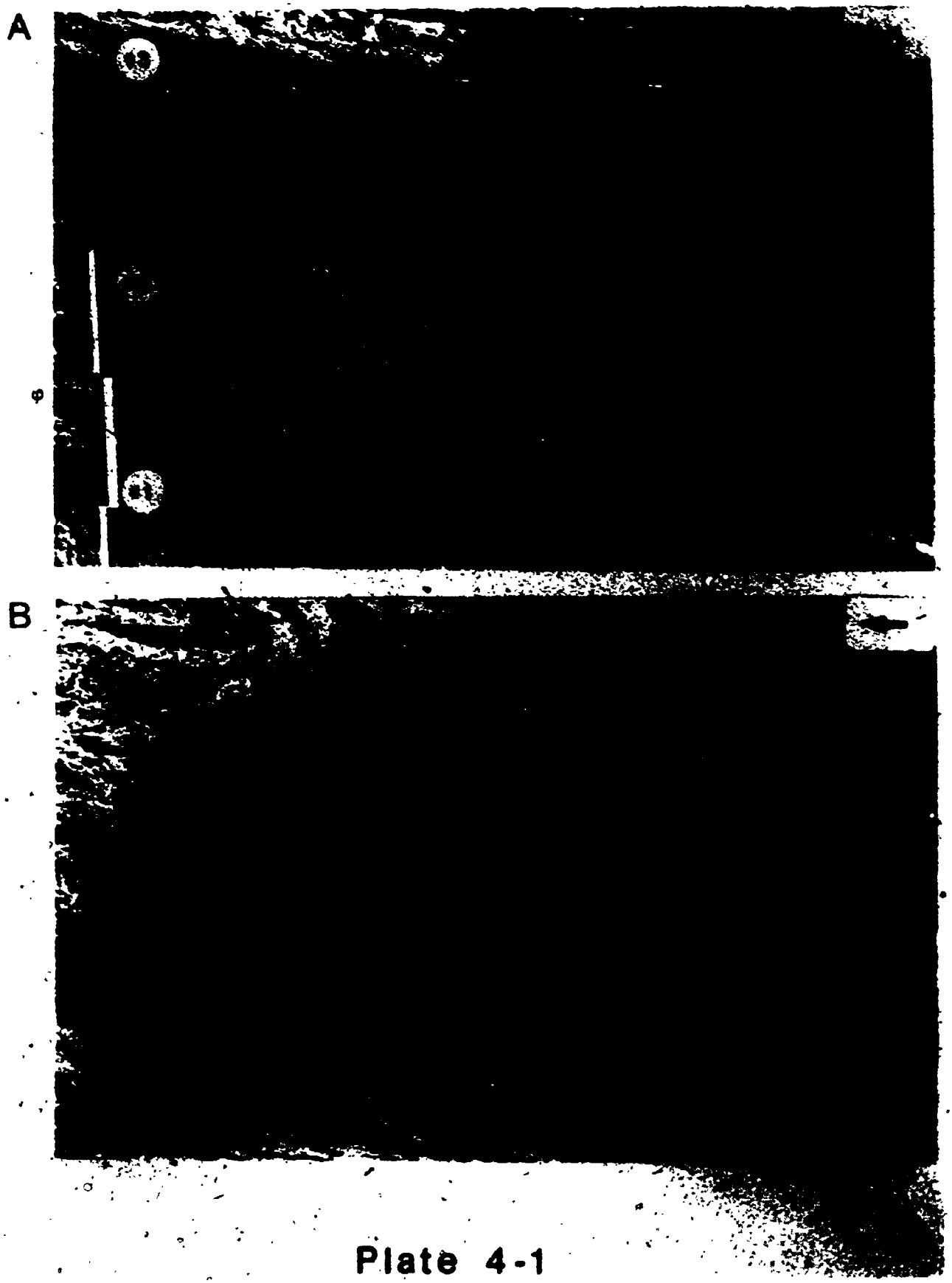

Plate 4-1

parallel orientation of the largest eigenvectors (V_1) for A-axis and C-axis data (Figure 4-2), there is no reason to believe that these may be transverse fabrics. Clast fabric data thus provide independent evidence of northward ice-flow during at least the closing stages of this glacial phase.

Clast fabrics were also measured in the lower part of drift unit A in subsection C (Figure 4-2: FT-24 and FT-30). FT-24 and FT-30 show strong preferred A-axis orientation plunging at shallow angles (5° in both cases) toward N 116° and N 097°, respectively. Because clast A/B planes lie close to the horizontal, there is a possibility that FT-24 and FT-30 are transverse fabrics. However, the alternate interpretation that both are parallel fabrics indicating westward ice-flow is preferred for the following reasons:

1) minute crag-and-tail striations trending N 265°, which cut across larger ones trending N 135°, are present on a bedrock outcrop less than 50 m east of subsection A; this indicates that there was at least one westward ice-flow episode in the immediate vicinity of the section;

2) westward-trending striations are common on outcrops of the Asbestos region (Lamarche, 1974; Lortie, 1976; see also Figure 3-1) and it is clear that at least some of them, perhaps all of them, are older than northward-trending striations (Plate 4-2A);

3) reports of clast fabrics measured in basal tills (lodgement or melt-out) deposited by modern glaciers (Boulton, 1970b, 1971; Lawson, 1979) indicate that the vast majority are parallel fabrics;

Although most compositional attributes of drift units A and C show much overlap (Table 4-1), the Ni and Cr content of the silt-clay fraction of till shows vertical variations that permit a clear distinction between the two units (Figure 4-4). Ni content is highest (65 to 87

Plate 4-2

A) Striations trending N 020° at the bottom of a westward-trending (N 280°) groove, south of Les Trois Lacs, near Asbestos. The pencil (14.5 cm-long), at the bottom of this large groove, points toward west (right). Abundant crag-and-tail striations were observed within this groove, and elsewhere on this group of outcrops (meta-volcanics). A few feet from this site, small crag-and-tail striations which trend in the same direction as simple striae within the groove suggest that the westward ice movement was followed by a northward ice-flow episode. Elsewhere on this group of outcrops, a few simple striae, which trend N 165°, cut across glacialy polished surfaces that were produced by the northward ice-flow event; however, the flow direction of the glacier which produced the latter striae cannot be established on the basis of glacial striations at this site.

B) Slightly oxidized (?) till of drift unit A overlain directly by non-oxidized till of drift unit C, Chemin des Ecossais section. Hammer head indicates the contact between the two till sheets. Hammer is 33 cm-long.

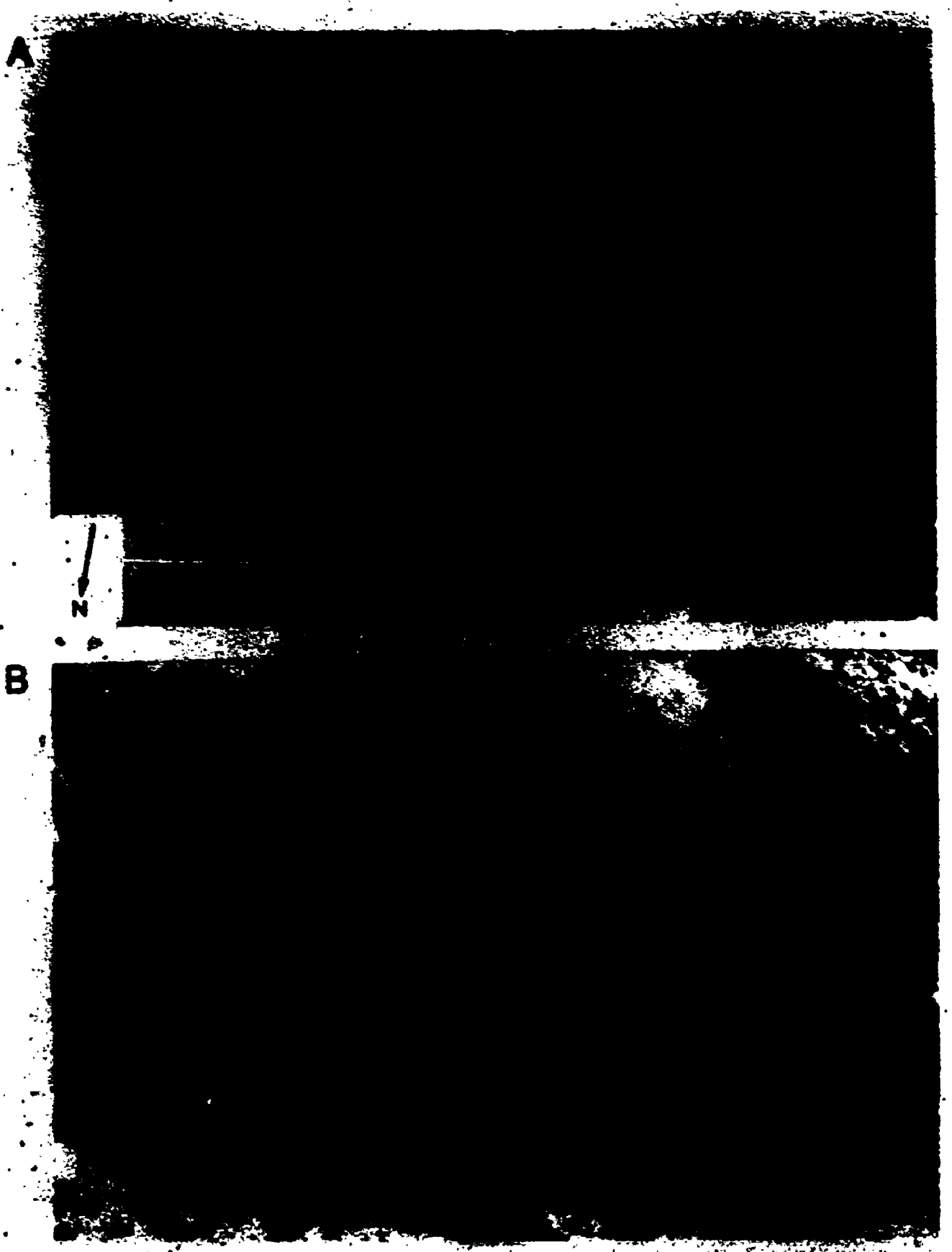

Plate 4-2

ppm) in the main part of drift unit A and drops to low values (23 - 24 ppm) in the top meter of the unit. Ni content in till of drift unit C is uniformly low (26 to 41 ppm), but slightly higher than at the top of drift unit A. As expected (Shilts, 1973a, 1975, 1978; Parent, 1978), variations of the Cr content show trends similar to those of the Ni content.

Since the ENE-trending ophiolite belt lies just south of the section, the high Ni and Cr content in the main part of drift unit A constitutes a clear indication that ultramafic debris were transported by ice advancing toward west or north during glacial phase A. Observed Ni and Cr values are not highly anomalous, but still well above background values (20 to 40 ppm Ni, and 10 to 20 ppm Cr). The drop of Ni and Cr values at the top of the unit is interpreted as resulting from the incorporation of ultramafic-poor glaciolacustrine muds into the basal load of glacier ice that readvanced toward north during the latter part of glacial phase A. These results are thus consistent with conclusions drawn from deformation structures, clast fabrics and granulometric trends.

The conclusions on provenance and ice-flow directions for drift unit A are also in keeping with field observations of clast lithology. Several ultramafic clasts can be observed in tills of drift unit A while Precambrian clasts derived from Shield terrain (northwest of study area) are almost absent. The reverse is true for drift unit C: Precambrian clasts are common and ultramafic clasts are rare.

In order to obtain a quantitative assessment of field observations on clast lithology, pebble counts were done on available bulk till samples (Table 4-2). Because the provenance of most other lithological types is equivocal at this locality, only distinctive indicator pebbles (Precambrian clasts and ultramafic clasts) were sought for counting. Samples consist of pebbles whose width (B-axis) ranges between 8.0 and 64.0 mm. Because the samples were extracted by sieving and because of the large sample size for each drift unit, totals shown in Table 4-2 can be safely considered as unbiased. Of the 306 pebbles extracted from

Table 4-2: Indicator pebbles (8.0 - 64.0 mm) in lithostratigraphic units of the Norbestos section

STRATIGRAPHIC UNIT	LITHOLOGY	SUBSECTION C N	SUBSECTION C (%)	SUBSECTION B N	SUBSECTION B (%)	SUBSECTION A N	SUBSECTION A (%)	TOTAL N	TOTAL (%)
DRIFT UNIT C (13 samples)	Ultramafic	0	(0)	0	(0)	1	(1)	1	(0)
	Precambrian	5	(2)	2	(2)	1	(1)	8	(2)
	Undifferentiated	227	(98)	88	(98)	71	(97)	386	(98)
	TOTAL	232	(100)	90	(100)	73	(99)	395	(100)
DRIFT UNIT A (9 samples)	Ultramafic	1	(1)	1	(1)	-	-	2	(1)
	Precambrian	0	(0)	0	(0)	-	-	0	(0)
	Undifferentiated	184	(99)	120	(99)	-	-	304	(99)
	TOTAL	185	(100)	121	(100)	(samples unavailable)		306	(100)
UNIT B Diamictons (3 samples)	Ultramafic	-	-	2	(2)	0	-	2	(2)
	Precambrian	-	-	2	(2)	0	-	2	(2)
	Undifferentiated	-	-	81	(95)	1	-	82	(95)
	TOTAL	(no pebbles)		85	(99)	1	-	86	(99)

drift unit A samples, none were Precambrian clasts and two (1%) were ultramafic clasts. These results, particularly when compared to those for drift unit C (2% Precambrian clasts), are an indication that very few Precambrian clasts were transported as far as the Norbestos section during glacial phase A. Precambrian clasts which are occasionally found in drift unit A may be reworked from older glacial sediments or may have been transported southeastward earlier during glacial phase A.

4.2.2 Rivière des Rosiers section (MP-79-9)

The Rivière des Rosiers section is located close to the outer margin of the Outer Appalachian Uplands, about 10 km northwest of the Norbestos section. For a distance of about of 4 km, the river cuts through thick Quaternary sediments and is entrenched to a depth of 20 to 30 m. Several sections occur along river banks but most are obscured by slumped sediments; the section selected for study (Figures 4-5 and 4-6) was the best exposure at the time of fieldwork.

In section MP-79-9, there are two superposed till sheets (drift units A and C) which ostensibly differ in colour, texture and stoniness. Lodgement till of drift unit C directly overlies stratified diamicton deposited at the close of glacial phase A. Evidence for a glaciolacustrine event (unit B) prior to glacial phase C comes from lenses and clasts of laminated silt and clay that are included in lodgement till of drift unit C. Till of drift unit C is in turn overlain by at least 1 m of graded silt and clay rhythmites deposited in a proglacial lake during the last deglaciation.

The lower 3 m of drift unit A consist of very compact, fissile, calcareous, rather pebbly, matrix-supported diamicton interpreted as lodgement till that probably extends down to bedrock (Caldwell Group: gray phyllite with abundant veins and pods of quartz). At a depth of 9.8 m, there is a sharp color change: below, the till is gray, fresh and strongly calcareous (about 15% total carbonates; see Figure 4-5) while it is pale olive (5Y 6/2.5 dry) and slightly oxidized above. The oxidized zone extends upward into and includes the overlying stratified

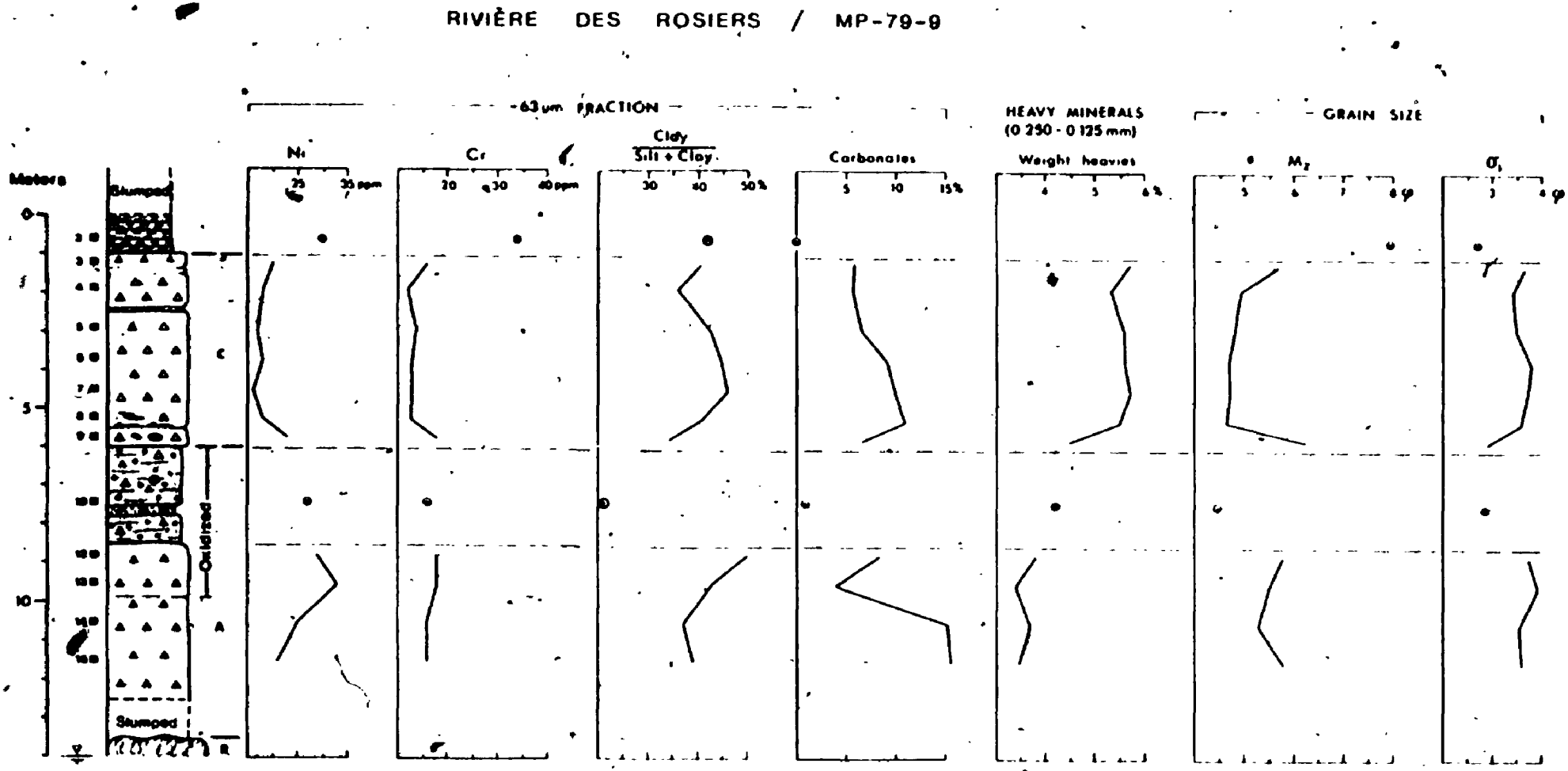

Figure 4-5 : Stratigraphic log and vertical variations of grain-size and compositional data, Rivière des Rosiers section (MP-79-9). (See legend in Figure 4-12).

diamicton. The olive lodgement till still contains between 4.0 and 8.3% carbonates (silt-clay fraction) and thus seems only moderately leached and oxidized. Colour changes and HCl- effervescence variations suggest that leaching and oxidation are less intense in the upper 1.5 m of the stratified diamicton than in the lower 1.1 m: sediment is olive and slightly calcareous in the upper part while it is buff and non-calcareous in the lower part. The fact that oxidation seems more intense in the sandy gravel bed (at 7.5 m) and in the underlying stratified diamicton suggests that it is caused by aeration of "modern" groundwater flowing through more permeable sediments that are underlain by an aquiclude (lodgement till). This interpretation is further supported by the fact that limestone pebbles are unweathered both in the stratified diamicton and in lodgement till.

Lodgement till of drift unit A shows some textural layering, particularly in the upper 1.2 m. As is shown in Figure 4-5, matrix grain size is rather homogeneous: M_z and σ_I average 5.6ϕ and 3.7ϕ respectively, which corresponds to an average content of 36% sand, 38% silt and 26% clay. Lodgement till matrix is finer-grained than that of a diamicton layer sampled in the overlying stratified diamicton (sample #10: 46% sand, 43% silt, 11% clay).

The stratified diamicton unit consists mainly of poorly sorted, pebbly, matrix-supported diamicton containing numerous layers and lenses of pebbly sand or sandy gravel. Because the unit was exposed laterally for only a few meters, it is difficult to tell whether or not some of the diamicton layers were emplaced as flow-tills, and whether the unit was deposited in a subaerial or a subaquatic environment. Observed features, together with the apparent lack of silt laminae within the unit, suggest that the stratified diamicton was deposited in a supraglacial environment. Particularly because of the presence of abundant gray and brownish sandstone pebbles which also abound in till of drift unit A but which are seemingly absent in till of drift unit C (see Table 4-3), clast lithology of the stratified unit resembles that of the underlying till sheet much more than that of the overlying one. Because of this and also because the overlying till sheet includes upsheared lenses and clasts of laminated silt and clay that are thought to lie stratigraphi-

cally above the stratified diamicton, the unit is assigned to drift unit A rather than to drift unit C.

Clast fabrics were measured at two levels within lodgement till of drift unit A (Figure 4-6). FT-45 is a type B fabric measured in the lower, gray subunit. Preferred A-axis orientation (V_1) plunges at a rather shallow but significant angle of 13° toward N 069°; clast A/B planes are also closely imbricated toward ENE. This suggests that glaciers advanced westward during at least part of glacial phase A.

FT-44 was sampled within the upper, olive lodgement till and it is also a type B fabric. Preferred A-axis orientation (V_1) plunges at an angle of 12° toward N 207° and clast A/B planes have a significant imbrication toward SSW. FT-44 thus suggests that ice-flow had shifted toward north during the latter part of glacial phase A.

Because compositional data obtained from till matrix analyses did not yield results which can be readily interpreted in terms of till provenance, the lithology of clast fabric samples was investigated. Results are listed in Table 4-3. Since samples include only elongated pebbles, some lithologic types are likely excluded from the samples; however, the resulting bias is expected to be evenly shared by all four samples. Because of the relatively small sample size (50 pebbles per sample), small variations between samples should not and will not be taken into account. As Table 4-3 reveals, the lithology of elongated pebbles in drift units A and C is nearly similar in some respects but differs significantly in others. Both units contain abundant pebbles of dark gray limestone and calcareous slate (#1) and phyllite and slate (#3-A) as well as occasional pebbles of red slate (#4). However, drift unit A also contains pebbles of sandstone (#2), quartz and quartz-veined phyllites (#3-B), graywacke (#3-C), volcanic rocks (#5) and muscovite schist (#6).

After due consideration is given to bedrock outcrop patterns in the vicinity of the section, two out of ten observed lithologic types can be used as till provenance indicators:

RIVIÈRE DES ROSIERS / MP-79-9

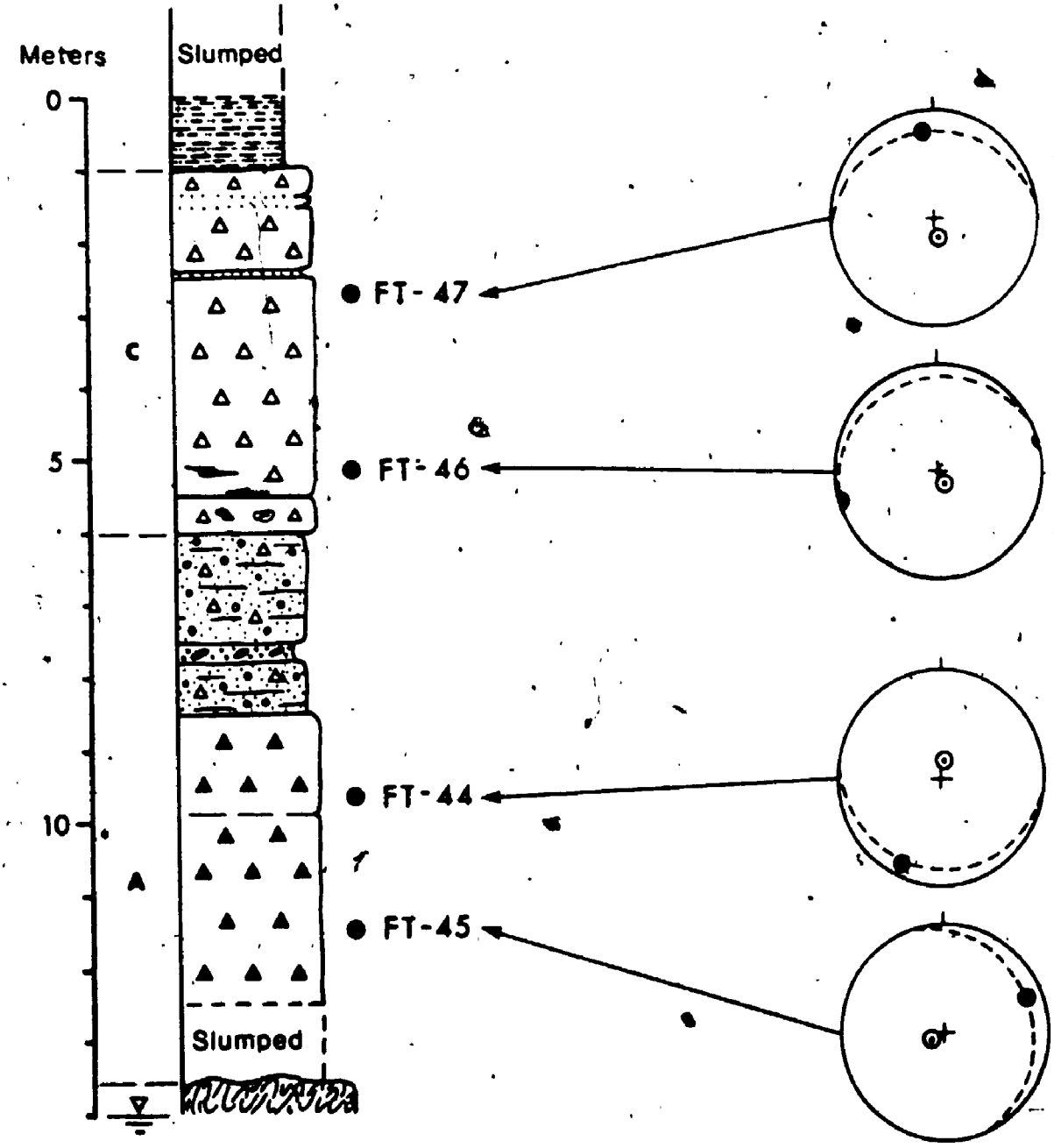

Figure 4-6 : Till clast fabrics from the Rivière des Rosiers section. (See legend in Figure 4-12)

Table 4-3: Lithology of elongated pebbles in tills of the Rivière des Rosiers section

	Drift Unit A (Gray till) FT-45	Drift Unit A (Olive till) FT-44	Drift Unit C Gray till FT-46	Drift Unit C Gray till FT-47
Indicators of northwest provenance (Bulstrode Fm)				
1-A) Dark gray limestone or calcareous slate	12	4	8	5
1-B) Gray slate with calcite veins	—	—	2	2
(SUBTOTAL)	(12)	(4)	(10)	(7)
Indicators of southeast provenance				
2-A) Brownish sandstone	—	7	—	—
2-B) Gray sandstone	—	3	—	—
(SUBTOTAL)	(0)	(10)	(0)	(0)
Other lithologies				
3-A) Gray and greenish phyllite or slate	29	24	39	42
3-B) Quartz or quartz-veined phyllite	5	3	—	—
3-C) Gray and greenish graywacke	4	5	—	—
4) Red slate	—	1	1	1
5) Volcanic	—	2	—	—
6) Muscovite schist	—	1	—	—
(SUBTOTAL)	(38)	(36)	(40)	(43)
TOTAL	50	50	50	50

1) dark gray limestone and calcareous slate of the Bulstrode Formation constitute unequivocal indicators of northwest provenance; starting less than 1 km northwest of the section, these distinctive rocks crop out as a 20 to 25 km-wide belt (Globensky, 1978; see also Figure 2-1: map-unit #12);

2) impure sandstone of the Caldwell Group is an excellent indicator of southeastern provenance, particularly if clasts are present in significant amounts; this reservation stems from the fact that sandstone is also common within rocks of the Granby Group which outcrop some 25 km northwest of the section.

Pebbles of dark gray limestone and calcareous slate derived from the Bulstrode Formation are common in samples of both drift units. Their presence in the lower, gray till of drift unit A is of particular interest: it indicates that ice advanced southeastward, at least as far as this section, during glacial phase A. This is in apparent contradiction with the westward ice-flow event deduced from clast fabric analysis (FT-45). A possible explanation is that glaciers first advanced southeastward across the Appalachian Piedmont and beyond at least this section and that this ice was subsequently replaced by westward-flowing ice. The alternative is that near-identical pebbles were transported from an unmapped bedrock source located somewhere east of the section. Recycling from older sediments is excluded because of the relative abundance of these pebbles in drift unit A.

Several distinctive pebbles of brownish and gray sandstone, typical of Caldwell Group rocks, are present in the olive till member of drift unit A and in the related stratified diamicton; and they are absent in other lodgement till units of this section (Table 4-3). Their absence in drift unit C which was unequivocally deposited by ice advancing toward southeast (see section 4.4.2) confirms their local value as southeast provenance indicators. Because of this and also because there is a significant two- to threefold decrease of northwest provenance indicators in the olive till, the possibility that the sandstone pebbles are derived from distantly located Granby Group rocks must be excluded.

Pebble lithology thus indicates that the olive till member has a south-eastern provenance, a conclusion that is in close agreement with the northward ice-flow event recorded by a till clast fabric (FT-44).

As shown in Figure 4-5, heavy mineral content is distinctly lower in till of drift unit A ($\bar{X}$ = 3.6%) than in that of drift unit C ($\bar{X}$ = 5.4%). The reason for this difference is not known; however, it seems unrelated to the magnetic mineral content which is nearly equal in tills of drift units A ($\bar{X}$ = 9.4%) and C ($\bar{X}$ = 9.5%). A small Ni peak in the olive till subunit of drift unit A (samples #13 and #12: 33 and 29 ppm Ni, respectively) may indicate some contribution from ultramafic sources located southeast of section MP-79-9 (see Figure 4-1); however, this higher Ni content (which is not paralled by a higher Cr content) may also be related to oxidation processes or to a higher clay content in the silt-clay fraction (Figure 4-5).

In any event, evidence gathered from this section as well as from the Norbestos section indicates that there was some transport of glacial debris during the northward ice-flow event which occurred during the latter part of glacial phase A.

4.2.3 Willow Brook section (MP-76-1)

The Willow Brook section is located within the Outer Appalachian Uplands, about 5 km southeast of the Asbestos ophiolite belt (Figure 4-1). In the vicinity of the section, the brook is entrenched into a till plain which has but a few glacigenic streamlined features; these are two small SE-trending drumlins located less than 1 km northwest of the section.

The section was summarily described in a previous report by this author (Parent, 1978: Figure 8) but was re-investigated and sampled for the purposes of the present study. A stratigraphic log, along with clast fabrics and other structural data, is presented in Figure 4-7. The 13.6 m-high section shows drift units A and C separated by a 6.8 m-thick sequence of glaciolacustrine sediments (unit B)..

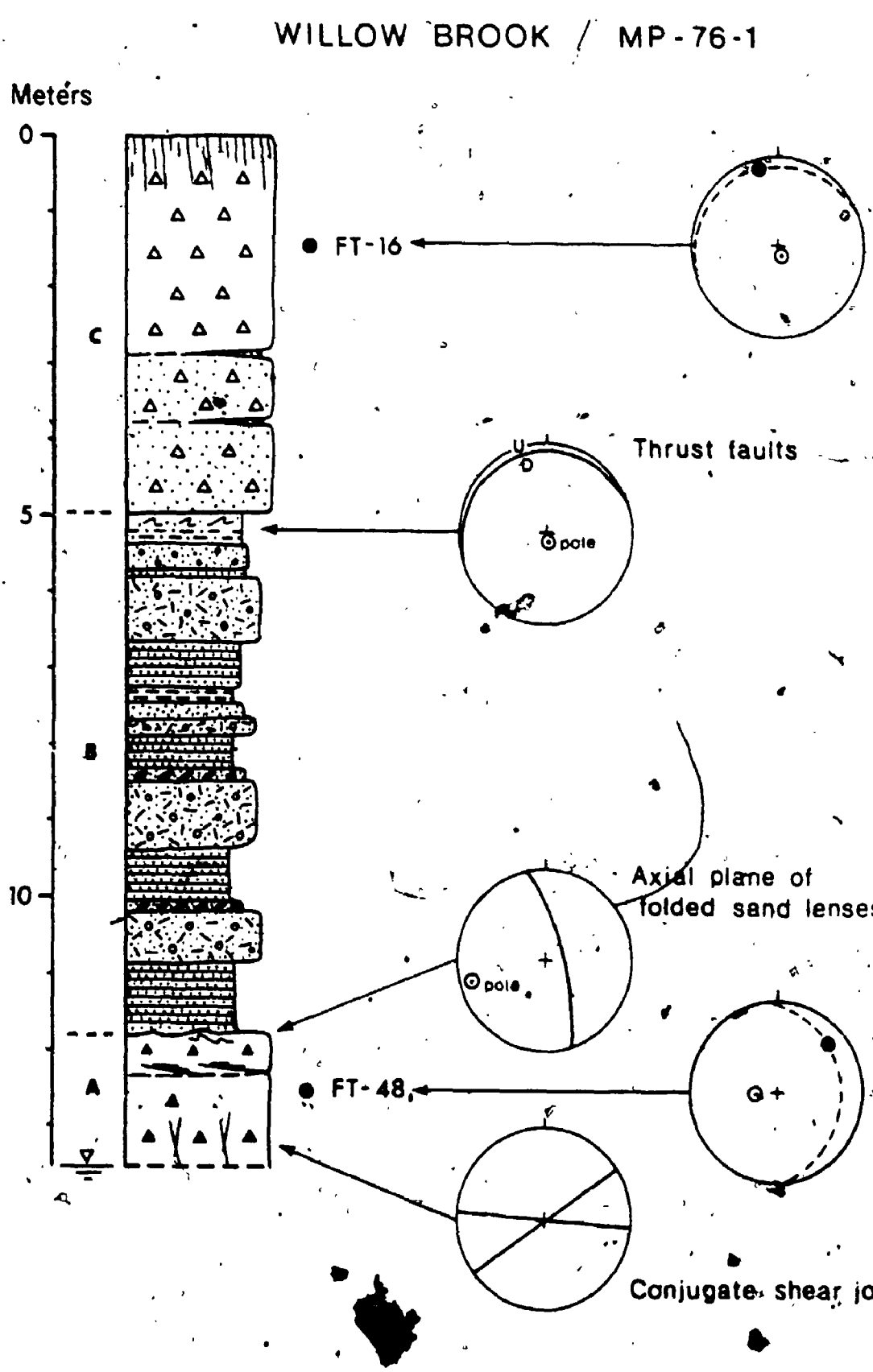

Figure 4-7 : Stratigraphic log, till clast fabrics and attitudes of glacitectonic deformations, Willow Brook section (MP-76-1). (See legend in Figure 4-12)


2
1.0
1.1
1.25
1.4
1.6
1.8
2.0
2.2
2.5
2.8
3.2
3.6
4.0
MICROCOPY

Drift unit A is exposed at the base of the section near river level; it consists of a single lodgement till unit. The till is a very compact, fissile, gray, calcareous, matrix-supported diamicton which has an exposed thickness of 1.8 m. "Etching" of the till exposure produced by flood-stage streamflow allows within-till structures to be observed. A conjugate set of loosely-spaced vertical joints extends upward to the level of well-defined shear planes (Figure 4-7). Main joints trend N 055° and secondary ones trend N 095°. The shear planes occur in the top 40 cm of the unit and dip toward east at shallow (<10°) angles.

The joints are thought to be shear joints induced by subglacial stresses; if so, the stresses were directed either toward N 075° or toward N 255°. The latter is preferred because shear planes above dip toward east and because axial planes of small overturned folds are also inclined toward east. The folds occur in a narrow zone where the till includes a few thin sandy lenses; they strike N 165° and dip 78° toward east and are interpreted as subglacial drag folds produced by a glacier moving toward WSW.

This ice-flow direction is corroborated by a clast fabric (FT-48) measured just below the shear zone. FT-48 is a type B fabric with preferred A-axis orientation (V_1) plunging toward N 047° at an angle of 19°. Since clast A/B planes dip at about the same angle toward east, there remains little doubt that FT-48 is a parallel fabric produced by ice moving toward WSW.

In the field, the lower till appears as a more homogeneous diamicton than the upper till and the lower variability of compositional data in drift unit A compared with that in drift unit C is in part a reflection of this (Figure 4-8). Of course, the smaller exposed thickness and lower number of samples must also contribute to this low variability. Matrix of the lower till has an average content of 43% sand, 49% silt and 8% clay, which corresponds to a mean grain-size (M_z) and sorting (σ_I) of 4.6φ and 2.4φ, respectively. The relatively high carbonate content ($\bar{x}$=7%) of the silt-clay fraction indicates that the lower till is unleached and unoxidized.

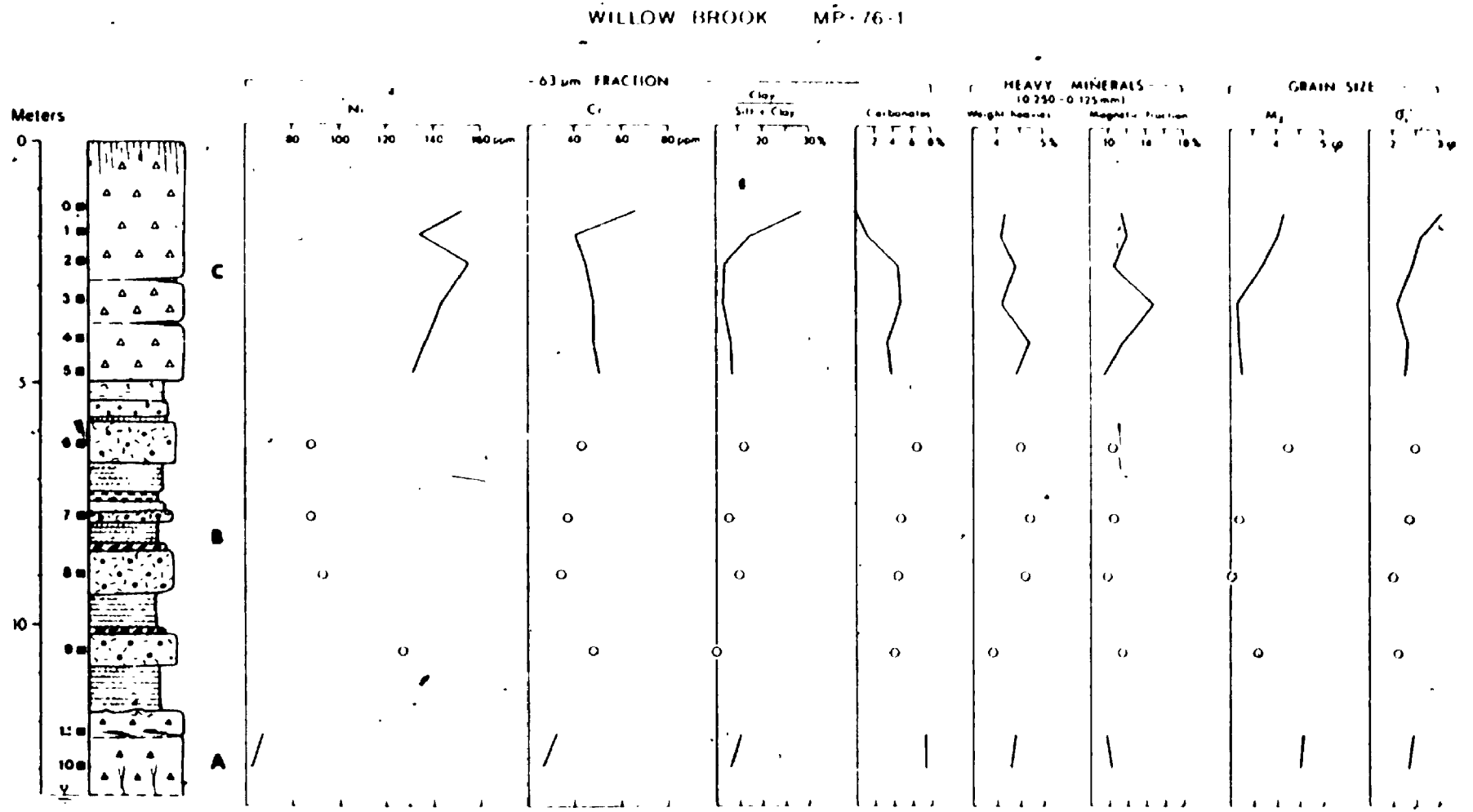

Figure 4-8 : Vertical variations of grain-size and compositional data, Willow Brook section. (See legend in Figure 4-12)

Ni and Cr contents in the lower till average 65 and 29 ppm respectively, which is above regional background but considerably less than in the upper till where Ni and Cr contents average 142 and 50 ppm respectively. Those values thus indicate that some ultramafic debris were transported to this site during glacial phase A, an interpretation which is confirmed by the presence of occasional ultramafic clasts and rare Precambrian clasts in drift unit A.

Considering the proximity and the outcrop pattern of the ultramafic belt on one hand and, on the other, the structural and clast fabric data, it seems difficult to escape the following provenance history:

1) ultramafic debris were transported by ice advancing toward the southeast sector during an earlier part of glacial phase A;

2) a subsequent episode of westward ice-flow caused the observed depletion of ultramafic components in till of drift unit A.

The scarcity of Precambrian clasts in the lower till further suggests that the early southeastward ice-flow phase may have been a short-lived event.

4.2.4 Chemin des Ecossais section (MP-79-1)

The Chemin des Ecossais section is located well within the Outer Appalachian Uplands, about 7 km northwest of Sherbrooke (Figure 4-1). The section was exposed for a few weeks during the summer of 1979 while a Transquébécoise Highway underpass was under construction.

The base of section MP-79-1 consists of glacially abraded bedrock (gray slate and metagraywacke) which is directly overlain by two superposed tills sheets which are in turn overlain by glaciolacustrine sediments (Figure 4-9). The contact of the two till sheets is marked by an unusually abrupt colour change: the upper till is olive gray in its basal zone while the underlying till is olive (Plate 4-2B). The colour

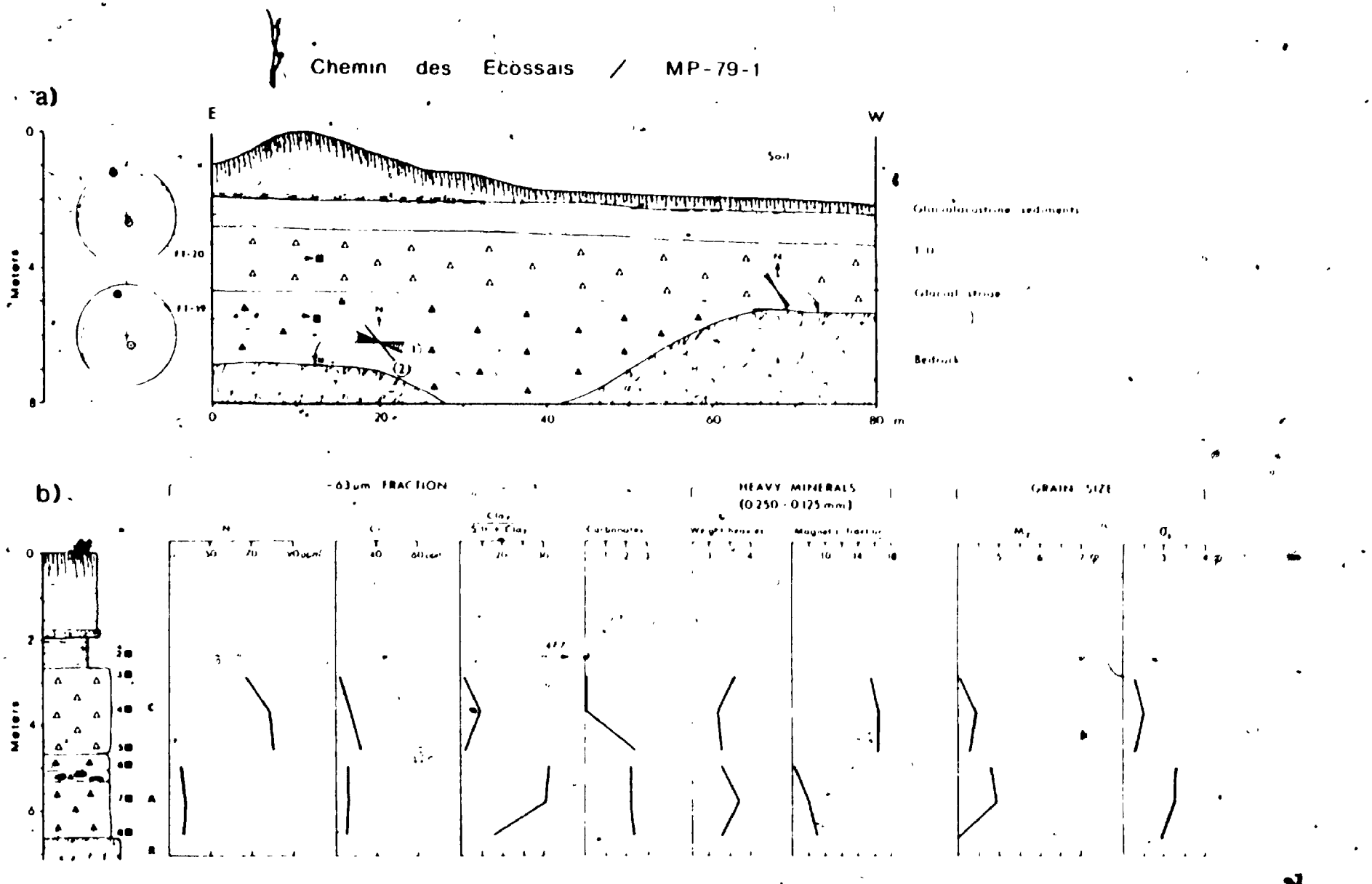

Figure 4-9 : Stratigraphy, till clast fabrics, vertical compositional trends and subtill glacial striae, Chemin des Écossais section (MP-79-1)
(See legend in Figure 4-12)

of the lower till is analogous to that which is commonly observed for slightly oxidized till, such as in the basal part of post-glacial weathering profiles in the region. However, the rather uniform 2.3% carbonate content of the lower till (Figure 4-9b) suggests that its olive colour may not have a pedogenic origin.

The two tills differ not only in colour but also in stoniness and clast composition. Although both tills are matrix-supported diamictons, the lower till is distinctly more pebbly and cobbly. Its clast lithology is also less diverse: most significantly, ultramafic clasts are absent in the lower till while they are quite common in the upper till.

This is corroborated by the uniformly low Ni content ($\bar{x}$=37 ppm) of the lower till compared to the fairly high Ni content ($\bar{x}$=75 ppm) of the upper till (Figure 4-9b). Because of this section's proximity and location relative to ultramafic rock outcrops (see Figure 4-1), the absence of ultramafic clasts and the low Ni content constitute evidence that the lower till has neither a northwest nor a west provenance. This is further confirmed by the fact that SE-trending tails of the younger (drift unit C) Asbestos ultramafic dispersal train run through a wide belt of terrain on both sides of the section (see Figure 4-21).

There are other compositional differences between the lower and upper tills, but these are of somewhat lesser interest. Matrix of the lower till contains an average of 43% sand, 42% silt and 15% clay and has an average grain-size mean (M_z) of 4.6ϕ and an average sorting (σ_I) of 3.2ϕ. The upper till has a slightly coarser matrix: it contains 46% sand, 47% silt and 7% clay and its average M_z and σ_I are 4.3ϕ and 2.4ϕ, respectively. Mainly because the lower till has a poorer sorting and a higher clay content, particularly in its upper half, this small grain-size difference is at a maximum near the contact between the two units (Figure 4-9b).

Carbonate content of the lower till is almost identical to that of unoxidized upper till (sample #5): average carbonate content is low

(2.3%) and this is likely a result of the remoteness of significant sources of carbonate bedrock (see Figure 2-1).

The fine sand fraction of both tills contains identical heavy mineral weight (3.4%). However, the average weight of the magnetic fraction in the lower till is only 7.7%, which is about half as much as in the upper till (16.1%). This contrast is likely related to the presence of ultramafic debris in the upper till, an interpretation which is similar to that of McDonald (1967a) and Shilts (1973a, 1975) for nearby areas.

Additional evidence on ice-flow directions during deposition of the lower till comes from glacial striations and till clast fabric. At the base of the measured section, an excellent exposure of glacially polished bedrock shows two sets of striations (Figure 4-9a). One set consists of abundant scratches and fine striae trending between N 90° and N 115°; this set is crosscut by another one consisting of a few deeper striae which trend N 140°. In both cases, there were no directional features, such as crag-and-tail striations, which would allow determining the direction of glacial movement. However, the absence of ultramafic debris in the lower till at this section strongly suggests that glaciers which produced the early set of east-trending striae advanced toward west rather than toward east.

A clast fabric sample (FT-19) provides evidence on the direction of ice-flow during the event that produced the younger set of striations. FT-19 is a type B fabric with preferred A-axis orientation (V_1) plunging toward N 347° at an angle of 16°. Since clast A/B planes also dip toward northwest, and at the same angle, FT-19 is interpreted as a parallel fabric produced by ice moving toward SSE. However, the absence of northwest provenance indicators throughout the lower till suggests that this southeastward ice-flow event was short-lived or, perhaps, that glacial transport was much more sluggish than during the later phase of southeastward ice-flow which deposited the upper till. Another possibility is that the glacial advance which deposited the upper till (drift unit C) caused re-orientation of all clasts within the upper meter of

the lower till, a suggestion which requires that a large number of closely-spaced shear planes be present within the lower till or that extensive post-depositional flowage occurred within the lower till; no field evidence was found that may support this "re-orientation hypothesis". Either interpretation finds some support in the fact that, where the upper till directly overlies bedrock, as at the west end of the roadcut (Figure 4-9a), the east-west striations were apparently obliterated by subglacial erosion and replaced by a set of striations trending between N 140° and N 150°.

To summarize, combined evidence from glacial striations, from a till clast fabric and from till provenance data suggests that:

1) the lower till records an early phase of westward ice-flow;

2) this westward ice-flow phase was probably followed, at least briefly, by a phase of southeastward ice-flow.

In spite of the absence of inter-till sediments or paleosol that would positively indicate a subsequent deglacial interval, the lower till is considered as an equivalent of drift unit A. The main reasons to do so are (1) that it records a significant westward ice-flow phase, as in drift unit A of previously described sections and (2) that the overlying till, which has an unequivocal northwest provenance and which is conformably covered by glaciolacustrine sediments, is obviously equivalent to drift unit C.

4.2.5 Rivière Noire section (MP-82-4)

The Rivière Noire section is located within the Appalachian Piedmont, about 14.5 km southeast of Acton Vale (Figure 4-1). In the vicinity of section MP-82-4, the river is entrenched to a depth of about 25 m into a till plain which features several SE-trending crag-and-tail ridges and drumlins (see Figure 3-1). A blanket of marine sand, as mapped by McDonald (1966), covers part of the till plain surface on both sides of the valley. McDonald (1967a: p. 143-144) previously investi-

gated this section and considered that it recorded a readvance to the Highland Front Moraine.

This section remains one of a few two-till localities of the Appalachian Piedmont; other known localities include the Ange Gardien section (Prichonnet, 1982a) and all are within the Granby map-area, west of the study area. The 24.5 m-high Rivière Noire section shows two till sheets (drift units A and C) separated by a 17.8 m-thick sequence of glaciolacustrine sand (Figure 4-10).

The top 5 m of the section are currently concealed by thick, vegetation-covered slumped sediments. As a result, the top and basal contacts of the upper till could not be investigated adequately during this study; the upper 6 m of the stratigraphic log are thus mostly drawn from observations recorded by McDonald (1967a). Although the upper till unit was poorly exposed, an in situ till sample (#1) could be recovered. Below 6 m however, the section is fairly well exposed.

The lower till unit has an exposed thickness of 1.5 m and extends below river level. It is a compact, fissile, gray, calcareous, matrix-supported diamicton. A single sample (#4) indicates that its matrix contains 31% sand, 53% silt and 16% clay, which corresponds to a granulometric mean (M_z) of 5.2ϕ and a sorting (σ_I) of 2.9ϕ. The lower till thus seems distinctly finer grained than the upper till (50% sand, 32% silt and 12% clay; M_z = 4.3ϕ and σ_I = 2.8ϕ). However, McDonald (1967a) had reported the presence of a 60 cm-thick silt-rich till layer at the base of the upper till unit.

The lower till is unoxidized and appears unleached of carbonates; its silt-clay fraction contains only 2.4% total carbonates, which is hardly a surprise since there are few carbonate bedrock sources in the vicinity of the section. Bright orange-red iron-oxide staining observed in the basal 1.5 m of the overlying cross-bedded sands does not seem related to an interstadial weathering episode; rather it appears to result from the aeration of modern groundwater.

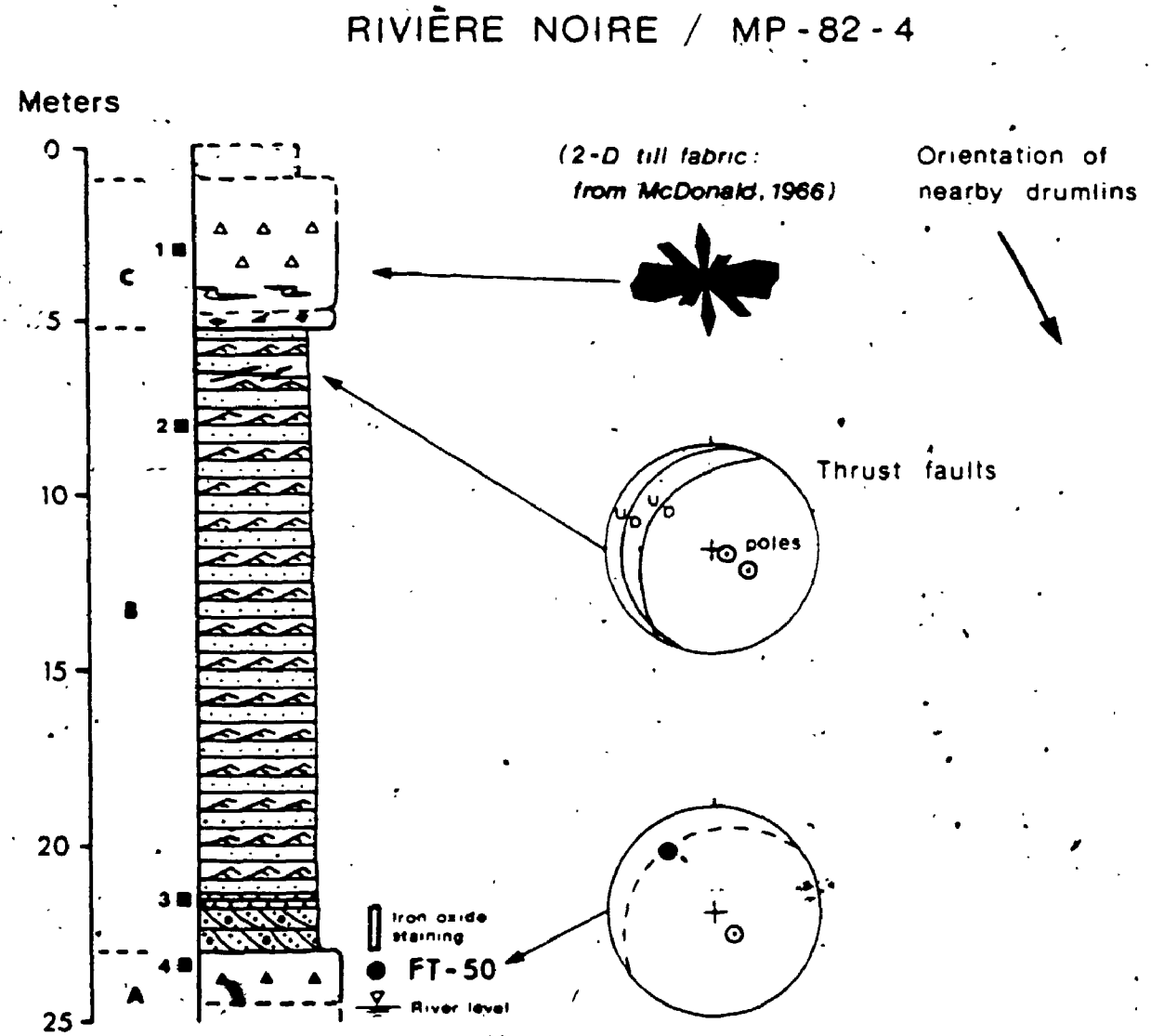

Figure 4-10 : Stratigraphic log, till clast fabrics and attitude of glacitectonic deformations, Rivière Noire section (MP-82-4). (See legend in Figure 4-12)

The lower till contains abundant clasts of green and red slate, typical of rocks of the Shefford Group and particularly of the Granby Formation (part of Shefford Group). These rocks outcrop in a wide NE-trending belt (see Figure 2-1) whose southeastern limit passes only 1.5 km northwest of section MP-82-4. This indicates that the lower till has a northwest provenance, an interpretation which is further supported by the presence of occasional Precambrian clasts and by the apparent absence of clasts derived from rocks of the Oak Hill and Caldwell Groups which outcrop only 3 km southeast of the section.

Moreover, a till clast fabric (FT-50) also indicates that the lower till was deposited by a glacier that advanced from northwest. FT-50 is a type B fabric with preferred A-axis orientation (V_1) plunging toward N 318° at a significant angle of 24°; clast A/B planes are also inclined toward northwest at an angle of 24°. These results are thus consistent with those of a two-dimensional till fabric reported by McDonald (1967a: figure 20).

The lower till of section MP-82-4, unlike that of all four previously discussed sections, contains no apparent record of a westward ice-flow episode and thus cannot be assigned to drift unit A on that basis. The difficulty is further compounded by the fact that the upper till, as indicated by nearby SE-trending crag-and-tail ridges and drumlins and by subtill thrust faults (Figure 4-10), was deposited by a glacier advancing toward southeast, as is the case for the lower till. Thus the suggestion by McDonald (1967a) that the lower till is equivalent to Lennoxville Till (surface till) and that the upper till sheet records a readvance to the nearby Highland Front Moraine remains at least a possibility.

However this author believes that the upper till sheet does not record a Late-Lennoxville readvance, but that it is equivalent to the regional surface till (drift unit C) and that the lower till sheet is equivalent to drift unit A. The main reasons for this interpretation are the following:

1) in upland sections that are located close to the Piedmont (MP-76-1 and MP-79-9), the lower till also contains the record of a southeastward ice-flow episode;

2) glacial striations indicating a westward ice-flow episode have not been reported from the Rivière Noire area (Lortie, 1976: carte 1); this may thus be an indication that there was no westward ice-flow event in this area;

3) surface till which can be observed in crag-and-tail ridges and drumlins located less than 1 km from the section has a sandy matrix, much like that of the upper till sheet (drift unit C);

4) perhaps more importantly, there is no evidence to indicate that the nearby Ulverton-Tingwick Moraine (local name for ice-marginal features which include sediment bodies formerly assigned to the Highland Front Moraine; see section 5.1.3) was formed during a significant glacial readvance; on the contrary, deglacial landforms and sediments (see Figure 3-1), surface till characteristics and glacial striations on record suggest that the Ulverton-Tingwick Moraine is simply a recessional ice-front position and that it does not represent a regional drift boundary.

The above interpretation which suggests that the upper till sheet is equivalent to drift unit C and that the lower till sheet is equivalent to drift unit A appears as a working hypothesis that is in much better agreement with the overall geologic record.

4.2.6 Summary of provenance interpretation and ice-flow sequences: evidence for Appalachian centers of glacial outflow

Characteristics of drift unit A were previously presented and discussed from a mainly site-specific point of view. The main ice-flow patterns and sequences which emerged from the analysis of both compositional and directional data are summarized in Figure 4-11. Evidence

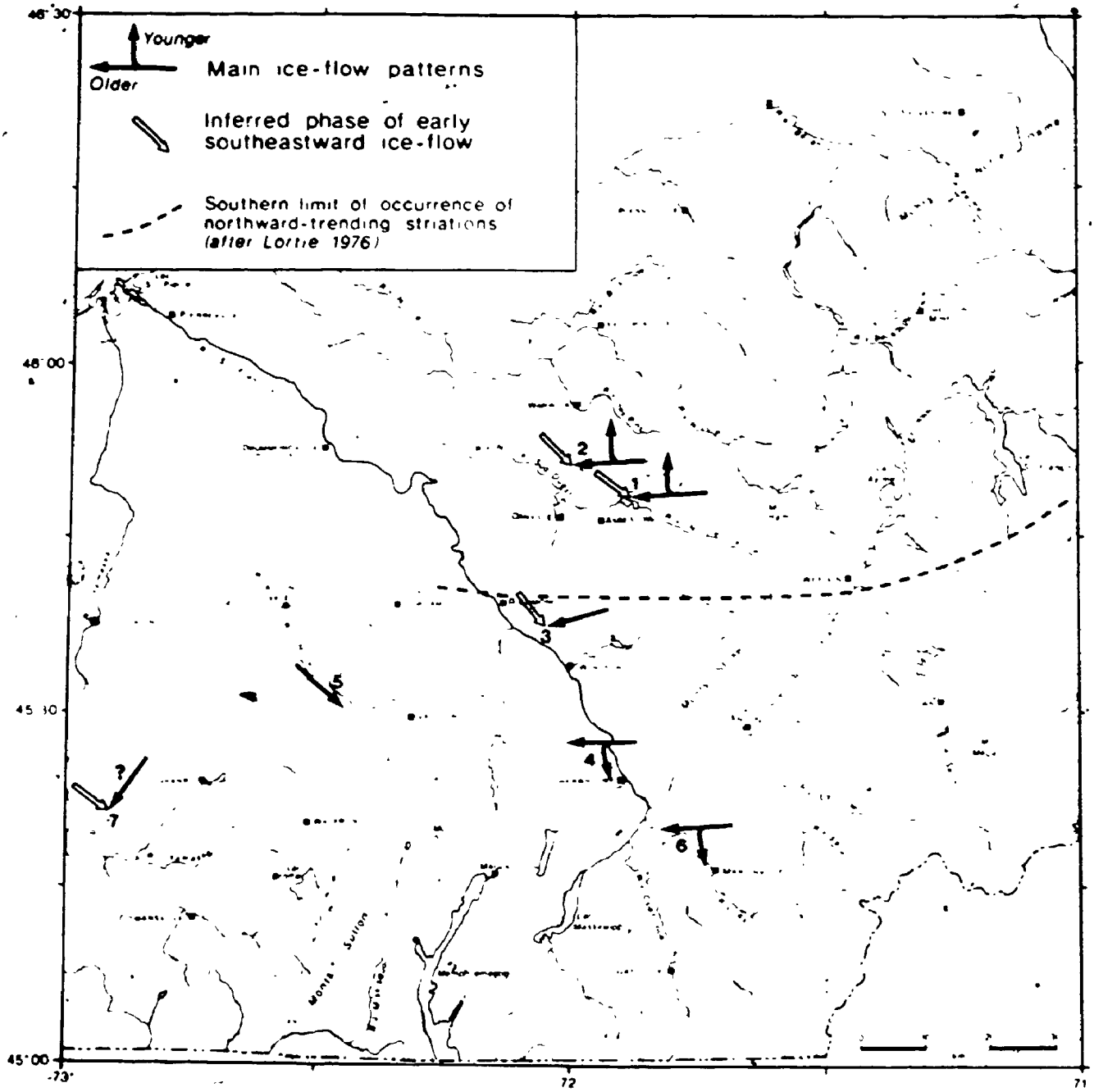

Figure 4-11: Ice-flow patterns and sequences for drift unit A and its suggested correlatives. The Ascot River (#6) and Ange-Gardien (#7) sections will be discussed in Chapter 6.

gathered from the five previously discussed sections reveals some consistent ice-flow and provenance characteristics of drift unit A as well as significant local variations. These are now examined in a more regional context.

Early phase of southeastward ice-flow

The only section which contains unequivocal evidence of southeastward ice-flow during glacial phase A is located within the Appalachian Piedmont (Riv. Noire / MP-82-4). At this site, both clast fabric and clast composition indicate that the lower till has a northwest provenance. However, only the top part of the till is exposed and, because of this constraint, it is not known whether or not any other ice-flow event, westward ice-flow for instance, occurred earlier in that area of the Piedmont. Nevertheless, it can concluded that Laurentide ice advanced southeastward at least as far as this section during the latter part of glacial phase A and that this may well be the only ice-flow event recorded in the lower till at the Rivière Noire locality.

An early southeastward ice-flow event is inferred from clast composition of the lower till in two other sections (Riv. des Rosiers / MP-79-9 and Willow Brook / MP-76-1). In both sections, the lower till contains only scarce Precambrian clasts but it does contain clasts which must have been transported southeastward from local Appalachian sources. Both sections are located within the Outer Appalachian Uplands but are situated in valleys that open widely toward northwest; this may have favored an early incursion of Laurentide ice in at least some valleys of the Outer Uplands. The scarcity of Precambrian clasts in the lower till at Norbestos further suggests:

- that Laurentide ice impinged only slightly upon the Outer Appalachian Uplands during the early part of glacial phase A,
- or that its advance was soon blocked and superseded by an ice mass that was advancing westward from Appalachian ice centers.

It must also be kept in mind that the base of lower till at Norbestos is not exposed and that an earlier ice-flow event, toward southeast for instance, may not have been directly recognized yet. The SE-trending striations which are crosscut by westward-trending striations are perhaps a record of this early southeastward ice-flow event.

Main phase of westward ice-flow: local evidence for Appalachian centers of glacial outflow

Westward-flowing ice deposited much of the lower till at all four sections located within the Outer Appalachian Uplands (Figure 4-11: sections #1 through #4). In sections that extend across much of the study area, from the vicinity of Asbestos to that of Sherbrooke, till clast fabrics and attitudes of glacitectonic deformations indicate a consistent pattern of westward to slightly southwestward ice-flow during deposition of drift unit A (Figure 4-11).

As indicated by clast lithology and by trace element data in conveniently located sections such as Norbestos, glacial phase A produced significant westward transport of local Appalachian indicators. In the three other Uplands sections, drift unit A is dominated by debris derived from local and eastern bedrock sources. Even in sections where an earlier phase of southeastward ice-flow is inferred, drift unit A contains few debris derived from northwest sources.

Evidence of westward ice-flow begins at or near the base of the lower till in sections where the unit is exposed more completely. Together with provenance and with directional data, this suggests that the westward ice-flow phase constitutes a prominent characteristic of glacial phase A in uplands of the Asbestos-Valcourt region. However, evidence from the Rivière Noire section indicates that westward-moving ice may not have reached that part of the Appalachian Piedmont; here again, it must be kept in mind that only the top part of the lower till sheet is exposed above river level.

Because of the consistent pattern of westward ice-flow recorded in drift unit A and because of the general eastern provenance of the unit, it is very tempting to suggest that Appalachian centers of glacial outflow were in existence throughout much of glacial phase A. The hypothesis is by no means entirely new; however, previous suggestions for Appalachian-based glaciers in this area were made in a different context and their discussion is thus withheld until after regional correlations have been considered (see sections 6.2 and 6.4). Only evidence from the Asbestos-Valcourt region is thus considered herein:

1) because a lasting phase of westward ice-flow is recorded in a belt of hilly terrain which is at least 50 km-wide and because this event is recorded in a variety of topographic situations, outflow from Appalachian centers appears as a realistic working hypothesis;

2) westward-trending striations occur throughout much of this region and are particularly abundant in uplands east of Asbestos (see Figure 1-3); these striations have been interpreted mainly as features of the last deglaciation by previous workers (Lamarche, 1974; Lortie, 1976); yet, the upper till sheet (drift unit C) as well as subsequent deglacial features contain no record of the "expected" phase of westward ice-flow (see section 4.3 and Chapter 5);

3) considering that the edge of the Canadian Shield is only about 100 km northwest of the edge of the Outer Appalachian Uplands and of the Richmond Hills, and considering that there are almost no topographic obstacles between the Shield and the Asbestos-Valcourt region, the scarcity of Precambrian clasts in drift unit A, particularly when compared with the overlying drift unit C, is considered as highly significant supporting evidence; this further suggests that Appalachian outflow centers are to be preferred over possible readjustments of Laurentide Ice Sheet flowlines in order to explain the westward ice-flow pattern.

Late phase of northward and southward ice-flow

In the two sections north of Asbestos, directional and compositional data from drift unit A indicate that the main phase of westward ice-flow was followed by a phase of northward ice-flow. Because a record of intermediate directions is lacking at both the Norbestos and Rivière des Rosiers sections, the change of direction is thought to have occurred quite suddenly. At Norbestos, slices of glaciolacustrine sediments were deformed and dragged at the base of the northward-moving glacier. This indicates that a glaciolacustrine water body entered into at least part of the Rivière Nicolet-Centre valley towards the close of the westward ice-flow phase or, alternatively, that there were local subglacial water bodies during the phase of northward ice-flow. If the first interpretation is retained, the proximal character of the deformed sediments then indicates that the northward readvance across the valley occurred only shortly after recession of the westward-flowing ice. In any event, the ensuing northward flow event lasted long enough to bring about significant compositional changes in the upper part of drift unit A at both Norbestos and Rivière des Rosiers.

The northward flow event is not recorded at other drift unit A localities. At Chemin des Ecossais, southward ice-flow replaced westward ice-flow for at least a short time prior to the end of glacial phase A. However, the ice-flow shift was apparently not paralleled by a significant compositional change at this locality. This is perhaps to be expected since monotonous slate-dominated bedrock outcrops for several kilometers east and north of the section. What is clear is that either the southward flow event did not last long enough for ice to transport ultramafic debris to this section or that the southward-flowing ice had not moved across ultramafic rocks.

The latter is possible only if an ice-divide was formed in the Appalachian Uplands between, say, Sherbrooke and Asbestos. This hypothesis is worth considering since both the northward and southward ice-flow events occur in a similar stratigraphic position. In this context, the southern limit of occurrence of northward-trending striations, as

delineated by Lortie (1976: carte 2), may tentatively be considered as the northernmost position of such a divide (Figure 4-11). Of course, Lortie (1976) interpreted this limit as a feature formed during the last deglaciation; as will be shown later (Chapter 6), most of the northward striations were likely produced prior to the last regional ice advance. The local ice-divide, which is herein proposed as a working hypothesis, probably did not extend as far west as the Rivière Noire locality. Perhaps because the Willow Brook locality is located very close to the expected position of the inferred ice-divide, a shift of ice-flow is not recorded at the top of drift unit A. Admittedly, there is only a limited stratigraphic record to support the proposed ice-divide. Yet the hypothesis presently appears as the only one which is capable of providing a consistent explanation for provenance and ice-flow patterns toward the close of glacial phase A.

4.3 Unit B - Interstadial glaciolacustrine sediments

Glaciolacustrine sediments assigned to unit B underlie lodgement till of drift unit C in all investigated sections (Figure 4-12); in sections where their basal contact is exposed, sediments of unit B directly overlie unweathered till of drift unit A. Sediments of unit B are not present between drift units A and C in only two of the sections shown in Figure 4-12; however, at one of these two localities (Rivière des Roßiers / MP-79-9), unit B is indirectly recorded by the presence of clasts and sheared lenses of laminated lake silt in lodgement till of drift unit C.

Glaciolacustrine sediments of probable equivalent age were observed below surface till at a few other localities; these include the open pit of Jeffrey Mine in Asbestos, a roadcut near the bridge over Rivière Nicolet-Centre at Moulin Plamondon, a gravel pit located about 1 km north of Saint- Fortunat (see Figure 3-1 for location) as well as several small exposures in the vicinity of most of the sections shown in Figures 4-12 and 4-1. However, because sediments were poorly exposed at those localities, they were examined mainly for the possible occurrence of organic debris. Further investigations could not be carried out at

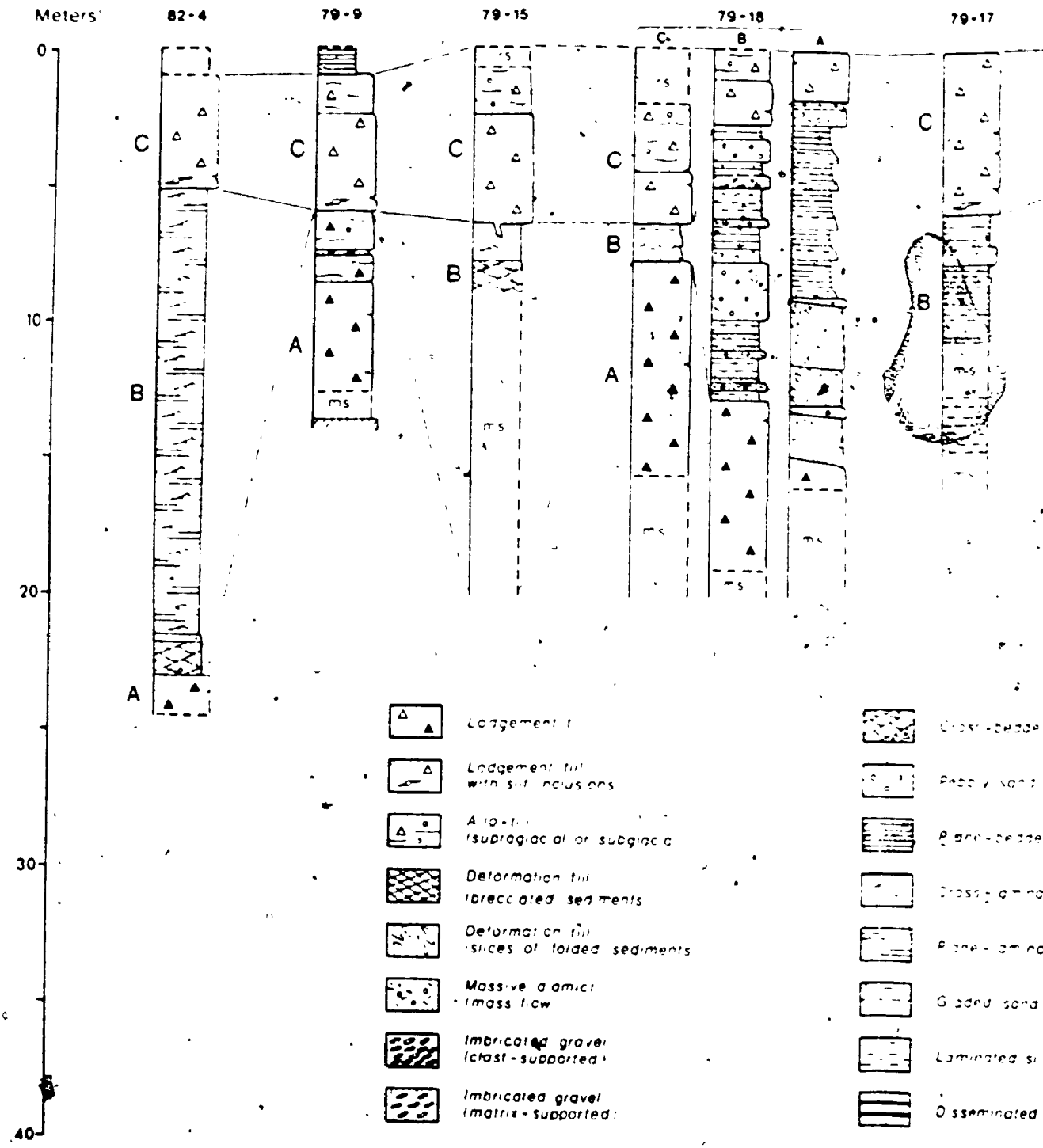

Figure 4-12 : Main stratigraphic sections of the Asbestos-Valcourt region. Correlations with units exposed

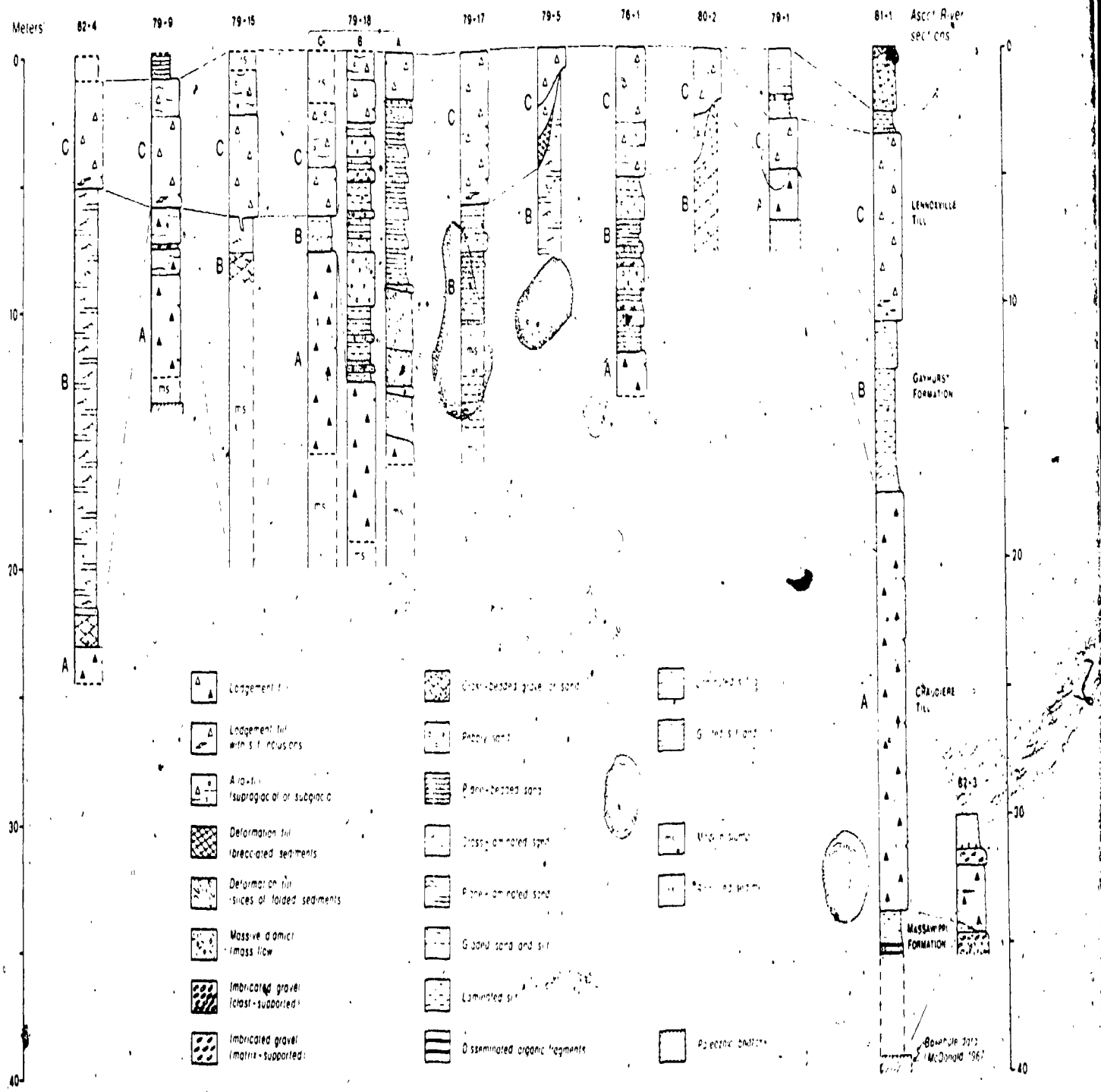

Figure 4-12 : Main stratigraphic sections of the Asbestos-Valcourt region. Correlations with units exposed at Ascot River will be discussed in section 6.2.

Jeffrey Mine because of hazardous conditions; moreover, important disturbances resulting from several phases of man-made reworking around the asbestos mine pit made it nearly impossible to obtain a reliable stratigraphic record. Figures 4-1 and 4-12 show that unit B is recorded at localities throughout much of the study area. Examination of aerial photographs further reveals that most of these localities are located within till plains which are underlain by thick Pleistocene deposits; since there are several similar terrains where no sections are available, it is strongly suspected that unit B underlies surface till over a more extensive area of the Outer Appalachian Uplands and Richmond Hills of the Asbestos-Valcourt region, particularly alongside valleys.

Glaciolacustrine sediments of unit B may be subdivided into two main lithofacies assemblages:

1) Facies group I: proximal deep-water muds and diamictons;
2) Facies group II: subaquatic outwash sediments (sand-dominated).

Since no single section contains a stratigraphic record which shows distinct superposition of the two facies groups and since both groups have been observed to extend from the top of drift unit A to the base of drift unit C, age relationships between the two groups cannot be unequivocally established. At the present time, the two facies groups are considered as laterally equivalent, time-transgressive subunits; facies differences are thus interpreted as resulting from lateral contrasts of glaciolacustrine depositional environments.

Because they lack dateable organic material, glaciolacustrine sediments were assigned to unit B without chronological control, mainly on the basis of their occurrence below drift unit C (surface till) which, as it will be shown in section 4.4, can be considered as a regionally distinctive marker bed. This assignment is further confirmed by the fact that, at least in a few sections (Norbestos / MP-79-18; Willow Brook / MP-79-1), sediments of unit B are superposed to drift unit A which, unlike drift unit C, has a distinctly Appalachian provenance.

4.3.1 Proximal deep-water muds and diamictons

Assemblages of glaciolacustrine muds and diamictons are exposed between drift units A and C in the Norbestos (MP-79-18) and Willow Brook (MP-76-1) sections. These assemblages consist of recurrent sequences which show distinct thinning-and-fining-upward internal trends (Figure 4-2). Some of the sequences are coarse-grained and diamict-dominated (sections MP-79-18B and MP-76-1) while others are rather fine-grained and mud-dominated (section MP-79-18A). In subsections A and B at Norbestos (MP-79-18), unit B consists of as much as seven such sequences, while the adjacent subsection C shows two sequences at the most (Figure 4-2).

Coarse-grained sequences show considerable lateral facies and thickness changes; these sequences typically consist of a basal bed of massive matrix-supported diamicton overlain by massive or plane-bedded pebbly sand which is in turn overlain by plane-laminated sand or by graded sand and silt. In some sequences, a layer of matrix-supported imbricated gravel may lie either above or below diamictic beds. Contacts at the base of sequences and within sequences are usually sharp and non-erosional; a channelized contact was observed only once, at the base of sequence #3 in section MP-79-18B (Plate 4-3A). Diamictic beds are generally less than 1 m thick; yet they make up 40 to 50% of the total thickness of unit B in sections MP-76-1 and MP-79-18B (Figure 4-12). Reverse grading was observed in the diamicton bed at the base of sequence #2 in section MP-79-18B (Plate 4-3A); other diamictic beds are massive. Their matrix grain-size composition resembles that of either overlying or underlying lodgement tills (see Debris flows in Figure 4-3). However the diamictic beds contain few boulders, if any; cobbles, and to a lesser extent pebbles; are noticeably less abundant than in lodgement tills.

Close relationships of diamictic beds with beds deposited by tractive undercurrents (imbricated gravel, plane-bedded pebbly sand, plane-laminated sand) and with typical turbidite beds (graded sand, graded sand and silt) suggest that these diamictons were deposited by sediment

Plate 4-9

A) Coarse-grained fining-and-thinning-upward sequences of sediment gravity flows and turbidites, unit B, Norbestos section (MP-79-18B). Sequence #2 shows an inversely graded diamicton overlain by mainly plane-laminated sand and massive silty sand layers; only minor ripple-laminated sand occurs immediately above the diamictic bed. Notice the channelized basal contact of the diamictic bed of sequence #3. Pencil is 15 cm-long.

B) Slump or drag fold overturned toward east in the upper part of sequence #5, unit B, Norbestos section (MP-79-18B). This and other similar folds are the result of syndepositional deformations. This fining-upward sequence of graded sand and graded silt layers contains abundant ice-rafted clasts. Staff intervals are 20 cm-long.

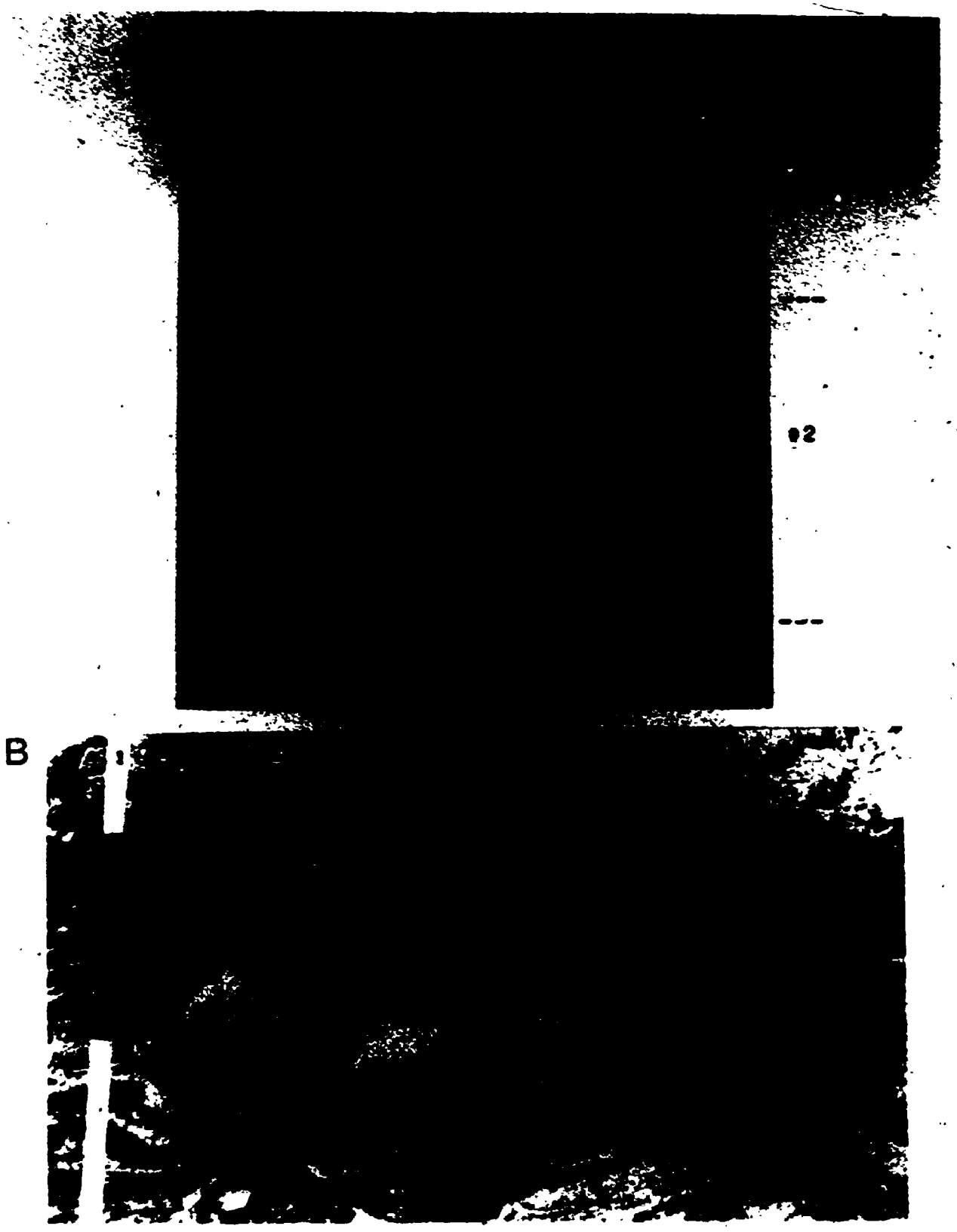

Plate 4-3

gravity flows rather than from grounded or floating glacier ice. Because primary structures are quite uncommon within diamictons, it is difficult to recognize whether they were emplaced by fluidized sediment flows, by grain flows or by debris flows (nomenclature of Middleton and Hampton, 1976). However, the lack of stratification or other internal contacts within diamictons, the fairly large maximum clast-size, as well as the near-absence of features indicative of grain flows or fluidized sediment flows suggest that most of the massive diamictic beds were deposited by debris flows. Coarse-grained sequences, such as those observed at Norbestos and Willow Brook greatly resemble sequences described as subaquatic mid-fan sediments by Walker (1984). If this interpretation is correct, these "distribution-graded" sequences are likely derived from unsorted glacial debris which were deposited subaquatically at a nearby ice margin and which episodically became liquefied, thus inducing debris flows or other types of sediment gravity flows, even on low-gradient depositional slopes; these flows may have initiated, or at least contributed to initiate, turbidity currents which deposited the stratified sandy sediments overlying the diamictons.

A clast fabric (FT-28) was sampled in an unusually thick (2 m), till-like diamictic bed in subsection B at Norbestos (sequence #4: see Figure 4-2). Although this sample consists of only 25 clasts, it shows that the attitude of clast A/B planes (normal to C-axes) is much less planar than that observed in lodgement tills of this region; C-axis fabric strength (C) is only 2.17, lowest of all measured C-axis fabrics (Table 3-1). A-axis data also show lowest fabric strength (C=1.84) of all samples (Figure 3-3) and their density distribution departs from that of the spherical normal distribution (k=2.1). Nevertheless, FT-28 shows a weak preferred A-axis orientation (V_1) plunging toward WSW; this A-axis plunge is not statistically significant (see Table 3-I), yet it may suggest that this diamicton was deposited by a debris flow moving toward ENE. This direction is the same as that indicated by small overturned folds observed in graded sand and silt of the overlying sequence (sequence #5 in Figure 4-2; Plate 4-3B); these folds may be interpreted as slump overfolds or as drag folds produced during deposition of sequence #6. If they are drag folds, it may be inferred that coarse-

grained glaciolacustrine sequences at Norbestos were deposited by sediment gravity flows and turbidity currents directed toward east; if they are slump overfolds, it may be further suggested that the subaquatic fan on which these sequences were laid down had a paleoslope dipping at a low angle toward east.

Over a distance of only about 65 m at Norbestos, diamict-dominated sediments pass laterally (eastward) to finer-grained, mud-dominated sediments. As mentioned earlier, these muds display several thinning-and-fining-upward sequences in subsection A (Figure 4-2). Each sequence begins with single or multiple layers of graded or massive silty sand whose overall thickness ranges from 3 to 30 cm; these are overlain by fairly thick (1 m or more) series of graded silt and clay layers. These sequences thus consist of series of (A) DE turbidites (nomenclature of Walker, 1984); B- and C-division layers are very uncommon, perhaps because of the high silt content and low fine sand content of tills and diamictons from which the turbidites are presumably derived. A-division layers are represented by the massive or graded silty sand layers which are present at the base of the thinning-and-fining-upward turbidite sequences and also by sandy partings which are frequently observed within the overlying silt and clay turbidites; diamictic layers, whose thickness varies between about 3 and 10 cm, commonly occur at the base of multiple layers of graded silt and clay in subsection A at Norbestos and may also be considered as A-division layers. A similar silt and clay turbidite sequence with thin diamicton layers was also observed near the middle of unit B at Willow Brook (Plate 4-4A). $DE_{(t)}$-division layers make up the major part of these turbidite sequences; they consist of multiple, thin (most are less than 1 cm-thick) layers of graded silt and clay which grade upward, at irregular intervals, into 1.5 to 2.0 cm-thick, clayey layers ($E_{(t,h)}$-division layers). These clay layers are interpreted as rain-out sediments deposited during intervals of reduced turbidity current activity; they may thus represent the winter layers of varves. If so, single varves in section NP-79-18A have a thickness on the order of 10 to 15 cm, and only a few tens of varves are recorded in unit B at Norbestos. DE layers also contain abundant ice-rafted clasts (small pebbles, granules, coarse sand) and

Plate 4-4

A) Fining-and-thinning-upward sequence of (A)DE turbidites, unit B, Willow Brook section (MP-76-1). A 10 cm-thick diamictic layer is present below massive sand layers (A-division) of the thickest turbidite unit. Arrowheads at right of photograph indicate the top of single turbidite units. This sequence, at a depth of 7.4 m, shows the most distal glaciolacustrine muds of unit B at Willow Brook. Pencil is 14 cm-long.

B) Ripple-laminated sand in subaquatic outwash sediments of unit B, Wotton section (MP-79-5). Paleocurrent is toward SE (right of photograph). The thrust fault (φ), which belongs to a series of glacitectonic deformations that were produced by subsequent glacial overriding (glacial phase C - southeastward ice flow), dips toward NW.

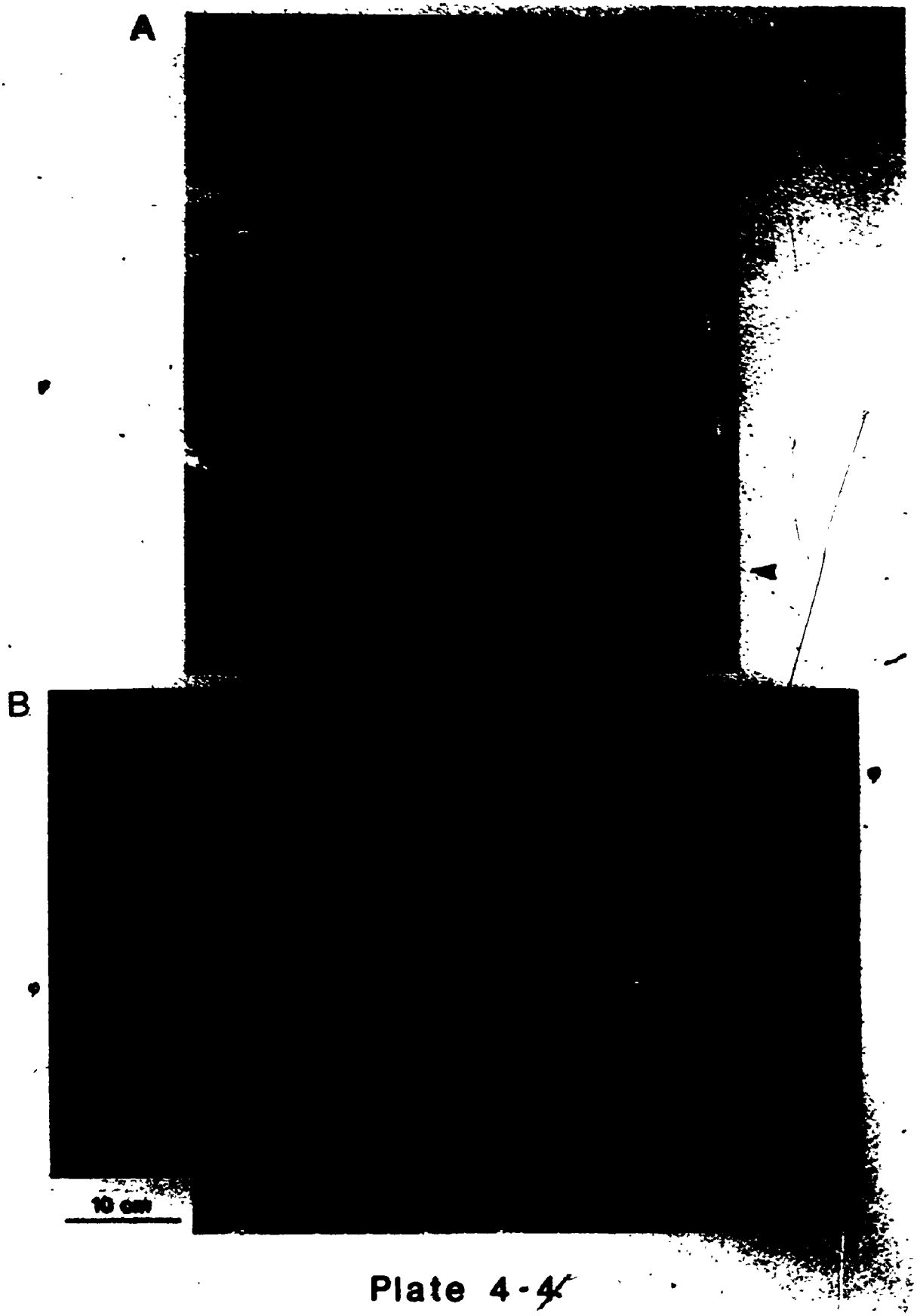

Plate 4-4

diamictic pellets. These fine-grained sequences may thus be interpreted as lower fan sediments or as proximal lake-bed sediments (see Walker, 1984).

4.3.2 Subaquatic outwash sediments

Unit B consists mainly of stratified sand in other investigated sections (Figure 4-12: sections MP-82-4, MP-79-15, MP-79-17, MP-79-5 and MP-80-2). Dominant lithofacies are cross-laminated and plane-laminated medium and fine sand at the Rivière Noire (MP-82-4) and Wotton (MP-79-5; Figure 4-13) localities; elsewhere, plane-bedded sand, trough-cross-bedded sand or pebbly sand, and graded sand and silt are more common lithofacies. Occasionally, these sandy sediments also contain diamictic beds that were deposited by sediment gravity flows; excellent examples of this were found at the Wotton (MP-79-5) and Notre-Dame-de-Ham (MP-79-17) localities.

These lithofacies assemblages are interpreted as subaquatic outwash sediments, mainly because there is ample evidence indicating that they were deposited in standing water by currents flowing toward southeast, thus in a direction opposite to that of modern drainage. Given the regional topographic context, this can only happen if glacial meltwater is introduced into a glaciolacustrine water body ponded by an ice-margin which is advancing toward south or southeast or which is retreating toward north or northwest. Moreover, these lithofacies assemblages closely resemble those of sediment bodies described as subaquatic fans deposited in a water body at the mouth of subglacial tunnels (Banerjee and McDonald, 1975) or as subaqueous outwash deposits (Rust and Romanelli, 1975; Rust, 1977).

The Wotton section (Figures 4-13 and 4-14) discloses several of the essential characteristics of subaquatic outwash sediments assigned to unit B. These glaciolacustrine outwash sediments underlie surface till (drift unit C) and have a maximum exposed thickness of only about 6 to 7 m; however the unit probably extends to a much greater depth. Exposed sediments consist mainly of alternating beds of plane-laminated and

cross-laminated (ripple-drift and climbing-ripple lamination; Plate 4-4B) medium and fine sand. Orientation measurements of cross-laminae cosets indicate that paleocurrent was toward southeast (Figure 4-14C). In pit C, near the base of the exposure, graded sand and silt layers (Plate 4-5A) are interbedded with cross-laminated sand but are absent higher in section.

This coarsening-upward trend, which is also present at the Rivière Noire and Notre-Dame-de-Ham localities, suggests that bodies of subaquatic outwash sediments prograded over more distal beds as ice which deposited drift unit C advanced southeastward into the region. Further evidence for increasingly proximal depositional environments toward the close of the glaciolacustrine episode is provided by the occurrence of a massive sand bed (sediment gravity flow; Plate 4-5B) and of debris flow units in the upper part of unit B at the Wotton locality; at Notre-Dame-de-Ham, a diamictic bed which is interpreted as a debris flow sediment also occurs near the top of unit B (Figure 4-12: section NP-79-17).

At the Bromptonville locality (section NP-80-2; Figure 4-17), plane- and cross-bedded sand and gravel beds which can now be seen underlying drift unit C are assigned to unit B mainly on the basis of previous observations by the author; during the summer of 1976, deltaic foreset beds, consisting of interbedded coarse gravel and sand layers and dipping toward southeast at an angle of about 30°, were exposed in the central part of this subtill sediment body. Unfortunately, these key sedimentary units were removed during subsequent gravel pit operations. The foreset beds are thought to have been deposited on a subaquatic delta fan, thus suggesting that stratified sand and gravel beds which are currently exposed were also deposited into a proglacial water body. This interpretation finds some support in the local occurrence of large, planar lenses of massive sand or silty sand (turbidites), particularly at the distal (southeast) end of the subtill sediment body. Alternatively, these sediments may have been deposited in a large water-filled subglacial cavity; this interpretation would suggest that the stratified sediments were deposited during glacial phase C rather than during the latter part of the previous interstade. However, subtill

Plate 4-5

A) Graded sand and silt layers within a sequence of plane- and cross-laminated sand near the base of subaquatic outwash sediments (unit B), Wotton section (MP-79-5: pit C). Convolute lamination indicates that intrastratal or syndepositional flowage was toward SE (right of photograph). Load structures are present at the top of the graded sand and silt unit (top of photograph). Pencil is 14 cm-long.

B) Till wedge at the base of drift unit C, Wotton section (MP-79-5: pit B). The SE-dipping till wedge extends to a depth of 1.8 m into subaquatic outwash sand of unit B (B-1 and B-2). The upper part of unit B consists of a large lens of massive fractured sand (B-2) which is interpreted as sediment gravity flow deposit. The upper lodgement till (C), which includes a thin basal zone of sheared silt lenses that also occur within the till wedge, was deposited by ice flowing toward SE (arrow). Staff is 1.6 m-long.

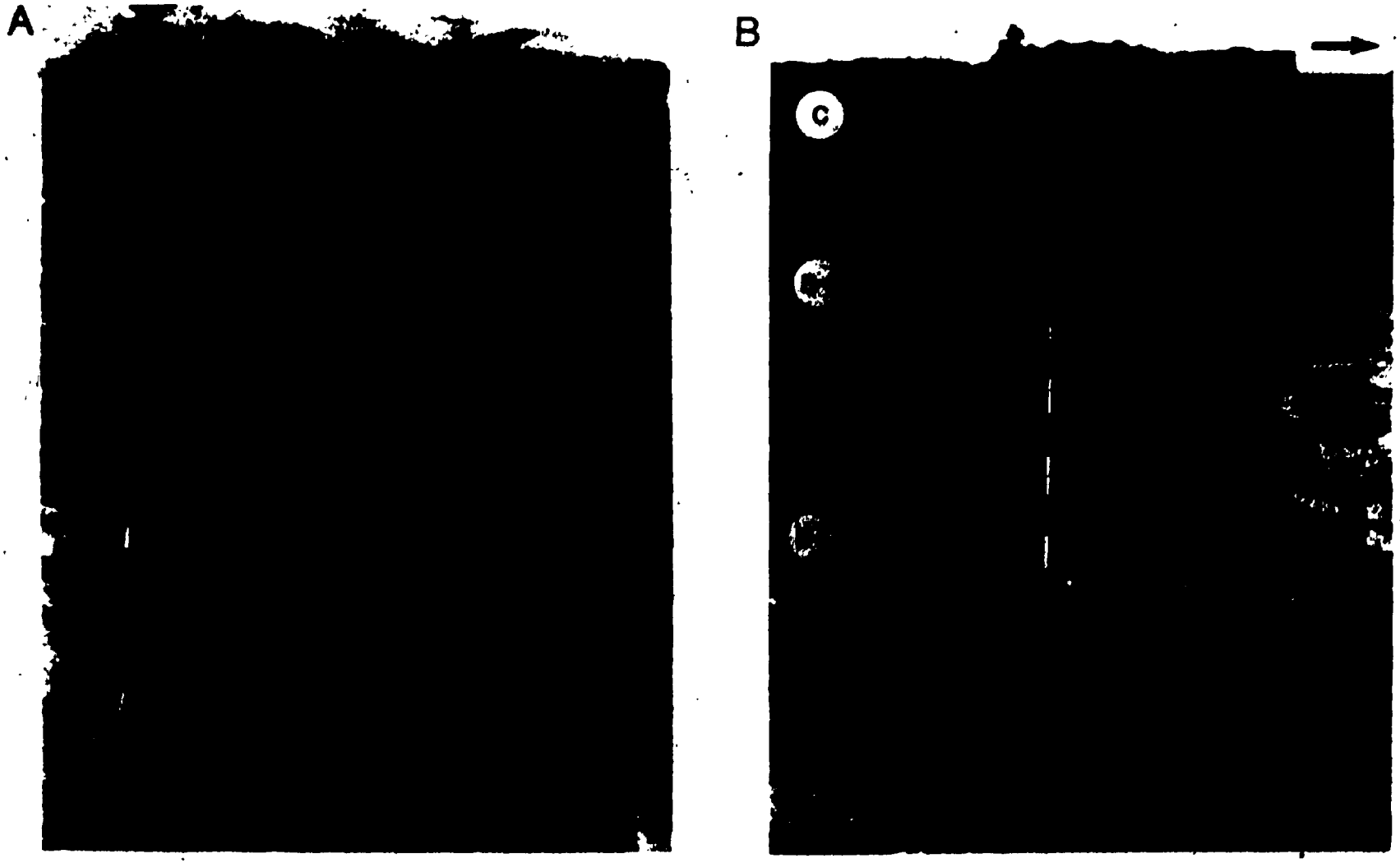

Plate 4-5

stratified sediments at Bromptonville are tentatively assigned to unit B, mainly because their origin compares well with that of sediments exposed at Wotton and other localities where straightforward evidence indicates that they were deposited in a proglacial lake by high-energy bottom currents which may have originated near the mouth of subglacial or englacial tunnels.

4.4 Drift unit C - Surface till

Characteristics of drift unit C were investigated in detail at all sections shown in Figures 4-1 and 4-12. The unit was also examined and sampled at over 200 surface till localities; while most of these localities are shown on the Ni dispersal map (see Figure 4-21), several others were examined or sampled outside of the limits of this main sampling area.

Because of its stratigraphic position, drift unit C is assumed to represent the regional surface till; however, this initial assumption was looked at as a simple working hypothesis and was thus repeatedly tested by means of site-specific and area-specific criteria. This approach was utilized at all localities shown in Figures 4-1 and 4-12. Section-to-section correlations shown in Figure 4-12 are the result of this work.

4.4.1 Norbestos section (MP-79-18; Figures 4-2, 4-3 and 4-4)

In subsection A, drift unit C consists of a single, 1.8 m-thick lodgement till sheet while in adjacent subsections B and C, the unit also includes a supraglacial till complex which has a thickness ranging between 1.1 m and 2.5 m and which overlies lodgement till (Figure 4-2). Although the basal contact of the lodgement till bed is sharp in all three Norbestos subsections, drift unit C appears to overlie conformably glaciolacustrine sediments of unit B; in fact, drift unit C does not show here a clearly erosional lower boundary.

However, the diamicton beds which are interpreted as lodgement till units rather than as debris flow sediments were investigated in detail and were found to contain several features which, when considered together, indicate a subglacial origin:

(1) the lodgement till unit, unlike debris flow diamictons previously described, does not appear to have an upper clast-size limit and it contains boulder zones whose level corresponds with that of apparent within-till shear planes (see Figure 4-2);

(2) till matrix has a distinctly planar fissility and, unlike fabrics reported from flow tills or debris flows (Boulton, 1971; Lawson, 1979), clast A/B planes were consistently found to have a strongly planar attitude dipping at a shallow (about 10°) angle in the same direction (toward north);

(3) during clast fabric measurements, the till was found to contain "break-away pebble fragments"; this newly coined term describes a situation where two flat-lying and perfectly matching fragments of the same till pebble are found, with an almost identical orientation but a few centimeters apart, at the same level in the diamicton; since it does not appear that there was any rotation of fragments about their A, B or C axes, it is inferred that a pebble fragment was simply broken off and dragged away for a short distance as a result of subglacial shear.

Lodgement till of drift unit C in the Norbestos section is a rather compact, fissile, olive to olive gray, generally oxidized and noncalcareous, matrix-dominated silty sand till. The till commonly shows textural layering that lies parallel to its subhorizontal fissility. Till matrix (-2.0 mm) has an average content of 55% sand, 34% silt and 11% clay; its average grain size mean (M_z) and sorting (σ_I) are 4.0ϕ and 3.0ϕ, respectively (Table 4-1; Figures 4-3 and 4-4). Matrix of this upper lodgement till unit is thus somewhat coarser than that of the

underlying lodgement till (drift unit A) and, as Figure 4-3 shows, its grain size composition is distinctly less variable.

In subsections B and C, lodgement till of drift unit C is overlain by loose, oxidized, crudely stratified, sandy to gravelly till; most commonly, this subunit consists of matrix-supported diamicton containing several lenses of waterlaid gravelly sand. Because the top part of subsections is usually slumped over at Norbestos, few distinctive sedimentary structures were clearly exposed. Nevertheless, this glacigenic material is interpreted as a supraglacial till complex which may include both melt-out and flow till layers in addition to lenses of poorly sorted glaciofluvial sediment. No features which may suggest a subaquatic origin were found within the subunit; it is thus suggested that these supraglacial sediments formed subaerially. Diamicton of this supraglacial complex is distinctly coarser-grained than that of the underlying lodgement till; a single diamicton sample was recovered from the subunit (sample #6 in section NP-79-18C) and was found to contain 68% sand, 24% silt and 8% clay (Figure 4-3).

In the absence of subtill glacitectonic deformations, directional data for drift unit C at Norbestos consist simply of till clast fabrics that were sampled in lodgement till at each of the three subsections (Figure 4-2). FT-25, FT-29 and FT-31 are type B fabrics showing preferred A-axis orientation (V_1) plunging toward north (N 008°, N 357° and N 345°, respectively) at angles of 16°, 13° and 19°, respectively (Table 3-1); clast A/B planes are also imbricated toward north at near-similar angles. These clast fabrics are thus interpreted as parallel fabrics indicating that lodgement till of drift unit C was deposited by a southward-flowing glacier.

The most significant compositional data for lodgement till of drift unit C were already discussed together with those of drift unit A (see section 4.2.1). Briefly, low Ni and Cr concentrations in the silt-clay fraction together with low percentage of ultramafic pebbles (0.3%) and "high" percentage of far-traveled Precambrian pebbles (2.0%) indicate that till of drift unit C has a northwest provenance, a conclusion which

is in close agreement with clast fabric data. Available heavy mineral and carbonate data (Table 4-1) seem to be of little use for differentiating tills of drift units A and C at Norbestos. On the other hand, it is tentatively suggested that the coarser-grained matrix of the upper lodgement till (drift unit C) may result from an increased content of sand-size debris derived from schistose rocks which lie northwest of the Norbestos section. By similar reasoning, slate-dominated bedrock that lies southeast of the ultramafic belt at Norbestos may explain the finer- grained matrix of the lower lodgement till (drift unit A) which was deposited by ice advancing from the east and, later, from the south.

4.4.2 Rivière des Rosiers section (MP-79-9; Figures 4-5 and 4-6)

In the Rivière des Rosiers section, drift unit C consists of three subunits: (1) a basal, brownish (2.5Y 6/2) lodgement till is overlain by (2) a thick, dark gray (5Y 5/1) lodgement till which is in turn overlain by (3) a series of three massive diamicton layers which are separated by thin sand layers and interpreted as subaquatic flow till units (Figure 4-5).

Both lodgement till beds consist of compact, fissile to massive, calcareous, matrix-dominated till; a sharply defined shear plane separates the lower, 50 cm-thick, brownish till bed from the overlying, 3.1 m-thick, dark gray till bed. The brownish till contains several pebble-size clasts of laminated silt and clay; because this till bed has a somewhat undulating lower boundary, its thickness may reach up to about 1 m. Matrix of this brownish till is distinctly finer-grained than that of the overlying dark gray till (Figure 4-5); sample #9 contains 22% sand, 51% silt and 27% clay and its mean (M_z) and sorting (σ_I) are 6.2φ and 2.9φ, respectively. The overlying dark gray till has a fairly uniform granulometric composition (Figure 4-5: samples #5 through #8); its matrix contains as average 53% sand, 27% silt and 20% clay and its average grain-size mean (M_z) and sorting (σ_I) are 4.7φ and 3.6φ, respectively. A few upsheared lenses of laminated silt and clay are present in the lower meter of the dark gray till bed.

Massive, dark gray, matrix-dominated diamictic layers which underlie glaciolacustrine turbidites (graded silt and clay couplets) at the top of the section closely resemble the underlying dark gray lodgement till; this is further reflected in compositional trends shown in Figure 4-5. However, these diamictons are interpreted as subaquatic flow till units because of the presence of intervening thin layers of massive sand and also because the wavy sand-diamicton contacts are parallel and distinctly non-erosional.

Two clast fabrics were measured within the dark gray lodgement till (Figure 4-6: FT-46 and FT-47). FT-46, which was sampled slightly above the basal shear plane, is a typical transverse fabric (type C); preferred A-axis orientation (V_1) is nearly horizontal, plunging at an angle of only 3° toward southwest (N 255°), while clast A/B planes have a strong preferred imbrication toward northwest (N 338°) at an angle of 11°. FT-46 thus indicates that the lower part of the dark gray till was deposited by ice advancing toward SSE. Transverse fabrics such as FT-46 are somewhat uncommon in lodgement tills; however, they may be formed by compressive stresses on the upglacier flank of subglacial obstacles (Boulton, 1971: p. 64). The presence of upsheared silt lenses at this level of the lodgement till bed indicates that there were indeed subglacial compressive stresses. The other till clast fabric (FT-47) was sampled near the top of the dark gray lodgement till bed. FT-47 is a type B fabric whose preferred A-axis orientation (V_1) plunges at an angle of 17° toward N 352°; clast A/B planes are also imbricated toward north (N 353°) at about the same angle (16°). FT-47 thus suggests that ice was still flowing more-or-less southward near the close of glacial phase C.

Southward to southeastward ice-flow is further corroborated by pebble lithology of drift unit C; as discussed earlier (see section 4.2.2), till of drift unit C contains abundant calcareous pebbles derived from the Bulstrode Formation which outcrops northwest of the section, but it contains no sandstone pebbles derived from nearby southeastern sources. Several Precambrian clasts were also found in drift unit C at this locality. Moreover, the dark gray colour of the main

lodgement till unit is characteristic of tills that overlie calcareous bedrock of the Bulstrode Formation on the adjacent Appalachian Piedmont. Very low Ni content (X = 19 ppm) and Cr content (X = 14 ppm) in tills of drift unit C provide negative evidence in favor of a north or northwest provenance; such low values suggest that drift unit C contains virtually no ultramafic debris that might have been transported from the ophiolite belt which is located only 10 km south of the Rivière des Rosiers section.

The origin of the brownish colour of the lower lodgement till bed is not known; however, since the unit contains 6.6% carbonates, which is as much as in the upper part of the overlying, dark gray, unweathered till, it may be tentatively suggested that the brownish colour is due to slight oxidation by groundwater, as in the upper part of drift unit A. In any event, the brownish lodgement till is interpreted as a local facies resulting from the incorporation of muddy glaciolacustrine sediments (unit B).

4.4.3 Willow Brook section (MP-76-1; Figures 4-7 and 4-8)

At the Willow Brook locality (Figures 4-7 and 4-8), drift unit C is the uppermost exposed lithostratigraphic unit and it consists of two subunits: a basal, vaguely stratified, rather pebbly till, which is interpreted as a subglacial melt-out till, is overlain by a typical lodgement till unit.

The subglacial melt-out till unit has a thickness of 2.1 m and directly overlies glaciolacustrine sediments of unit B; it consists of compact, gray (5Y 6/1), calcareous, pebbly, matrix-supported till containing a few sand lenses which have a maximum thickness of about 15 cm. This till unit is distinctly coarser-grained than the overlying lodgement till unit. Its matrix, for instance, contains an average 70% sand, 26% silt and 4% clay; this corresponds to an average grain-size mean (M_z) and sorting (σ_I) of 3.2φ and 2.2φ, respectively.

The overlying lodgement till has a thickness of 2.9 m and consists of compact, fissile matrix-dominated till; the till is yellowish brown (2.5Y 6/4) and oxidized above a depth of 1.7 m while it is olive gray (5Y 6/2) and calcareous below that depth. Vertical trend of carbonate content (Figure 4-8) suggests that the zone of leaching extends to a depth of about 2.3 m; below that zone, till of drift unit C contains an average 4% carbonates. Matrix of the upper till has an average content of 57% sand, 35% silt and 8% clay; average grain-size mean (M_z) and sorting (σ_I) are 3.9ϕ and 2.7ϕ, respectively.

Graded silty sand layers which immediately underlie drift unit C are cut across by small thrust faults which strike N 072° and dip 8° toward NNW; their throw ranges from 1 cm to about 3 cm. These subtill thrust faults were produced by an overriding glacier which was advancing toward SSE. Ice-flow toward SSE is also indicated by a till clast fabric which was sampled in the upper lodgement till. FI-16 is a type B fabric which shows preferred A-axis orientation (V_1) plunging at an angle of 9° toward N 345°; clast A/B planes are also closely imbricated at an angle of 9° toward N 341° (Figure 4-7). Ice-flow direction indicated by this till clast fabric and by subtill thrust faults is nearly parallel to the southeast trend of two small nearby drumlins (Figure 3-1); there is thus little doubt that ice-flow toward approximately southeast lasted throughout glacial phase C.

This conclusion finds additional support in the high Ni and Cr concentrations in the silt-clay fraction of both melt-out and lodgement tills (Figure 4-8); as mentioned earlier (section 4.2.3), drift unit C at Willow Brook has an average Ni content of 142 ppm and an average Cr content of 50 ppm. The section is within the head of the Asbestos ultramafic dispersal train (see Figure 4-21). Drift unit C also contains several ultramafic clasts as well as far-traveled Precambrian clasts.

4.4.4 Chemin des Ecossais section (MP-79-1; Figure 4-9)

At the Chemin des Ecossais locality, lodgement till of drift unit C has a thickness of 2.0 m and is overlain by late-glacial glaciolacustrine sediments which have a maximum thickness of 2.7 m (Figure 4-9). The lodgement till unit consists of compact, fissile, matrix-dominated till. Below the zone of leaching, at a depth of 4 m, the till is olive gray (5Y 6/2) and its silt-clay fraction contains 2.4% carbonates; above that depth, the till is olive (5Y 6/3) and non-calcareous. Several of the characteristics of this till unit were discussed previously (see section 4.2.4) and will not be repeated here. The till has unequivocal northwest provenance and this section is located well within prominent tails of the Asbestos ultramafic dispersal train (see Figure 4-21).

Southeastward ice-flow during glacial phase C is further confirmed by a till clast fabric (FT-20) sampled about in the middle of the lodgement till bed (Figure 4-9a). FT-20 is a type B fabric which shows strong preferred A-axis orientation (V_1) plunging at an angle of 10° toward NNW (N 343°); clast A/B planes also show a strong 10° imbrication toward NNW.

4.4.5 Rivière Noire section (MP-82-4; Figure 4-10)

Till stratigraphy of the Rivière Noire section (Figure 4-10) was described and discussed at some length in section 4.2.5; as earlier mentioned, till of drift unit C was extensively slump-covered and could not be properly investigated during the course of this study. However, for the purposes of further discussion, the following description of the upper till by McDonald (1967a: p. 143) may be added: "Till (Lennoxville): buff-brown and sandy near top, becoming darker brown and silt-rich toward base; non-calcareous; contorted sand lenses between depths of 13 and 15 feet, clasts of "varved" lake silts in basal, silt-rich, 2 feet of unit;". The lowermost 60 cm of drift unit C may therefore be interpreted as a local lodgement till facies resulting from subglacial incorporation of glaciolacustrine muds, while the overlying till (sample

f1) appears as typical, well-mixed, lodgement till. Till facies sequence in drift unit C at Rivière Noire thus closely resembles that observed in drift unit C at Rivière des Rosiers.

Southeastward ice-flow during deposition of the upper till at Rivière Noire is inferred from the southeastward trend of nearby crag-and-tail ridges and drumlins (Figures 3-1 and 4-10). A two-dimensional clast fabric which was sampled by McDonald (1960, 1967a) shows a strong A-axis maximum trending east-west and may be tentatively interpreted as a transverse fabric. In any event, the presence of small, subtill thrust faults dipping toward northwest suggests that the glacier which overrode glaciolacustrine sediments of unit B was advancing toward southeast during the early part of glacial phase C as well. Two of these small thrust faults could be measured at a depth of about 1 m below the base of drift unit C: respective strikes and dips are N 018°, 12° NW and N 030°, 26° NW (Figure 4-10).

4.4.6 Wotton section (MP-79-5)

The Wotton section is located well within the Outer Appalachian Uplands, about 3 km southeast of the Asbestos ophiolite complex (Figure 4-1). The section consists of three adjacent excavations which provide a good opportunity to study Pleistocene sediments underlying an upland till plain. Because of continued gravel pit operations, thickness and facies of exposed sediments show interesting changes from year to year; Figure 4-13 shows the section as it appeared during the summers of 1979 and 1980. Because the till plain surface lies several tens of meters above the level of adjacent streams, its edges have been somewhat dissected by postglacial gullying; this explains the rather abrupt topographic variations shown in Figure 4-13 as well as the occurrence of slope lag deposits.

For the purpose of present descriptions and discussions, pit A constitutes the main reference section; unless otherwise indicated, basic descriptions will refer to this main section and more specifically, to a vertical section which includes the location of FT-21. Two

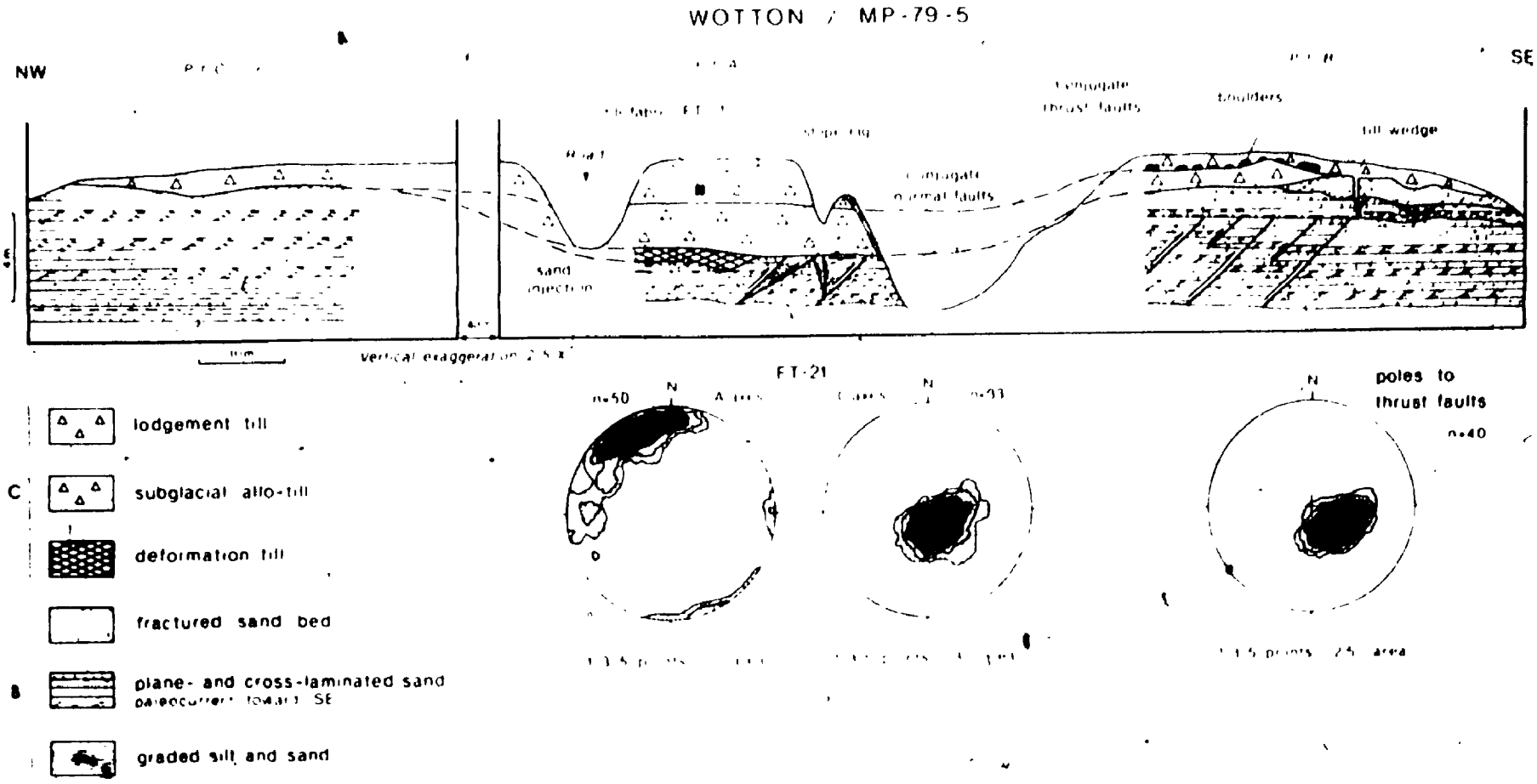

Figure 4-13 : Stratigraphy and lithofacies at the Wotton section (MP-79-5), showing lateral relationships of lithofacies units and glaciotectonic deformations. Contoured stereograms of poles to thrusts faults and of a till clast fabric are also shown.

main lithostratigraphic units are exposed in these three 8 m-deep borrow pits (Figure 4-13); from top to bottom, there are:

1) drift unit C, which consists of three main till facies (lodgement till, subglacial allo-till and deformation till);

2) unit B, which consists mainly of plane- and cross-laminated sands that are interpreted as subaquatic outwash sediments deposited in a proglacial lake.

Lodgement till of drift unit C is a compact, fissile, oxidized, yellowish brown (2.5Y 6/4), matrix-dominated sandy till. This till unit reaches a maximum thickness of 2.2 m in the main section but thins out to 1 m or less in adjacent pits. The till has a sharply defined lower boundary in the main section and has a distinctly erosional basal contact in adjacent pits; in pit B, the base of the lodgement till is marked by a boulder zone, that extends over a lateral distance of about 20 m. A few meters southeast of this boulder zone, a 2 m-deep, 40 cm-wide till wedge protrudes from the base of the lodgement till bed into the underlying glaciolacustrine sands (Figure 4-13; Plate 4-5 B). The till wedge strikes N 020°E and dips 75° toward ESE; its tapered lower end is slightly curved, a feature which is commonly observed in till wedges (Mörner, 1972, 1973; Humlum, 1978). The attitude and shape of the wedge constitute clear evidence that the overriding glacier was advancing toward southeast. A till clast fabric (FT-21), measured at a depth between 1.4 and 2.0 m (Figure 4-13), provides further evidence of southeastward ice-flow during deposition of the lodgement till unit. FT-21 is a type B fabric with preferred A-axis orientation (V_1) plunging at an angle of 18° toward northwest (N 332°); the attitude of C-axes indicates that clast A/B planes are also imbricated toward northwest (N 320°) with a near-identical, 16° dip (Figures 4-13 and 4-14 B).

Unlike the underlying till subunits, the upper lodgement till at Wotton has a well-mixed matrix and a well-mixed clast lithology, two features which are typical of the regional surface till. The till contains several ultramafic clasts and, although it is less pebbly than

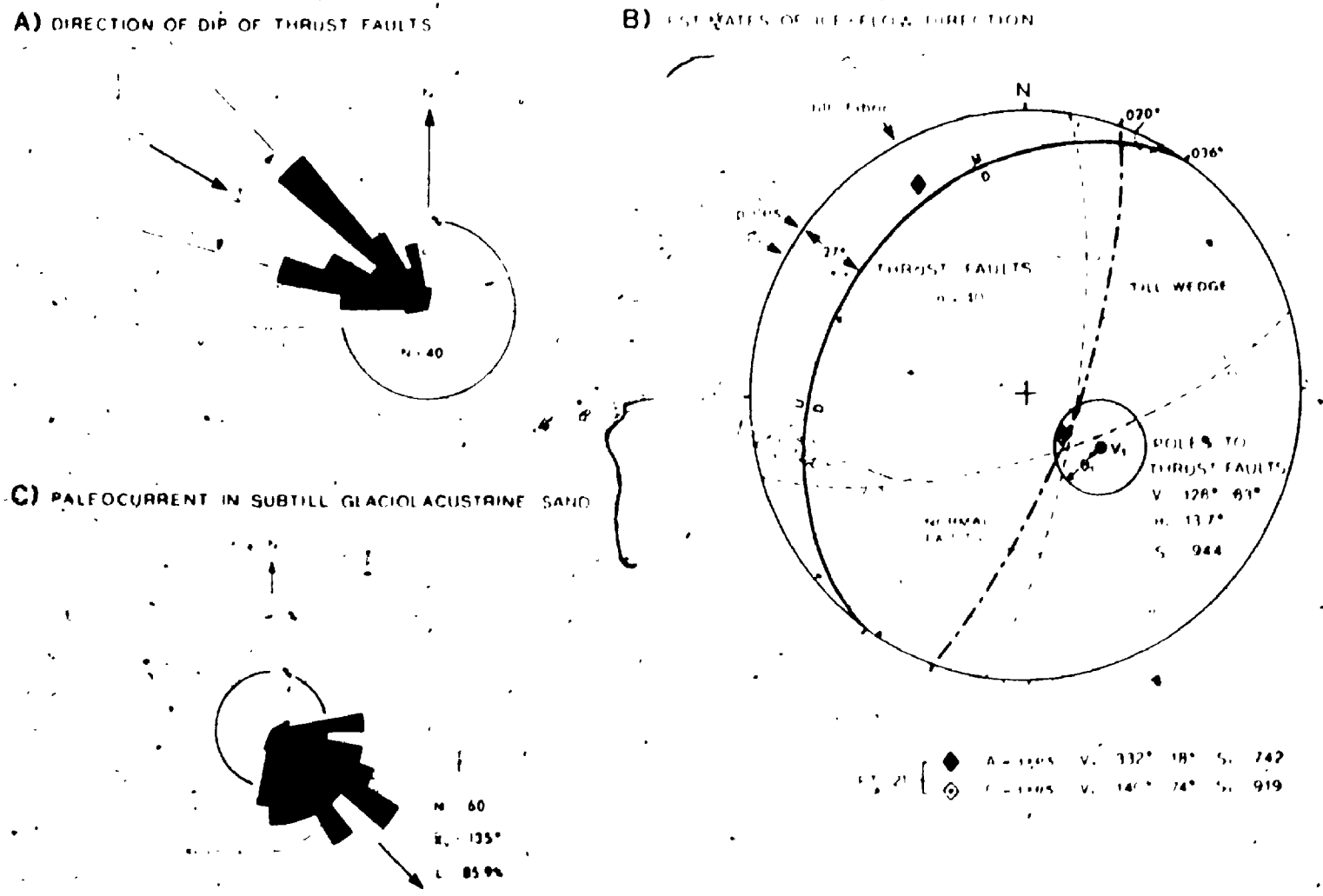

Figure 4-14 : Summary of orientation data for subtill glaciotectonic deformations (A and B), for till clast fabric measurements (B) and for subtill glaciolacustrine sand (C), Wotton section.

lodgement till beds observed at most other localities in the study area, it also contains a few Precambrian clasts. This, together with the fairly high Ni content (x̄=74 ppm) of its silt-clay fraction, indicates that it has a northwest provenance.

A large, lens-shaped body of glacigenic sediment which is interpreted as subglacial allo-till locally underlies the upper lodgement till sheet (Figure 4-13). The allo-till is also oxidized and it consists of substratified to massive, matrix-dominated sandy till. Its matrix has an average content of 69% sand, 26% silt and 5% clay; although it appears to be less well mixed, this compares well with the matrix of the overlying lodgement till (68% sand, 27% silt, 5% clay; M_z=3.3φ ; σ_I=2.2φ). In places, the allo-till contains abundant sheared silt clasts and lenses and may then be interpreted as a deformation till (Elson, 1981; Dreimanis, 1983) or as a local lodgement till; in other cases, the till contains sandy and silty lenses which show little or no deformations and may then be considered as a subaquatic melt-out till (Dreimanis, 1983). Several intergradational genetic types of till are likely present in this subunit and it seems preferable to simply call it a subglacial allo-till.

In the main section, the subglacial allo-till is underlain by a small, lens-shaped body of typical deformation till. This brecciated material contains clasts of massive and substratified till as well as clasts of laminated silt and silty sand together with admixed foreign stones, much as that described by Elson (1961, 1981). The deformation till unit has an erosional basal contact below which SE-dipping extension fractures and wedges can be seen extending into glaciolacustrine sand of unit B (Figure 4-13; Plate 4-6A). These small extension fractures form a conjugate set whose attitude seems similar to that of a nearby set of conjugate normal faults (Figure 4-14B). These fractures and wedges can be seen to intersect NW-dipping shear fractures; this confirms the subglacial origin of these subtill fractures and thus of the overlying deformation till and allo-till as well.

Plate 4-6

A) Erosional contact between deformation till (drift unit C) and underlying glaciolacustrine sand (unit B), Wotton section (MP-79-5: pit B). Notice that SE-dipping extension fractures and wedge cut across NW-dipping shear fractures. Ice flow toward SE (arrow).

B) Thrust faults in glaciolacustrine sand of unit B, Wotton section (MP-79-5: pit C). Notice that thrust faults die out in very fine sand beds (top end of staff) which are locally densely fractured and which probably acted as décollement planes. Staff divisions are 30 cm-long. Ice flow toward SE (arrow).

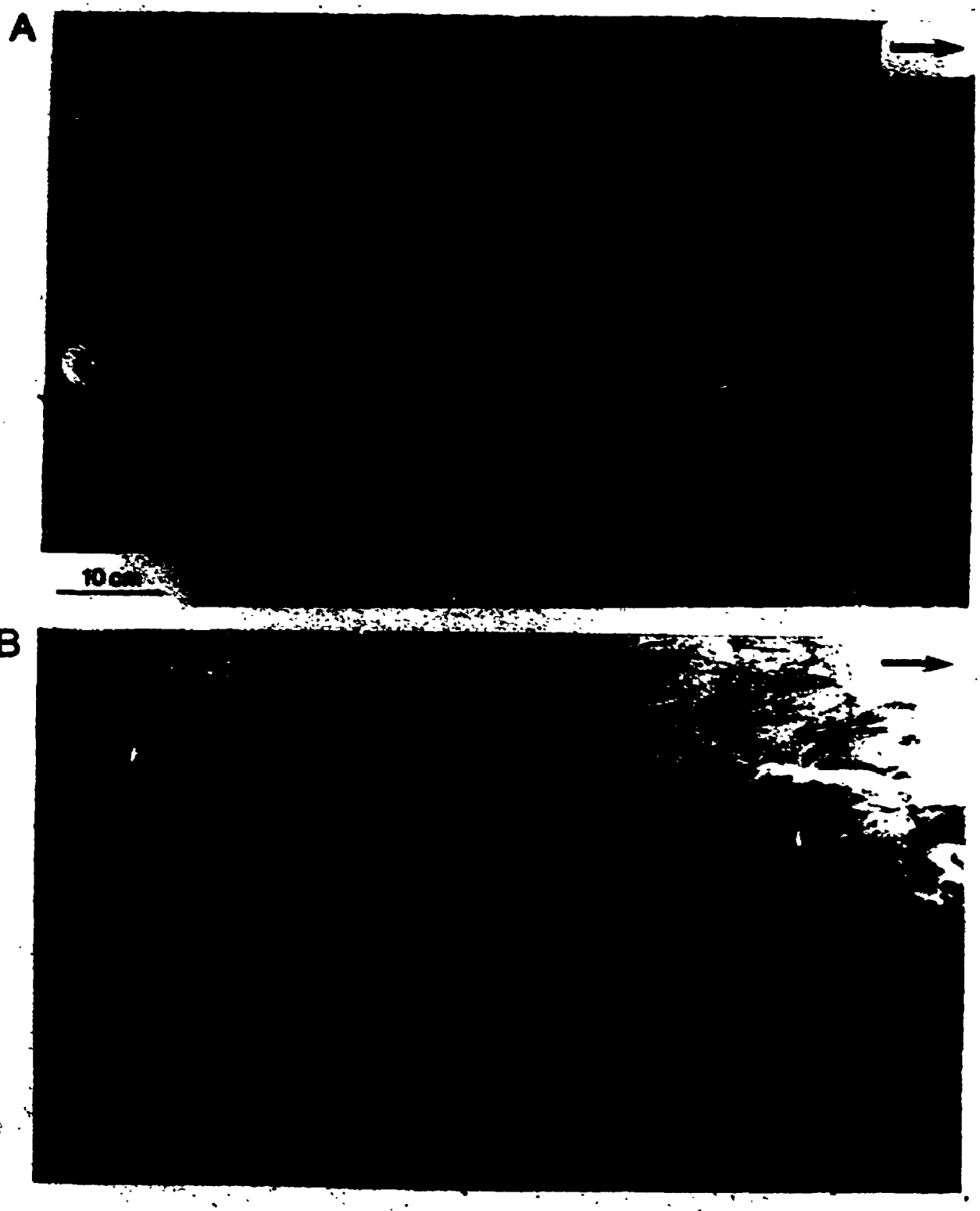

Plate 4-6

In pits A and B, subtill glaciolacustrine sands are intersected by a series of closely-spaced thrust faults (Figure 4-13; Plate 4-4B). None were seen in pit C where the upper lodgement till directly overlies these laminated sands along an erosional, but otherwise featureless, basal contact. Several thrust faults were observed to "die out" in finer-grained beds (ripple-laminated very fine sand; Plate 4-6B) which may have acted as décollement planes. Observed throws vary between only 1 and 25 cm; thrust slices thus appear to have undergone only minor forward displacement. The faults were observed and measured in exposure faces trending in a variety of directions; no relationships were found between their attitude and exposure face or location. This is further confirmed by the fact that poles to thrust faults are tightly clustered about a mean axis (V_1) plunging 63° toward N 126° (Figures 4-13 and 4-14B). The 40 thrust faults that were measured thus have a preferred strike of N 036° and a preferred dip of 27° toward northwest. This indicates that the overriding glacier was advancing toward southeast. Moreover, the 27° dip indicates that the major shear stress (σ_1) was nearly horizontal, much as that expected from subglacial drag.

Further analysis of the attitude of thrust faults reveals that their strikes form a conjugate set rather than a parallel set. This is shown in Figure 4-14 A where dip directions are clustered into two main modes trending N 285° and N 315°, thus with a dihedral angle of 30°. Maximum principal shear stress, as inferred from this simple diagram, was directed toward N 120°, which compares very well with the direction (N 126°) determined by the eigenvalue method (V_1). More importantly, this analysis reveals that the intermediate principal stress (σ_2) was subvertical, thus suggesting that thrust faults were formed at a fairly large confining pressure (at low confining pressures, it is the minimum principal stress (σ_3) which is expected to have a subvertical direction). These thrust faults were thus probably produced under a fairly substantial ice thickness.

The till wedge in pit B intersects an intensely fractured (shear fractures), massive sand bed as well as the already discussed NW-dipping thrust faults in the underlying laminated sands (Plate 4-5B; Figure

4-13). This indicates that subglacial tensional stresses were subsequently transmitted into the glaciolacustrine sand body. The brecciated material (deformation till) which fills in the wedge is in structural continuity with the basal "layers" of the lodgement till bed, indicating that at least part of the subglacial debris load was not frozen. This may also suggest that the subtill sand body was not frozen during formation of the thrust faults, a suggestion which finds additional support in the presence of a thin, presumably upsheared, silt layer along some of the fault planes.

4.4.7 Notre-Dame-de-Ham section (MP-79-17)

The Notre-Dame-de-Ham section (MP-79-17) is located on the southwest flank of the upper Rivière Nicolet valley (Figure 4-1); this site thus lies within the Outer Appalachian Uplands, near the southwest extremity of the Notre-Dame Mountains. The section is exposed in a small borrow pit excavated along the edge of an upland till plain which, as with the Wotton locality, has been dissected by postglacial gullying. At this locality however, the till plain surface is capped by small till ridges and intervening ice-marginal channels formed during the last deglaciation.

In the 16 m-deep borrow pit, lodgement till of drift unit C overlies sandy glaciolacustrine sediments (Figure 4-15). The latter unit (B) consists of graded sand and silt layers which grade upward into plane-bedded medium sand. Unit B also includes a 70 cm-thick bed of sandy matrix-supported diamicton which contains a few flowage structures and which shows overall grading; the diamicton unit is interpreted as a debris flow sediment.

The upper 5 m of the lodgement till unit consist of compact, fissile, oxidized, olive to olive gray (5Y 6/3, 6/2), matrix-dominated, silty sand till which contains a few thin, discontinuous sand lenses. This well-mixed lodgement till sheet is underlain by a 0.9 m-thick bed (or lens?) of rather sandy lodgement till which contains upsheared silt lenses and which is interpreted as local lodgement till. The two till

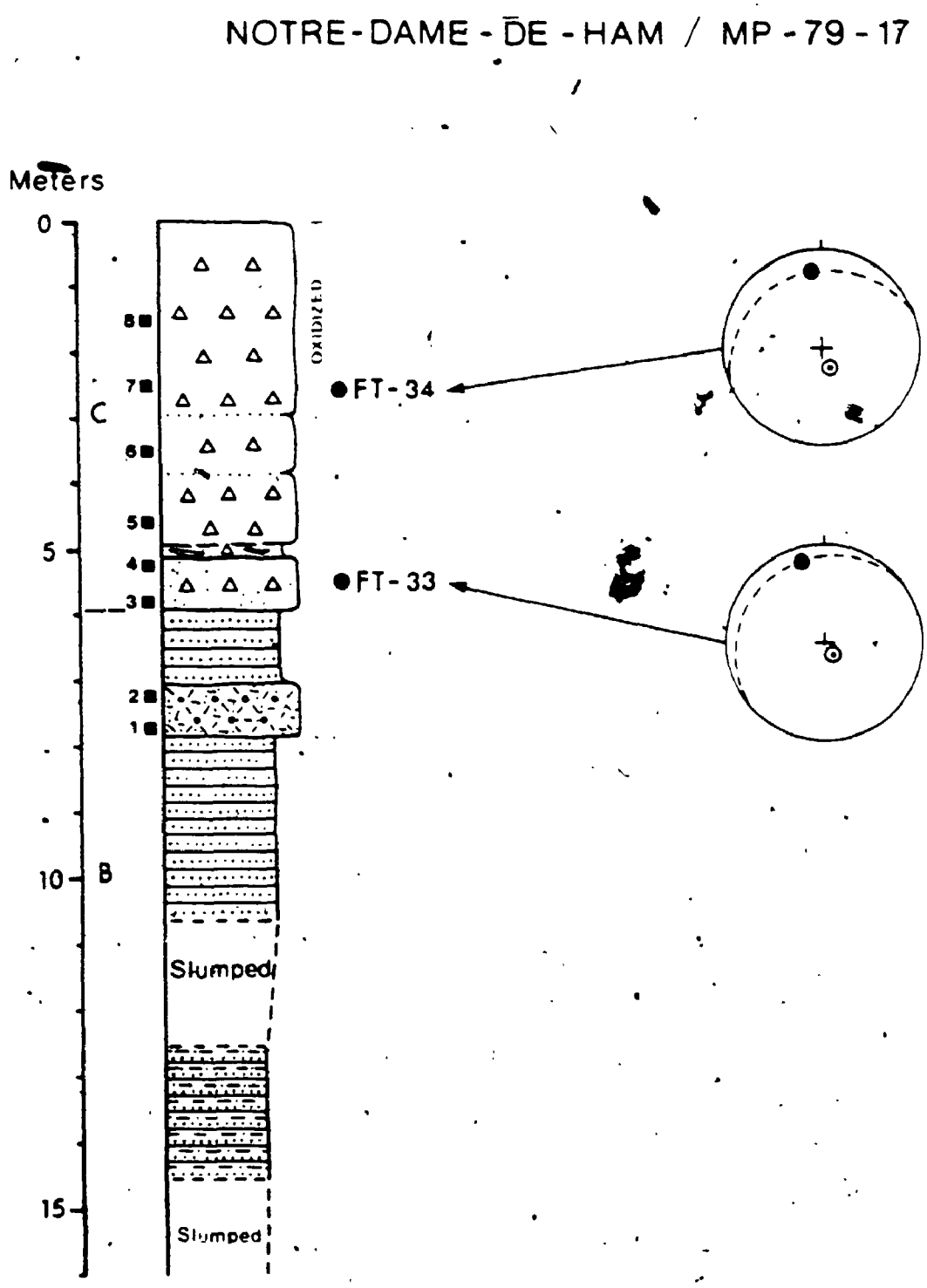

Figure 4-15 : Stratigraphic log and till clast fabrics, Notre-Dame-de-Ham section (MP-79-17). (See legend in Figure 4-12)

units are separated by a distinctive, 25 cm-thick till layer containing sandy lenses and which may be interpreted as a shear zone. Only the lower till bed is below the zone of weathering; its silt-clay fraction contains about 3% carbonates.

Matrix of the lower, local lodgement till bed contains an average 69% sand, 25% silt and 6% clay, which corresponds to an average grain-size mean (M_z) and sorting (σ_I) of 3.3φ and 2.4φ, respectively. Matrix of the upper lodgement till is better mixed and somewhat finer-grained; it contains on average 59% sand, 35% silt and 6% clay, and its mean (M_z) and sorting (σ_I) are 3.8φ and 2.4φ, respectively. Sub-glacial incorporation of glaciolacustrine sand during the early part of glacial phase C likely produced the coarser grain-size of the local lodgement till unit.

This is to some extent corroborated by the fact that the lower till bed has a heavy mineral content ($\bar{x}$=5.1%) which is about intermediate between that of the underlying debris flow unit ($\bar{x}$=5.7%) and that of the overlying lodgement till unit ($\bar{x}$=3.9%). Other compositional attributes show rather uniform trends within tills of drift unit C; this suggests that there were no significant changes of provenance during till deposition. Average magnetic mineral weight is about 7.8% while average Ni and Cr contents are about 15 and 11 ppm, respectively. Such low Ni and Cr contents indicate that drift unit C contains virtually no ultramafic debris: given the location of section MP-79-17 relative to ultramafic outcrops (see Figure 4-1), this suggests that drift unit C has a northwest provenance.

Till clast fabrics were measured in both till beds (Figure 4-15). FT-33 and FT-34 are both type B fabrics which show preferred A-axis orientation (V_1) plunging toward northwest (N 344° and N 352°, respectively) at angles of 13° and 21°, respectively; clast A/B planes are also imbricated toward northwest. These two parallel fabrics thus indicate that tills of drift unit C were deposited by ice that advanced toward more-or-less southeast; the fabrics further suggest that southeastward ice-flow was maintained throughout glacial phase C.

4.4.8. Tingwick section (MP-79-15)

The Tingwick section (MP-79-15) is located about 10 km southeast of the northwest edge of the Outer Appalachian Uplands (Figure 4-1). The section is exposed in a small borrow pit excavated into the left (southwest) flank of the Rivière des Pins valley. In the vicinity of the section, the river is entrenched to a depth of about 20 m into a till plain which is locally overlain by ice-contact stratified drift (see Figure 3-1).

In the 20 m-deep borrow pit, subaquatic outwash sediments of unit B are overlain by lodgement and melt-out tills of drift unit C (Figure 4-16). Because of a thick slump cover at the base of the section, the lower 11 m could not be properly investigated. However a few test pits that were dug out indicate that glaciolacustrine sands extend at least to the level of the pit floor. The upper few meters of unit B as well as the contact with the overlying lodgement till bed were well exposed over about 30 m laterally.

Lodgement till of drift unit C has a thickness of 3.9 m and consists of very compact, fissile, brownish gray (2.5Y 6/3), calcareous, matrix-dominated silty sand till. It is overlain by loose, oxidized, yellowish brown (2.5Y 6/4), massive, matrix-supported sandy till which is interpreted as a supraglacial melt-out till. The contact between the two till subunits is sharply defined by the colour change as well as by contrasts of till compaction and grain-size. Matrix of the lower lodgement till contains an average 54% sand, 33% silt and 13% clay and its average grain-size mean (M_z) and sorting (σ_I) are 4.2φ and 3.0φ, respectively. The overlying melt-out till has a somewhat coarser matrix containing 63% sand, 24% silt and 13% clay; this corresponds to a grain-size mean (M_z) of 3.8φ and to a sorting (σ_I) of 3.1φ.

Several southeast-dipping till injections are present along the basal contact of the lodgement till bed; the largest one consists of a 60 cm-deep, 15 cm-wide, dike-shaped till wedge which protrudes, without any discontinuity, from the base of the lodgement till bed (Figure 4-16;

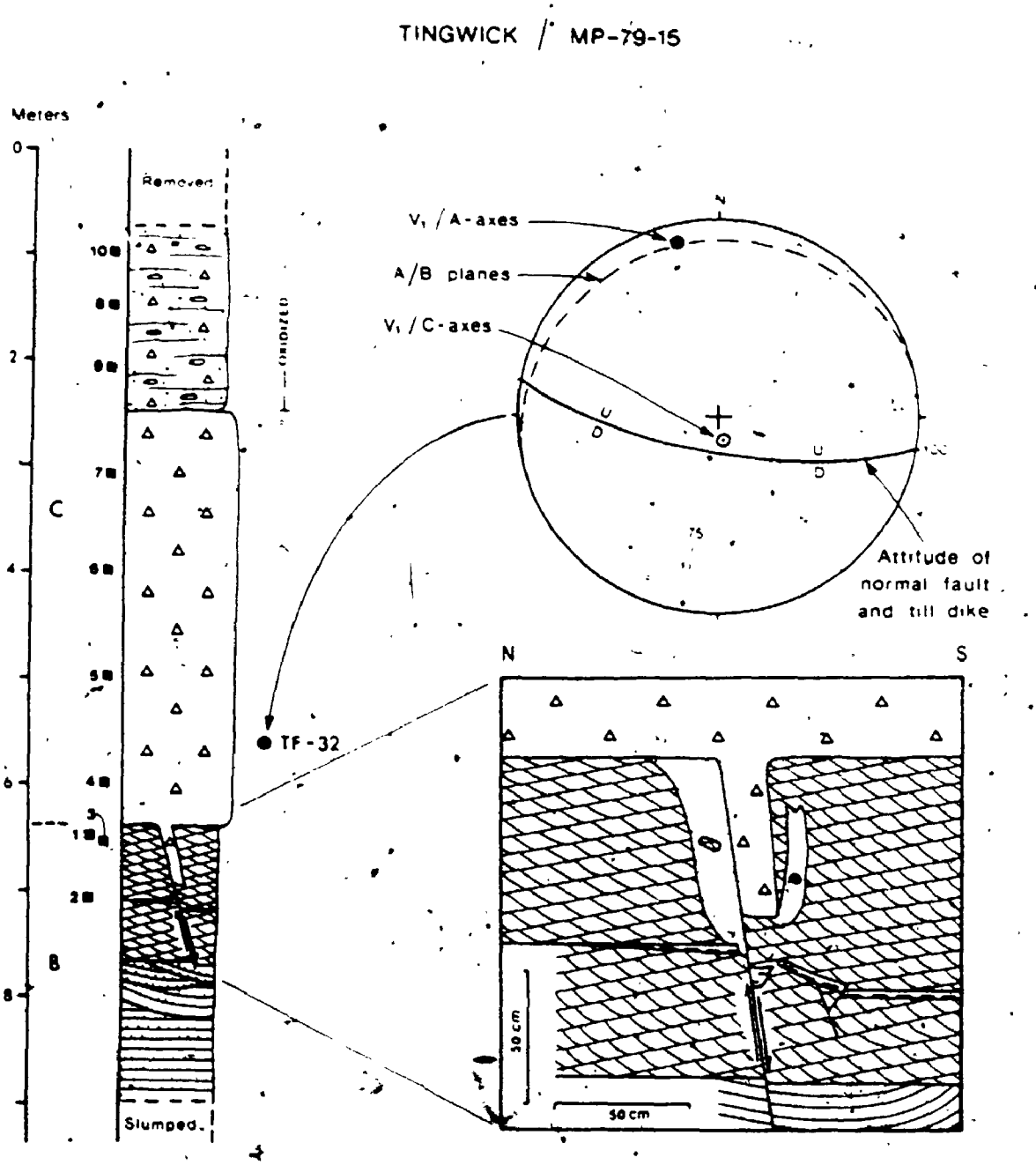

Figure 4-16 : Stratigraphic log and till clast fabric, Tingwick section (MP-79-15). Also shown are the attitude and a close-up sketch of a till dike at the base of drift unit C. (See legend in Figure 4-12)

Plate 4-7A). A normal fault with a downthrow of only 2.5 cm extends downward from the north edge of the till wedge into subtill glaciolacustrine sand; it strikes N 100° and dips 75° toward south. This also gives the attitude of the till wedge. Field relationships (see inset of Figure 4-16) indicate that formation of the till wedge and of the normal fault is coeval; subglacial shear toward the south caused extension (normal fault) of glaciolacustrine sands which also slipped forward along a plane of décollement (silt lens), at which time the till wedge was instantaneously injected. Subsequent build-up of subglacial hydrostatic pressure caused the obliteration of primary sedimentary structures (cross-lamination) within a narrow zone on the upglacier (north) side of the rather impervious till wedge; release of hydrostatic pressure under the wedge in turn produced the flame structure observed on the lee side of the till wedge.

Subtill glacitectonic deformations at this locality were clearly produced by southward-flowing ice. This is further corroborated by a till clast fabric measured about 1 m above till base. FT-32 is a type B fabric which shows preferred A-axis orientation (V_1) plunging toward N 347° at an angle of 9°; clast A/B planes are also imbricated toward NNW (Figure 4-16).

Lodgement and melt-out till subunits both contain several Precambrian clasts; this suggests a northwest provenance for drift unit C at the Tingwick locality. The melt-out till subunit also contains several clasts of red slate that are likely derived from the belt of Granby Group rocks which outcrop about 25 km northwest of the section. The 6.5% average carbonate content of the silt-clay fraction of the underlying lodgement till subunit suggests that calcareous debris were transported at least 10 km southeast of the Bulstrode Formation outcrop belt. Other measured compositional attributes provide little direct evidence for assessing till provenance. Heavy mineral content and magnetic mineral content average 4.55% and 9.64%, respectively, and are quite uniform throughout drift unit C; uniformly low Ni ($\bar{X}$=22 ppm) and Cr ($\bar{X}$=13 ppm) contents indicate that no ultramafic debris were transported northward to the Tingwick locality during glacial phase C.

Plate 4-7

A) Dike-shaped till wedge protruding from the base of lodgement till (drift unit C) into glaciolacustrine sand of unit B, Tingwick section (MP-79-15). Notice the zone of obliterated lamination (quick sand) on the upglacier side of the till wedge and the flame structure on the down-glacier side. Ice flow toward S$E.

B) Small till wedge protruding from the base of lodgement till (drift unit C) into subaquatic outwash sandy gravel (unit B, Bromptonville section (MP-80-2). Ice flow toward SE.

Plate 4-7

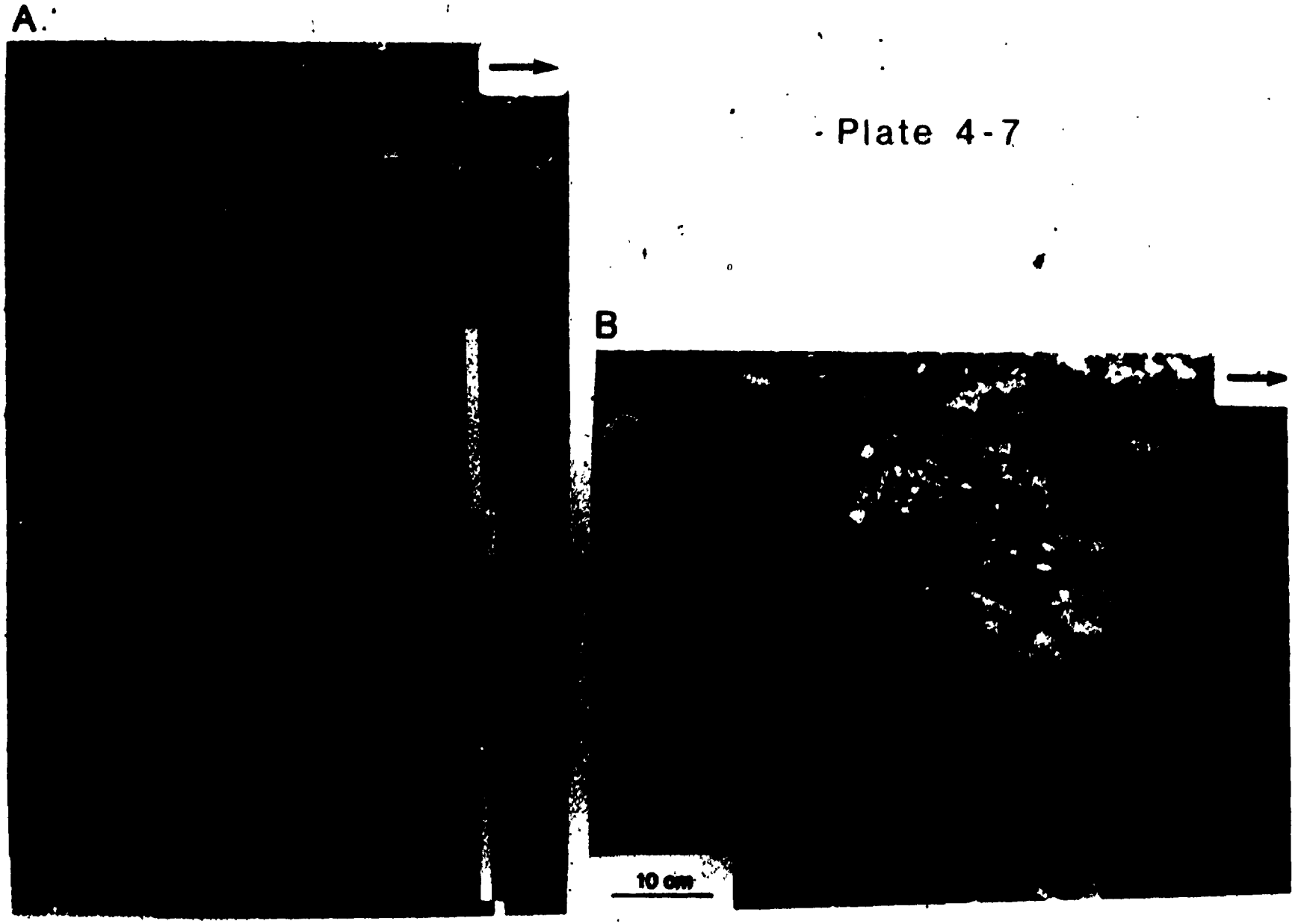

4.4.9 Bromptonville section (MP-80-2).

The Bromptonville section (MP-80-2) is located in a gravel pit excavated within the core area of a small SE-trending drumlin (Figure 4-17). This drumlin is one of a few streamlined subglacial landforms that occur on low uplands east of the middle Saint-François River valley (see Figure 3-1); there is little doubt that these streamlined features were formed during glacial phase C. During the summer of 1980, the northeast face of the pit provided an almost continuous, 250 m-long, 8 to 10 m- high section along one flank of the drumlin.

In section MP-80-2, a sheet of lodgement till, which is locally underlain by lenses of substratified till, overlies stratified sand and gravel beds that are assigned to unit B. As mentioned earlier (section 4.3.2), these subtill stratified sediments are interpreted as subaquatic outwash sediments; they were deposited in a proglacial water-body, by southeastward currents that were presumably issued from subglacial or englacial streams as ice advanced southeastward into the region. High shear strength and permeability of this outwash sediment body may be factors that favored subsequent drumlin formation (Menzies, 1979).

Lodgement till of drift unit C was closely inspected in six well-exposed subsections (A through F in Figure 4-13); it generally consists of fairly compact, fissile, massive, olive to olive gray, sandy silt till. Its basal contact is sharp and erosional in four of the subsections (A, B, C, E); in subsection C, a small, SE-dipping till wedge which protrudes from the base of the till sheet into slightly deformed gravel beds (Plate 4-7B) provides independent evidence of southeastward ice-flow. Elsewhere, subtill sediments seem undeformed. In subsections D and F, the till unit has a sharp but conformable basal contact and its lower part, which is substratified, may consist of subglacial melt-out till. In subsection A, at the upglacier end of the drumlin, the lodgement till bed is underlain by a 2 m-thick, lens-shaped unit of coarse substratified till which contains numerous striated boulders and large cobbles. This till unit, which locally contains clast-supported lenses as well as a few waterlaid gravel lenses, is tentatively interpreted as

BROMPTONVILLE

/ MP-80-2

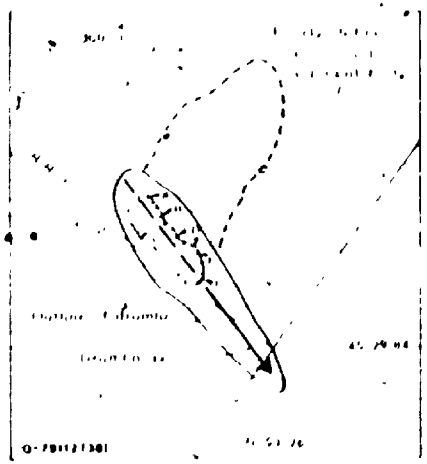

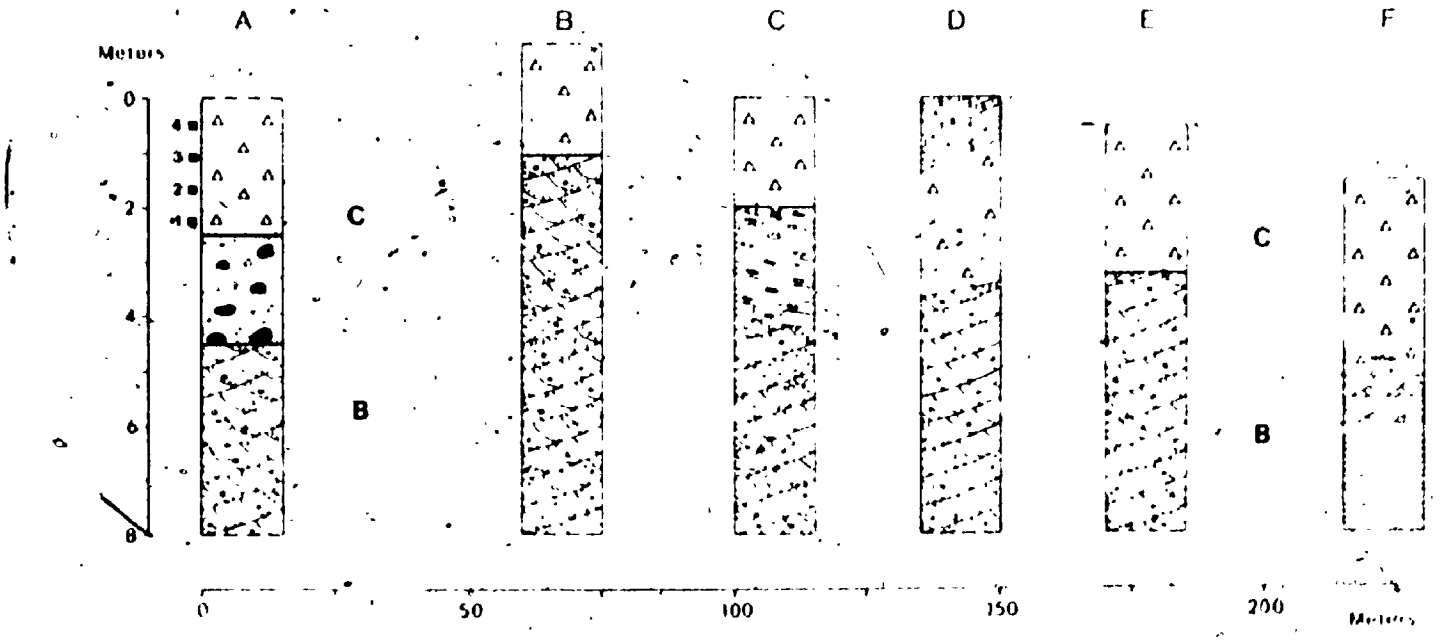

Figure 4-17 : Stratigraphic logs and lateral facies changes within a drumlin near Bromptonville (section MP-80-2). (See legend in Figure 4-12)

a subglacial clay-till. Few features were found that can further clarify its origin; a subglacial origin is inferred because of its stratigraphic position and also because of the occurrence of SE-trending striations on the top surface of some boulders.

Drift unit C contains several Precambrian and ultramafic clasts; this indicates that it has a northwest provenance. Four samples which were taken in lodgement till at subsection A indicate that the unit has a fairly uniform matrix composition. Till matrix contains an average 46% sand, 41% silt and 13% clay and its grain-size mean (M_z) and sorting (σ_I) average 4.5φ and 2.9φ, respectively. Although the unit is generally thoroughly oxidized, the silt-clay fraction of the lowermost till sample, at a depth of 2.3 m, still contains 4% carbonates. The fine sand fraction of the till contains an average 3.3% heavy minerals; this compares well with that of the upper till sheet at the nearby Chemin des Ecossais locality (MP-79-1). However its magnetic mineral content (x=11.7%) is somewhat lower.

Fairly high Ni ($\bar{x}$=73 ppm) and Cr ($\bar{x}$=28 ppm) concentrations in the silt-clay fraction indicate that drift unit C contains ultramafic debris that is likely derived from outcrops located some 20 km northwest of section MP-80-2 (Figure 4-1). Moreover, regional geochemical sampling indicates that this section is located within a prominent SE-trending tail of the Asbestos ultramafic dispersal train (see Figures 4-21 and 4-22 A).

4.4.10 Arthabasca section (MP-79-14)

The Arthabasca section (MP-79-14) is located on a small bedrock-controlled bench lying on the lower slopes of the northeast flank of the Rivière Nicolet valley (Figure 4-1). Although this site is located within the Outer Appalachian Uplands, it lies only about 1 km from the southeastern limit of the Appalachian Piedmont. Because drift unit C is the only exposed lithostratigraphic unit, this section has not been included in the correlation diagram (Figure 4-12). However this locality is an important one as it may serve as a reference section for a

reddish-brown surface till unit which is quite common in the vicinity of Victoriaville, both near the edge of the Outer Appalachian Uplands and on the adjacent Appalachian Piedmont.

Section MP-79-14 shows two sheets of brown (10 YR 5/3), sandy lodgement till that are separated by a 0.8 m-thick unit of stratified drift and flow till (Figure 4-18). The unusually reddish hue and sand-dominated matrix of these tills are outstanding field characteristics. The lower lodgement till unit has a thickness exceeding 2.4 m and consists of very compact, fissile, brown, slightly calcareous, matrix-dominated, silty sand till. The upper 30 cm contains a few sheared sand stringers that rise toward SE. Till matrix is well-mixed and contains on average 76% sand, 21% silt and 3% clay; its average grain-size mean (M_z) and sorting (σ_I) are 2.9φ and 1.9φ, respectively.

The overlying, 0.8 m-thick unit is best described as an assemblage of flow till and ice-contact stratified drift. Most commonly, the unit consists of brown, substratified, matrix-supported sandy diamicton containing numerous lenses and pods of stratified medium sand; since these waterlaid inclusions have been slightly deformed by flowage rather than by shearing, the enclosing diamicton is considered as a flow till. In other parts of the borrow pit, this unit consists of stratified sand and gravelly sand containing abundant lenses of brown flow till. A single sample (#4) taken from a flow till layer was found to contain 83% sand, 14% silt and 3% clay.

The upper till bed has an observed thickness of 1.4 m, to which should be added about 50 cm of removed solum; it consists of compact, massive, brown, oxidized, matrix-dominated sandy till. Basal contact of the unit is sharp. Matrix of this till is also well-mixed and has an average content of 85% sand, 13% silt and 2% clay; its average grain-size mean (M_z) and sorting (σ_I) are 2.3φ and 1.6φ, respectively. The upper till bed is thus somewhat coarser-grained than the lower one.

Till clast fabrics were measured in each of the two till beds. FT-35 is a transverse (type C) fabric that was measured in the lower

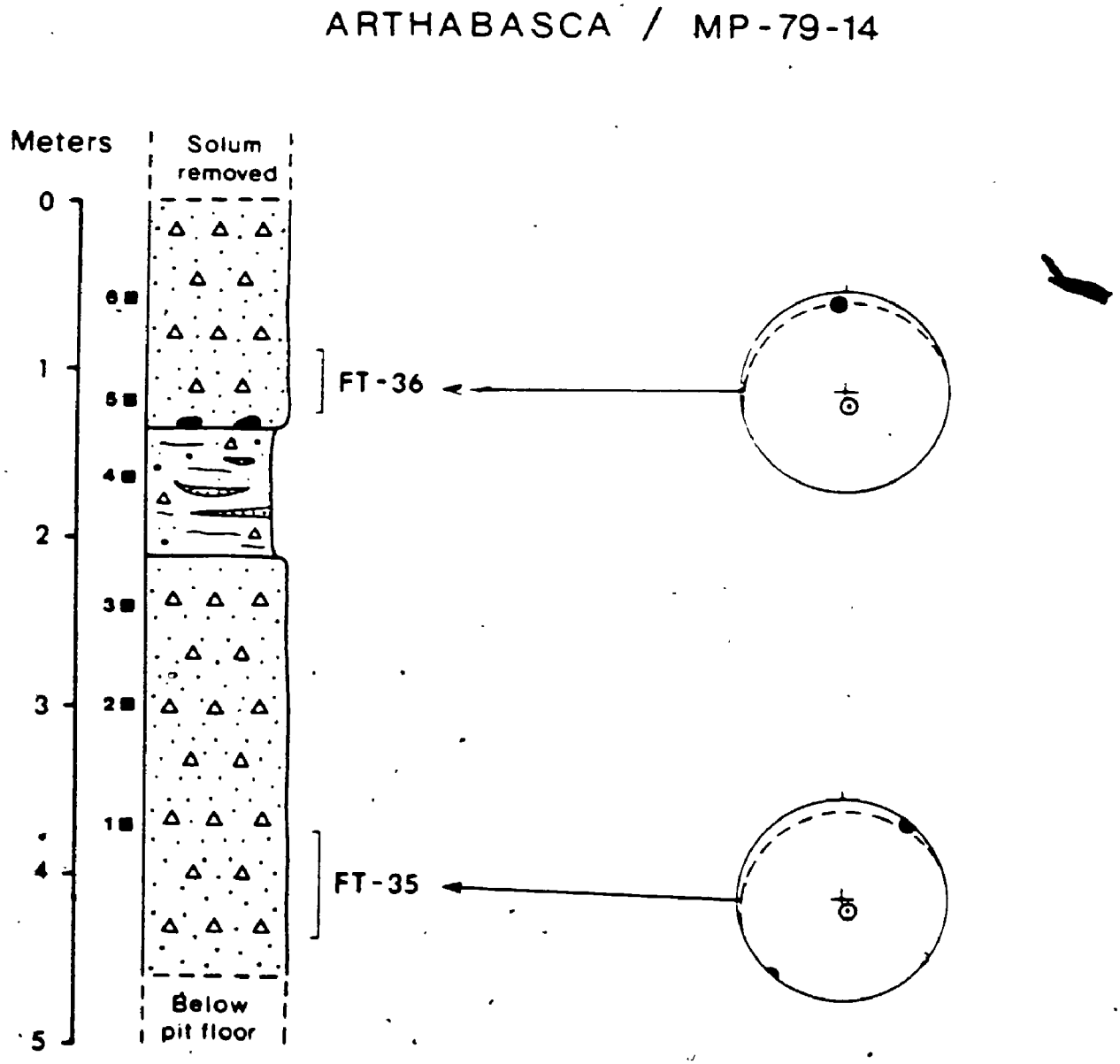

Figure 4-18 : Stratigraphic log and till clast fabrics, Arthabasca section (MP–79–14). (See legend in Figure 4-12)

till; preferred A-axis orientation (V_1) plunges at a very shallow 5° angle toward northeast (N 038°) while clast A/B planes are imbricated at a preferred angle of 11° toward northwest (N 347°). FT-35 thus suggests that the lower lodgement till was deposited by ice that advanced from northwest. As discussed earlier (section 4.4.2), transverse fabrics such as FT-35 may form as a result of compressive stresses transmitted into till on the stoss side of subglacial bosses; this is a situation that applies particularly well to the Arthabasca site which is located less than 1 km northwest of a large strike ridge that obstructs the course of the Nicolet River valley.

FT-36, which was measured in the upper till bed, is a type A fabric with preferred A-axis orientation (V_1) plunging at a non-significant, 11° angle toward north (N 356°). However clast A/b planes do have a strongly preferred imbrication that dips at a significant 9° angle toward NNW (N 341°). FT-36 is therefore interpreted as a parallel fabric and thus suggests that the upper lodgement till was also deposited by ice that advanced from approximately northwest.

Both reddish-brown till beds contain several northwest-derived Precambrian clasts as well as abundant clasts of red and green slate that are most likely derived from bedrock sources (Granby Group: map-unit #7 in Figure 2-1) which outcrop less than 12 km northwest of the Arthabasca locality. Since Granby Group rocks and equivalent units (Sillery Group) also contain abundant sandstone beds (Globensky, 1978; Clark and Globensky, 1973), it is further inferred that the high sand content of the reddish-brown tills at Arthabasca and at other nearby localities very likely owes its origin to sand-sized glacial debris derived from these rocks. Lastly, the reddish hue of these tills is most likely due to thin reddish coatings on particles; these coatings may reflect the presence of minor amounts of red shale debris derived from the Bécancour Formation (Figure 2-1: map-unit #23) in the St. Lawrence Lowlands. Alternatively, this reddish debris may originate from Granby Group rocks which, as mentioned above, contain much red slate. However, this would not alter the basic inference that reddish-

brown tills in the vicinity of Victoriaville were deposited by ice that advanced southeastward across the St. Lawrence Lowlands and Appalachian Piedmont.

Except for the minor grain-size difference previously noted, the two till beds at Arthabasca have an essentially similar composition. Average heavy mineral content of their fine sand fraction is 7.3%; this is distinctly higher than in other lodgement tills of the study area. However, no reasonable explanation for this can be offered. Magnetic mineral content averages about 12.3%, a fairly common value in the region, and therefore provides no explanation for the high weight of the heavy mineral fraction. Although large sources of carbonate bedrock (Bulstrode Formation) lie only about 1 km northwest of the section, both reddish-brown tills contain only up to about 1% carbonates (silt-clay fraction). This may of course be a result of postglacial weathering. However, the lower till bed, particularly at depths below about 3 m, seems to have undergone only slight to moderate weathering; yet it contains only 1% carbonates at a depth of 3.6 m (sample #1). If the lack of carbonate debris is indeed a primary characteristic of these reddish-brown tills, this may suggest that their constituent debris are derived chiefly from englacial transport; this would not only explain the near-absence of debris derived from nearby carbonate bedrock sources but it would also explain low comminution rates of sand-size debris derived from more distal sources (Granby Group).

The superposition of two reddish-brown till beds at Arthabasca seems to be a rather local occurrence. Other nearby sites, although less well exposed, showed little evidence that may lead one to infer that a significant glacial readvance took place during the latter part of glacial phase C. Moreover, there remains at least a possibility that the upper till bed at Arthabasca may be a flow till bed rather than a lodgement till bed; however this possibility has been set aside because the strong planar attitude of clast A/B planes (FT-36) in the upper till is a fairly good indicator of subglacial deposition.

4.4.11 The Asbestos ultramafic dispersal train

The Asbestos ophiolite complex which extends across the study area as a narrow, 0.5 to 5 km-wide, outcrop belt (Figures 4-1 and 4-21) includes distinctive ultramafic rocks that not only constitute excellent area- specific provenance indicators in multiple-till exposures but also provide an excellent opportunity to study glacial dispersal patterns in surface till. These ultramafic rocks consist mainly of serpentinized peridotite (harzburgite) but also include some dunite, pyroxenite and chromitite as well as undifferentiated serpentinite (Lamarche, 1973). Detailed studies of till provenance in the neighboring Thetford-Mines and Lac-Mégantic regions (Shilts, 1973a, 1973b, 1975, 1976a, 1978, 1981) have shown that the high Ni and Cr contents in the silt-clay fraction (- 0.063 mm) of tills derived from ultramafic rocks provides a very effective method of establishing glacial dispersal patterns.

Surface till was sampled at 204 localities distributed over an area of about 1800 km^2 that extends both northwest and southeast of the Asbestos ophiolite complex. This sample suite includes a representative sample of drift unit C for each of the eight sections that are located within the sampling area. Ni concentrations in the silt-clay fraction of till range between 11 and 450 ppm and average 73.6 ppm (Figure 4-19); however their frequency distribution is positively skewed (towards high values). Cr concentrations range between 8 and 160 ppm and average 31.4 ppm; their frequency distribution is also positively skewed, but to a lesser extent than that of Ni concentrations (Figure 4-19). Analytical results from tills (drift unit C) that contain virtually no ultramafic debris, such as at the Tingwick and Arthabasca localities, reveal that regional background values are as low as about 20 ppm for Ni and about 15 ppm for Cr. This indicates that:

1) most of the 204 surface till samples contain at least minor quantities of ultramafic debris and are thus "anomalous";

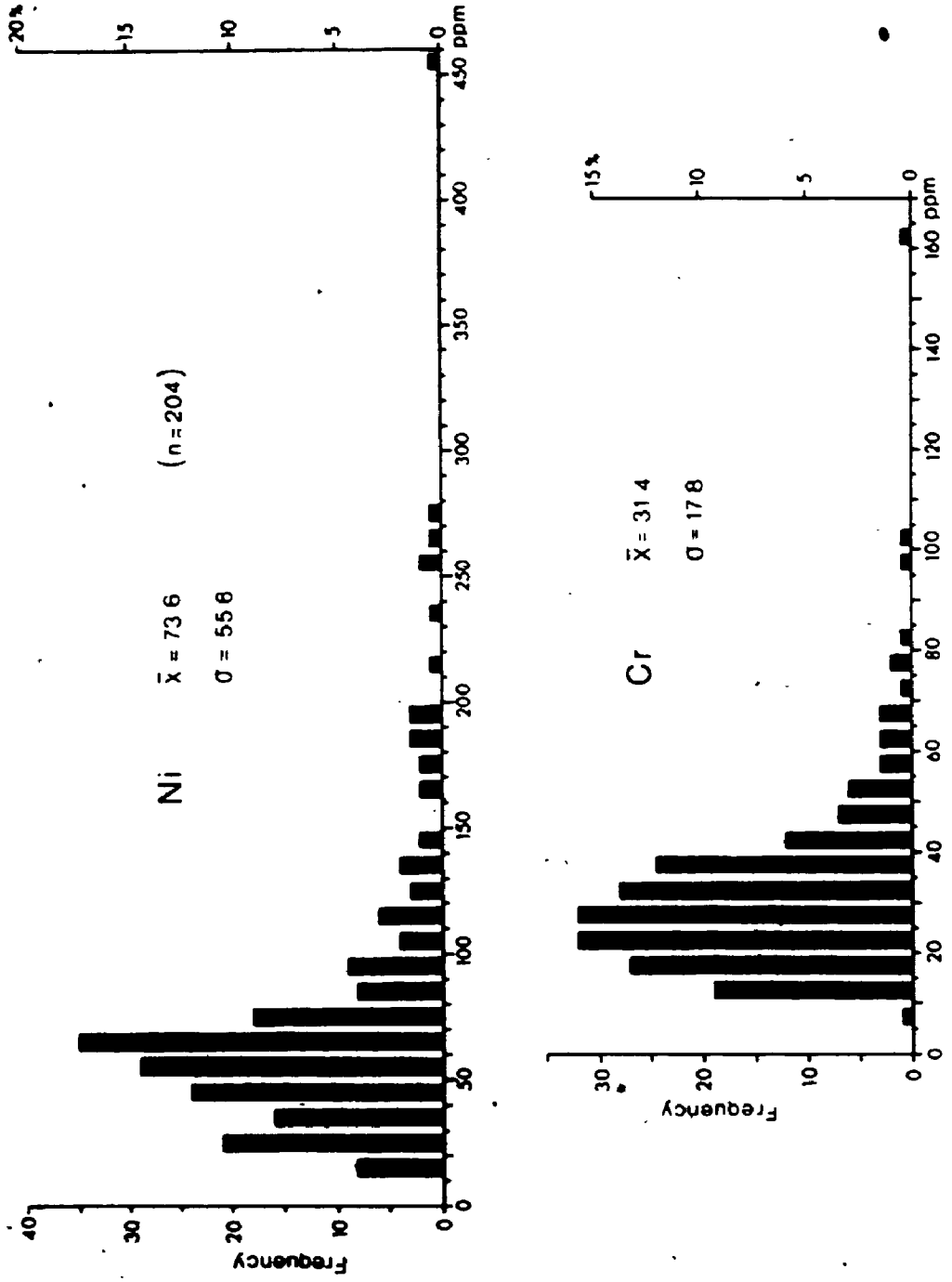

Figure 4-19 : Frequency distribution of Ni and Cr concentrations in the silt-clay fraction (<0.063 mm) of surface till samples (hot HCl – HNO_3 extraction).

2) background concentrations for Ni and Cr in this sample suite may not be established by statistical procedures (e.g. lognormality test) based on frequency distribution analysis.

The ratio of average Ni content (73.8 ppm) to background (about 20 ppm) is 3.7:1 while the ratio of average Cr content (31.4 ppm) to background is only 2.1:1. This explains, at least in part, why variations of Cr concentrations in stratigraphic sections as well as in surface tills were found to be less contrasted than variations of Ni concentrations. Because Ni and Cr concentrations are strongly correlated (r = 0.88; Figure 4-20) and also because previous work by Shilts (1975, 1976a) has shown that ultramafic dispersal patterns based on Cr concentrations are essentially the same as those based on Ni concentrations, it is most reasonable to assume that above-background concentrations of Ni and Cr in tills of the study area are essentially similar indicators of ultramafic provenance. Therefore, in order to ease forthcoming discussions, Cr data will no longer be illustrated nor referred to.

The Asbestos ultramafic dispersal train is distinctly recorded by contour lines of Ni concentrations in the silt-clay fraction of surface till samples (Figure 4-21). The Ni dispersal map shows that the dispersal train consists of two main zones:

- Zone I: This zone features a typical dispersal train extending southeast of a series of rather prominent ultramafic rock outcrops. Dispersal trends in zone I are exemplified by the A-A' profile (Figure 4-21 and 4-22A). In this zone, two distinct tails (Ni > 90 ppm) of the dispersal train can be traced southeast of ultramafic outcrops over a distance of about 25 km; these tails must extend for at least a few additional kilometers beyond the sampling area. The head (Ni > 130 ppm) of the dispersal train extends up to about 10 km southeast of the outcrop belt. The dispersal train in zone I thus greatly resembles typical dispersal trains, such as those in the nearby Thetford-Mines region and in other glaciated

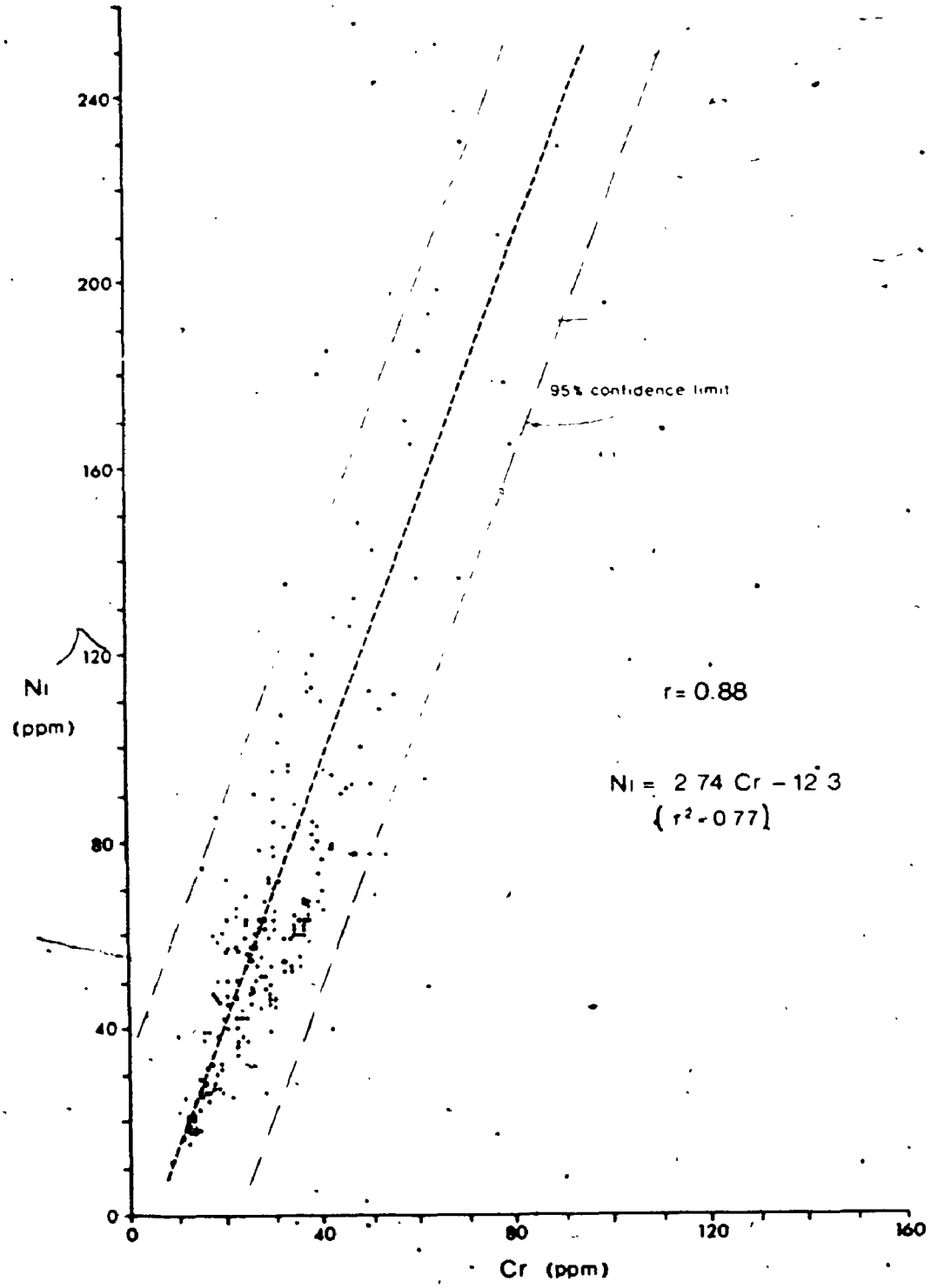

Figure 4-20 : Scatter diagram showing the strong correlation between Ni and Cr concentrations in the silt-clay fraction (<0.063 mm) of surface till samples. Results of a regression analysis are also shown.

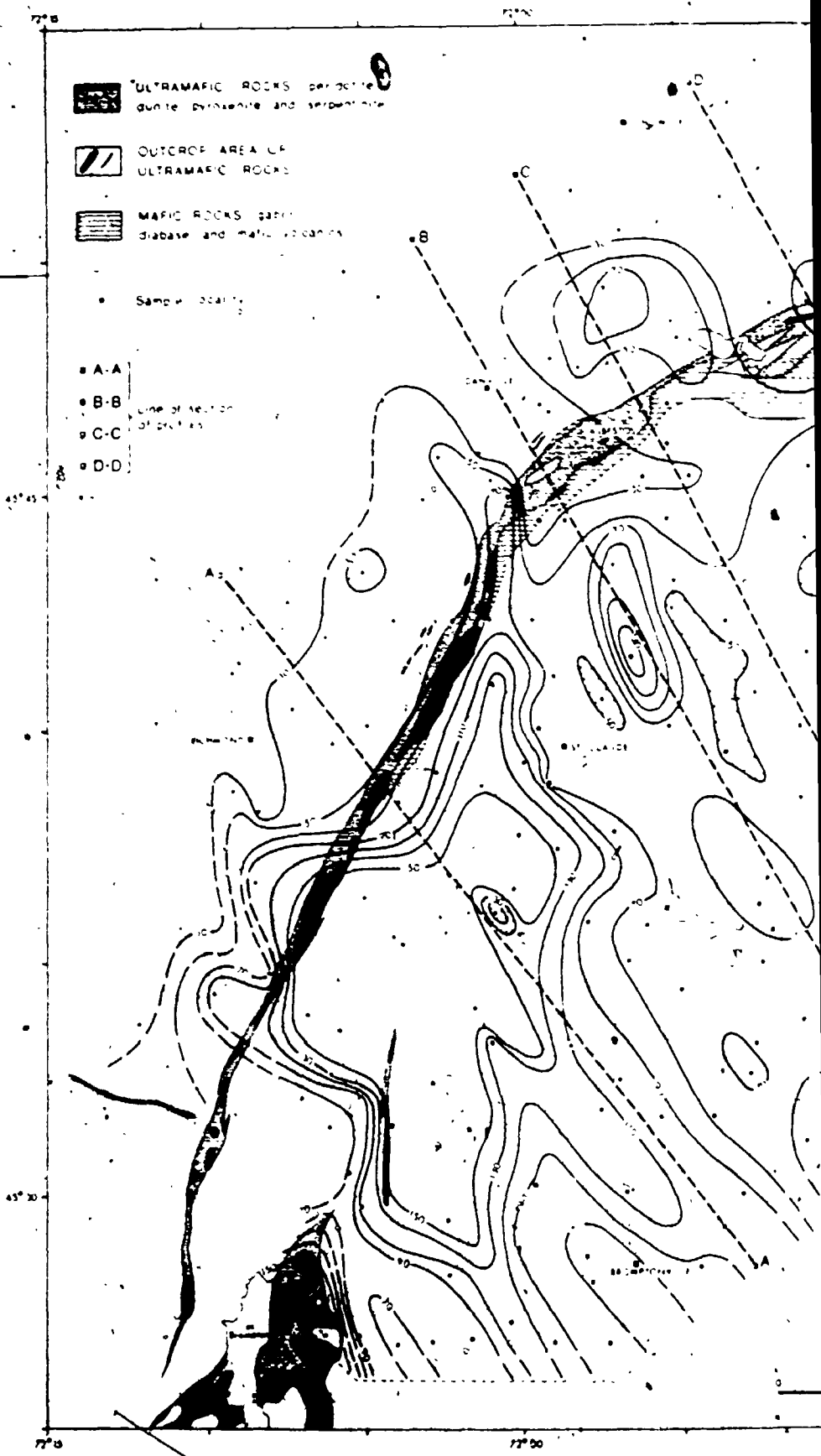

Figure 4-21: The Asbestos ultramafic dispersal train, as recorded by contour
till. Bedrock outcrop patterns are after Lamarche (1973), St-
content / topographic profiles depicted in Figure 4–22.

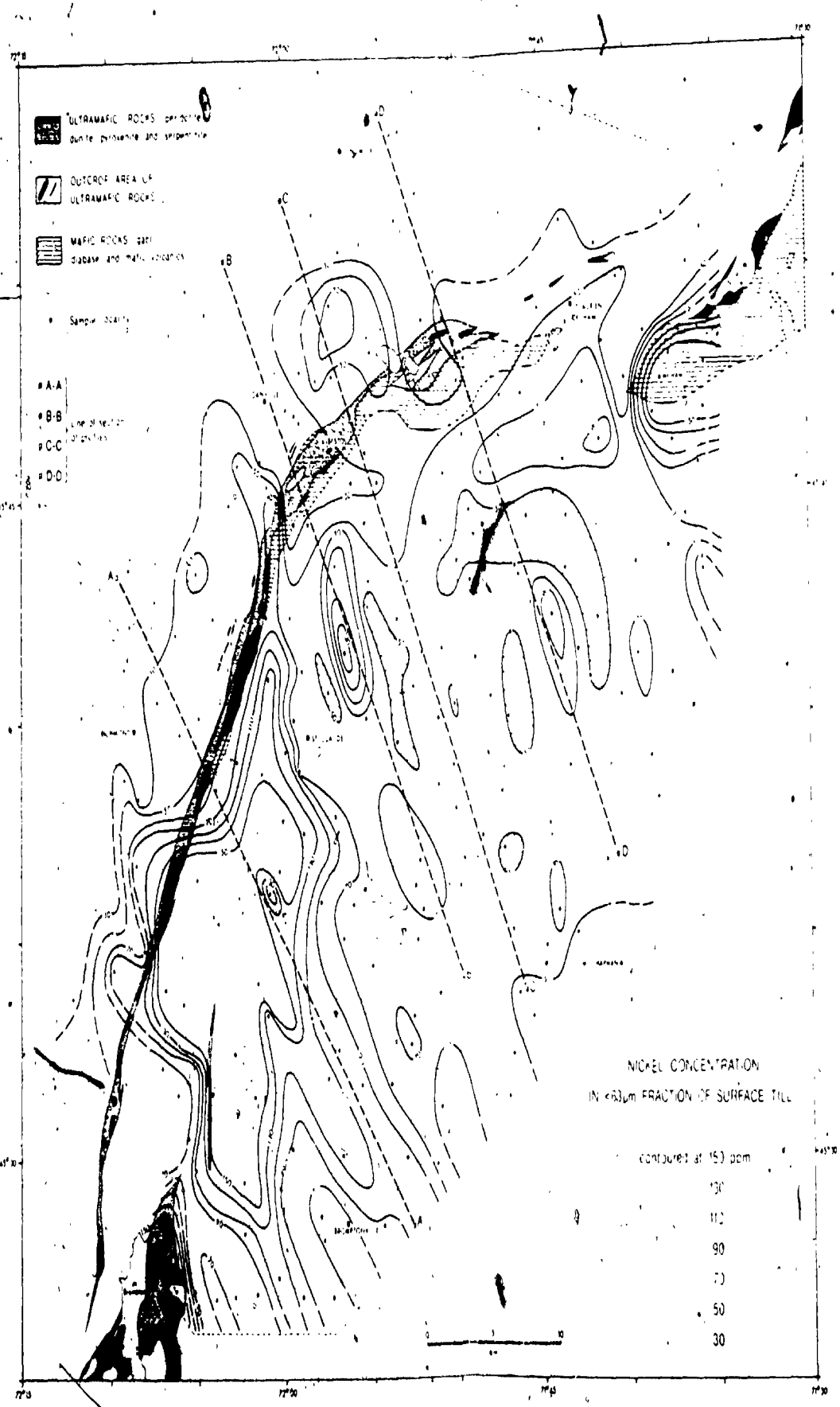

Figure 4-21. The Asbestos ultramafic dispersal train, as recorded by contour lines of Ni concentration in the silt-clay fraction (<0.063 mm) of surface till. Bedrock outcrop patterns are after Lamarche (1973), St-Julien (1970) and Hébert (1982). Also shown are the locations of Ni content / topographic profiles depicted in Figure 4–22.

regions (Shilts, 1975, 1976a; Siegel, 1974). Probably because of the low topographic roughness of uplands and valleys in zone I, the location and pattern of dispersal tails show only slight topographic influence: for instance, the -90 ppm re-entrant around Bromptonville is somewhat unexpectedly located in the Saint-François River valley.

- Zone II: This zone is characterized by a much more diffuse dispersal train that extends southeast of an area where ultramafic rocks are largely covered by older Quaternary sediments (drift unit A and unit B) and crop out only occasionally (Figure 4-21). Profiles C-C' and D-D' (Figures 4-21, 4-22C and 4-22D) show typical examples of dispersal trends within zone II. The absence of a dispersal head is a typical feature of zone II and is explained mainly by the fact that very few ultramafic outcrops were available for subglacial erosion during glacial phase C. Only a few discontinuous, rather diffuse dispersal tails are present in zone II; more commonly, Ni concentrations simply oscillate between about 50 and 70 ppm. Profile B-B' (Figures 4-21 and 4-22B) illustrates dispersal trends southeast of an area where small ultramafic outcrops were exposed to glacial erosion; in this case, only a low-amplitude, diffuse dispersal head lies 5 to 8 km southeast of the ultramafic belt.

The Ni dispersal map together with profiles of Ni content reveal other key facts:

1) At distances of less than 10 km northwest of the ultramafic belt, Ni content in surface till falls to values of 20 to 25 ppm. Since till in that area contains virtually no ultramafic clasts, this indicates that the "true" regional background for Ni is only about 20 ppm.

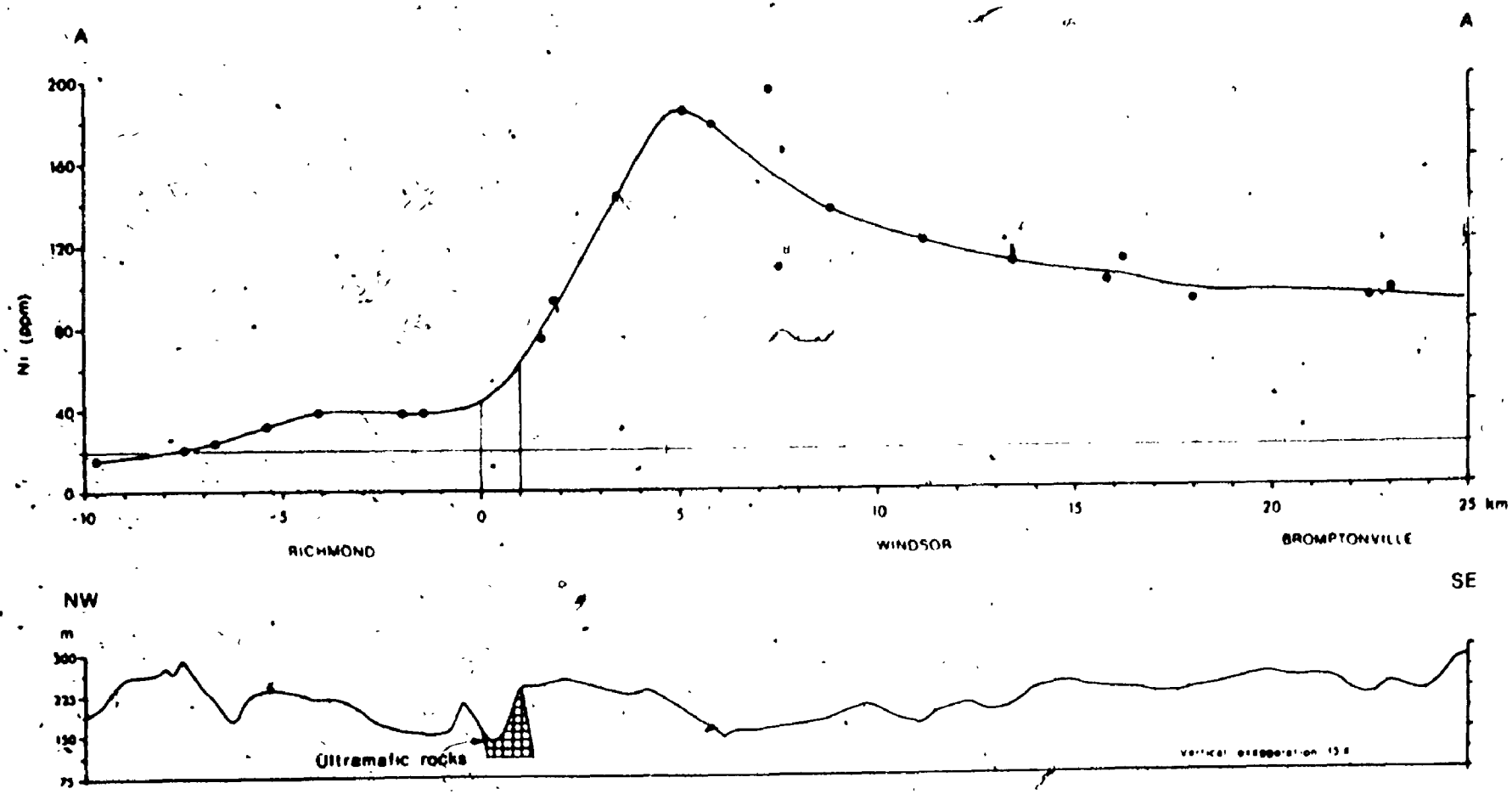

Figure 4-22 A : Topography and Ni concentration in the silt-clay fraction of surface till along profile A–A'. This profile is characteristic of Zone I of the Asbestos ultramafic dispersal train.

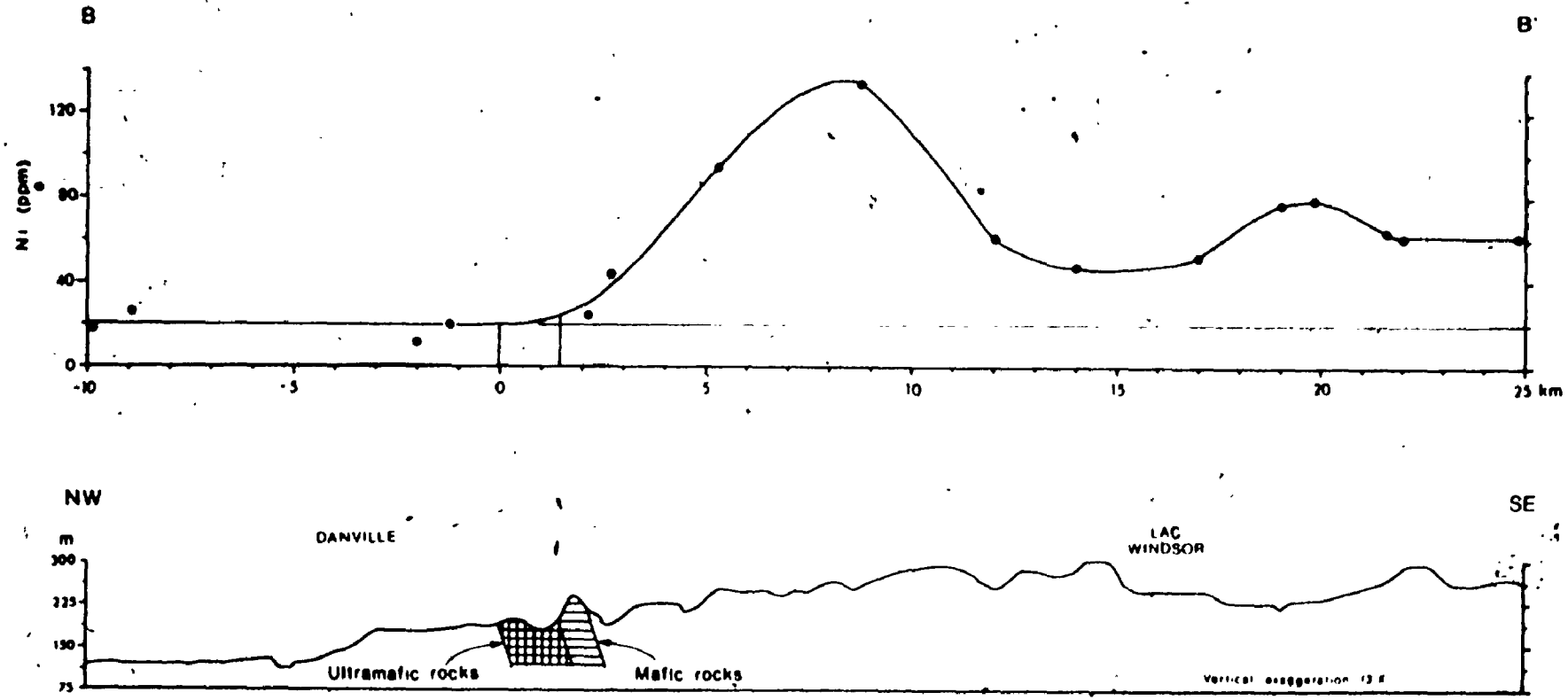

Figure 4-22 B : Topography and Ni concentration in the silt-clay fraction of surface till along profile B–B'. Ultramafic components are almost absent in the valley northwest of the ultramafic belt, but only a diffuse dispersal head occurs between 5 and 8 km southeast of the ultramafic belt.

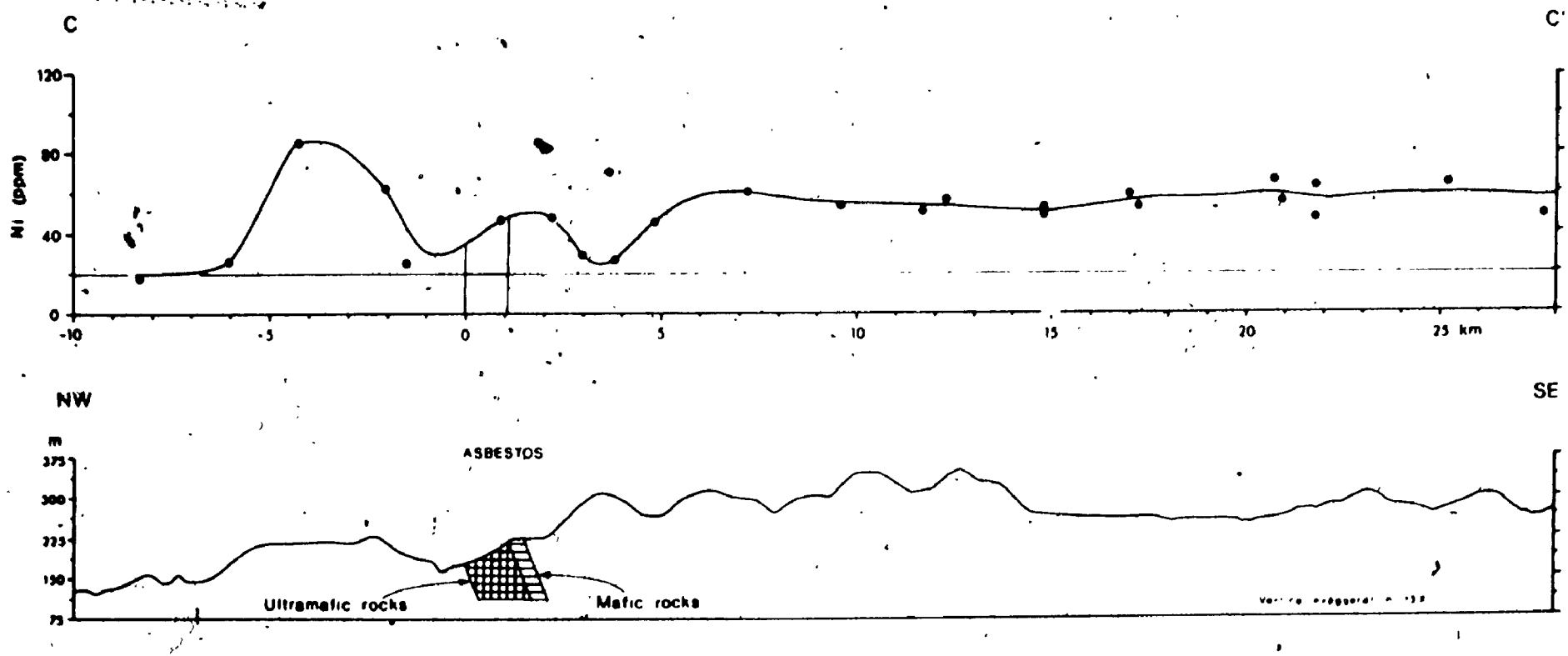

Figure 4-22 C : Topography and Ni concentration in the silt-clay fraction of surface till along profile C–C'. Ni dispersal trend southeast of the ultramafic belt is characteristic of Zone II of the Asbestos ultramafic dispersal train. A small anomaly (Ni > 60 ppm), located on low uplands northwest of the ultramafic belt, is interpreted as a residual feature (see text).

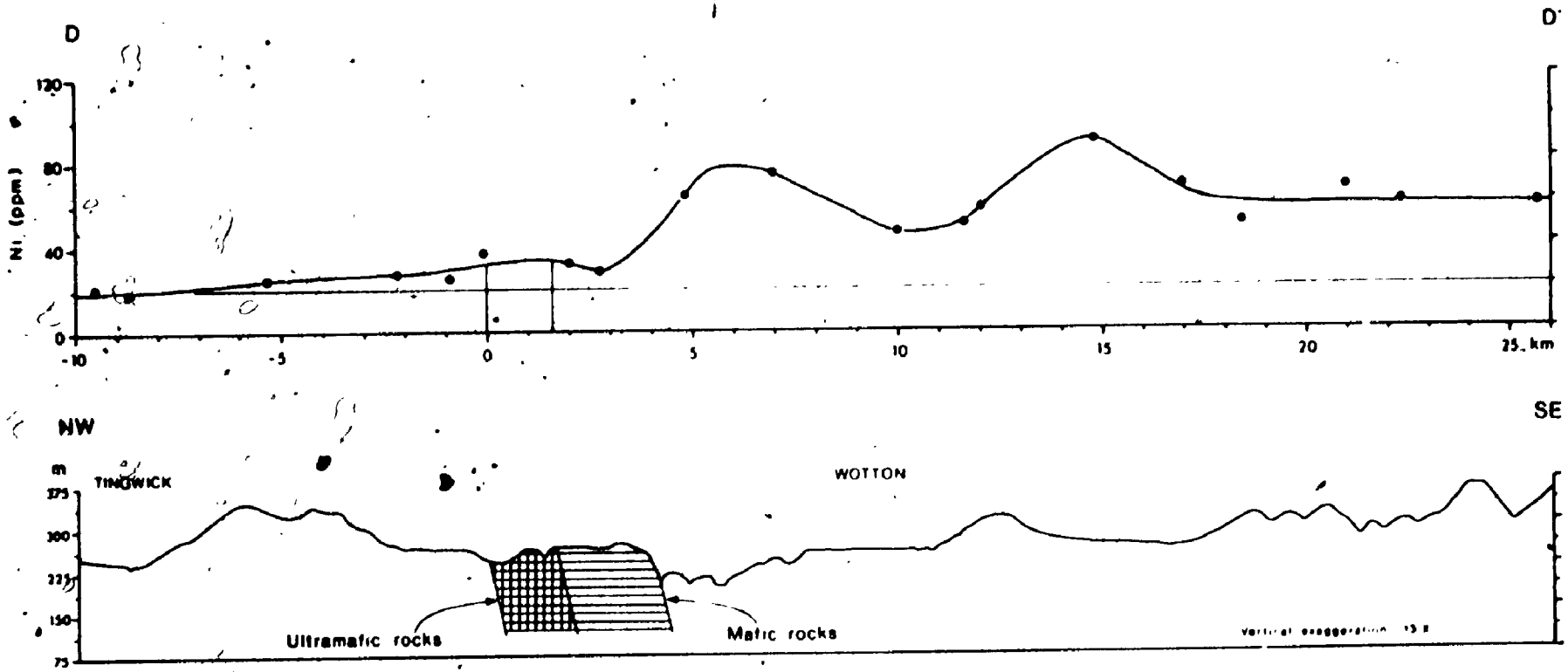

Figure 4-22 D : Topography and Ni concentration in the silt-clay fraction of surface till along profile D–D'. This profile is characteristic of Zone II of the Asbestos ultramafic dispersal train.

2) In uplands northwest of the ultramafic belt, surface till commonly contains 30 to 70 ppm Ni; this belt of "anomalous" Ni content has a width of up to about 8 km and extends along almost the entire length of the ultramafic belt, from the vicinity of Lake Brompton to that of Lake Nicolet. Since surface till of this terrain belt also contains occasional ultramafic clasts, the presence and extent of this "anomalous" surface till belt are considered to be very significant. This indicates that ultramafic debris which had been transported westward and northward during glacial phase A were not completely re- entrained by southeastward ice-flow during glacial phase C. The presence of contour re-entrants (Ni < 30 ppm) in valleys, near Asbestos for instance (see also profile B-B'), indicates that southeastward glacial transport was more effective in valleys and gaps than on adjacent uplands (profiles A-A', C-C', D-D').

The Ni and Cr contents of surface till thus not only serve to establish that the SE-trending Asbestos ultramafic dispersal train was formed during glacial phase C but they also provide an indirect record of westward and northward ice-flow during the earlier glacial phase (drift unit A).

4.4.12 Summary of provenance interpretation and ice-flow patterns

Observations in stratigraphic sections and in numerous shallow surface exposures indicate that typical till of drift unit C contains at least minor amounts of Precambrian clasts; yet, because of the abundance of debris derived from local bedrock sources (mainly slate, sandstone and schist), Precambrian clasts commonly make up less than one percent of till clasts. However, by comparison with the underlying drift unit A, Precambrian clasts are abundant in drift unit C; an excellent example of this is provided by pebble counts in tills of the Norbestos section (Table 4-2).

The best overall provenance record of drift unit C is provided by the SE-trending Asbestos ultramafic dispersal train (Figure 4-21). The dispersal train extends over a distance of at least 25 km southeast of the ultramafic belt; this distance, given the fact that the Asbestos ultramafic belt is much narrower and has a much smaller outcrop area than the Thetford-Mines ultramafic belt, compares well with that of the Thetford-Mines ultramafic dispersal train (about 80 km-long; Shilts, 1973a, 1975). Additional site-specific provenance criteria, such as those discussed for the Arthabasca and Tingwick localities, provide further evidence indicating that drift unit C was deposited by the Laurentide Ice Sheet.

Till clast fabrics and subtill glaciotectonic deformations at all investigated localities (Figure 4-23: localities #1 to #10) consistently indicate that drift unit C was deposited by ice that advanced toward approximately southeast throughout the study area. Moreover, available directional and provenance data strongly suggest that southeastward ice-flow was maintained until the Laurentide Ice Sheet had finally retreated from the study area; surface till in uplands surrounding Asbestos provides no evidence that may lend support for a late-glacial northward (or westward) ice-flow event.

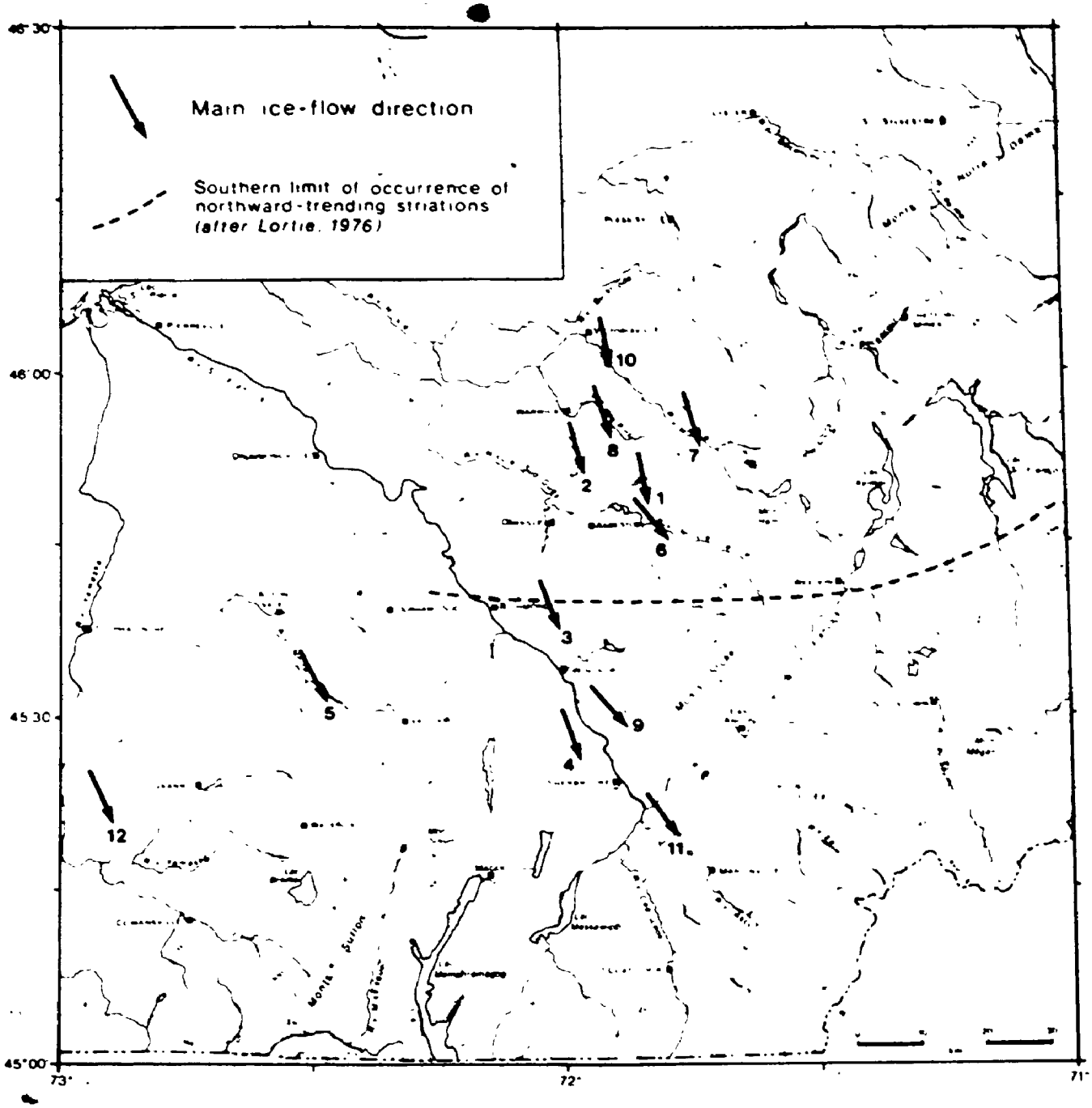

DRIFT UNIT C		SUGGESTED CORRELATIVES	
1. Norbestos	6. Wolton		
2. Riv des Rosiers	7. N-D-de-Ham	11. Lennoxville Till (Ascot River section)	
3. Willow Brook	8. Tingwick	12. Upper till (Ange-Gardien section)	
4. Ch des Ecossais	9. Bromptonville		
5. Riv Noire	10. Arthabasca		

Figure 4-23 : Southeastward ice-flow pattern recorded in drift unit C and suggested correlatives. Till of drift unit C contains no evidence which may suggest that a northward ice-flow reversal took place toward the close of glacial phase C. The Ascot River (#11) and Ange-Gardien (#12) sections will be discussed in Chapter 6.

CHAPTER 5

LATE WISCONSINAN STRATIGRAPHY AND DEGLACIAL EVENTS

Because it has proven difficult to reconcile a late-glacial ice-flow reversal event with significant aspects of the deglacial record (see section 1.3.2), an assessment of deglacial patterns and events is required as it places a series of constraints on any attempt to reconstruct late-glacial ice-flow patterns. Deglacial features shown in Figure 5-1 combine the results of work previously carried out by McDonald (1966, 1967a, 1967b, 1968) and by the author (Parent, 1978; Clément and Parent, 1977). Additional fieldwork was done by the author throughout the Asbestos-Valcourt region, particularly in areas that were previously unmapped, for instance east of Asbestos and Warwick (21 E/13) and south of Valcourt (31 H/8 W). A detailed map of deglacial landforms and sediment bodies is presented in Figure 3-1. Although the investigation of new exposures and the mapping of new areas call for some modifications to regional deglaciation patterns and in the history of deglacial events, the basic deglacial history remains essentially similar to that proposed earlier by McDonald (1967a, 1968). His work is aptly summarized by this statement: "An active ice-front retreated northward and northwestward down the topographic gradient in the Appalachian region and deposited a series of discontinuous moraines, largely composed of ice-contact stratified drift, in the glacial lakes at the ice-front" (Gadd, McDonald and Shilts, 1972a: p. IV).

5.1 Morainic belts

Three main recessional morainic belts extend across the Asbestos-Valcourt region (Figure 5-1; see also Figure 3-1). From oldest to youngest, these are (1) the Cherry River / East-Angus Moraine, (2) the Mont Ham Moraine and (3) the Ulverton-Tingwick Moraine. These are discontinuous end-moraines which mainly consist of ice-contact sediment bodies and of assemblages of morainic ridges and intervening ice-marginal meltwater channels (Figure 3-1). On the basis of the extent and

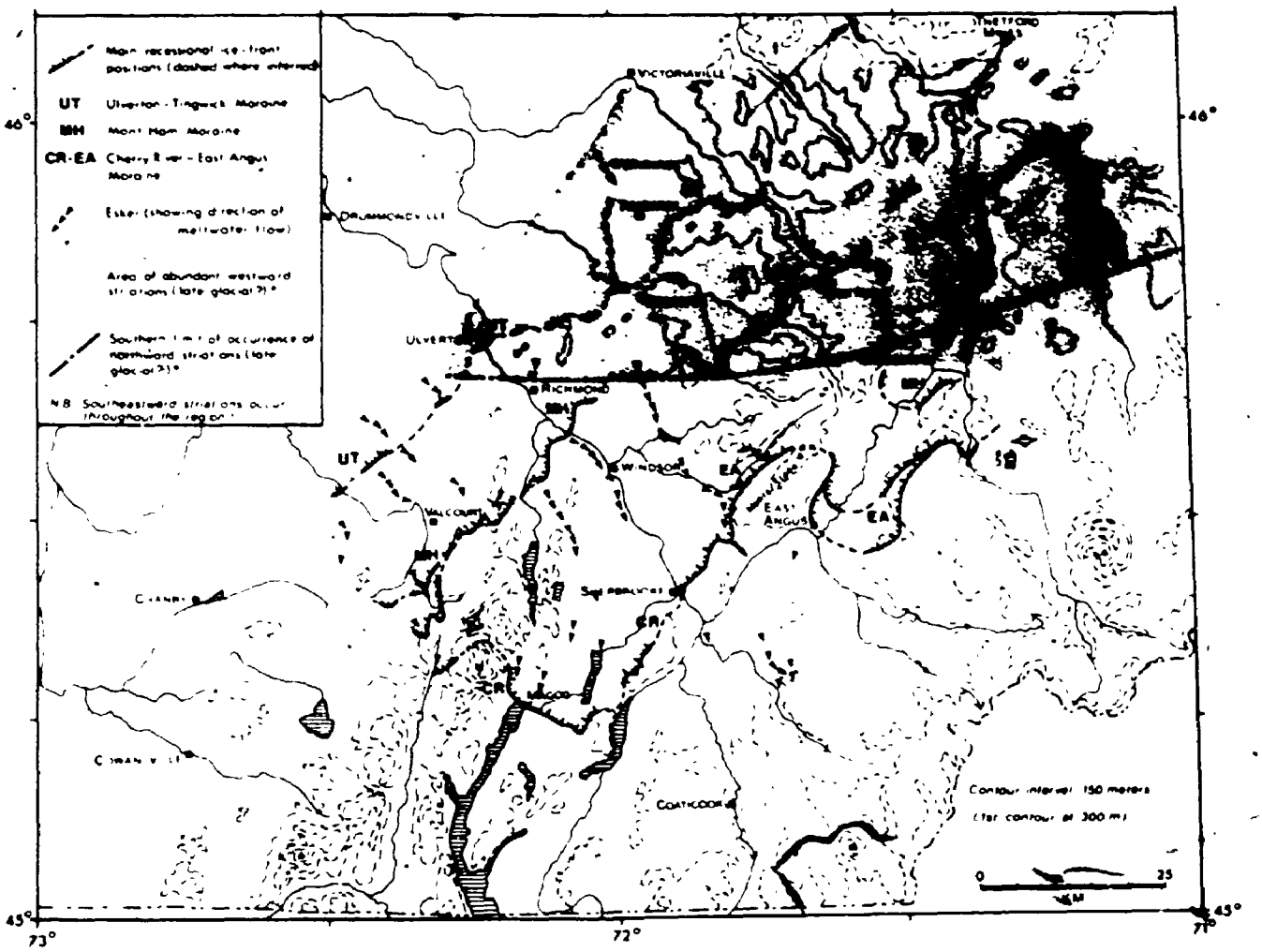

Figure 5-1: Main Late Wisconsinan recessional moraine belts of the Asbestos-Valcourt region, also showing the areal extent of northward- and westward-trending striations. Notice that the Ulverton-Tingwick and Mont Ham Moraines extend deeply into terrains where late-glacial northward and westward ice-flow reversal events have been suggested by earlier authors. (* after Lortie, 1976).

depth of proglacial lakes impounded by the retreating ice-front, two main types of ice-marginal environments can be recognized in the study area:

1) In terrains where large, deep proglacial lakes were impounded at the ice-margin, such as in the Saint-François River valley between, say, Sherbrooke and Richmond and on low adjacent uplands, morainal sediments consist mainly of subaquatic outwash deposits, several of which are evidently esker-fed sediment bodies. End-moraine segments are particularly discontinuous in such areas; however, numerous esker ridges and small streamlined subglacial landforms (drumlins, drumlinoid ridges, crag-and-tail ridges, lineaments) are commonly present in low-relief terrains. The area of occurrence of these ice-marginal environments is approximately given by the area of occurrence of eskers in Figure 5-1. The fact that McDonald's mapping work was mostly carried out in such areas seems to explain the previously cited statement that moraines are "largely composed of ice-contact stratified drift".

2) In terrains where only small or shallow proglacial lakes were impounded at the ice-margin, morainic belts consist mainly of assemblages of till ridges and intervening meltwater channels. These transverse morainic landforms, which most commonly lie on north- or northwest-facing slopes, may extend over distances of up to 8 km; their trend reflects quite closely that of the retreating ice-front (Parent, 1978; Clément et Parent, 1977). Small bodies of ice-contact stratified drift, which locally include deltas, commonly occur at the downstream extremity of ice-marginal meltwater channels; when present, these deltas allow specific ice-front positions to be tied with levels of coeval ice-dammed lakes. Similar, though much more scattered, transverse landforms are present on terrains between the main morainic belts. This type of deglacial environment in which eskers seem virtually absent occurs mainly in the eastern part of the Asbestos-Valcourt region (Figure 5-1).

5.1.1 Cherry River / East-Angus Moraine

The Cherry River / East-Angus Moraine extends along the southern edge of the study area (Figure 5-1; see also Figure 3-1). It consists of two main segments:

1) the Cherry River Moraine (McDonald, 1967a, 1968), which is a rather discontinuous morainic belt extending from the vicinity of Magog to that of Sherbrooke;

2) the East-Angus Moraine (Clément et Parent, 1977; Parent, 1978), which is a fairly continuous morainic belt that wraps around the northwest and northeast flanks of Monts Stoke and which includes a few ice-contact sediment bodies (near Stoke) that had been previously assigned to the Cherry River Moraine by McDonald (1967a, 1968).

The two segments are separated by yet unexplained gaps in the vicinity of Sherbrooke (Figure 5-1). These gaps have led to slightly different reconstructions of ice-retreat patterns near Sherbrooke (McDonald, 1967a; Clément et Parent, 1977; Boissonnault et Gwyn, 1983). Since little firm evidence has been presented to suggest that the earlier interpretation must be changed, the outline of the Cherry River Moraine depicted in Figure 5-1 is essentially that proposed by McDonald (1967a, 1968) for the area between Sherbrooke and Magog. In any event, these slightly different interpretations of ice-retreat patterns do not alter two basic facts:

1) the Cherry River Moraine consists mainly of ice-contact stratified drift bodies that were deposited by southward-flowing meltwater streams as they entered a proglacial lake (McDonald, 1967a, 1967b, 1968);

2) the altitude of ice-contact deltas associated with the morainic belt indicates that it was built while Glacial Lake Memphre-

magog stood at the level of the Sherbrooke phase (McDonald, 1968).

Because of this, the matter of ice-retreat patterns near Sherbrooke seems of rather local interest and was not further investigated in the course of the present study. On the other hand, McDonald's proposed outline of the Cherry River Moraine between Magog and the vicinity of Valcourt (see Figure 1-3) has been dropped: between these two localities, there are almost no ice-marginal deposits (see Figure 3-1) to support the suggested ice-front position. Instead it is suggested that ice-marginal deposits in the vicinity of Valcourt, because they are in line with deposits of the Mont Ham Moraine, are a southwestern extension of this younger morainic belt (Figure 5-1).

The East Angus Moraine consists mainly of assemblages of till ri[illegible] and ice-marginal meltwater channels. The moraine was fully destribed and discussed in earlier reports (Parent, 1978; Clément et Parent, 1977); this material will not be repeated here. This morainic belt was also built while Glacial Lake Memphremagog stood at the level of the Sherbrooke phase, hence the suggested correlation with the Cherry River Moraine. The East-Angus Moraine is named after the town of East-Angus (Clément et Parent, 1977), near which McDonald (1967a, 1969) first described and mapped large cross-valley morainic ridges underlain by a distinctive clay-till sheet and by deformed varves. McDonald (1967a) inferred that a glacial lobe, flowing southwestward down the upper Saint-François River valley, readvanced over glacial-lake sediments to build the morainic ridges.

The best reference locality for the East-Angus Moraine is a clay pit in the town of East-Angus, originally described by McDonald (1967a: p. 37-38). The clay pit (Figure 5-2) was visited by the author mainly for the purpose of sampling calcare[illegible] concretions which had been observed by McDonald within deformed varves. It was hoped that radiocarbon dating of these concretions might provide at least an estimate of the age of the deformed varves and, hence, of the overlying till. No concretions were found.

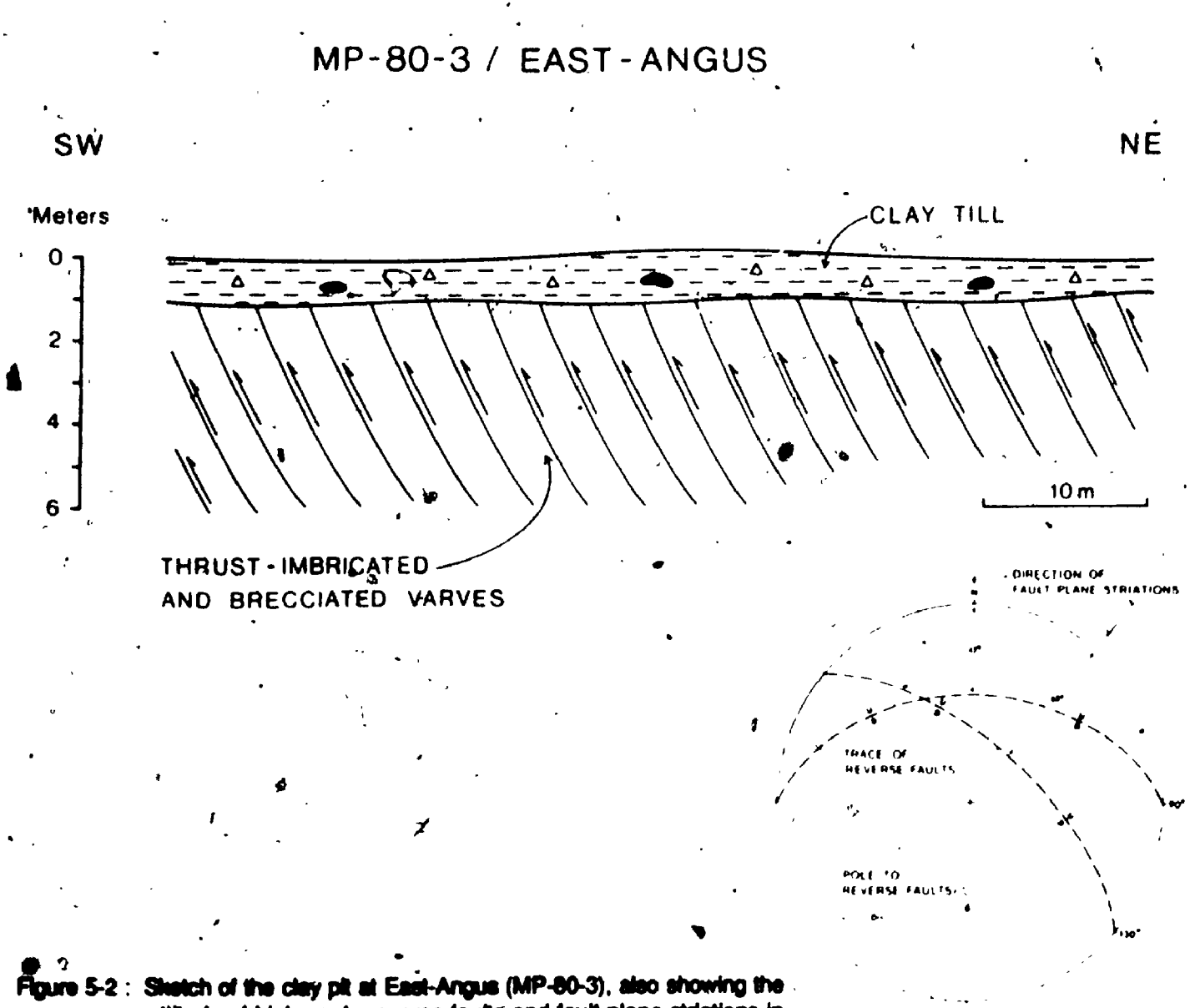

Figure 5-2 : Sketch of the clay pit at East-Angus (MP-80-3), also showing the attitude of high-angle reverse faults and fault plane striations in the thrust-imbricated and brecciated varves that underlie the clay till unit.

The clay pit is excavated within a large morainic ridge. Exposed sediments consist of a 0.9 to 1.2 m-thick bed of clay till that overlies unconformably thrust-imbricated and brecciated silty clay varves (Figure 5-2), much as McDonald had described. The subtill deposit is cut across by a series of high-angle, subparallel, slightly concave-up, closely spaced (5 to 30 cm apart), and striated fault planes. Their attitude, which was measured at two well-exposed sites within the pit, is given in Figure 5-2. The high angle of these reverse faults suggests that shearing occurred at low confining pressure and thus tends to support McDonald's view that the deformations were produced near or at the margin of a glacier which was advancing toward SW. A suggestion by Shilts (1978, pers. comm.) that the origin and age of the deformed varves-clay till sequence at East-Angus may be similar to that of the "early Lennoxville" Drolet Lentil of the Lac-Mégantic region (Shilts, 1973a; see also Figure 1-2) cannot be confirmed nor denied: there are, within or above the clay till bed, almost no stones whose provenance might have allowed the inference that a significant episode of southeastward ice-flow (drift unit 8) succeeded the local southwestward ice-flow event that deformed the varves and deposited the clay-till unit.

In any event, the East-Angus Moraine is recorded by a series of rather prominent ice-marginal features (see Figure 3-1) that stand on their own as evidence for this ice-front position. These may or may not be related to events recorded in the East-Angus clay pit. However, the occurrence of the clay till sheet overlying deformed glaciolacustrine muds does suggest that a glacial lobe readvanced for at least a few kilometers in the vicinity of East-Angus to build the East-Angus Moraine.

5.1.2 Mont Ham Moraine

The Mont Ham Moraine designates a series of discontinuous ice-marginal deposits that extend from the vicinity of Valcourt to that of Weedon (Figure 5-1). This morainic belt was originally described and defined by the author (Parent, 1978: figures 24 and 25; see also Figure 1-3). At that time, the belt was named "moraine du Nicolet" (Nicolet

River Moraine) but it was later renamed Mont Ham Moraine (Parent, 1984a) in order to avoid confusion with stratigraphic terms in current usage (Nicolet Stadial and Nicolet Formation) as well as to better reflect the region where it was first recognized (Rivière Nicolet, although its upper watershed is within the Outer Appalachian Uplands, is much better known as a stream of the St. Lawrence Lowland and Appalachian Piedmont).

Features of the Mont Ham Moraine are best developed in the area east of Asbestos where they consist of assemblages of morainic ridges and intervening meltwater channels that rest on north-facing slopes of the Outer Appalachian Uplands (Figure 3-1). The morainic belt also includes large cross-valley ridges of ice-contact stratified drift that were built on the left flank of the Saint-François River valley between Windsor and Richmond (Parent, 1978). Recent field work indicates that the morainic belt extends southwestward into uplands near Valcourt where it consists of a mixed assemblage of till ridges and ice-contact sediment bodies (Figure 3-1).

Relationships between the morainic belt and coeval ice-dammed water bodies defined by McDonald (1967a, 1968) allow firm correlations to be made between discontinuous segments of the moraine. On the basis of his study and of earlier work by McDonald (1966, 1967a, 1968), Parent (1978) established that the Mont Ham Moraine was built during the maximum extent of the Sherbrooke phase of Glacial Lake Memphremagog. This interpretation is based on three main lines of evidence:

1) Ice-marginal retreat from the position of the Cherry River / East-Angus Moraine allowed glacial-lake waters to expand northward in the Saint-François River valley and on low adjacent uplands. Several small ice-contact deltas between Sherbrooke and Windsor were built at the level of the Sherbrooke phase during this ice-retreat interval; several shoreline features that were formed at the level of the Sherbrooke phase have also been recorded throughout that area (see Figure 3-1).

2) Ice-contact deltas associated with the Mont Ham Moraine were built at altitudes that correspond to the level (265 - 270 m ASL) of the warped waterplane of the Sherbrooke phase (Parent, 1978). For instance, ice-marginal features suggesting that a small late-glacial lobe occupied the upper Saint-François River valley upstream of Weedon (Figure 5-1) are assigned to the Mont Ham Moraine because associated ice-contact deltas were formed at an altitude (about 240 m) corresponding to the local level of the Sherbrooke phase.

3) Strandline features of the Sherbrooke phase are absent on the proximal side of the Mont Ham Moraine (Parent, 1978). Field evidence acquired earlier (McDonald, 1967a, 1968; Parent, 1978) as well as during this study indicates that Glacial Lake Memphremagog drained following ice-retreat from the position of the Mont Ham Moraine and that water levels fell by about 50 m.

5.1.3 Ulverton-Tingwick Moraine

Judging from the weak development of ice-marginal deposits, except perhaps for a few till ridges (and meltwater channels) resting on north-facing slopes near Asbestos and on the north side of the Ham Hills (see Figure 3-1), ice-retreat that followed deposition of the Mont Ham Moraine must have been quite rapid. However ice-marginal retreat slowed down or halted about 15 km northwest of the Mont Ham Moraine to build the Ulverton-Tingwick Moraine (Figure 5-1). This morainic belt may be subdivided, on the basis of geomorphic characteristics, into two main segments, the Ulverton and Tingwick segments.

The Ulverton morainic segment, which rests on the inner Appalachian Piedmont a few kilometers northwest of the Richmond Hills, extends from Colline Elliot (near Asbestos) southwestward to the vicinity of Béthanie (northwest of Valcourt) where it may extend beyond the study area. This 30 km-long morainic segment is particularly discontinuous since it consists mainly of esker-fed subaquatic outwash bodies that were deposited in a proglacial lake at the ice-front. Several well-defined strandline

features (deltas, wave-cut terraces, beaches) which have been recorded by both McDonald (1966, 1967a) and the author (see Figure 3-1) in terrains lying on the distal side (southeast) of the morainic segment indicate that the warped water-plane of this proglacial lake stood at an altitude of about 230 m ASL near the Ulverton ice-margin.

Numerous sand or gravel pits which have been excavated into deposits of the Ulverton segment reveal that the subaquatic outwash bodies consist mainly of plane-and ripple-laminated sand that was deposited by currents flowing toward the southeastern sector. Eskers on both the distal and the proximal side of the morainic segment were also deposited by southeastward paleocurrents. These observations essentially corroborate those of McDonald (1966, 1967a) who had assigned these morainal deposits to the Highland Front Moraine (Gadd, McDonald and Shilts, 1972; see Figure 1-3). Although the Ulverton morainic segment generally lies above the marine limit (165-175 m ASL), a few of its deposits, such as those at Ulverton, are below the marine limit and their upper surface has been reworked by current and wave action or partly buried during the Champlain Sea episode.

One of the most significant localities of the Ulverton morainic segment is the Colline Elliott delta-kame (Figure 5-3): at this locality, over 40 m of subaquatic outwash sediments, consisting mainly of plane- and ripple-laminated sand but also including a few flow till or debris flow beds, are capped by discontinuous, up to 1 m-thick, topset beds consisting of trough-cross-bedded sandy gravel. It is inferred that the high rate of sediment supply, provided by englacial or subglacial tunnels (recorded by the Warwick-Asbestos esker), allowed the subaquatic outwash fan to build up to water level, at which time the cross-bedded gravels were deposited in shallow channels that formed at the surface of the flat-topped sediment body. The surface of the Colline Elliott delta-kame lies at an altitude of about 226 m.

The Tingwick morainic segment, which extends northeast of the Colline Elliott locality, is also coeval with this proglacial lake: near Tingwick, ice-contact deltas and lake terraces were built at alti-

tudes between 225 and 230 m by ice-marginal meltwater channels that are associated with the morainic belt. Unlike the Ulverton segment, the Tingwick segment consists mainly of series of till ridges and intervening meltwater channels that rest on north-facing slopes of the Outer Appalachian Uplands (see Figure 3-1). Deposits of this part of the morainic belt extend northeastward to the vicinity of Notre-Dame-de-Ham where they lie at an altitude of about 300 m. However the morainic belt could not be traced further northeast into the Notre-Dame Mountains.

The Ulverton-Tingwick Moraine is therefore coeval with a proglacial lake whose water-plane stood at an altitude of about 230 m near the glacier-lake interface; this proglacial lake thus covered much of the Appalachian Piedmont in the Asbestos-Valcourt region. McDonald (1967a; 1968) had also reported strandline features at altitudes between 220 m and 230 m on the Appalachian Piedmont west of Richmond; he assigned those features to a "lower lake system" which extended up in the Saint-François River valley to at least the vicinity of Sherbrooke and whose isobases "... conform roughly to levels of the Fort Ann phase of Lake Vermont, described in the Lake Champlain Basin by Chapman (1937)..." (McDonald, 1968: p. 672). Recent surveys by Prichonnet (1982a, 1982b, 1984) and co-workers (Prichonnet, Doiron et Cloutier, 1982; Prichonnet, Cloutier et Doiron, 1982; Doiron, 1981; Cloutier, 1982) in the Granby and Cowansville areas also include reports of glaciolacustrine strandline features at altitudes between 210 and 230 m in the Appalachian Piedmont southwest of the Asbestos-Valcourt region. Therefore, evidence from the study area and from adjacent areas strongly suggests that waters of Glacial Lake Vermont (Fort Ann phase) had expanded onto the Appalachian Piedmont of southeastern Quebec during construction of the Ulverton-Tingwick Moraine. This conclusion is further corroborated by the fact the altitude difference separating the "Fort Ann" strandline features from the upper Champlain Sea strandline features varies between 50 and 60 m in the study area, much as in the Lake Champlain and Upper St.Lawrence valleys (Chapman, 1937; Denny, 1974; Clark and Karrow, 1984).

5.2 Warwick-Asbestos esker

Deposits of the Warwick-Asbestos esker (Figure 5-3) were originally mapped as an "ice-front accumulation" which Gadd, McDonald and Shilts (1972) considered as part of the Highland Front Moraine (see Figure 1-3). However, judging from the areal extent of surficial geology mapping that had been carried out at the time of their regional synthesis, one may suppose that these deposits had not been fully investigated. Because of this difference of interpretation, deposits of the Warwick-Asbestos esker were investigated more specifically. Other eskers of the study area (Figure 5-1) were simply checked for direction of meltwater flow; all were found to have been deposited by paleocurrents flowing toward S or SE, much as suggested by McDonald (1966, 1967a, 1967b). Except for the Warwick-Asbestos esker and for a few eskers located in the previously unmapped west half of the Orford map-area (31 H/8), eskers shown in Figure 5-1 were already reported by McDonald (1966, 1967a, 1967b).

The Warwick-Asbestos esker consists of a series of diachronous esker segments that were deposited as the ice-front retreated northward from the position of the Ulverton-Tingwick Moraine; typically, subaquatic outwash bodies lie at the distal end of single-ridged esker segments (Figure 5-3). Sediments of these segments consist mainly of plane- and cross- bedded pebble gravel and pebbly sand; cobble gravel beds were also observed, particularly in the core area of single-ridged segments. Excellent exposures reveal that only minor faulting or collapse has occurred and thus that these segments were probably deposited in subglacial tunnels, much as in the Windsor esker (Banerjee and McDonald, 1975; McDonald and Shilts, 1975). Paleocurrent was toward south, more-or-less parallel to esker ridge; an example of this is provided by the orientation of cross-beds at locality #1, just south of Pine Hill (Figure 5-3).

Subaquatic outwash bodies consist mainly of plane- and ripple-laminated fine to medium sand but also include plane- and cross-bedded sand; sand beds most commonly appear as tabular sets or as very broad trough sets with almost no sedimentary dip or with low-angle (< 5°)

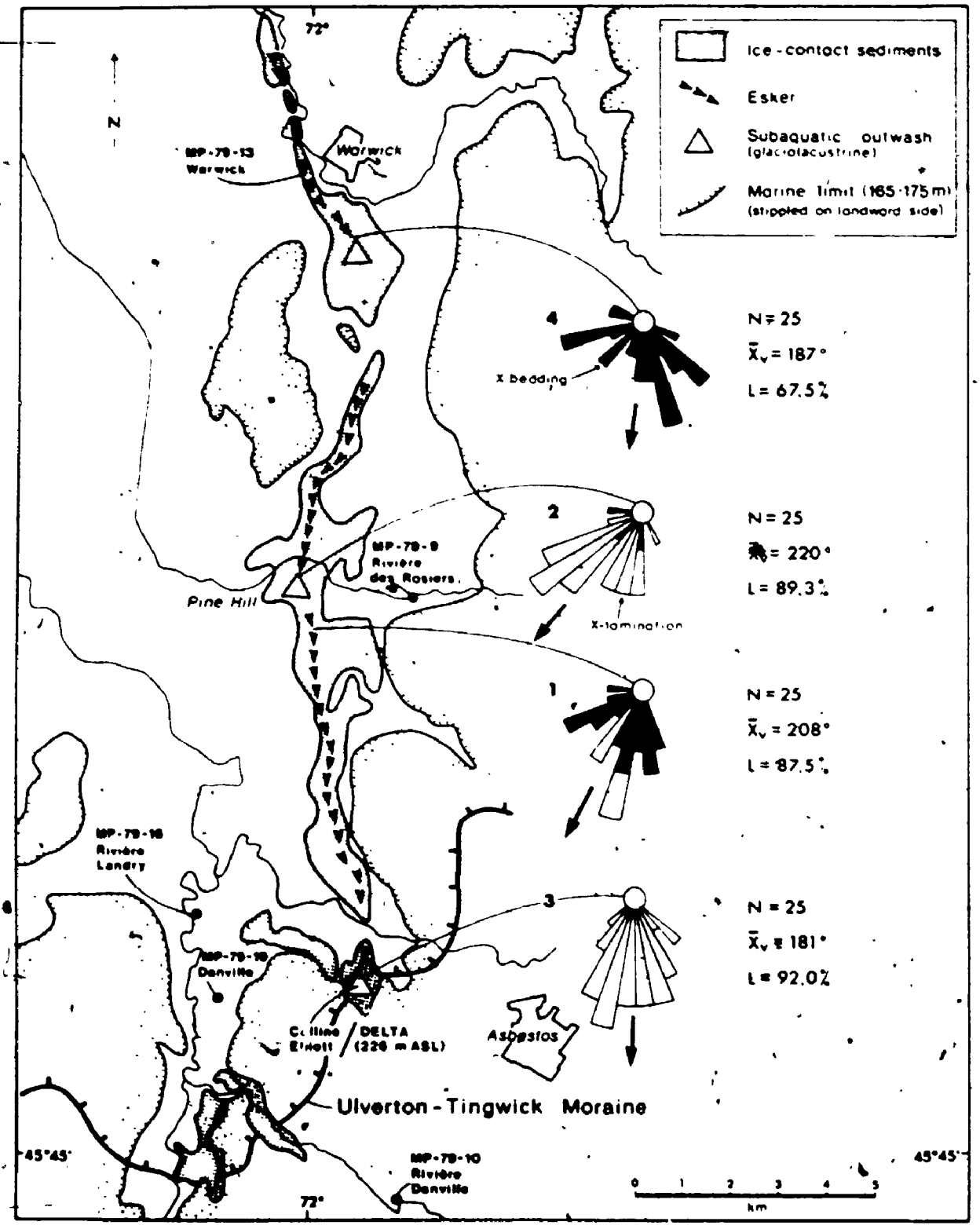

Figure 5-3 : The Warwick-Asbestos esker and its relationships with the Ulverton–Tingwick Moraine, the Colline Elliott delta-kame and the upper marine limit. Paleocurrent data indicate that the esker was deposited by southward-flowing meltwater. Also shown are the locations of several of the sections described in this chapter.

southward dips. Exposed thickness of these sandy outwash bodies is usually about 20 m, but reaches 40 m at Colline Elliott. Orientation measurements from cross-bedded and cross-laminated cosets (Figure 5-3: rose diagrams #2, #3 and #4) indicate that paleocurrent was toward the south; this provides further evidence that these sediments were not deposited on the east side of an ice-front with a local north-south trend, as should be expected if this sediment body were part of the Highland Front Moraine.

Except for the Colline Elliott delta-kame, all deposits of the Warwick-Asbestos esker lie below marine limit (165-175 m ASL). Distinctive outwash bodies at Colline Elliott, Pine Hill and Warwick allow convenient subdivision of the esker complex into three main segments for the purpose of further description and discussion. The west side of the Colline Elliott esker segment has been extensively reworked by wave action and is partly buried under deltaic and littoral sands deposited during the Champlain Sea incursion (see Figure 3-1); its east side however has retained typical esker morphology (ice-contact slopes) except at the north end of the segment, near Rivière des Rosiers, where it is contiguous with thick, poorly exposed, sandy sediments which have been mapped as ice-contact stratified drift but which may eventually prove to be deltaic sediments deposited over stagnant ice blocks. The Pine Hill segment, because it lies east of a large bedrock ridge that formed an island during the marine episode, was well protected from wave action and has retained a typical esker ridge morphology (Figure 5-3). However, the Warwick esker segment was not only reworked by wave action but it was largely buried under fossiliferous marine silts as well as by deltaic sediments supplied by Rivière des Pins (see Figure 5-8); the existence of this segment would have likely remained unsuspected were it not for the series of gravel pits that have been excavated into it. On the other hand, the Warwick subaquatic outwash body was well protected from wave action, much as the Pine Hill esker segment, and has retained its kettled surface.

5.3 Glaciolacustrine and marine sediments younger than drift unit C

Glaciolacustrine and marine sediments younger than surface till (drift unit C) have been mapped by a number of authors (McDonald, 1966, 1967b; Warren et Bouchard, 1976; Parent, 1978; Chauvin, 1979b) in terrains that lie within the study area; sand-gravel facies of littoral or deltaic origin as well as silt-clay facies deposited at greater water-depths (below wave-base) have been reported and mapped for both glaciolacustrine and marine sediments. Because facies of glaciolacustrine sediments may resemble those of marine sediments, particularly when only small or shallow exposures are available, the presence of marine fossils (mainly shells) remains the best way of distinguishing Champlain Sea sediments from those deposited in anterior glacial lakes.

However, marine sediments, particularly littoral or deltaic sands and gravels, are commonly unfossiliferous or only sparsely fossiliferous; this seems to be the result of several combined factors:

1) harsh environmental conditions (low temperature and salinity) that prevailed during at least the early part of the Champlain Sea incursion (Wagner, 1970; Hillaire-Marcel, 1979, 1980; Cronin, 1977a, 1977b, 1979a) may have caused not only low faunal diversity but also low faunal density;

2) abundant detritus derived from freshly deglaciated, sparsely vegetated (Richard, 1977, 1978; 1985; Davis and Jacobson, 1985) adjacent terrains as well as from glaciers within the marine basin (Hillaire-Marcel and Occhietti, 1980; Occhietti, 1980) must have resulted in high sedimentation rates, hence further decreasing apparent faunal density;

3) marine shells lying at shallow depths, particularly in sandy or gravelly deposits, may have been dissolved as a result of intense Holocene weathering.

As a result, marine sediments cannot be consistently identified on the basis of their faunal content.

In areas such as the Asbestos-Valcourt region where proglacial lakes likely extended into terrains that were later invaded by marine waters, this problem is especially critical: McDonald (1966), for instance, mapped glacial-lake sediments in the Appalachian Piedmont but added in the map-legend "(possibly includes some marine material below altitude 540 feet)". This may also explain why Prichonnet (1982a) placed the marine limit at 190 m ASL in the nearby Granby area whilst Chapman (1937) placed it at only about 160 m ASL in the same area. Moreover, Gadd (1983) recently proposed that the highest marine beaches lie at only about 100 m ASL near Granby and Cowansville; however his evidence was strongly disputed by the author (Parent, 1984c) and is squarely contradicted by the presence of marine shells in deltaic sediments at an altitude of 145 m, dated 11 740 ± 200 BP (I-4489), near Frelighsburg in the vicinity of Cowansville (Parrott and Stone, 1972; Wagner, 1972).

5.3.1 Pre-Champlain Sea varved sediments

Although the occurrence of pre-Champlain Sea varves in the Appalachian Piedmont has been recognized for some time (McDonald, 1967a; Gadd, McDonald and Shilts, 1972a; Warren et Bouchard, 1976), very few good varve exposures seem to have been found or reported; as a result, no reference or type sections have been described. During this investigation, several varve exposures were recorded in sections that lie both below and above marine limit (Figure 5-4). Two of these sections, Melbourne (MP-82-1) and Rivière Danville (MP-79-10), are located on the distal (southeast) side of the Ulverton-Tingwick Moraine; they provide a record for a glaciolacustrine episode, presumably Fort Ann phase of Glacial Lake Vermont, that took place after deposition of the Mont Ham Moraine but prior to or during deposition of the Ulverton-Tingwick Moraine.

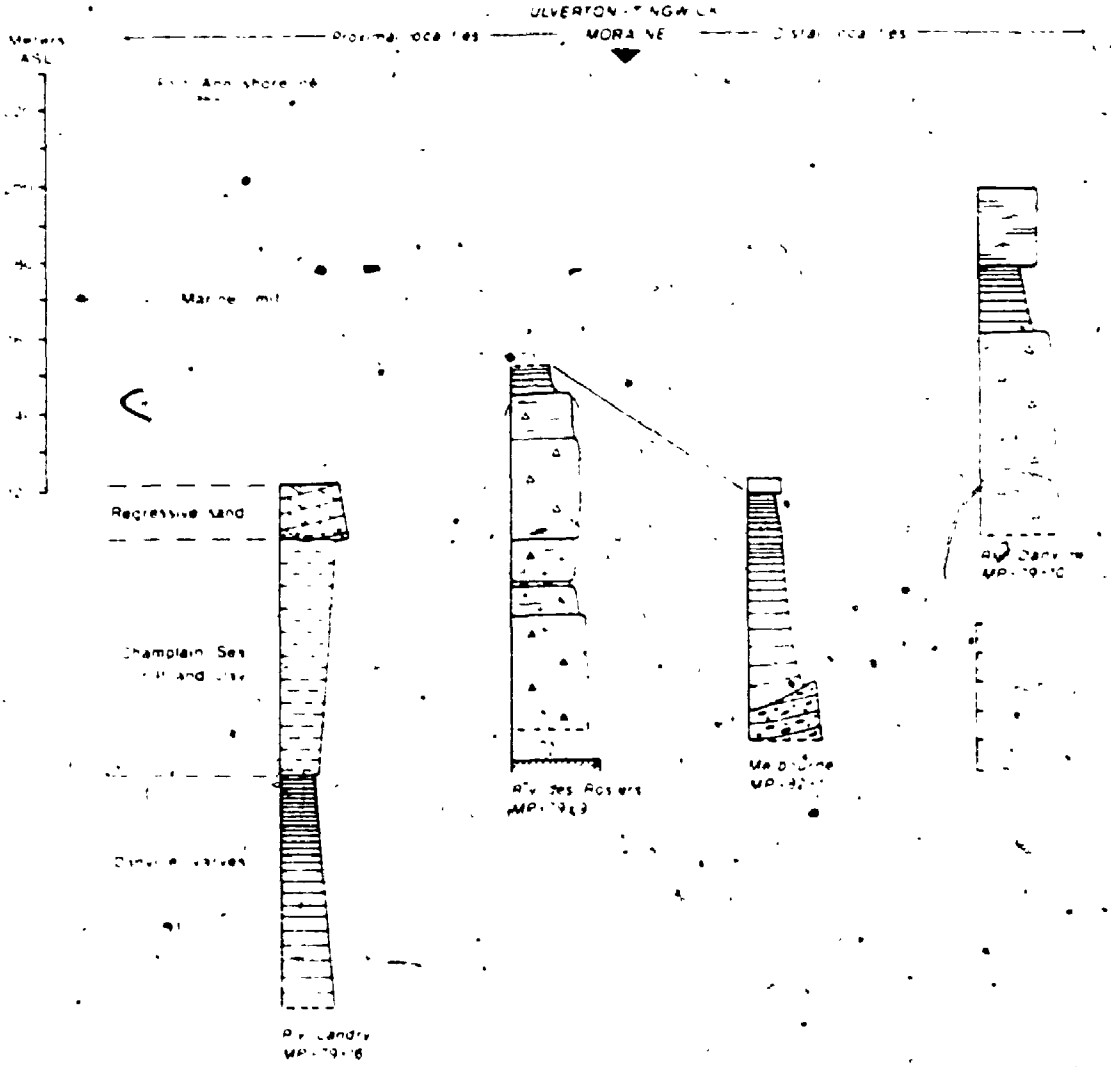

Figure 5-4 : Measured sections recording occurrences of pre-Champlain Sea varves along the northwest edge of the Appalachian uplands, Asbestos-Valcourt region. Relationships with the elevation of the Fort Ann shoreline and of the marine limit are also shown. (See legend in Figure 4-12)

Rivière Danville section (MP-79-10)

At Rivière Danville near Asbestos, about 3 km southeast of the Ulverton-Tingwick Moraine (Figure 5-3), lodgement till of drift unit C is overlain by a 2.2 m-thick varve sequence which is in turn overlain by 2.8 m of plane- and cross-laminated glaciolacustrine sand. Varve couplets consist of 2 to 3 cm-thick summer layers (single- or multiple-graded silt layers) overlain by thinly laminated clayey winter layers. The thinning-upwards trend which characterizes the summer layers rather than the winter layers suggests that the Rivière Danville site became increasingly distal during the glaciolacustrine episode. The overlying sand unit may reflect either shoaling of the impounded water-body or perhaps a return to proximal (deep-water) sedimentation.

Melbourne section (MP-82-1)

In the Melbourne section (MP-82-1), which lies at an altitude of only 122 m in the Saint-François River valley near Richmond, about 7 km southeast of the Ulverton-Tingwick Moraine (see Figure 3-1), a 7.0 m-thick varve series directly overlies ice-contact stratified drift (Figure 5-4). The varve series consists of two thinning-and-fining-upwards sequences that are essentially recognized through changes of thickness and texture of the summer layers. The upper sequence is at least 1.9 m-thick (top of section has been extensively disturbed); it consists of 23 or more couplets whose silty summer layers contain trace fossils (*Paeichnia*: grazing traces; nomenclature of Seilacher, 1964; see also Frey and Pemberton, 1984). The lower sequence has a thickness of 3.6 m and consists of 33 couplets whose summer layers decrease in thickness from 1.1 m in the basal varve to 0.5 cm in varve #33; thickness of winter layers (thinly laminated clay) decreases only slightly, from 3 to 2 cm. Summer layers grade from thick sandy turbidites in basal varves, to graded sandy silt, and to laminated calcareous silt near to top of the sequence, much as in some sequences reported by Banerjee (1973). Ripple-lamination in turbidite layers indicates that paleocurrent was toward southeast (upvalley) and thus that turbidity

currents must have originated at an ice-front located northwest of the Melbourne locality.

Rivière des Rosiers section (MP-79-9)

In the Rivière des Rosiers section (MP-79-9), which lies about 15 m below marine limit, but a few km northwest of the Ulverton-Tingwick Moraine (Figure 5-3), till of drift unit C is overlain by a 1 m-thick, thinning-upwards sequence of graded silt and clay couplets which are most likely varves. Because the upper part of the section was not fully exposed, it remains somewhat uncertain that these rhythmites are true glacial-lake varves; however, given the thinning-upwards sequence and given the shallow water-depth (about 15 m) that nearby Champlain Sea deltas would imply, a marine origin seems unlikely.

Rivière Landry section (MP-79-16)

The Rivière Landry section (MP-79-16), near Danville (Figure 5-3), is the most significant of these sections that provide direct evidence for the existence of deep-water glaciolacustrine environments in the Appalachian Piedmont, prior to Champlain Sea incursion (Figure 5-4); since this is the only currently reported section where varves can be observed directly underlying fossiliferous marine clay in this region, the section was the object of detailed investigations. At Rivière Landry, a 9 m-thick, silt and clay varve sequence that extends to an unknown depth below river level is overlain by 8 m of laminated fossiliferous (Macoma balthica and Hiatella arctica) marine silt which are in turn overlain by a 2 m-thick regressive sand unit (Figures 5-4 and 5-5).

The exposed varve sequence consists of 103 couplets whose average thickness (5-year running mean) decreases from about 25 cm near the base of the unit to about 2.5 cm near the top (Figure 5-6); however, this overall thinning-upwards trend, which is predominantly recorded within summer layers, shows several secondary cycles. Summer layers consist mainly of plane-laminated, light gray, calcareous, slightly bioturbated

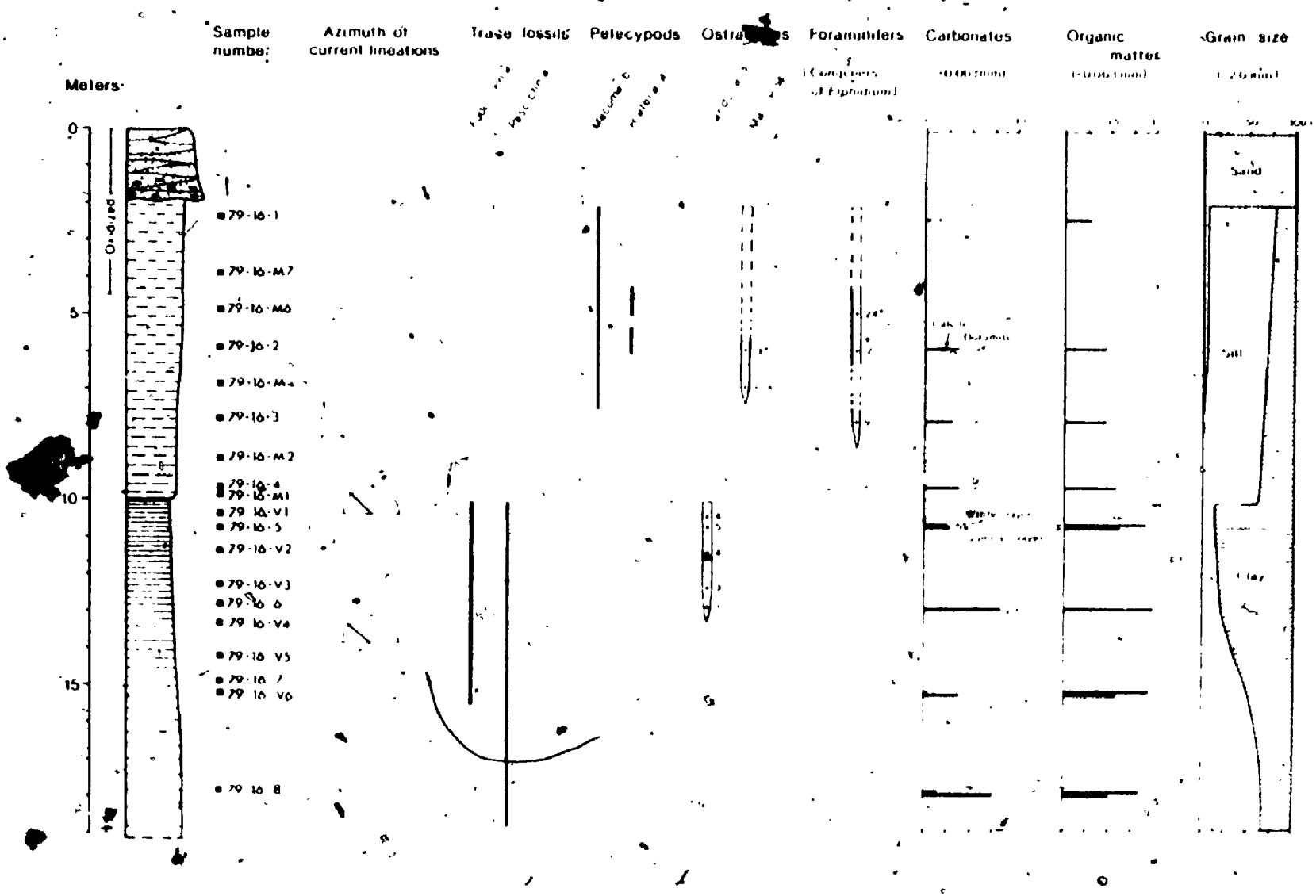

Figure 5-5 Faunal and sedimentologic record of the Rivière Landry type section (MP-79-16) (See legend in Figure 4-12)


3
1.0
1.1
1.25
1.4
1.6
2.8
3.2
3.6
4.0
2.5
2.2
2.0
1.8
MICROD

silt. Very fine sand partings are present within almost all summer layers; in two varves, these partings show distinct, NW-SE trending, parallel lineations that must have been produced by turbidity currents. Moreover, following examples given by Banerjee (1973) and Ashley (1975) for instance, these varves are best interpreted as turbidites with $(C)DE_{(t,h)}$-divisions (nomenclature of Walker, 1984). A few thick (30 cm or more), contorted (convolute lamination) summer layers occur in the lower 3.5 m of the varve unit (varves #4, 7, 12 and 17). A plot of mean grain size (M_Z) versus depth shows that the thinning-upwards trend is paralleled by a fining-upwards trend which is best recorded within summer layer samples (Figure 5-7). The winter layers consist mainly of thinly laminated or faintly laminated, stiff, non calcareous, dark gray clay.

Annual rhythmicity of these varves is demonstrated by the fact that the occurrence of trace fossils is restricted to the coarser, light-coloured, summer layers. Trace fossils are most common in sandy partings that are present in summer layers throughout the varve unit; they consist mainly of grazing traces (**Pascichnia**), but crawling traces (**Repichnia**) were also observed together with grazing traces in a few varves. Feeding structures (**Fodinichnia**) which are present within laminated silt layers above a depth of 15.5 m disappear at the contact with the overlying marine silt, much like **Pascichnia** and **Repichnia** (Figure 5-5). Above a depth of 13 m, the varves contain sparse valves of **Candona subtriangulata**, a benthic ostracode species which typically inhabits arctic freshwater lakes but which, according to Cronin (1977a, 1977b), may also be tolerant to low salinity environments such as those which he thought characterized the Transitional phase of the Champlain Sea. However, given the characteristic sedimentology of the varves and given the absence of other ostracode or foraminifer species that characterize Cronin's Transitional phase, this author believes that the varves were deposited in a typical glaciolacustrine environment. In samples below 13 m, **Candona s.** is apparently absent (Figure 5-5); this however may well be a consequence of the high sedimentation rates (10 to 20 $cm.a^{-1}$) recorded in the lower part of the varve unit. A fragment of **Candona** sp. which was found in sample

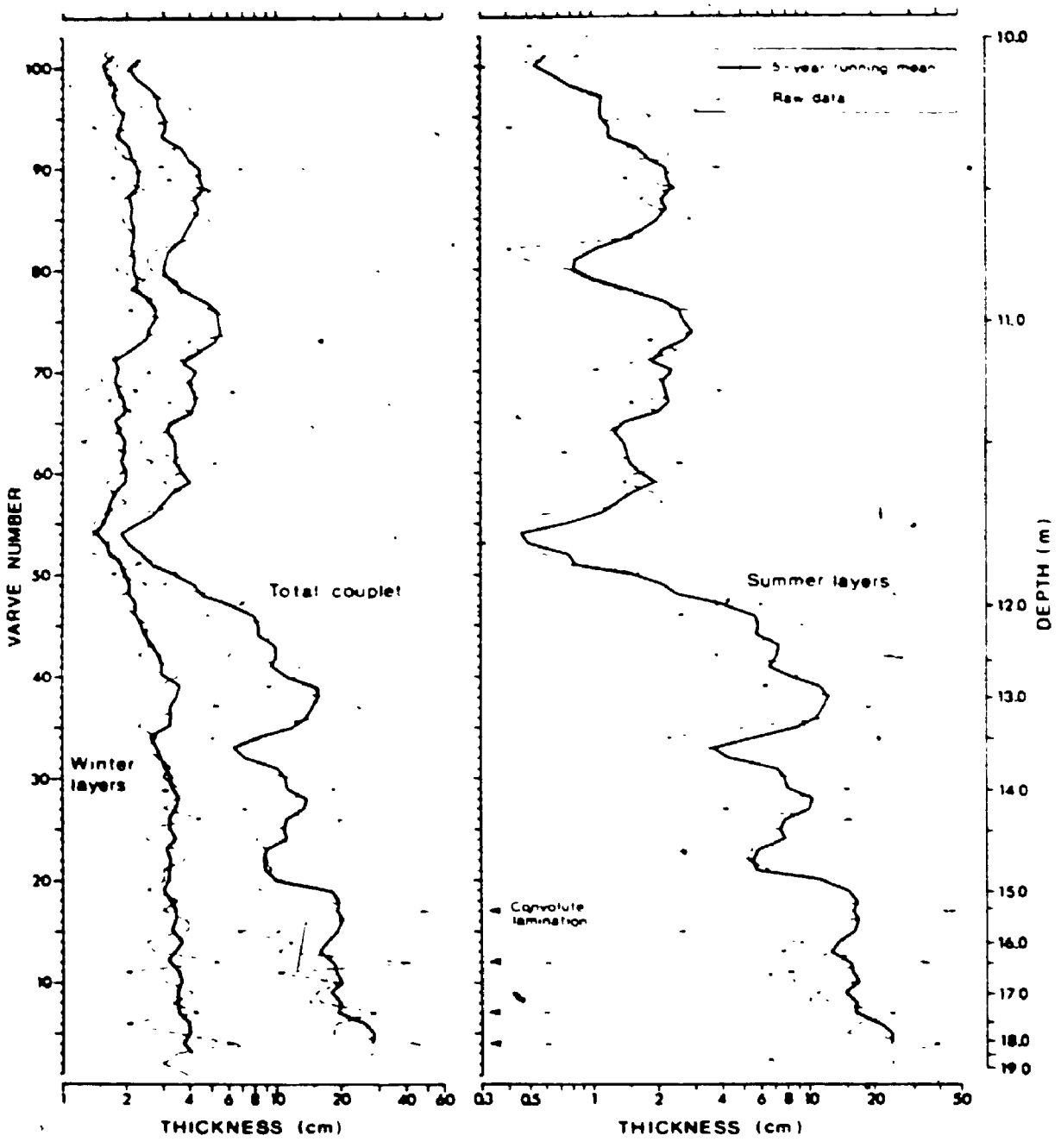

Figure 5-6 : Varve thickness diagram, Danville Varves (Rivière Landry section).

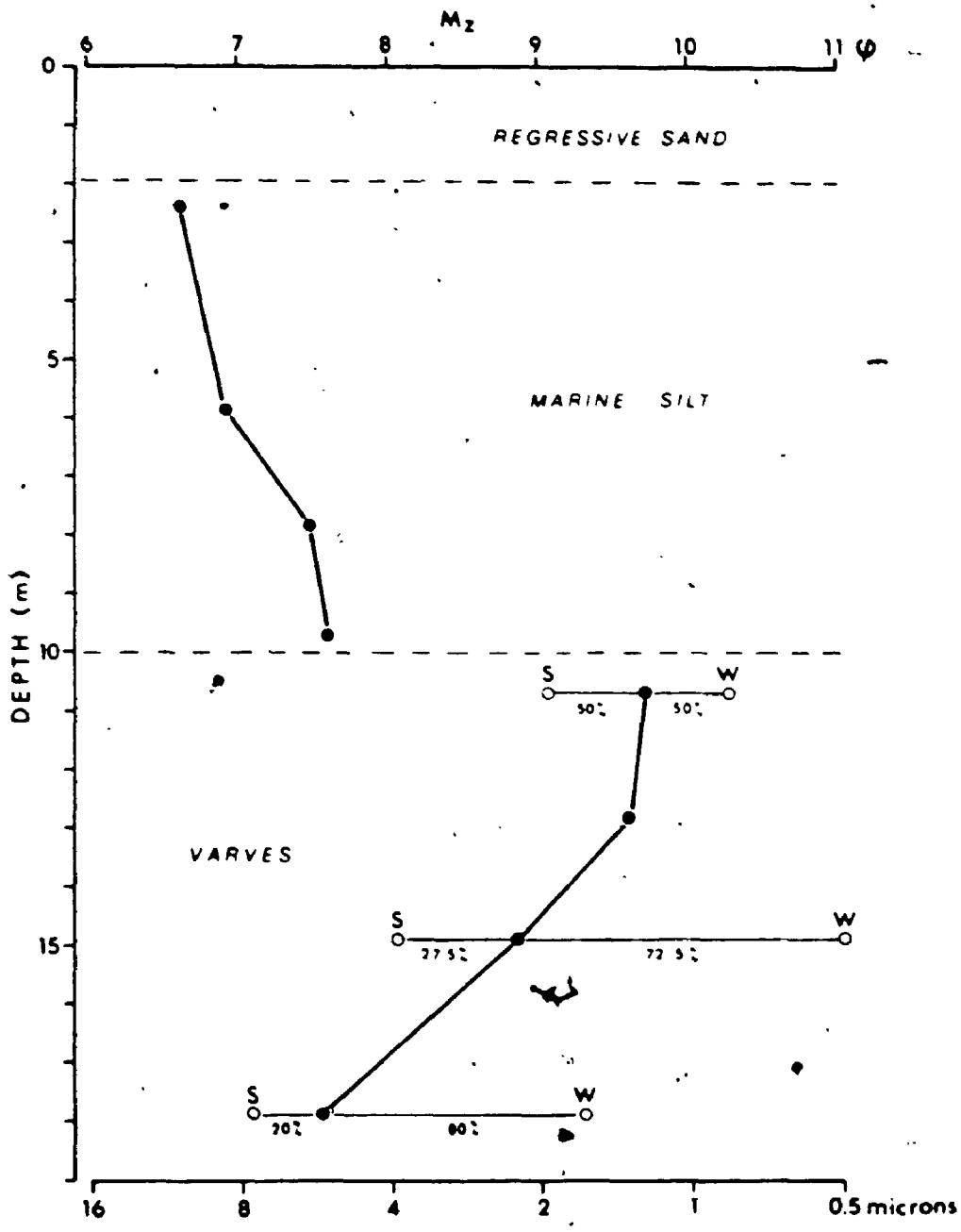

Figure 5-7 : Vertical variations of grain-size mean (M_z), Rivière Landry section. The varves show a fining-upward trend while the marine silt unit shows a coarsening-upward trend. S = summer layer ; W = winter layer. Solid dots in the varve series represent weighted average for total varve couplet; percent figures represent weighting factors based on thickness data.

species belong to faunal assemblages that characterized the Hiatella arctica phase of the Champlain Sea (prior to about 11 000 years BP).

Above a depth of 4.5 m, the marine silt unit contains sandy interbeds whose thickness varies from 2 to 3 cm and is fairly oxidized; presumably as a result of dissolution during the Holocene, the upper part of the marine unit was found to be devoid of microfossils. However several molds of **Macoma balthica** (in growth position) were observed in silt layers up to the base of the regressive sand unit (Figure 5-5).

5.3.2 Champlain Sea sediments

A full description of marine sediments observed in the Asbestos-Valcourt region is beyond the scope of this thesis; excellent summaries and descriptions of Champlain Sea sediments and fauna are available elsewhere (Hillaire-Marcel, 1977, 1979, 1980; Occhietti, 1977, 1980; McDonald, 1967a, 1968; Elson, 1969a, 1969b; Cronin, 1977a, 1979a, 1979b; Gadd, 1971; Wagner, 1970). Let us simply say that numerous marine beaches, deltas and littoral terraces have been recognized up to altitudes of about 175 m in the Asbestos-Valcourt region (see Figure 3-1); however, the marine limit decreases to altitudes of about 165 m in marginal embayments (Saint-François River and Landry River valleys). This assessment of the marine limit (from 165 to 175 m ASL, depending upon location) is essentially in agreement with a previous assessment (165 m ASL) by McDonald (1967a, 1968) and with surficial geology maps published since (Warren et Bouchard, 1976; Chauvin, 1979a, 1979b). The fairly large altitude difference (50 to 60 m) which separates marine-limit strandline features from those formed during the earlier glaciolacustrine episode (Fort Ann phase of Lake Vermont) provides fairly conclusive evidence, even in the absence of marine fossils, for the recognition of marine-limit features. Moreover marine shells are now being reported up to altitudes of 149 m in the Asbestos-Valcourt region (Table 5-1; Figure 3-1). The main purpose of this section is to present the stratigraphic context of marine faunas that were ^{14}C dated in the course of the present study.

species belong to faunal assemblages that characterized the **Hiatella arctica** phase of the Champlain Sea (prior to about 11 000 years BP).

Above a depth of 4.5 m, the marine silt unit contains sandy interbeds whose thickness varies from 2 to 3 cm and is fairly oxidized; presumably as a result of dissolution during the Holocene, the upper part of the marine unit was found to be devoid of microfossils. However several molds of **Macoma balthica** (in growth position) were observed in silt layers up to the base of the regressive sand unit (Figure 5-5).

5.3.2 Champlain Sea sediments

A full description of marine sediments observed in the Asbestos-Valcourt region is beyond the scope of this thesis; excellent summaries and descriptions of Champlain Sea sediments and fauna are available elsewhere (Hillaire-Marcel, 1977, 1979, 1980; Occhietti, 1977, 1980; McDonald, 1967a, 1968; Elson, 1969a, 1969b; Cronin, 1977a, 1979a, 1979b; Gadd, 1971; Wagner, 1970). Let us simply say that numerous marine beaches, deltas and littoral terraces have been recognized up to altitudes of about 175 m in the Asbestos-Valcourt region (see Figure 3-1); however, the marine limit decreases to altitudes of about 165 m in marginal embayments (Saint-François River and Landry River valleys). This assessment of the marine limit (from 165 to 175 m ASL, depending upon location) is essentially in agreement with a previous assessment (165 m ASL) by McDonald (1967a, 1968) and with surficial geology maps published since (Warren et Bouchard, 1976; Chauvin, 1979a, 1979b). The fairly large altitude difference (50 to 60 m) which separates marine-limit strandline features from those formed during the earlier glaciolacustrine episode (Fort Ann phase of Lake Vermont) provides fairly conclusive evidence, even in the absence of marine fossils, for the recognition of marine-limit features. Moreover marine shells are now being reported up to altitudes of 149 m in the Asbestos-Valcourt region (Table 5-1; Figure 3-1). The main purpose of this section is to present the stratigraphic context of marine faunas that were ^{14}C dated in the course of the present study.

Table 5-1 : RADIOCARBON DATES

LABORATORY NUMBER	AGE (years BP)	ALTITUDE (m ASL)	LOCALITY (latitude, longitude)	DATED MATERIAL	SEDIMENT	COLLECTOR	REFERENCE
1. Early Champlain Sea fauna, southeastern part of central basin							
I- 13342	11 700 ± 170	127	Warwick, Qc (45°58'29" N) (72°00'05" W)	Hiatella arctica, *Balanus crenatus	Reworked esker gravel and silty sand	Parent	Parent, 1984c
GSC-187	11 410 ± 150	122	Kidgeey Falls, Qc	Macoma calcarea Mya truncata Hiatella arctica	Stratified silty sand and clay	Gadd	Dyck et al. 1965
GSC-290	11 370 ± 200	149	Danville, Qc (45°46'49" N) (72°01'28" W)	Macoma balthica	Deltaic sand	Parent	Parent, 1984c
GSC-505	11 880 ± 180	122	L'Avenir, Qc	Macoma balthica (90%) Hiatella arctica (8%) Mya sp. (1%) Yoldia sp. (1%)	Pebbly gravel and sand	McDonald	Loudon and Blake, 1970
GSC-936	12 000 ± 230						
GSC-475-2	11 500 ± 160	145	Ste-Christine, Qc	Hiatella arctica (mostly) Macoma sp. (fragments) Yoldia sp. (fragments) Mytilus edulis (fragments)	Silt	McDonald	Loudon and Blake, 1970
GSC-475	11 530 ± 160						
BQ-29	11 360 ± 110	105	Adamsville, Qc	Macoma balthica	Sand	Prichonnet	Prichonnet, 1982a, 1984
I-4489	11 740 ± 200	145	Preligheburg, Qc	Macoma balthica	Lens of sand and clay in deltaic material	?	Parrott and Stone, 1972 Wagner, 1972
QC-200	11 665 ± 175	79 (95?)	Plattsburg, NY	Macoma balthica	Unspecified	Cronin	Pardi, 1977 Cronin, 1977
GSC-2338	11 900 ± 120	101	Peru, NY	Macoma balthica	Pebbly sand	Cronin	Loudon and Blake, 1979
GSC-2366	11 800 ± 150	96	Plattsburg, NY	Macoma balthica	Silty sand	Cronin	Loudon and Blake, 1979

Table 5-1 (continued)

QC-475	12 480 ± 240	61	St-Dominique, Qc	Mya sp.	Unspecified	Prichonnet	Prichonnet, 1982a
GrN-1697	11 490 ± 110	171	Mont Royal, Qc	Unidentified shells	Unspecified	Elson	Elson, 1962, 1969a
ooo-2311	11 420 ± 350	58	Burlington, Vt	Unidentified pelecypods	Silt and clay	Hunt and Wagner	Wagner, 1972 Spiker et al., 1978
2. Early Champlain Sea fauna, Québec City region							
GSC-1533	12 400 ± 160	110	Charlesbourg, Qc	Portlandia arctica	Clayey sand	LaSalle	Loudon and Blake, 1973
QU-93	12 230 ± 250	104	St-Henri-de-Lévis, Qc	Hiatella arctica	Interbedded gravel and clay	LaSalle	Samson et al., 1977
GSC-1235	11 600 ± 160	176	N.-D.-des-Laurentides, Qc	Mya truncata	Glaciomarine sediment	LaSalle	Loudon and Blake, 1976
3. Dates pertaining to regressive marine levels, Asbestos-Valcourt region and immediate vicinity							
oooQQ-289	10 780 ± 190	132	Warwick, Qc (45°56'28" N) (72°00'09" W)	Hiatella arctica Macoma balthica °Balanus crenatus °Mytilus edulis °Mya truncata ovata	Reworked esker gravel and sand	Parent	Unpublished
UQ-947	10 350 ± 100	81	St-Wenceslas, Qc (46°09'06" N) (72°18'50" W)	Mya arenaria °Macoma balthica	Sand	Parent	Unpublished
GrN-2034	10 590 ± 100	81	Duncan, Qc	Mya arenaria °Mytilus edulis °Macoma balthica	Sand	Elson	Elson, 1969a
L-441 C	9 500 ± 300	91	St-Germain, Qc	Non-calcareous gyttja at base of core		Terasmae	Gadd et al., 1972

° Other species present, but not submitted for dating.
oo This date relates to a regressive sea level stand at 153 m ASL.
ooo Used from the same silt and clay unit was dated 10 950 ± 300 years BP (W-2309).
oooo This date relates to a regressive sea level stand at 136 m ASL.

Warwick section (MP-79-13)

Though the Rivière Landry section provides an excellent stratigraphic record of regional events prior to and during the marine incursion, its disseminated molluscan fauna could not be ^{14}C-dated. The Warwick section (MP-79-13) provides an excellent opportunity to date the marine incursion as well as to further clarify relationships between ice-contact sediments and early Champlain Sea sediments (Figure 5-8). The section actually consists of several subsections that are exposed in a gravel pit which has been excavated mainly into sediments of the Warwick-Asbestos esker (see Figure 5-3 for location). Near Warwick, the esker is largely buried by marine and deltaic sediments whose surface lies between 136 and 138 m ASL; present relief of the esker has been reduced to only a few meters.

The most complete stratigraphic record is provided by subsection A where esker gravels are overlain by fossiliferous marine silts which are in turn overlain by regressive deltaic sands (Figure 5-8). At the very base of the marine silt unit, a 30 cm-thick bed of resedimented silty gravel and sand contains a slightly displaced fauna consisting of **Hiatella arctica** (valves commonly unbroken and closed) and of **Balanus crenatus** (commonly unbroken and still attached to pebbles). According to Hillaire-Marcel (1980), this type of epibiontic assemblage commonly inhabited coarse-grained substrates at intermediate water-depths (0-30 m). Since the overlying laminated clayey silts which contain only sparse shells of **Macoma balthica** must have been deposited mainly below wave base, it is inferred that the **Hiatella arctica - Balanus crenatus** assemblage, dated 11 700 ± 170 years BP (I-13 342), was displaced from the ridge or flank of the esker during occasional large storms. At that time, water level may have already started to recede from beaches at the marine limit (about 175 m ASL in the vicinity of the section). The resedimented sand and gravel unit which overlies esker gravel in the contiguous subsection (B) includes abundant, slightly displaced specimens of **Hiatella arctica, Balanus crenatus** and **Macoma balthica**, a few valves of **Mya truncata uddevalensis** and some fragments of **Mytilus edulis**; this mixed faunal assemblage (f-3)

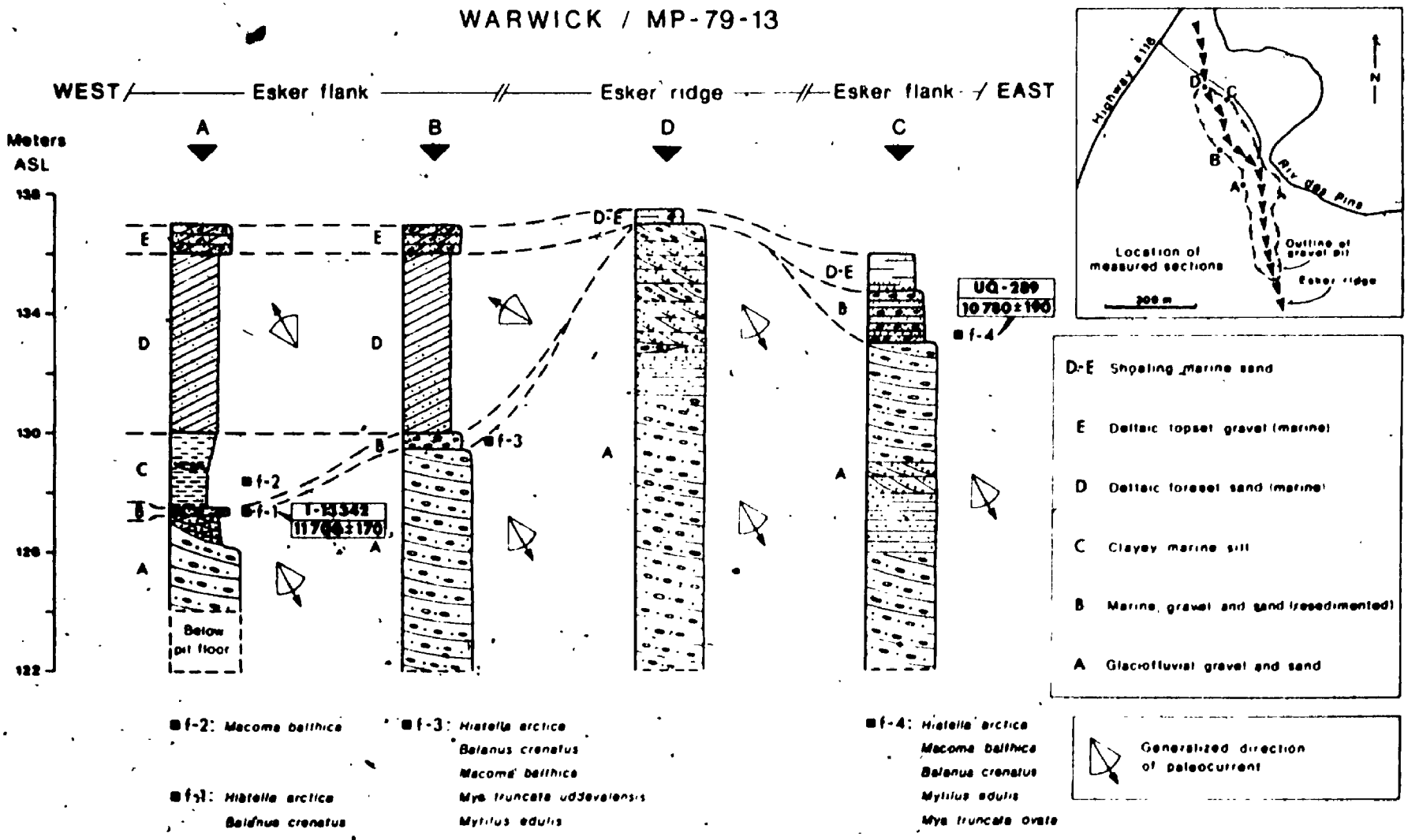

Figure 5-8 : Lateral facies relationships, marine faunal assemblages (f-1 through f-4) and radiocarbon dates, Warwick section (MP-79-13). The age of resedimented esker sediments spans about 1000 years.

may be slightly younger than or contemporaneous with the **Macoma balthica** fauna of the clayey silt unit. In subsection A, the silt unit grades upward into foreset sands which are also present in subsection B. The age of the foreset and topset beds is given by a ^{14}C date (10 780 ± 190 years BP, UQ-289) on a shallow-water faunal assemblage that was found in well-sorted sand and gravel overlying esker gravel on the opposite flank (Figure 5-8); shells of this assemblage consisting of **Hiatella arctica, Macoma balthica, Balanus crenatus, Mytilus edulis** and **Mya truncata ovata** (in order of decreasing abundance) were mostly unbroken and in growth position.

Danville section (MP-79-19)

The 1000-years offlap history provided by the Warwick locality is nicely supplemented by a ^{14}C-dated deltaic sequence near Danville (see Figure 5-3 for location); the Danville section (MP-79-19) is exposed in a gravel pit excavated into a regressive delta whose surface stands at 153 m ASL. In the gravel pit and adjacent roadcut, an 8 m-thick unit of bottomset silt and sand is overlain by foreset sands and topset gravels (Figure 5-9). The bottomset beds consist of a coarsening-and-thickening-upwards rhythmite sequence; the rhythmites consist of alternating silt and fine sand layers. The faintly laminated silt layers contain sparse shells of **Macoma balthica** that are in growth position throughout the unit, and they also contain burrow pits (**Domichnia**) that were most likely made by **Macoma balthica**. Thickness of the sand interbeds reaches up to 15 cm in the upper bottomset beds but decreases gradually downward to become simple partings in the lower 2 m of the unit. The contact of the silt and sand rhythmites with the overlying foreset sands is gradational and this contact zone is deformed by ball-and-pillow structures throughout much of the exposure. The contact zone locally contains a slightly displaced molluscan fauna (valves attached and mostly closed) consisting of a single species, **Macoma balthica**, dated 11 370 ± 200 years BP (UQ-290). This date gives the age of a regressive sea-level stand at 153 m ASL, about 12 m below the local altitude of the marine limit; this date is thus consistent with

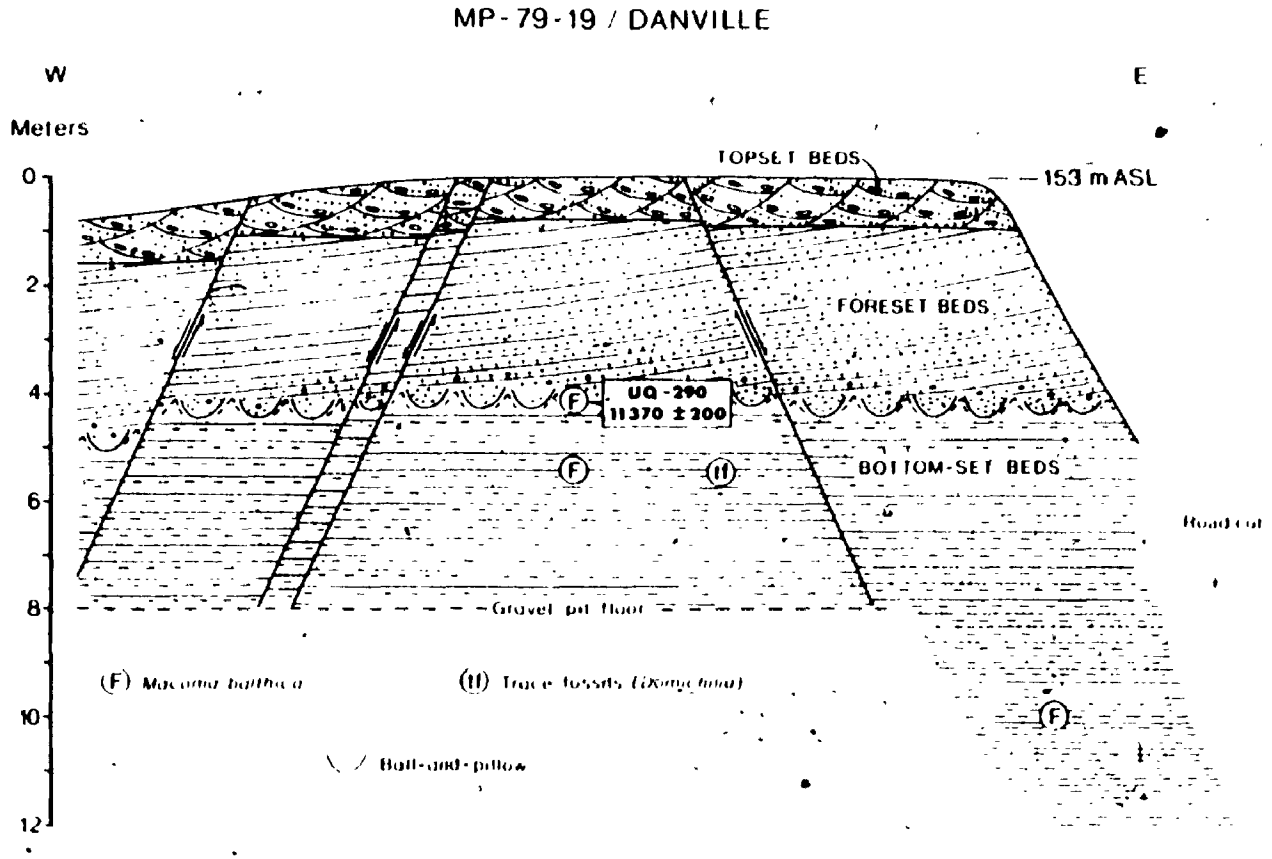

Figure 5-9 : Lithofacies and ^{14}C-dated marine fauna in a prograding Champlain Sea delta (Danville section, MP-79-19). This delta, which likely overlies the Danville Varves and which was formed during marine regression (local marine limit stands at ~165 m ASL), was formerly assigned to the Highland Front Moraine System (Gadd et al., 1972 a : Map 10-1971). (See legend in Figure 4-12)

^{14}C dates from the Warwick section and with dates previously obtained by McDonald (1967a, 1968) in the western part of the study area (listed in Table 5-1).

The occurrence of minor step faults that cut across all units of the Danville section (Figure 5-9) suggests that small blocks of stagnant ice persisted during construction of early Champlain Sea deltaic terraces in the Danville embayment. Elsewhere in the study area, particularly in more open sites, little evidence was found to suggest that early marine sediments were deposited over, or adjacent to, stagnant ice blocks.

Near St-Wenceslas, a few km northwest of the study area (co- ordinates are given in Table 5-1), at an altitude of 81 m, a 1 m-thick littoral sand unit which overlies deep-water marine silt contains a typical intertidal faunal assemblage consisting of **Mya arenaria** and **Macoma balthica**, dated 10 350 ± 100 years BP (UQ-947). This date, together with GrN-2034 (10 590 ± 100 years BP) obtained on a similar faunal assemblage (Elson, 1969a; see Table 5-1) near Duncan, also at 81 m ASL, just west of the study area, indicates that, by about 10 500 years BP, level of the Champlain Sea had regressed to altitudes of 90 m or less and thus that the marine incursion had ended in the Appalachian Piedmont of the Asbestos-Valcourt region.

5.4 Late Wisconsinan glaciolacustrine episodes

Proglacial lakes impounded at the ice-front provide a relatively independant means of testing deglacial patterns depicted in Figure 5-1. Strandline features consisting mainly of ice-contact and fluvial deltas, ice-contact lake terraces, littoral terraces (mainly wave-cut) and beach sediments have been recognized throughout much of the Asbestos-Valcourt region (see Figure 3-1) during this and earlier studies (McDonald, 1967a; Parent, 1978). Elevations of features that were compiled from previous reports or determined during this investigation are plotted in Figures 5-10, 5-11, 5-12 and 5-13 and listed in Tables A-5 and A-6. The shoreline diagram (Figure 5-10) and paleogeographic maps (Figures 5-11,

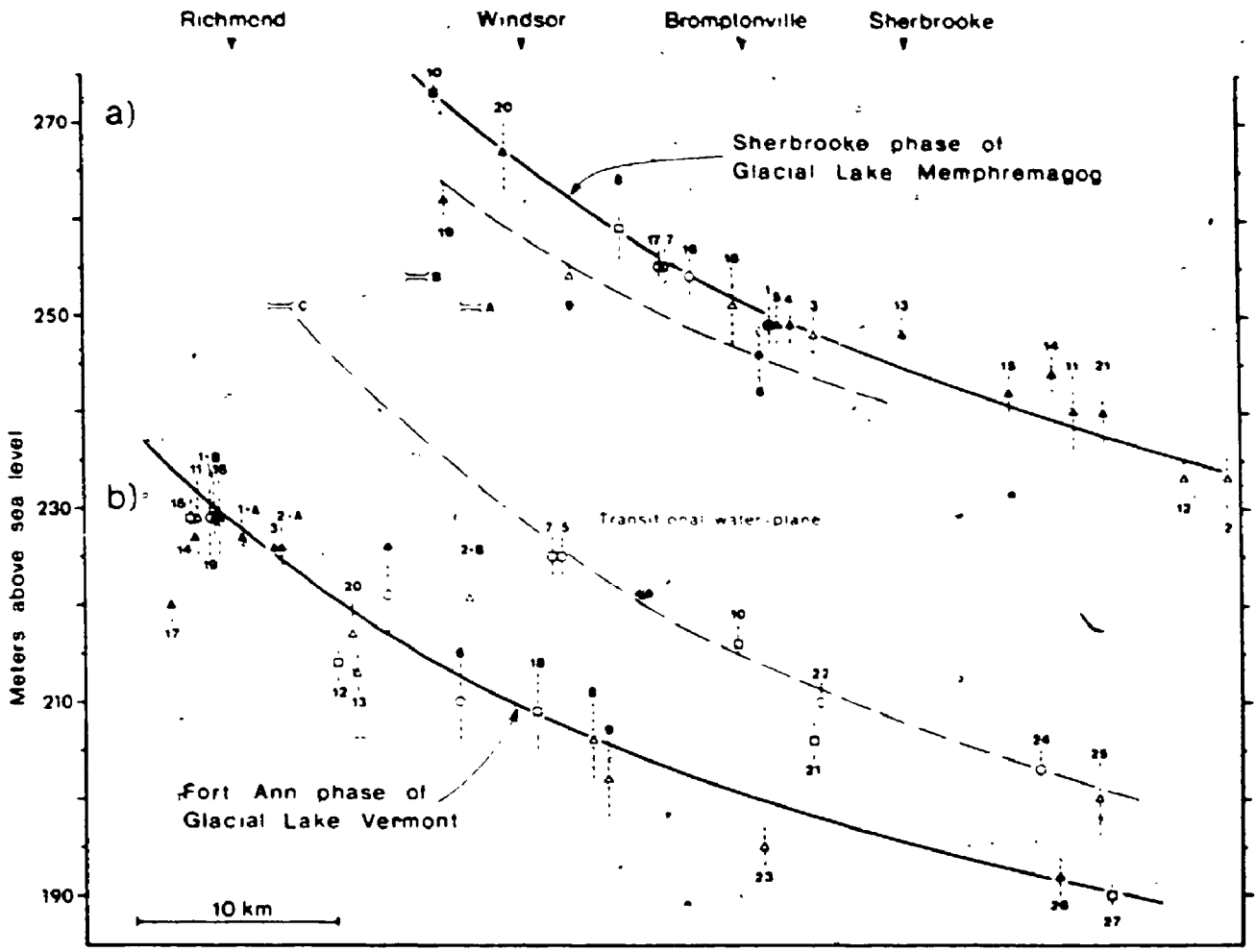

Figure 5-10 : Shoreline diagram for the Sherbrooke phase of Glacial Lake Memphremagog (a) and for the Fort Ann phase of Glacial Lake Vermont (b). Location of shoreline features and line of section are given in Figures 5-11 and 5-12 with the same symbols. Dashed vertical lines represent probable measurement errors of altitude data.

5-12 and 5-13) were constructed so that data points show minimum overall departure from reconstructed isobases; given the flexural rigidity of the lithosphere in tectonically stable areas (Walcott, 1970, 1972, 1973), isobases were constructed so as to show only smooth variations of trend and gradient.

The shoreline diagram indicates that, in addition to features related to the marine limit, two main groups of strandline features are recorded within the study area:

(1) A series of features whose altitudes rise northwestward from about 233 m south of Sherbrooke to about 270 m near Windsor (Figure 5-10a). Most of these features belong to the warped water-plane of the Sherbrooke phase of Glacial Lake Memphremagog (McDonald, 1968); maximum tilt of the water-plane is about 1 $m.km^{-1}$ toward northwest (N 320°).

(2) A series of features whose altitudes rise northwestward from as low as 190 m near Sherbrooke to about 230 m near Richmond (Figure 5-10b). The features belong to two distinct warped water-planes that are only about 10 to 15 m vertically apart. The lower features of this series are thought to belong to the Fort Ann phase of Glacial Lake Vermont while the upper ones probably belong to a fairly short-lived, intermediate glacio-lacustrine water-body which had only local extent. Maximum tilt of these water-planes is also about 1 $m.km^{-1}$ toward northwest (N 310°); their parallelism with earlier water-planes suggests that the lakes were short-lived and that deglaciation was quite rapid.

5.4.1 Sherbrooke phase of Glacial Lake Memphremagog

As stated by McDonald (1967a, 1978), the level of the Sherbrooke phase of Glacial Lake Memphremagog was controlled by the Lac Nick outlet (Figure 5-11: feature #1) through which waters impounded within the Saint- François River watershed drained into Glacial Lake Vermont via

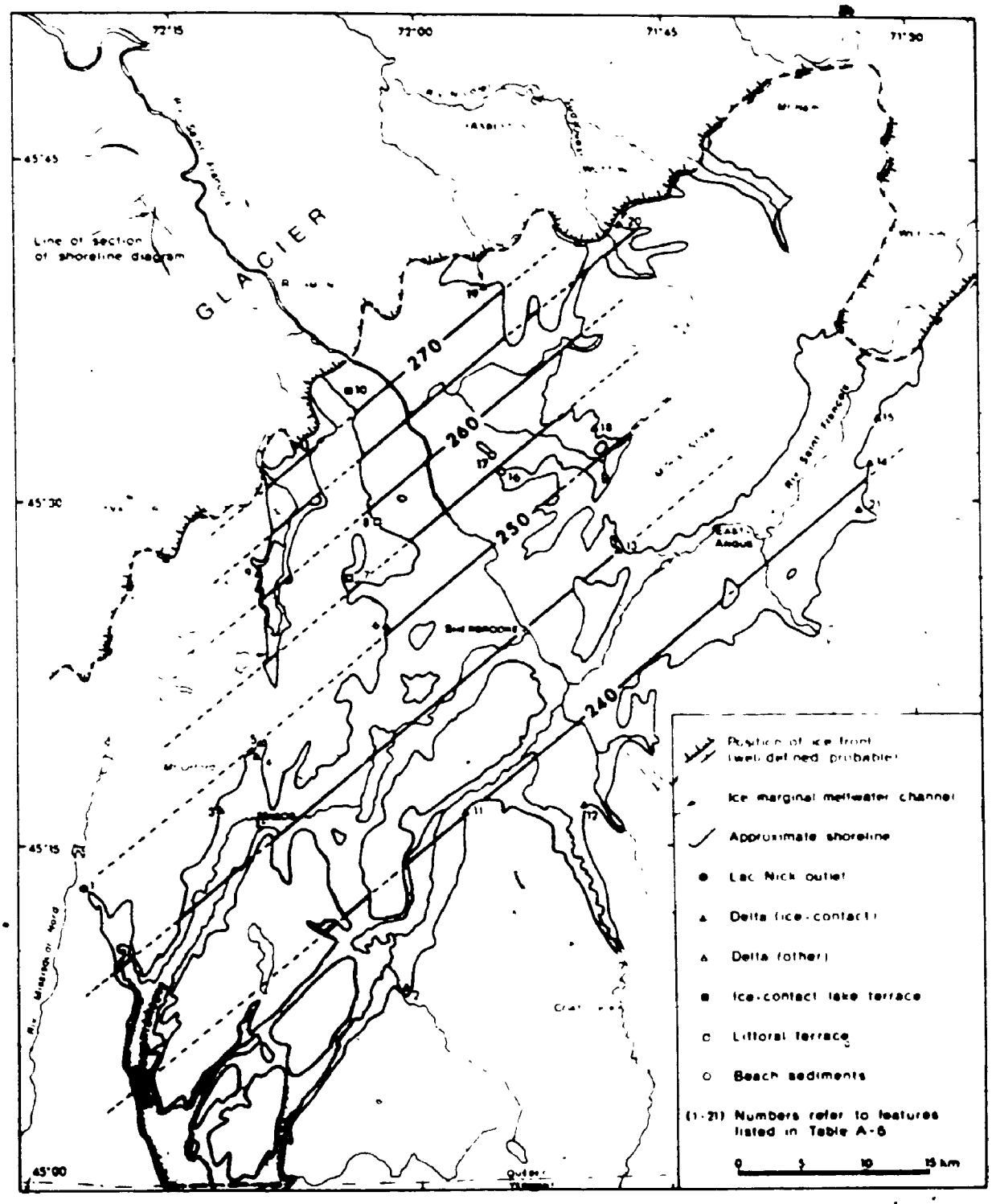

Figure 5-11: Sherbrooke phase of Glacial Lake Memphremagog during construction of the Mont Ham Moraine. Isobases on the former water-plane are in m ASL ; elevations of shoreline features are shown in Figure 5-10a and listed in Table A-5.

the Rivière Missisquoi Nord valley. During at least the latter part of the Sherbrooke phase, waters of Lake Vermont had fallen to the level of the Fort Ann phase (Dubé, 1983; Parent et al., 1985).

The Sherbrooke phase is the last of a series of glacial-lake levels that have been recognized mainly in the southern part of the Lake Memphremagog basin (McDonald, 1967a, 1968; Boissonnault et Gwyn, 1983; Dubé, 1983); however, contrary to terminology utilized by Boissonnault and Gwyn (1983), subsequent water-bodies that may have existed in the Lake Memphremagog basin at levels slightly above present-day level should not be assigned to Glacial Lake Memphremagog since their outlets must have been located well outside of the lake basin drainage area (see Figure 5-12) and since these lake levels had little, if anything, to do with high-level glacial lakes that were impounded in the Lake Memphremagog basin during deglaciation. Much as McDonald (1967a, 1968) had realized, strandline features of the Sherbrooke phase are absent on the proximal (northwest) side of the Mont Ham Moraine (Figure 5-11); this indicates that glacial-lake levels fell rapidly after the ice-front retreated from the position of the Mont Ham Moraine.

The occurrence of ice-contact and fluvial deltas (#3 and #11) which lie on the distal side of the Cherry River Moraine and which were built into Glacial Lake Memphremagog indicates that the Sherbrooke phase was already in existence at the time that the moraine was emplaced. Retreat from the position of the Cherry River Moraine (see Figure 5-1) allowed waters of the Sherbrooke phase to expand into the Saint-François River valley north of Sherbrooke; the areal extent that was reached by the proglacial water-body favored fairly strong beach development in the vicinity of Windsor and Bromptonville (features #8, #16 and #17). It is probably during this ice-retreat episode that, given the required water depth, thick varve series, which were observed by the author at several localities in the Saint-François River valley near Windsor and Bromptonville, were deposited.

The occurrence of ice-retreat deltas on the proximal (northeast) side of the East-Angus Moraine (features #14, #15 and #21) provides

independent evidence that a small glacial lobe retreated northeastward in the upper Saint-François River valley and that this lobe remained active until the ice-front had retreated from the position of the Mont Ham Moraine south of Richmond; hence, the suggested correlation between these two parts of the morainic belt (Figures 5-1 and 5-11). As indicated earlier, it is uncertain whether or not varves that underlie the clay till at East-Angus (Figure 5-2) were deposited in Glacial Lake Memphremagog prior to construction of the East-Angus Moraine. Small glacial lakes that were impounded in the upper Nicolet River valley drained southwestward into Glacial Lake Memphremagog via ice-marginal meltwater channels; the altitude of a small ice-contact delta south of Wotton (feature #20) further suggests that one of these lakes became confluent with waters of the Sherbrooke phase during construction of the Mont Ham Moraine (Figure 5-11).

5.4.2 Fort Ann phase of Glacial Lake Vermont

During ice retreat from the position of the Mont Ham Moraine, low cols southwest of Richmond became ice-free, causing level of proglacial lakes in the Saint-François River valley to fall rapidly. Prior to lowering to the level of the Fort Ann phase of Glacial Lake Vermont, water levels stabilized at least briefly 10 to 15 m above the level of the Fort Ann phase (Figure 5-10b); the level of this transitional water-plane may have been controlled by one of three possible outlets at altitudes between 251 and 254 m in the area south of Valcourt (Figure 5-12). As shown in Figure 3-1, all three outlets were utilized as meltwater channels at some time during deglaciation: however, on the basis of altitude relationships (Figure 5-10b), outlet C probably controlled the level of the transitional water-plane.

Subsequent ice-retreat to the position of the Ulverton-Tingwick Moraine caused glaciolacustrine water-levels to fall to the level of the Fort Ann phase of Glacial Lake Vermont (Figure 5-12). Strandline features recording this water plane occur within the middle Saint-François River valley and along the edge of the uplands (Richmond Hills and Outer Appalachian Uplands) throughout much of the Asbestos-Valcourt region.

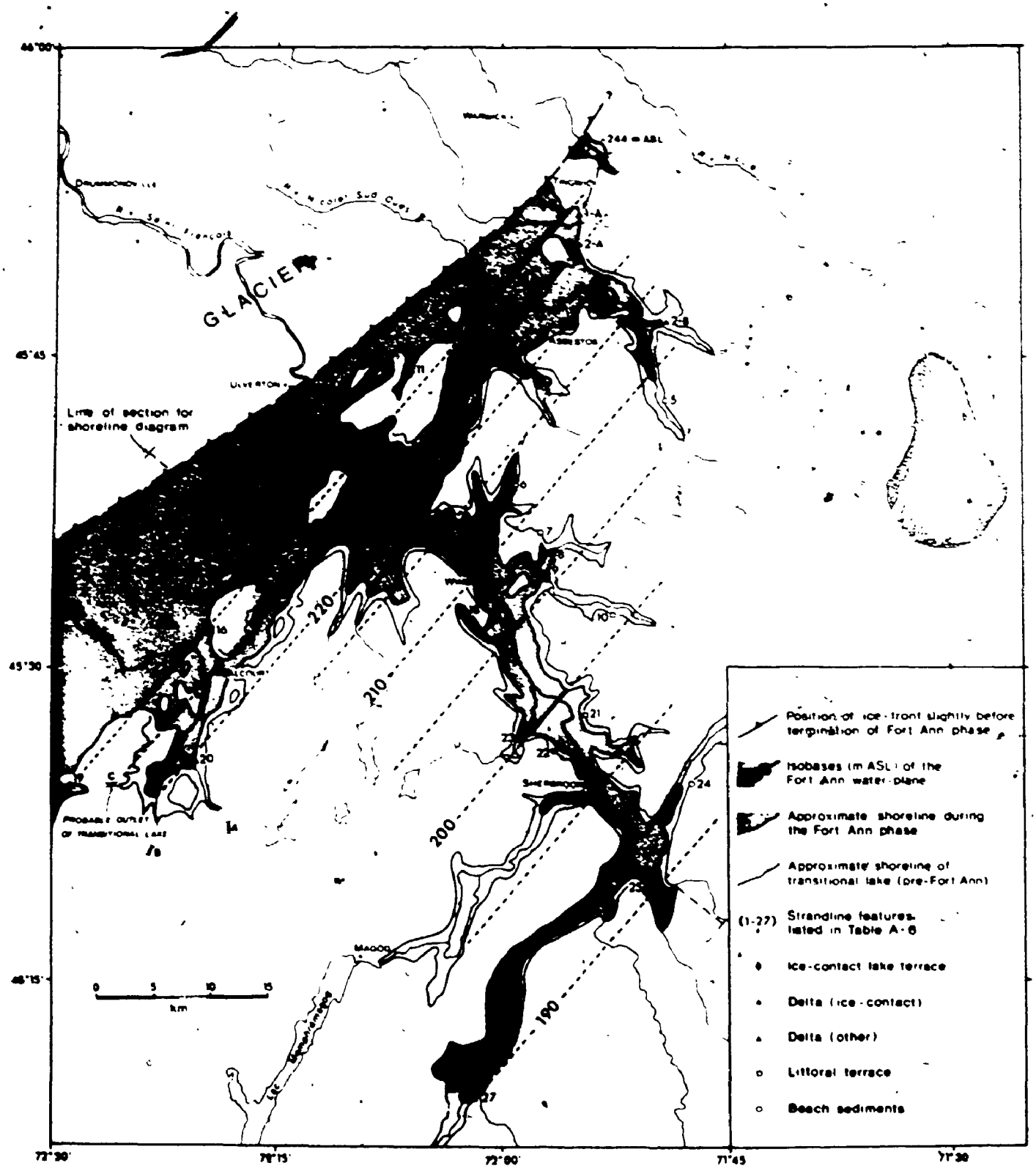

Figure 5-12 : Fort Ann phase of Glacial Lake Vermont in the Asbestos-Valcourt region, showing isobases (m ASL) on the former water-plane. Extent of pre-Fort Ann transitional lake is also shown. Elevations of features are shown in Figure 5-10b and listed in Table A-6.

Littoral features such as beaches and wave-cut terraces are particularly well developed in the vicinity of Valcourt perhaps because of the longer fetch in that area; on the other hand, mainly ice-contact deltas and terraces associated with the Ulverton-Tingwick Moraine are recorded in the vicinity of Asbestos. Investigation of areas northeast of Warwick have failed to provide any evidence that the Fort Ann phase may have extended beyond Warwick along the edge of the Appalachian uplands, an observation which is an agreement with mapping by both Chauvin (1979a) and Dubé (1971).

The occurrence of both varves and Fort Ann strandline features on the proximal side of the Ulverton-Tingwick Moraine indicates that Glacial Lake Vermont continued to expand onto the Appalachian Piedmont for some time prior to Champlain Sea incursion. Figure 5-12 gives the probable ice-front position near the close of the Fort Ann phase of Glacial Lake Vermont.

Reconstructed water-planes shown in Figures 5-10b and 5-12 differ somewhat from those suggested by McDonald (1967a, 1968) for his "lower glacial-lake system" perhaps because the limited number and areal distribution of strandline features which were available to him did not allow differentiating features of the transitional water-plane from those of the Fort Ann phase. Recognition of the Fort Ann phase of Glacial Lake Vermont in the Asbestos-Valcourt region rests mainly:

(1) on the 50 to 60 m altitude difference which separates the lower glaciolacustrine strandline features from marine-limit features,

(2) and on the absence of possible outlets that may have controlled the level of the lower water-plane; fieldwork in the area east of Warwick and Victoriaville showed no evidence that cols in that area were ever utilized as northeastward drainage routes; on the contrary, a small glacial lake which was impounded in the upper Rivière des Pins valley overflowed southwestward into Glacial Lake Vermont via a distinctive meltwater channel (Figure 5-12).

In order to further verify correspondance of the lower glacio-lacustrine water-plane of the Asbestos of the Asbestos-Valcourt region (Figure 5-12) with the water plane of the Fort Ann phase of Glacial Lake Vermont in its "type" area, the Lake Champlain valley (Chapman, 1937; Denny, 1974), strandline features recognized by earlier authors in the intervening areas of southeastern Québec and northwestern Vermont were compiled (Figure 5-13 and Table A-6). In Vermont (including the upper Missisquoi River valley in adjacent Québec), only features (#38 to #53) which were previously assigned to the Fort Ann phase (Parrott and Stone, 1972; Wagner, 1972; Dubé, 1983) are included in Figure 5-13; however, features that were located upstream in narrow valleys were deleted from the reconstruction as they may have formed in small, local lake basins.

In the Granby area of southeastern Québec, recorded shoreline features (#29 to #37) have not been assigned to a given phase of Glacial Lake Vermont by Prichonnet and co-workers (Prichonnet, 1982a, 1982b; Prichonnet et al., 1982a, 1982b; Doiron, 1981; Cloutier, 1982). Since these authors have recognized abundant littoral features between about 245 m ASL (Coveville phase ?) and about 210 m ASL (Fort Ann phase ?), only features which could be identified on aerial photographs have been included in the reconstruction (Figure 5-13). Fort Ann features in New York and adjacent Québec (#54 to #71) were compiled from the original work of Chapman (1937) as well as from more recent work by Denny (1974) and Clark and Karrow (1984) which have essentially confirmed Chapman's main interpretations; features of the Upper Fort Ann level of Clark and Karrow (1984) were utilized since their lower, better developed set of features lie somewhat below the level of the Fort Ann phase of Chapman (1937).

The latter problem is not especially critical since the occurrence of several ice-contact deltas and terraces (features #1-A, 2-A, 3, 14, 17, 32 and 49) confirms earlier suggestions that the Fort Ann water-plane is diachronous and thus that glacio-isostatic uplift likely took place throughout the duration of the episode. A perfect fit of shoreline features with reconstructed isobases should therefore not be expected. Analysis of Table A-6 reveals that departures from the proposed

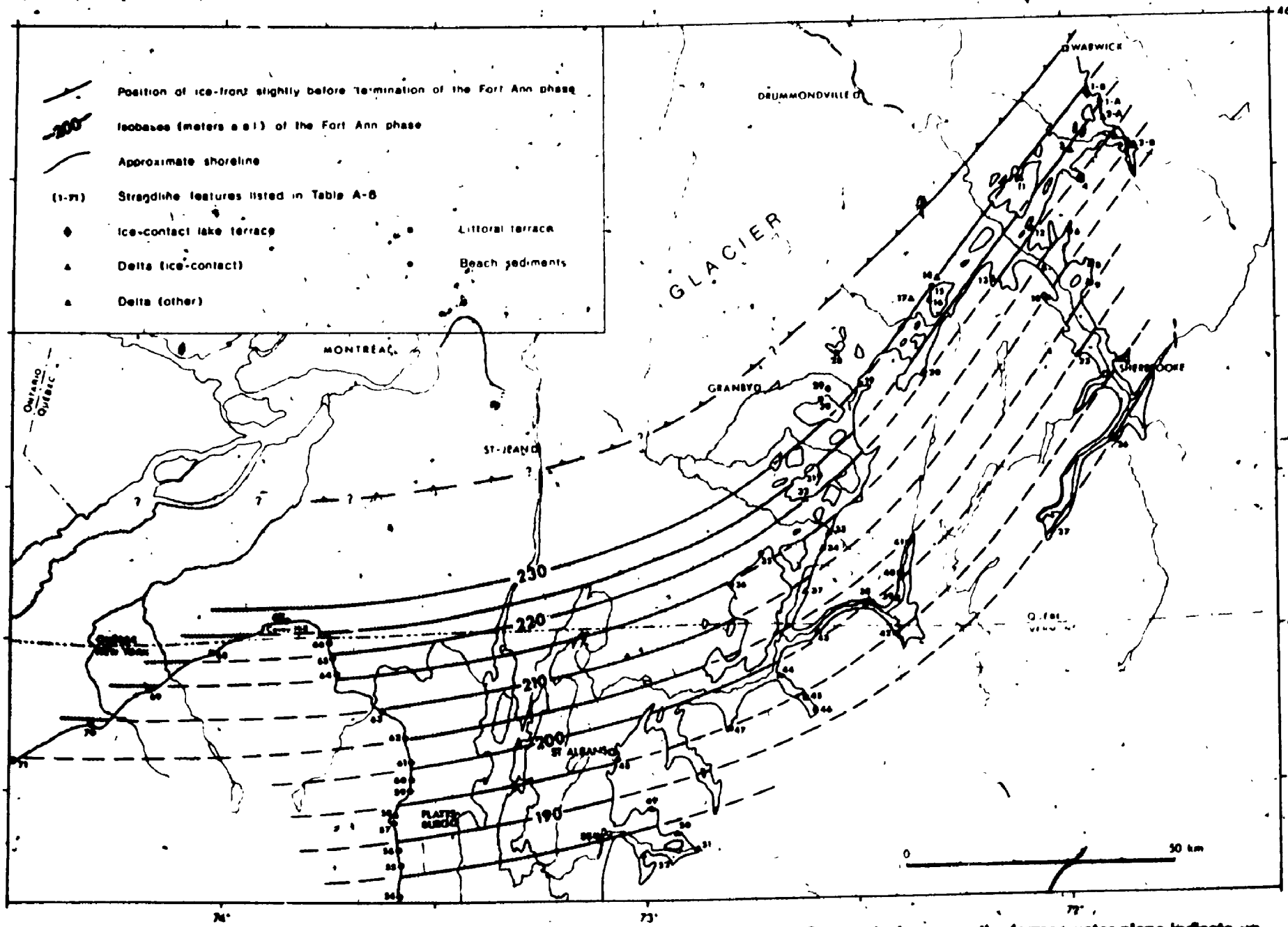

Figure 5-13 : Fort Ann phase of Glacial Lake Vermont in southern Québec and adjacent United States. Isobases on the former water-plane indicate an average geoidal flexure of ~ 1 m/km. Lake level fell when low terrains northeast of Warwick became ice-free.

isobases in the Asbestos-Valcourt region (features #1-A through #27) and in the Granby-Sutton region (features #28 through #38) average only -1.8 and -2.2 m, respectively; average departure in northern New York (features #54 through #71) is only -0.7 m while it is -9.6 m in the Vermont-Missisquoi region (features #39 through #53). Several features of the latter region may thus correspond to the Lower Fort Ann level of Clark and Karrow (1984).

Reconstructed Fort Ann isobases (Figure 5-13) show that the ice-marginal geoidal flexure in the Asbestos-Valcourt region had a similar gradient (about 1 $m.km^{-1}$) to that recorded in the Lake Champlain valley. The two regions must therefore have a fairly similar history of glacial unloading. The possible ice-front position near the close of the Fort Ann phase, as given in Figure 5-13, is drawn so as to conform roughly to the pattern of isobases. Reports of varved sediments at the base of marine clay in the Montreal region (Prest and Hode-Keyser, 1977) and in the Saint-Jean region (LaSalle, 1981) suggest that Glacial Lake Vermont which had become confluent with Glacial Lake Iroquois (Prest, 1970; Denny, 1974; Clark and Karrow, 1984) may have extended at least briefly into those areas, perhaps as a result of rapid calving at the ice-front.

5.5 Chronology and stratigraphic relationships

The onset of the Champlain Sea incursion into the Asbestos-Valcourt region is defined stratigraphically at the Rivière Landry section where fossiliferous marine silt conformably overlies the Danville Varves. Available ^{14}C dates on early Champlain Sea fauna (**Hiatella arctica** or **Macoma balthica**) from the study area and from elsewhere in the southeastern part of the central marine basin (Figure 5-14 and Table 5-1) strongly suggest that the event took place about 12 000 years BP.

However, this proposal is apparently contradicted by a date of 12 480 $\pm$ 240 years BP (QC-475) on **Mya** sp. collected in the Appalachian Piedmont, near St-Dominique (Prichonnet, 1982a), just west of the study area. Being almost 500 years older than any other shell date from the southeastern part of the central basin, QC-475 is unique and

poses a problem. Lack of information on the dated species (**Mya arenaria** or **Mya truncata** ?) and on associated biofacies or lithofacies makes it difficult to assess the validity of this date; the problem was previously discussed in a regional context by the author (Parent et al., 1985) and will not be repeated here. Let us simply say that such an early age for a faunal assemblage dominated by any species of the genus **Mya** would be very surprising. It seems best to consider QC-475 as anomalous.

In order to assess possible synchroneity of the marine limit along the Appalachian uplands of southeastern Québec and in the adjacent Lake Champlain valley, altitudes of upper marine shoreline features were compiled from much the same sources as for Fort Ann strandline features (Figure 5-14 and Table A-7). Isolines drawn on these marine features indicate that the average gradient of the geoidal flexure during the early Champlain Sea incursion is about 0.9 $m.km^{-1}$, slightly less than during the Fort Ann episode. This may suggest that, as a result of northward ice-retreat, the marginal zone of steeper geoidal flexure had already undergone slight northward migration or, alternatively, that the marine limit is slightly diachronous in the area (stippled) shown in Figure 5-14. In any event, marine-limit isolines show patterns and gradients that are nearly similar to those shown by isobases on Fort Ann features. However, marine-limit features at the edge of the Appalachian uplands near Laurierville (#41, 42 and #43) show appreciable departures from the projected 175 m ASL isoline; this may reflect a somewhat different deglacial history of the Appalachian uplands in the area south of Québec City. Features on Mont St-Hilaire (#44) and Mont Royal (#45) were dropped during construction of the isolines as they may be significantly younger than other marine-limit features plotted in the stippled area of Figure 5-14.

Stratigraphic relationships that were established between Late Wisconsinan glacial, glaciolacustrine and marine sediments during this investigation are schematically depicted in Figure 5-15. This NW-SE cross-section summarizes the following conclusions:

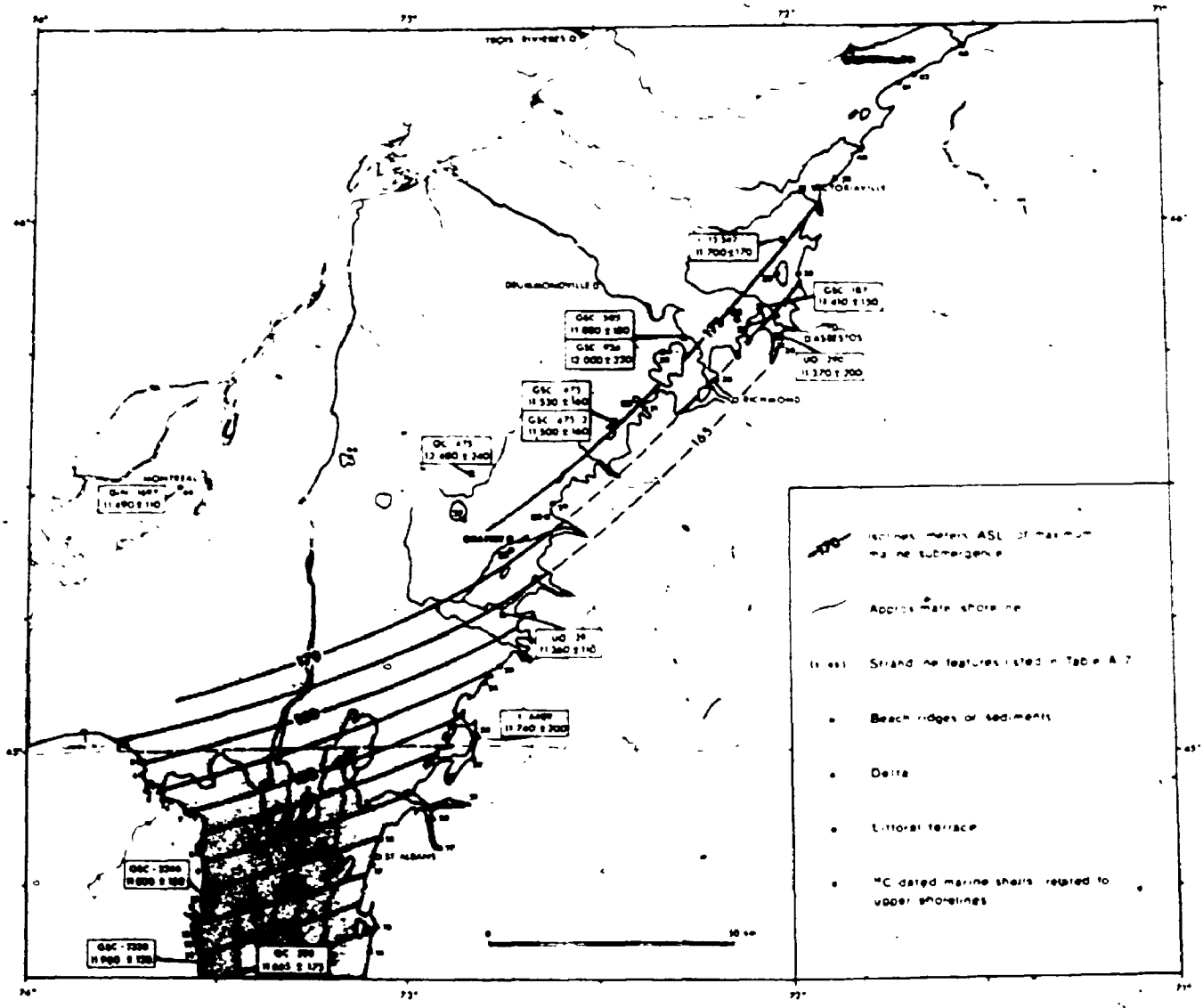

Figure 5-14 : Early Champlain Sea incursion in southern Québec and adjacent Lake Champlain valley. Isolines on marine-limit features (Table A-7) suggest an average geoidal flexure of ~0.9 m/km during early marine submergence, about 12 000 years BP (shell dates).

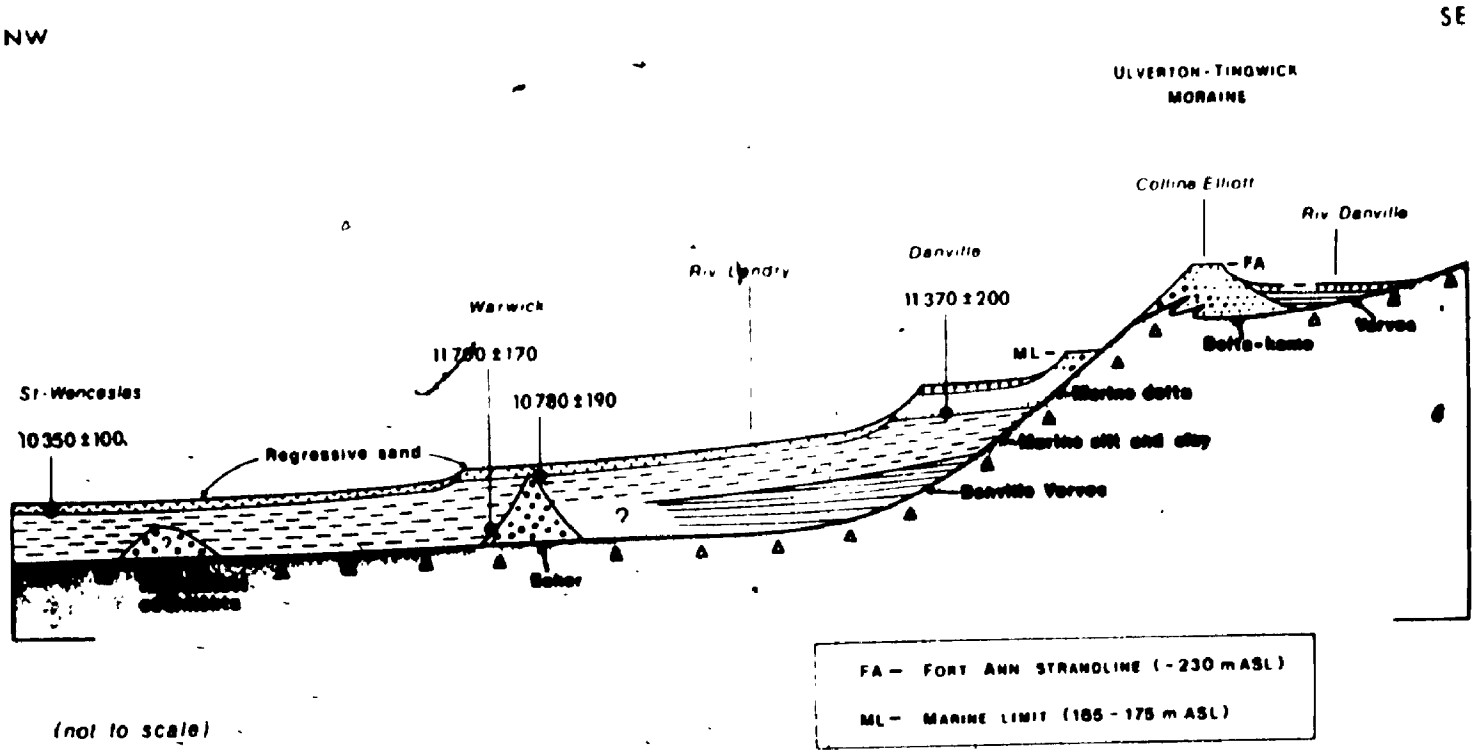

Figure 5-15 : Schematic cross-section showing stratigraphic relationships between Late Wisconsinan glacial, glaciolacustrine and marine sediments in the vicinity of Asbestos.

1) During construction of the Ulverton-Tingwick Moraine, a proglacial lake whose level stood at 230 m ASL near the glacier-water interface (Fort Ann phase of Glacial Lake Vermont) was impounded in terrains southeast of the ice front.

2) Northward ice-retreat from the position of the Ulverton-Tingwick Moraine was soon followed by drainage of Fort Ann water levels; Fort Ann strandline features are recorded in terrains lying just a few kilometers northwest of the morainic belt and are conspicuously absent in valleys east of Victoriaville.

3) At Rivière Landry, glaciolacustrine sedimentation (Danville Varves) lasted slightly more than 100 years after construction of the Ulverton-Tingwick Moraine and prior to Champlain Sea incursion.

4) By about 12 000 years BP, marine waters had replaced glacial-lake waters in the Appalachian Piedmont of southeastern Québec; Champlain Sea incursion likely took place only after the ice-margin had retreated from the edge of the Outer Appalachian Uplands in the vicinity of Warwick.

5) Regression of the Champlain Sea had already begun by about 11 500 years BP; as a result of rapid isostatic recovery, and in spite of globally rising sea levels (Milliman and Emery, 1968; Clark, Farrell and Peltier, 1978), marine waters had evacuated this part of the Appalachian Piedmont by about 10 500 years BP.

CHAPTER 6

CORRELATION WITH SELECTED REGIONS, AND REGIONAL IMPLICATIONS

Because the stratigraphic records of the combined Sherbrooke and Lac-Mégantic regions (McDonald and Shilts, 1971; Shilts, 1981) and of the Central St. Lawrence Lowland (Gadd, 1971; Occhietti, 1980; Lamothe, 1985) have direct bearing on the stratigraphic record of the Asbestos-Valcourt region, correlation with these two regions will be discussed primarily. Moreover, these two stratigraphic records are well documented and are more comprehensive than those of other regions of southeastern Québec (Prest and Hode-Keyser, 1977; Prichonnet, 1982a, La Salle et al., 1977b; La Salle, 1984; Chauvin, 1979a, 1979b) or adjacent New England (Borns and Calkin, 1977; Genes et al., 1981; Lowell et al., 1986; Koteff and Pessl, 1985; Stewart and MacClintock, 1969).

The stratigraphic record of the Asbestos-Valcourt provides key evidence for the existence of Appalachian outflow centers during Early (?) to Middle Wisconsinan time as well as for the assessment of Late Wisconsinan deglacial events prior to and leading to the Champlain Sea incursion.

6.1 Stratigraphic record of the Ascot River sections

The Quaternary record of the Sherbrooke region is based mainly on stratigraphic units exposed in two sections located on the banks of Ascot River (McDonald, 1967a: fig. 4 and 5); units that McDonald (1967a: fig. 11) considered as correlatives are exposed in other sections located between Sherbrooke and the international boundary. The stratigraphy of the Sherbrooke region was subsequently extended into the Lac-Mégantic region (Shilts, 1970).

Because of its exceptionally good record, the main Ascot River section (herein labelled MP-81-1) was selected by McDonald and Shilts (1971) as the type section for Lennoxville Till, Chaudière Till and

Massawippi Formation and as a reference section for Gayhurst Formation. A close-by section (herein labelled MP-82-3) was selected as the type section for Johnville Till and pre-Johnville sediments (McDonald and Shilts, 1971). Their interpretation of these units was summarized earlier (see Chapter 1).

The Ascot River sections were investigated by the author mainly for the purpose of obtaining a data base which could then be compared directly with that utilized in the adjacent Asbestos-Valcourt region.

6.1.1 Ascot River I section (MP-81-1)

Except for minor thickness and facies differences which are likely due to retreat of the exposure caused by recent slumping and fluvial erosion, the stratigraphic log of the Ascot River I section (Figure 6-1: MP-81-1) is essentially the same as that recorded by McDonald (1967a; see also McDonald and Shilts, 1971). Stratigraphic units shown in Figure 6-1 are described in Appendix I and will therefore not be repeated in full.

At the base of section MP-81-1, non calcareous, organic-bearing lacustrine silts of the Massawippi Formation (dated > 54 000 years BP, Y-1683, in McDonald, 1967a) are directly overlain by the 16.3 m-thick Chaudière Till. The latter consists mainly of gray, unoxidized, matrix-dominated lodgement till which also includes a few thin (less than 30 cm-thick) lenses or layers of sorted sand or pebbly sand. The basal 2 m of the till unit locally contain sheared lenses of slightly oxidized laminated silt; these lenses are located on the southwest side of sub-till bosses of compact lacustrine sediments (Massawippi Formation). The lenses were obviously dragged subglacially toward west or southwest; this direction is further corroborated by the occurrence of minor, NE-dipping thrust faults in the upper part of the Massawippi Formation.

Five till clast fabrics that were measured within Chaudière Till suggest that ice-flow shifted from westward to approximately southward during the Chaudière episode. This shift of ice-flow direction is re-

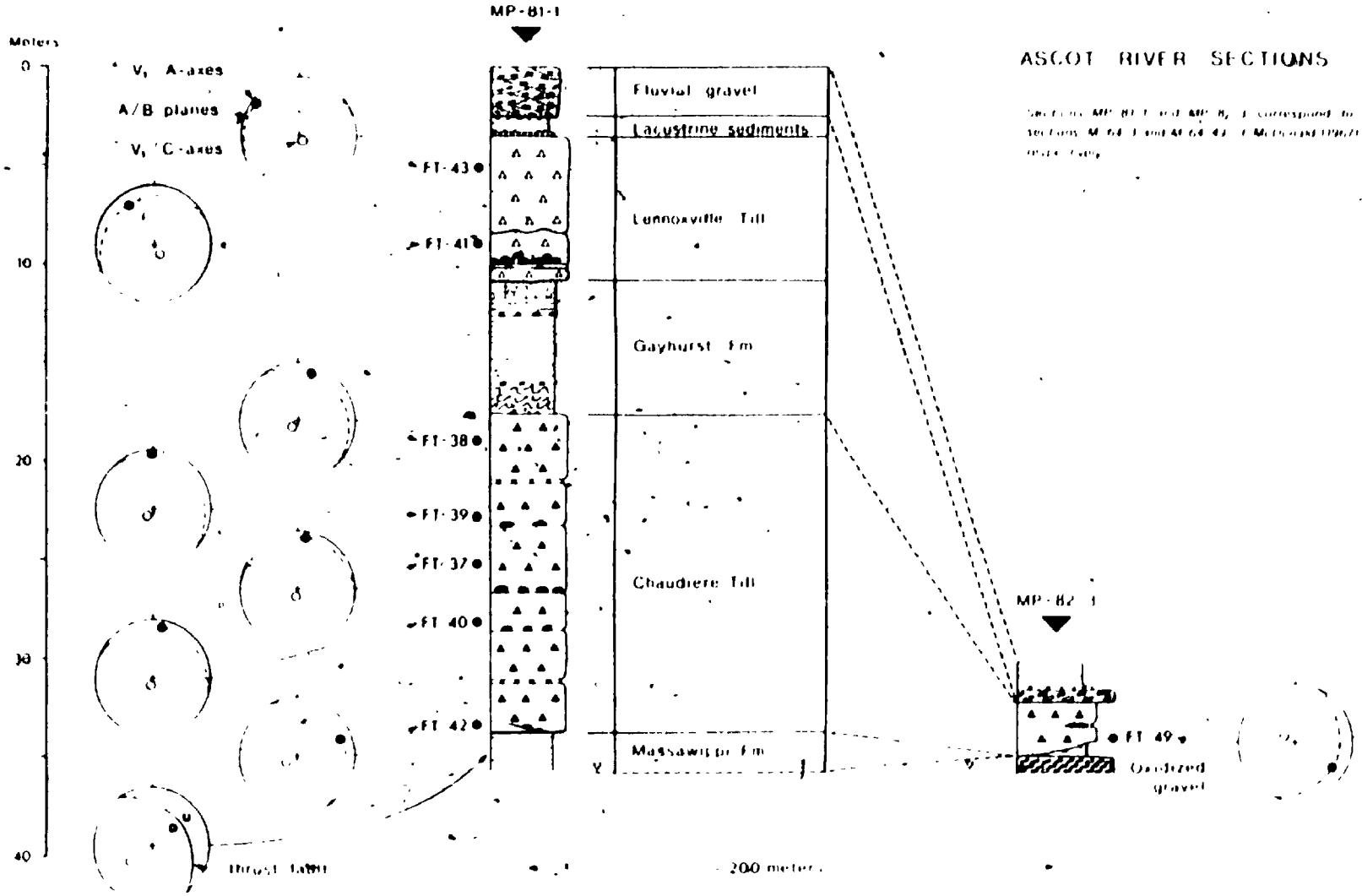

Figure 6-1: Stratigraphic logs, till clast fabrics and glacitectonic deformations, Ascot River sections (MP-81-1 and MP-82-3). (See legend in Figure 4-12)

corded by changes of A-axis orientation that are paralleled by orientation changes of clast imbrication. The best examples of this are provided by FT-42, FT-40 and FT-38: these are unequivocal parallel (type B) fabrics whose preferred A-axis orientation (V_1) plunges toward N 070°, N 010° and N 015°, respectively. The other two fabric samples, FT-37 and FT-39, also show preferred imbrication of clast A/B planes toward north (N 011°) and northeast (N 042°), respectively; however, FT-37 is rejected on statistical grounds (A-axis distribution is probably not spherically normal; see Table 3-1) while it is somewhat uncertain that FT-39 is a parallel (type A) fabric. Yet, it must be noticed that, even if FT-39 were interpreted as a transverse (type C) fabric, the overall interpretation of clast fabric data in Chaudière Till would remain essentially unchanged.

Till clast fabrics measured by the author at the base (FT-42) and at the top (FT-38) of Chaudière Till are almost identical to those reported by McDonald (1967a) at equivalent levels (his fabrics g and b, respectively). Clast fabrics from the middle part of Chaudière Till, though they cannot be compared directly with two-dimensional fabrics reported by McDonald (1967a), also seem in agreement with previous measurements; however, these fabrics do not show intermediate directions that may support the idea that the change from westward to southward ice-flow was gradual, as had been suggested earlier (McDonald, 1967a; McDonald and Shilts, 1971).

Striations were measured on the top surface of a few boulders belonging to boulder zones within Chaudière Till. Striae trend between N 080° and N 120° on large embedded boulders at the base of Chaudière Till, an observation which is in agreement with the inferred westward ice-flow direction. Striae recorded in boulder zones at depths of 23.2 and 26.5 m trend mainly within a sector comprised between N 330° and N 030°; again, these are in broad agreement with the southward ice-flow direction inferred from till clast fabrics in the upper part of Chaudière Till.

Chaudière Till is overlain by a 4.8 m-thick unit of laminated silt which constitutes the basal member of the Gayhurst Formation; because of its distinct fining-upwards trend (Figure 6-2), the silt unit is believed to have been deposited in a deep proglacial lake during retreat of Chaudière ice. However, the paleo-environmental context in which the overlying, 1.9 m-thick, slightly oxidized, sandy silt unit was deposited seems less clear: the unit may record a significant drop of lake level or, alternatively, it may simply signal the encroachment of glacier ice (Lennoxville ?) in the vicinity of the section. At this time, the second interpretation, that is a return to proximal sedimentation, is tentatively retained because of the occurrence of pebbles that were probably ice-rafted and also because of the occurrence of black lenses which likely consist of disseminated sulfides: if so, a reducing environment is implied, which is in agreement with proximal, deep-water conditions.

The upper member (sandy silt unit) of the Gayhurst Formation is much thinner than the 5.6 m observed by McDonald (1967a); this is probably due to the absence, at the time of McDonald's fieldwork, of a 2.5 m-thick local till unit which now occurs at the base of Lennoxville Till and which overlies intensely deformed silty sand of the Gayhurst Formation. The lower half of the local till unit consists of deformation till containing numerous sheared lenses and layers of sorted material (laminated clayey silt and sandy silt) as well as a bouldery zone. The textural variability of the unit (Figure 6-2) reflects the admixture of debris derived from both members of the Gayhurst Formation. A till clast fabric (FT-41) was measured within the better mixed, matrix-dominated, upper half of the local till unit: FT-41 is a parallel (type B) fabric which shows preferred A-axis orientation (V_1) plunging toward northwest (N 326°) and which also shows significant imbrication of clast A/B planes toward northwest.

A till clast fabric (FT-43) was also measured within the overlying "normal" lodgement till member of Lennoxville Till. FT-43 is a parallel (type A) fabric which shows significant northwestward (N 341°) imbrication of clast A/B planes; however, preferred A-axis orientation (V_1)

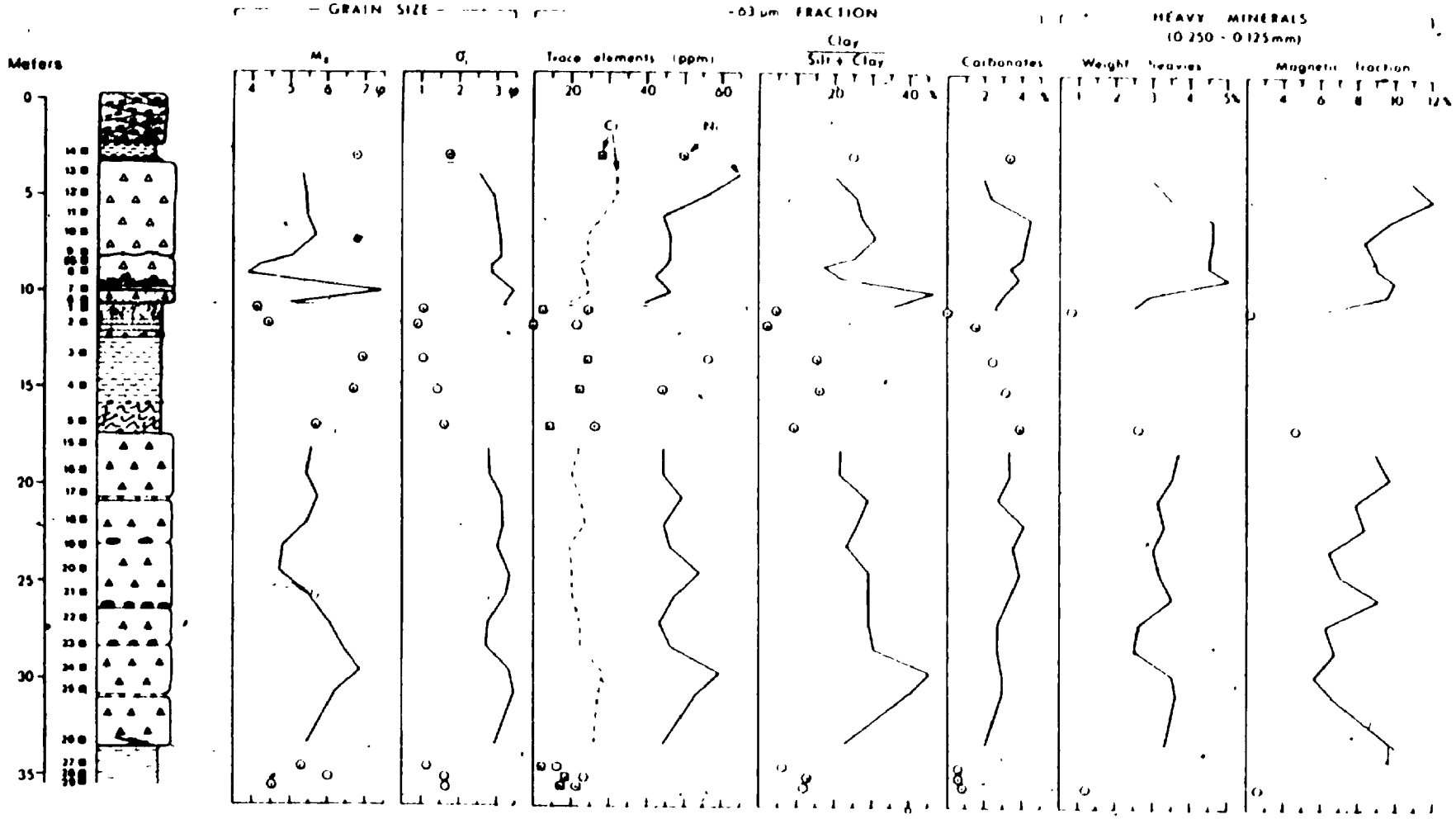

Figure 6-2 : Vertical variations of grain-size and compositional data, main Ascot River section (MP-81-1). Lennoxville Till and Chaudière Till are best differentiated on the basis of clast lithology and fabric (see text). (See legend in Figure 4-12)

only plunges at a shallow 6° angle toward northwest (N 305°). A-axis distribution pattern of FT-43 greatly resembles that measured previously at an equivalent level (McDonald, 1967a: fig. 5, fabric a).

Lennoxville Till is overlain by a 0.9 m-thick lacustrine silt unit; however the thickness of this unit varies laterally and, since McDonald (1967a) had reported a 1.2 m-thick lacustrine sand unit, significant lateral facies changes are also inferred. The lacustrine unit is overlain by a 2.5 m-thick unit of sandy fluvial gravel in which modern soil has developed.

Investigation of matrix composition of till units exposed at Ascot River, along with field observations of clast lithology, has revealed that:

1) provenance of Chaudière and Lennoxville Tills cannot be clearly differentiated on the basis of compositional data (grain size, trace element geochemistry, carbonates, weight of heavy and magnetic minerals) obtained thus far from till matrix samples (Figure 6-2); however, the increase of Ni content at the top of Lennoxville Till (samples #12 and #13) suggests that a dispersal tail of ultramafic debris may extend to the vicinity of the section (see Figure 4-21); this Ni peak, in contrast to that recorded near the base of Chaudière Till (sample #24), coincides with an increased content of magnetic minerals and, since it does not coincide with a higher clay content, it may not be attributed to a textural control effect (see section 3.2.3);

2) distinctive granodiorite and granite clasts, presumably derived from Devonian intrusives located northeast of the section (Figure 4-1), occur in low abundance throughout Chaudière Till, but are absent in Lennoxville Till;

3) Chaudière Till contains virtually no Precambrian clasts, and only rare ultramafic clasts were found near the top of the unit;

on the other hand, ultramafic and Precambrian clasts are quite common, though in low abundance (< 1%), in Lennoxville Till.

These investigations further indicate that provenance signals at Ascot River are somewhat diffuse because the section is remotely located from distinctive bedrock sources (see Figure 4-1). Except for a few details, the above observations on clast lithology are in agreement with earlier observations and pebble counts by McDonald (1967a).

6.1.2 Ascot River II section (MP-82-3)

As a result of bank undercutting caused by floods, the base of section MP-82-3 was particularly well exposed during the fall of 1982. At the base of the section, oxidized cobble gravel is directly overlain by laminated, organic-bearing silt of the Massawippi Formation which is in turn overlain by Chaudière Till (Figure 6-3); these units are unconformably overlain by Recent fluvial sediments (cobble gravel and stratified sand) that underlie a 5 m-high post-glacial terrace.

The oxidized cobble gravel is imbricated toward east (upstream of Ascot River in this area), thus indicating that free drainage conditions were in existence at the time of fluvial sedimentation; however, the presence of Precambrian clasts in the gravel unit suggests that Laurentide glaciers had invaded the Appalachians at least once prior to this fluvial episode, much as McDonald and Shilts (1971) have suggested. In subsection D, a bed of unoxidized, cross-laminated sand is both underlain and overlain by oxidized gravel beds (Parent, 1984b: photo 3.2); this indicates that oxidation and cementation of the gravel unit did not occur during an episode of "... prolonged weathering prior to deposition of Johnville Till" (McDonald and Shilts, 1971: p. 685-686). However, no evidence was found to indicate the presence of Johnville Till in this section where this 30 cm-thick till unit had been reported to overlie the oxidized gravel and to underlie sediments of the Massawippi Formation (McDonald, 1967a). The difference of interpretation is perhaps related to the presence of interstitial muds in the upper part of the clast-supported gravel unit; the author believes that these muds

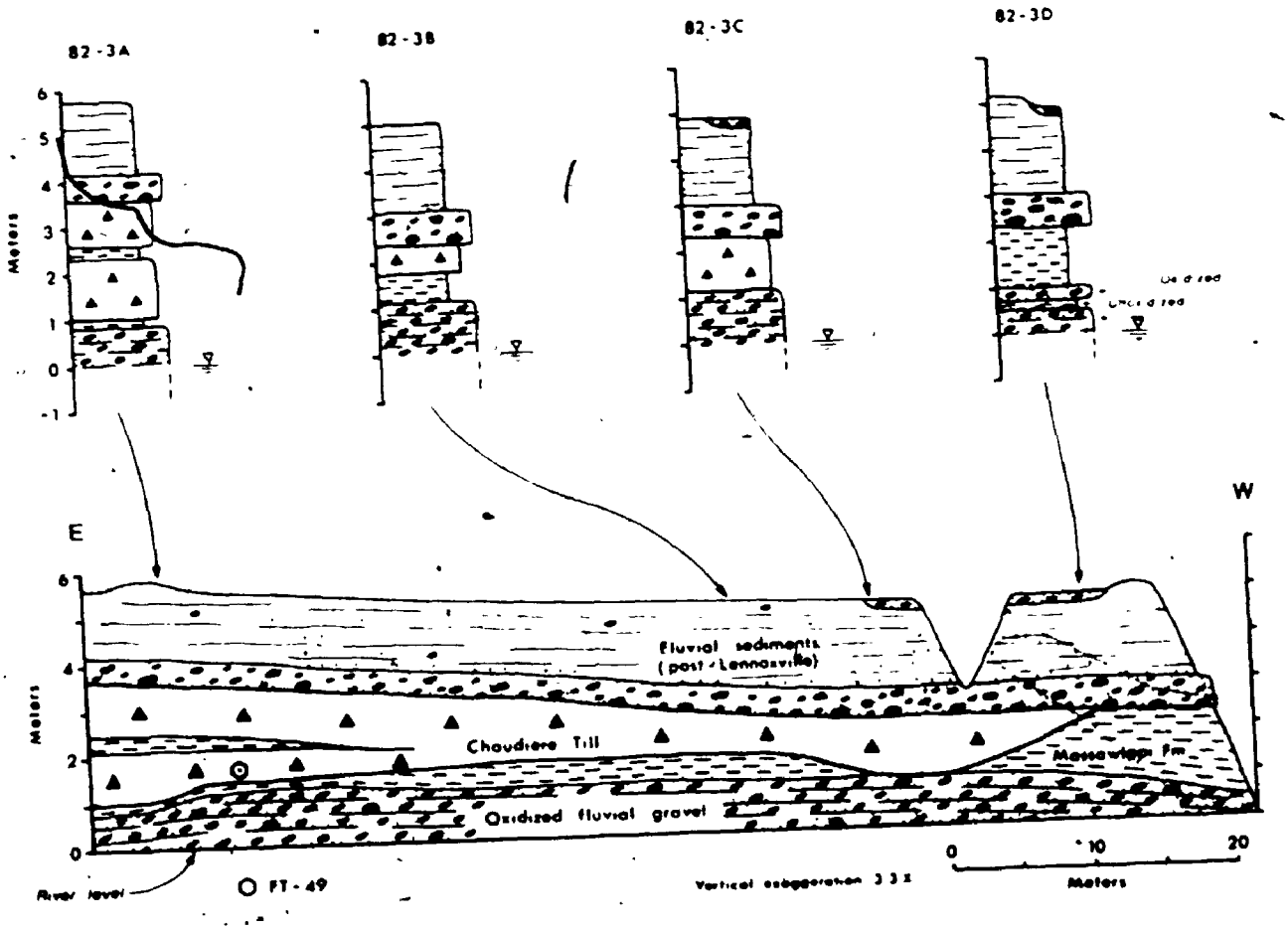

Figure 6-3 : Lateral relationships of units exposed in the second Ascot River section (MP–82–3). Notice the absence of Johnville Till between the oxidized fluvial gravel and the Massawippi Formation. Oxidation of the lowermost fluvial gravel unit is interpreted as the result of modern groundwater aeration (see text).

seeped into large interstices during the subsequent Massawippi lacustrine episode, an interpretation which is in agreement with the absence of such interstitial muds in places where the gravel is matrix-supported, such as in subsection D.

Non-calcareous laminated silt and fine sand of the Massawippi Formation overlies the oxidized gravel unit in all subsections except in subsection C where it has apparently been eroded away by the Chaudière ice advance. The overlying Chaudière Till is a non-calcareous, matrix-dominated, lodgement till which locally includes upsheared silt lenses derived from the Massawippi Formation (subsection A); these observations are analogous with those made in the basal part of the stratotype at the Ascot River I locality. A till clast fabric (FT-49) was measured at the base of Chaudière Till in subsection A (Figure 6-3): FT-49 is a parallel (type B) fabric with preferred A-axis orientation (V_1) plunging toward ESE (N 126°) and with preferred imbrication also dipping toward ESE (Figure 6-1). The approximately westward ice-flow direction recorded by FT-49 is thus in agreement with that recorded at the base of Chaudière Till in the nearby Ascot River I section.

In subsection A, fine sand laminae within the upsheared silt lens are oxidized at the surface of the exposure but not a few centimeters inwards; below this silt lens, Chaudière Till is stained with bright orange-red oxide only along subhorizontal fissility planes and these stains can be seen to "intersect" within-till pebbles. This, along with the occurrence of non-oxidized sand within the fluvial gravel unit, suggests that the bright orange-red oxides which partly cement the fluvial gravel (and which locally stain the overlying units) are the result of modern groundwater oxidation rather that the result of a subaerial weathering episode prior to deposition of the Massawippi Formation. Moreover, the degree of oxidation seems directly related to differential permeability of the sediments; the occurrence of Mn-oxides within the oxidized cobble gravel further suggests that modern water-table fluctuations play a role in the oxidation processes.

As a result of these observations, the lithostratigraphic record of the Ascot River sections, hence of the Sherbrooke region, now stands as follows (from top to bottom):

1) fluvial gravel (a post-Lennoxville informal unit);
2) lacustrine sediments (a post-Lennoxville informal unit);
3) Lennoxville Till;
4) Gayhurst Formation: - upper member;
   - lower member;
5) Chaudière Till;
6) Massawippi Formation: - lacustrine member;
   - fluvial member.

It is proposed that the lithostratigraphic terms "Johnville Till" and "pre-Johnville sediments" (an informal unit) be abandonned:

- because Johnville Till as well as the Laurentide ice advance it was meant to designate are not recorded at the type section or in its vicinity;

- because the name "pre-Johnville sediments" as well as the events that the unit was meant to represent have lost their meaning (the Massawippi Formation includes fluvial gravels in reference sections of the Lac-Mégantic region; see McDonald and Shilts, 1971).

It is also recommended that new stratotypes for lithostratigraphic units older than Massawippi Formation be found and defined, preferably in the Sherbrooke region so as to avoid possible correlation problems. Pre-Massawippi units have been reported in the Chaudière valley (Shilts, 1981; Shilts and Smith, 1986) and may also occur in the Sherbrooke region.

6.2 Correlation between the Asbestos-Valcourt and Sherbrooke regions

Following the previous assessment of glacial and non-glacial events in the Asbeatos-Valcourt region (see Chapters 4 and 5) and following the re-assessment of glacial and non-glacial units at Ascot River, a correlation scheme between the Sherbrooke and Asbestos- Valcourt regions may now be discussed. It is herein proposed that drift unit A, unit B and drift unit C of the Asbestos-Valcourt region are correlatives of Chaudière Till, Gayhurst Formation and Lennoxville Till, respectively (Figure 6-4).

In the absence of sound chronological control, particularly for unit B and Gayhurst Formation, the proposed correlation is based mainly:

1) on similar stratigraphic position of the correlated units;
2) on the similarities of glacial and deglacial events recorded in both regions.

Till clast fabrics from local and well-mixed lodgement facies of Lennoxville Till indicate that ice initially advanced toward southeast at Ascot River and that southeastward ice-flow was maintained throughout the Lennoxville episode, much as McDonald (1967a) had suggested. The common occurrence of Precambrian and ultramafic clasts in Lennoxville Till further indicates that it is a Laurentide till unit, a conclusion which is in excellent agreement with earlier reports (McDonald and Shilts, 1971). This fully supports the proposed correlation with drift unit C of the Asbestos-Valcourt region: drift unit C is also a Laurentide till unit that was deposited by an ice-sheet that maintained southeastward ice-flow until final deglaciation (see section 4.4.12). Deglacial events that postdate drift unit C and Lennoxville Till will be discussed in section 6.6.

Regional ice-flow patterns during this last major glacial episode are given in Figure 4-23. It may also be suggested, on the basis of clast composition and fabric data reported by Prichonnet (1982a), that

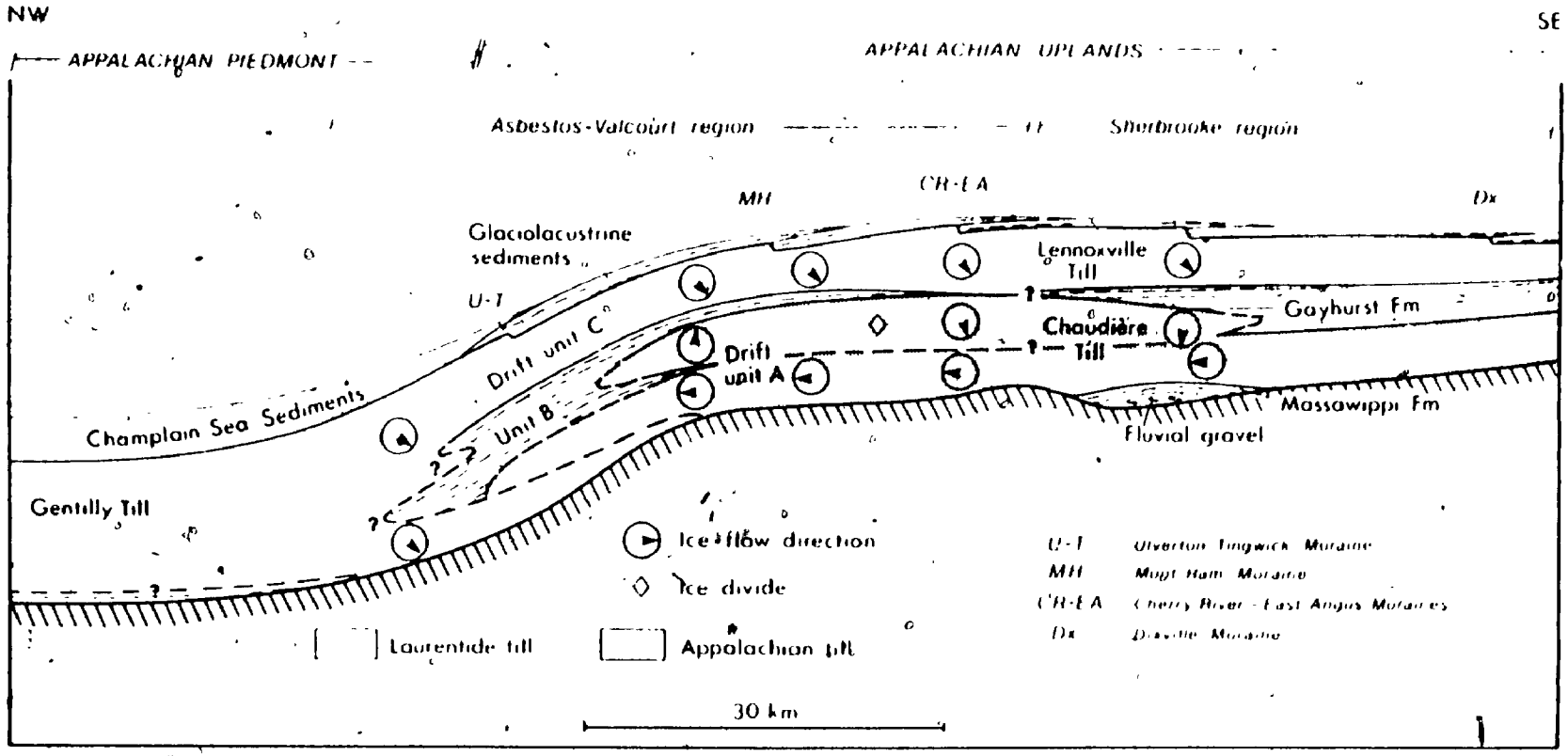

Figure 6-4 : Schematic cross-section showing vertical and lateral relationships of Late Pleistocene units in the Asbestos–Valcourt and Sherbrooke regions, southeastern Québec

the upper till in the Ange-Gardien section (Prichonnet, 1982a: fig. 29.3) is at least a partial correlative of drift unit C.

Directional and compositional data recorded by the author (see section 6.1) as well as by McDonald (1967a) suggest that Chaudière Till is an Appalachian till unit and that it is a correlative of drift unit A of the Asbestos-Valcourt region. Like most of the till units assigned to drift unit A (the lower till at Rivière Noire is the only exception), Chaudière Till at its type section has a distinctive eastern provenance and records a regional episode of westward ice-flow (Figures 4-11 and 6-4). This interpretation of an "Appalachian" Chaudière Till rests on the fact that the shift to southward ice-flow, which was previously thought to represent a significant southeastward advance of Laurentide ice across southeastern Québec (Shilts, 1981; see also Figure 1-2), failed to produce expected compositional changes. Rather this work suggests that the shift to southward ice-flow at Ascot River was produced by a shift of Appalachian ice-dispersal centers (Figure 6-4).

The proposed sequence of ice-flow patterns can also account for changes in clast lithology that were documented by McDonald (1967a) at Ascot River; not only had he pointed out the significance of Devonian granite erratics in Chaudière till, but he also showed that volcanic clasts (presumably derived from rocks of the Ascot-Weedon Formations) as well as other clasts derived from local "northwest" sources are more abundant at the top than at the base of Chaudière Till. Provenance and ice-flow patterns recorded in drift unit A and in Chaudière Till will be further discussed in section 6.4.

Correlation of unit B and Gayhurst Formation is based mainly on the fact that both units consist of glaciolacustrine sediments that were deposited prior to the last regional ice advance (drift unit C - Lennoxville Till) and also on the fact that both units were apparently neither followed nor preceded by an episode of weathering or fluvial erosion. As McDonald and Shilts (1971) rightly pointed out (see also Shilts, 1981), this means that glacial lakes remained impounded in the Appalachian Uplands of southeastern Québec throughout the interstadial. The

proximal nature of glaciolacustrine sediments assigned to unit B throughout the study area indeed suggests the nearby presence of glaciers; coarsening-upwards sequences recorded at Rivière Noire (MP-82-4), Notre-Dame-de-Ham (MP-79-17) and Wotton (MP-79-5) further suggest that at least part of unit B was deposited during advance of glacial phase C.

However, the present correlation scheme, as depicted in Figure 6-4, raises the question of the paleogeographic context that was defined by McDonald and Shilts (1971: fig. 3) for Glacial Lake Gayhurst. For instance, glaciolacustrine sediments of unit B are recorded at several localities north of their "inferred ice-front position at maximum retreat during the lake episode"; the occurrence of unit B at several localities well north of the Mont Ham Moraine makes it unlikely that a large glacial-lake could have remained impounded throughout southeastern Quebec at a level as high as that (about 370 m ASL) suggested by McDonald and Shilts (1971). Considering the levels of glacial lakes that were impounded in the study area during late-glacial time (see Chapter 5), lake levels must have fallen to at least about 300 m ASL in the Saint-François River watershed. However, Shilts (1981) has argued convincingly that the level of Lake Gayhurst in the upper Chaudière valley did not fall below about 370 m ASL; this may also suggest that the lowest col (at La Guadeloupe: 305 m ASL) between the Saint-François and Chaudière Rivers watersheds remained obstructed by a remnant ice mass (or ice cap) that may have persisted on Appalachian uplands in the vicinity of Thetford-Mines, a situation which would be analogous to that suggested in Figure 6-4 for the closing stages of glacial phase A.

In any event, the extent of glacier ice in southeastern Quebec prior to the last regional ice advance (drift unit C - Lennoxville Till) remains, in the author's opinion, an open question. Glaciolacustrine sediments recorded in sections reported in this thesis and in other studies (Chauvin, 1979a, 1979b; Shilts and Smith, 1986) suggest that large areas, valleys and low uplands in particular, were at least partly deglaciated prior to the last advance of the Laurentide Ice Sheet; on the other hand, these sections also indicate that only proximal glacio-

lacustrine sedimentation took place in Lake Gayhurst and its correlatives at sites located within the area of occurrence of northward-trending striations (see Figure 1-3 for location). It is thus possible that the northward ice-flow event which occurred towards the close of glacial phase A and which probably contributed to maintaining proximal glaciolacustrine environments (unit B) in the Asbestos-Valcourt region (Figure 6-4) also occurred in the Thetford-Mines and Beauceville areas. If so, the presence of local, remnant ice masses in uplands of those areas prior to the last Laurentide ice advance is a possibility.

6.3 Correlation with the St. Lawrence Lowland

The traditional stratigraphic framework of the St. Lawrence Lowland (Gadd, 1971; Occhietti, 1980) as well as long-held correlations with units of the Appalachian uplands (McDonald, 1971; Gadd et al., 1972b; Gadd, 1976; Shilts, 1981) were presented in Figure 1-2. The traditional framework holds that the last episode of glacial coverage in the Lowland, represented by Gentilly Till and related sediments, lasted from about 65 ka until about 12 ka, at which time the Lowland was invaded by the Champlain Sea. This traditional framework has been challenged by Lamothe (1984, 1985; see also Lamothe et al., 1983) who reported several TL and ^{14}C dates which suggest that deposition of Gentilly Till may have commenced as recently as about 30 ka.

Since both Chaudière Till and drift unit A (except at Rivière Noire) are herein considered as essentially Appalachian till units (Figure 6-4), the chronology of glacial and non-glacial events which predate drift unit C becomes partly detached from the chronology of the Lowland. The stratigraphic record of the Asbestos-Valcourt can be correlated with that of the Lowland in the context of either a long-span or a short-span Gentilly Till.

Schematic correlations depicted in Figure 6-4 suggest that drift unit A at Rivière Noire (MP-82-4) records an "early" advance of the Laurentide Ice Sheet to at least the edge of the Appalachian Uplands, an event which is tentatively correlated with an early southeastward ice-

flow episode inferred from clast lithology of drift unit A in the Norbestos (MP-79-18), Rivière des Rosiers (MP-79-9) and Willow Brook (MP-76-1) sections (see section 4.2.6 and Figure 4-11). Because of the suggested correlation between drift unit A and Chaudière Till, it is implicitly suggested that drift unit A is younger than the Massawippi Formation and its probable correlative in the Lowland, the St-Pierre Sediments. If so, Gentilly Till, which was deposited by the last major advance of the Laurentide Ice Sheet across the Lowland and the Appalachian Piedmont, may then be a correlative of both drift units A and C; in this context, Gentilly Till and drift unit A at Rivière Noire may have been preceded by an episode of impounded drainage and hence be underlain by glaciolacustrine sediments as shown in Figure 6-4.

This hypothesis indirectly supports the view that Gentilly till records a prolonged glacial episode in the St. Lawrence Lowland. This correlation may find some support in the stratigraphic record of a section just recently reported by La Salle et al. (1986): according to their abstract, the Béthanie section, which is located in the close vicinity of the Rivière Noire section (MP-82-4), shows 6 m of varved sediments (unit B?) overlying 3.5 m of organic-bearing fluvial sediments which apparently lie above a till unit (drift unit A?). The varved sediments were TL-dated about 56 ka and fluvial sediments yielded pollen spectra similar to those of the St-Pierre Sediments. The Béthanie section thus suggests that ice-retreat prior to deposition of unit B may have been more extensive than shown in Figure 6-4; the occurrence of fluvial sediments at Béthanie re-opens the possibility that zones of oxidation observed at the top of drift unit A in the Rivière des Rosiers (MP-79-9) and Chemin des Ecossais (MP-79-1) sections may represent bona fide weathering episodes. However, the absence of weathering zones at the top of drift unit A in other sections of the Asbestos-Valcourt region would remain unexplained.

However, because of significant chronological uncertainties in the Lowland and because of the lack of sound chronological control for Gayhurst Formation and unit B in the Appalachians, correlations between

the two regions are tentative and must be considered as such. The problem is further compounded by several stratigraphic uncertainties in the Lowland (Lamothe, 1985). For instance, new exposures along the St. Lawrence River and recent borehole data (Lamothe, 1986, written communication) indicate that two units of organic-bearing fluvial sediments underlie Gentilly Till and that a till bed and varved sediments are intercalated between the two organic-bearing units.

6.4 Evidence for Appalachian outflow centers throughout the Chaudière glaciation

The expression "Chaudière glaciation" is used informally for the purpose of the following discussion; it is understood as a diachronous unit represented by Wisconsinan till units deposited during the penultimate glacial "maximum" in southeastern Quebec. As used herein, the Chaudière episode thus encompasses Chaudière Till of the Sherbrooke and Lac-Mégantic regions as well as drift unit A of the Asbestos-Valcourt region.

Evidence for Appalachian outflow centers during the Chaudière episode was presented some time ago by McDonald and Shilts (1971). Evidence then available suggested that Chaudière Till "... was likely deposited by a glacier which entered the area from an ice-flow centre to the east and which, after coalescing with the continental Laurentide Ice Sheet flowing from north and northwest, was incorporated into a general southeastward glacial flow" (Shilts, 1978: p. 2). Figure 1-2 which is partly based on a schematic cross-section by Shilts (1981: fig. 11), summarizes previous thinking on the subject.

Sequences of ice-flow patterns recorded in sections of the Asbestos-Valcourt region show that, if indeed there was coalescence of the two glaciers during the Chaudière glaciation, westward ice-flow was re-established and maintained during much of the episode. Because this prominent westward ice-flow event is recorded in sections close to the St. Lawrence valley and because it was followed by a northward ice-flow event rather than by southeastward ice-flow, it is suggested that Appa-

lachian outflow centers probably persisted throughout the Chaudière glaciation. Evidence to support this hypothesis comes from a variety of observations by this author as well as by previous authors.

As mentioned earlier, drift unit A of the Asbestos-Valcourt region contains very few Precambrian erratics and the few which could be found occur in till that was deposited by ice advancing from the east. At Ascot River, Chaudière Till contains virtually no Precambrian erratics; the same was noticed also in the Lac-Mégantic region where Shilts (1981, p. 21) observed that: "In all exposures Chaudière Till... has few, if any, Precambrian 'shield-type' erratics".

Westward transport of ultramafic debris during the Chaudière glaciation is indicated by the relatively high Ni content of drift unit A at Norbestos. Many of these ultramafic components were re-entrained by ice advancing toward southeast during the next regional glacial phase; however, "residual" amounts are present in surface till west and north of the Asbestos ophiolite complex. Their minimum area of occurrence in surface till outside of the southeast-trending Asbestos ultramafic dispersal train is given by the 30 ppm Ni contour line (Figure 6-5). Ultramafic debris was thus transported westward, and locally northward, over at least 10 km during the Chaudière glaciation. Moreover, the presence of occasional ultramafic clasts in late-glacial ice-contact sediment bodies in the vicinity of Durham-Sud (McDonald and Shilts, 1971: fig. 2) suggests that these clasts were transported westward over as much as 30 km during the episode.

In areas south of Sherbrooke, at the Ascot River locality for instance, the occurrence of distinctive granitic clasts throughout Chaudière Till provides direct evidence of regional westward glacial transport during the Chaudière glaciation. Investigations by this author fully support the earlier interpretation by McDonald (1967a) that these clasts are derived from Devonian granitic stocks located in the vicinity of Scotstown and Lakes Aylmer and Saint-François (Figure 6-5), northeast of the Ascot River section. Devonian granite erratics also occur as surface boulders at a number of localities outside of main

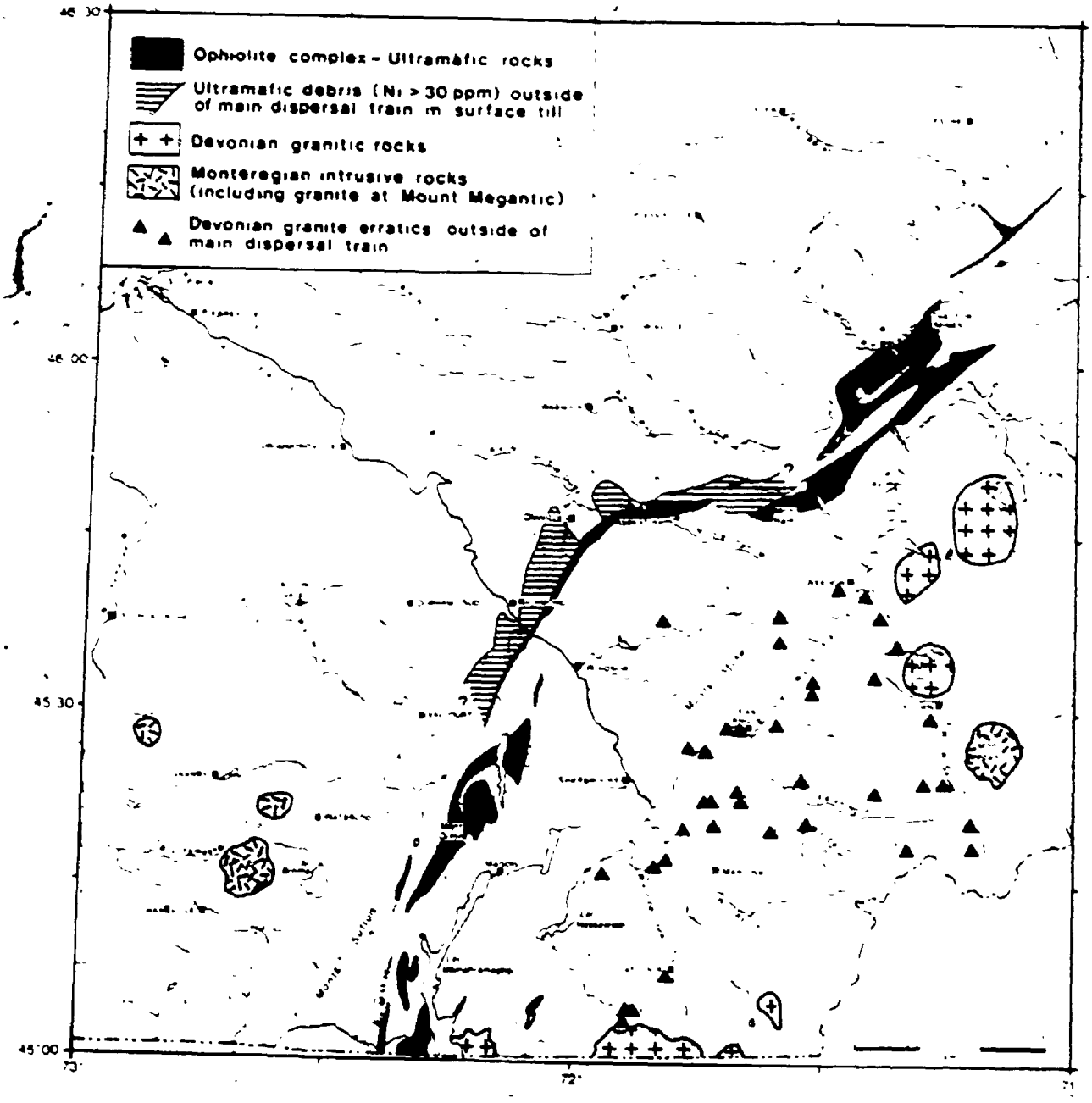

Figure 6-5 : Residual evidence for regional westward and northward glacial transport during the Chaudière glaciation. The regional occurrence of distinctive indicators (ultramafic debris and Devonian granite erratics) outside of southeastward dispersal trains that were formed during the last regional ice advance provides indirect evidence for Appalachian outflow centers during the earlier (Chaudière) glaciation. Occurences of Devonian granite erratics are mostly from McDonald (1967a : his fig. 9).

southeastward-trending dispersal trains (McDonald, 1967; McDonald and Shilts, 1971). Additional localities north and northwest of the Stoke Mountains were found by this author; these, along with localities previously reported by McDonald and Shilts (1971), are plotted in Figure 6-5. The areal distribution of these occurrences discloses a fairly distinct, although residual, dispersal pattern extending westward of Devonian granitic stocks; this provides further evidence of westward transport over distances exceeding 40 km during the Chaudière glaciation.

Whether or not the Laurentide Ice Sheet advanced into or across southeastern Quebec during the latter part of the episode, as it has been suggested earlier by McDonald and Shilts (1971), remains an important question. However, compositional changes that can be expected as a result of such an event have yet to be recorded. At Norbestos and Rivière des Rosiers, near the edge of the Appalachian uplands, the upper part of drift unit A contains no record of an "expected" influx of Precambrian clasts; instead, a shift to northward ice-flow is recorded. At Ascot River, changes in till clast composition and fabric in the upper part of Chaudière Till are explained equally well, perhaps even better, by a late shift to southward ice-flow which is currently interpreted as the counterpart of the northward flow event recorded at Norbestos and Rivière des Rosiers (Figures 6-4 and 4-11). An hypothetical late Chaudière ice-divide, such as that shown in Figure 6-4, may also explain why Shilts (1981, p. 20) could not find evidence for an expected enrichment in feldspar and granodiorite within the upper portion of Chaudière Till in his provenance region III near Lac-Mégantic. This lack of evidence for significant southward or southeastward glacial transport during the Chaudière episode was recently extended to sections along Rivière des Plantes and to Rivière Gilbert boreholes in the vicinity of Beauceville (Shilts and Smith, 1986).

6.5 Ice-flow sequences recorded by glacial striations - A discussion

Irrespective of interpretation differences that may occur between different observers on a given outcrop (see section 3.1.3), studying

ice-flow directions and sequences of ice-flow directions recorded by glacial striations remains an important research tool in southeastern Québec and elsewhere. However this study indicates that results can be sometimes misleading. Ice-flow histories, such as those arrived at by Lamarche (1971, 1974), Lortie (1976), Chauvin et al., (1985);, Lowell (1985), Lowell and Kite (1986) and several others, are mainly based on:

- relative frequency of directions recorded by glacial striations
- and inferred relative age of sets of striations, as revealed by cross-cutting or similar relationships.

In regions where striations have been investigated together with the stratigraphic and paleogeographic record of deglacial events (e.g. Chauvin et al., 1985; Lowell, 1985; Lowell and Kite, 1986), they have been found in fair agreement with the deglacial record. The Asbestos region stands out as one of the few areas known to this author where the deglacial record seems at variance with the ice-flow history inferred from studies of glacial striations (see Chapters 1 and 5); however it may be noticed in passing that relatively little was known of the deglacial record of the Asbestos area at the time of studies by Lamarche (1974) and Lortie (1976).

The few sites where striations were investigated during this study (Figure 3-1) indicate that westward-trending striations are by far the most abundant in the Asbestos region, much as earlier reports had indicated. However these sites also show that northward-trending striations are commonly superimposed on westward-trending striations; also superimposed on westward-trending striations are "simple" north-south striae and even southward-trending striations. In about the same area, Lamarche (1974) and Lortie (1976) report other sites where northward-trending striations are younger than westward-trending striations and where westward-trending striations are younger than southeastward-trending striations. In view of ice-flow directions recorded in stratigraphic sections (see Figure 6-4 for a summary), all the aforementioned cross-cutting relationships seem possible on a given outcrop. In fact, what seems to be lacking here is a well-defined "datum", that is a set

of glacial striations whose relative age can be independently established and consistently tested. This author believes that drift unit C and the associated deglacial record provides such a datum; this leads to the conclusion that many of the glacial striations found on outcrops of the Asbestos region are most likely residual features that were formed prior to glacial phase C.

This proposal may explain why glacial dispersal studies have failed to find significant evidence for northward and westward transport in surface till of the Asbestos (this study; see also Lortie, 1976) and Thetford-Mines (Shilts, 1973b; Lortie, 1976) regions in spite of the large number of westward- and northward-trending striations that have been recorded throughout much of the southeastern Québec Appalachians. Gadd (1978) also observed that "... little erosion or sediment transportation was effected during the northward flow event." (p. 3) in the Saint-Sylvestre area. A main exception is the occurrence of large amounts of amphibolite boulders that Lortie (1976) reported in terrains northwest of their presumed bedrock sources (about 10 km^2) at Belmina ridge, near Thetford-Mines; however, Caron (1983a) subsequently mapped a 14 km^2 amphibolite outcrop located just northwest of the amphibolite dispersal train. Boulders counted by Lortie (1976) may therefore be derived from both bedrock sources.

This author finds it difficult to reconcile the idea of finding little or no evidence of northward glacial transport in areas where northward-trending striations are so common: the very presence of these striations indicates that northward-flowing glaciers had a significant basal debris load and that those debris were indeed transported. Moreover, maps prepared by Lortie (1976) as well as observations made during this investigation show that northward- and westward-trending striations are just as "pervasive" on outcrops of their area of occurrence as southeastward- or southward-trending striations are in areas where no late-glacial ice-flow reversal event has been inferred; this argues against the often cited idea of "short-lived" or "ineffective" ice-flow reversal events. This further suggests that northward- and westward-trending striations reported as late-glacial features in other Appala-

chian regions may be, as they are in the Asbestos region, residual features; yet this does not exclude the possibility that some of these striations may be true late-glacial features.

Sudden shifts of ice-flow direction, such as that recorded during the latter part of the Chaudière glaciation in the Asbestos-Valcourt and Sherbrooke regions (Figure 6-4), may be typical deglacial events in the Appalachian Uplands; however their context (shift or reversal) and their areal extent may have differed depending on whether the last deglaciation (Lennoxville) or prior ones are considered. Investigations such as those carried out by Lamarche (1971, 1974), Lortie (1976) and several others are extremely valuable as they at least provide regional data on the direction and areal extent of glacial movements.

6.6 Regional deglacial patterns

An updated map of selected deglacial features (eskers and morainic belts) was compiled from the available literature (mainly McDonald, 1967a, 1969; Clément et Parent, 1977; Parent, 1978; Gadd, 1964, 1978; Shilts, 1970, 1981; Prichonnet et al., 1982a, 1982b; Gadd, McDonald and Shilts, 1972a; Dubé, 1971; Chauvin, 1979a, 1979b; Dubé, 1983) and from the author's field investigations (Figure 6-6). As a result of several new regions being investigated since the last regional compilation map of deglacial features (Gadd, McDonald and Shilts, 1972) was published, the regional picture of ice-retreat patterns and associated deglacial events contains significant changes. Considering the fairly advanced state of surficial geology mapping in southeastern Quebec, ice-retreat patterns depicted in Figure 6-6 seem generally robust.

Brief comments and discussion on salient points shown by Figure 6-6 now follow:

(1) Eskers are relatively common in the southwestern half (west of longitude 71°30") of the southeastern Québec Appalachians; investigations carried out thus far reveal that most of these eskers formed subglacially as fairly short diachronous seg-

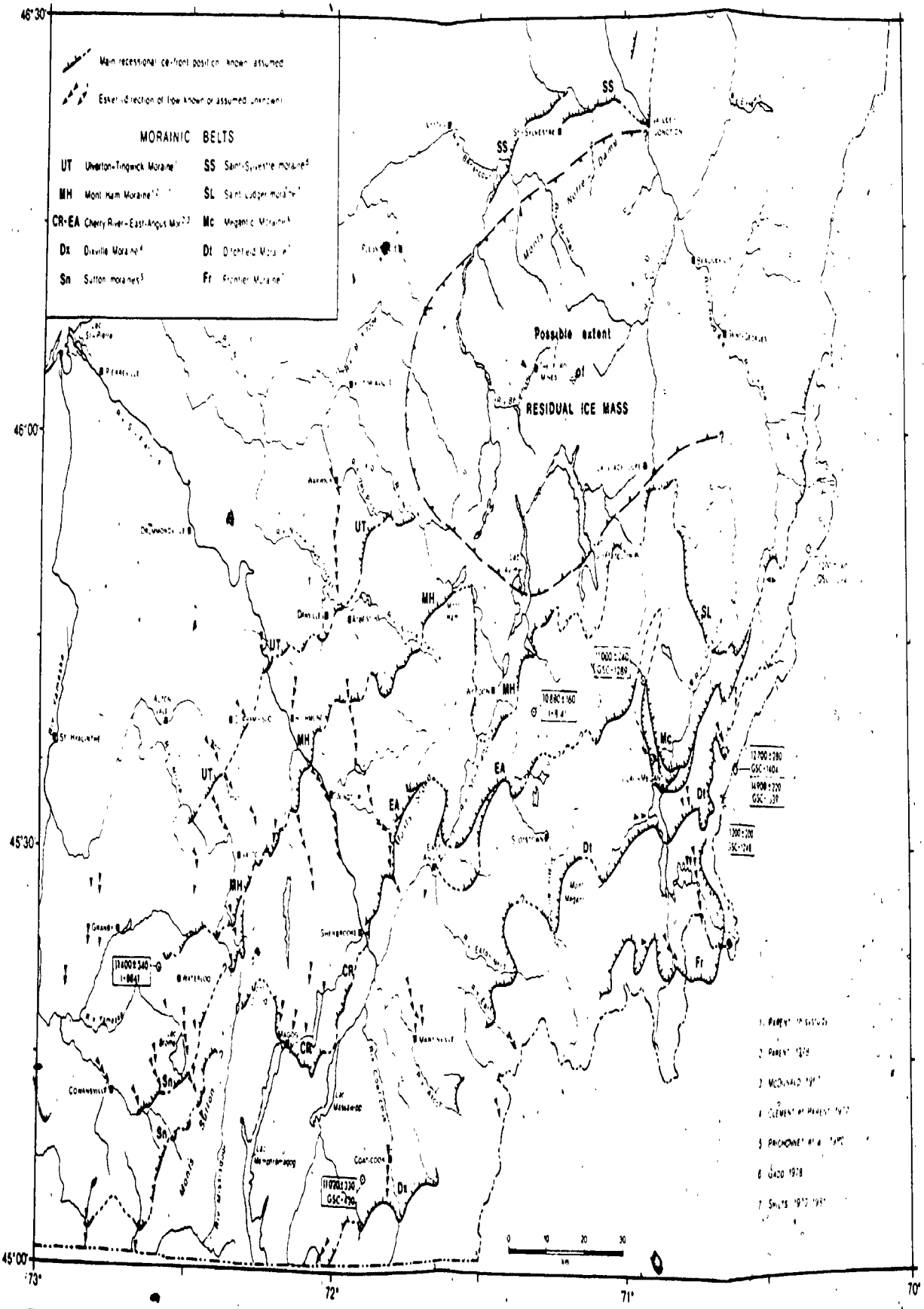

Figure 6-6 : Main recessional moraine belts in southern Québec, also showing the possible extent of a residual ice mass in uplands of the Thetford-Mines region. Radiocarbon dates obtained on terrestrial plant material are from Gadd et al. (1972 a), Mott (1977) and Richard (1977, 1978).

ments (Banerjee and McDonald, 1975; Parent, 1978, 1984c, this study; Gadd, 1983: p. 411). This suggests that, west of this Warwick - Martinville line, the predominant subglacial thermal régime during deglaciation was one of basal melting (Boulton, 1972), an idea which finds additional support in the common occurrence of streamlined subglacial landforms in low-relief terrains of that region (Figure 3-1; see also Gadd, McDonald and Shilts, 1972, and Prichonnet, 1984). Although no causal relationship is inferred, it may be further noticed that large proglacial lakes were impounded at the ice-front during deglaciation of this region (see Chapter 5).

(2) In uplands lying east of the Warwick-Martinville line, eskers seem almost totally absent; this suggests that the predominant subglacial thermal régime during deglaciation was one of either basal freezing or of cold-based ice (Boulton, 1972). If so, this may have been a region of weak subglacial erosion during the last deglaciation; moreover, this hypothesis may provide at least a partial explanation for the preservation of older (westward and northward, and (?) southeastward) striations in the Asbestos region and perhaps in the Thetford-Mines region as well.

(3) Known recessional ice-front positions indicate that northward retreat of an active ice-front took place in the southern and western regions of the southeastern Québec Appalachians; except for the fact that ice-front positions trend about WSW-ENE rather than SW-NE, this ice-retreat pattern resembles that suggested by Gadd, McDonald and Shilts (1972a). As a result, the Dixville Moraine, a previously unnamed morainic belt whose features were first reported and discussed by Clément and Parent (1977), now appears as a correlative of either the Ditchfield or the Frontier Moraine of Shilts (1970, 1981). The next younger morainic belt, the Cherry River / East-Angus Moraine, may be of about the same age as the Mégantic Moraine of the upper Chaudière valley. The Sutton moraines, a conve-

nient name for a series of slightly diachronous morainic deposits mapped by Prichonnet et al., (1982a, 1982b) on the northwest flank of the Sutton Mountains, record ice-retreat positions which seem roughly coeval with the Cherry River / East-Angus Moraine and slightly older than the Mont Ham Moraines; ice-contact deltas and terraces associated with the Sutton moraines (Prichonnet et al., 1982b) suggest that waters of Glacial Lake Vermont (Chapman, 1937) fell from the level of the Coveville phase to that of the Fort Ann phase during ice-retreat from the outer to the inner Sutton moraines. The Fort Ann phase is therefore a partial correlative of the Sherbrooke phase of Glacial Lake Memphremagog (Parent et al., 1985); the Sherbrooke phase reached its maximum extent during construction of the Mont Ham Moraine (Parent, 1978, this study) which may be nearly coeval with construction of the Saint-Ludger moraine (a convenient name that designates morainic deposits mapped by Shilts (1981) near Saint-Ludger, in the upper Chaudière valley).

(4) Ice-retreat from the position of the Mont Ham Moraine allowed incursion of Glacial Lake Vermont (Fort Ann) onto increasingly large areas of the Appalachian Piedmont of southeastern Quebec (See Chapter 5). As discussed earlier, the next younger Ulverton-Tingwick Moraine was formed only slightly more than 100 varve years prior to final drainage of the Fort Ann phase of Lake Vermont and hence prior to Champlain Sea incursion about 12 000 years BP (shell dates). Absence of Fort Ann strandline features and of glaciolacustrine sediments in the vicinity of Victoriaville suggests that Lake Vermont did not drain northeastward along the Appalachian Piedmont of the Plessisville area.

(5) Deglacial patterns along the edge of the Appalachian uplands, between Lac Brome and Plessisville, have little in common with the concept of the Highland Front Morainic System as defined by Gadd, McDonald and Shilts (1972a); the concept is now obso-

lete and the name should definitely be abandoned and replaced by local names, such as the Ulverton-Tingwick Moraine, in order to designate morainic deposits that were formerly assigned to the Highland Front Morainic System. Similar reasoning has already been applied in the Lower St. Lawrence region (Chauvin et al., 1985). In order to avoid possible confusion, it is informally suggested that morainic deposits which were mapped by Gadd (1978) in the vicinity of Saint-Sylvestre be simply called Saint-Sylvestre moraine. As Figure 6-6 shows, there are virtually no morainic deposits that support the connection between the Saint-Sylvestre moraine and the Ulverton-Tingwick Moraine. Chronological relationships between the two features remain to be worked out; nowever, the Saint-Sylvestre moraine seems younger than the Ulverton-Tingwick Moraine.

(6) In a large area surrounding Thetford-Mines, very few ice-marginal deposits or eskers have been reported. However, Chauvin (1979a) reports that the youngest lodgement till sheet is commonly overlain by a melt-out till unit (his "membre supérieur") in sections of the Thetford-Mines region. This, together with the absence of eskers and ice-frontal deposits, suggests that a large mass of cold-based (?), stagnant ice may have been left stranded on uplands of the Thetford-Mines region. A small esker with northward paleocurrent which has been reported by Lortie (1976) and Gadd (1978) near Saint-Sylvestre may be associated with the residual ice mass. A similar ice mass may also have been isolated on uplands east of the Chaudière valley (Shilts, 1981; Lowell, 1985; Lowell et al., 1986). Isolation of this residual ice mass may have followed an ice-flow reversal event and may have occurred as a result of the retrogradation of a marine calving bay up the St. Lawrence River estuary to the vicinity of Québec city, much as Chauvin et al. (1985) and Parent et al. (1985) and several other previous authors (see Chapter 1) have inferred. Parent et al. (1985: fig. 1) also suggested that incursion

of the calving bay to vicinity of Québec City, about 12.5 to 12.2 ka, may be approximately coeval with constructions of the Mont-Ham Moraine and of its correlatives.

(7) Because periglacial desert and tundra conditions succeeded deglaciation of the southern Québec Appalachians (Richard, 1977, 1978, 1985; Mott, 1977), a fairly long delay between deglaciation and the onset of organic sedimentation is inferred. Available bog-bottom dates (Figure 6-6) seem of little help for assessing deglacial patterns, particularly since palynological studies by Mott (1977) have shown that GSC-1339 (14 900 ± 220 years BP) and GSC-1404 (12 700 ± 280 years BP) which were obtained from calcareous organic sediments (Mott, 1977; Gadd, McDonald and Shilts, 1972a) are probably contaminated by old carbonates; dates from other sites indicate that terrestrial organic sedimentation was well underway in the region by about 11 000 years BP.

CHAPTER 7

CONCLUSIONS AND RECOMMENDATIONS FOR FUTURE STUDY

7.1 Conclusions

The main conclusions of this study are:

(1) During the Wisconsinan stage, the Asbestos-Valcourt region was invaded by at least two regional glacial advances (drift units A and C) with an intervening, rather short-lived, glaciolacustrine episode (unit B).

(2) Drift unit A, which was deposited during the earlier glacial advance and which is considered as a correlative of Chaudière Till, was deposited by a glacier that advanced mainly toward west or WSW from Appalachian outflow centers. This Appalachian till unit contains some northwest-derived debris that provides evidence for an earlier phase of southeastward ice-flow which may either predate or postdate deposition of the Massawippi Formation (Early Wisconsinan). The upper part of drift unit A contains no record of an influx of northwest-derived debris that should be expected from a long episode of coalescence with the Laurentide Ice Sheet, such as that proposed by earlier workers. Instead, recorded ice-flow patterns suggest that a shift of outflow centers within an Appalachian-based glacier took place toward the close of glacial phase A; it is during this part of glacial phase A that a northward ice-flow episode took place in uplands of the Asbestos region.

(3) Glaciolacustrine sediments of unit B were deposited in a glacial lake (or a series of glacial lakes) that was impounded in front of the glacier which subsequently deposited drift unit C. However, the lower part of these sediments may be locally coeval with the northward ice-flow episode which occurred

during the latter part of glacial phase A. Sediments of unit B, which are probable correlatives of the Gayhurst Formation, were deposited in mainly proximal glaciolacustrine environments. Because of the apparent lack of dateable organics, the age of this Middle Wisconsinan interstade remains poorly known.

(4) Drift unit C was deposited during the last regional advance of the Laurentide Ice Sheet and is believed to be a correlative of Lennoxville Till. Available evidence indicates that southeastward ice-flow was maintained throughout glacial phase C in the Asbestos-Valcourt region. Northward- and westward- trending striations which were interpreted by previous authors as the result of a late-glacial ice-flow reversal are best interpreted as residual features that were formed during the earlier glacial phase A.

(5) Three main recessional morainic belts (Cherry River / East-Angus, Mont Ham and Ulverton-Tingwick Moraines, in order of decreasing age) were constructed during northward retreat of the Laurentide Ice Sheet. These morainic belts have yet to be dated directly; nowever, varve series that overlie drift unit C suggest that the Cherry River / East-Angus Moraine probably formed some 500 years prior to Champlain Sea incursion (about 12 ka) and that the Ulverton-Tingwick Moraine was constructed at least 100 years prior to marine incursion.

(6) Deglacial patterns along the edge of the Appalachian Uplands have little in common with the concept of the Highland Front Morainic System as defined by previous authors; this pioneer concept is now obsolete and should be abandoned and replaced by locally defined morainic belts, such as the Ulverton-Tingwick Moraine. Regional ice-retreat patterns bring some support to the hypothesis that a large residual ice mass became isolated in uplands of the Thetford-Mines region, northeast of the Asbestos-Valcourt region. Northward ice-flow may

also have taken place within this cut-off mass of Laurentide ice; if so, this northward ice-flow reversal may be the result of early marine incursion (12.5 to 13.0 ka) in the St. Lawrence River Estuary, as postulated by several authors, and may therefore be correlative with the northward ice-flow event recorded by Chauvin et al. (1985) and by Lowell (1985) in uplands east of the Chaudière River valley and in the northern Maine uplands.

(7) Glacial lakes were impounded south of the ice-front during Late Wisconsinan deglaciation of the Asbestos-Valcourt region. As a result of differential post-glacial isostatic rebound, shoreline features of the former water-planes are tilted upward to the northwest with a gradient of about 1 $m.km^{-1}$. During construction of the Cherry River / East-Angus Moraine, waters of Glacial Lake Memphremagog had already fallen to the level of the Sherbrooke phase; ice-dammed waters remained at the level of the Sherbrooke phase until the ice-front had retreated slightly northwest of the position of the Mont Ham Moraine. Glacial retreat to the position of the Ulverton-Tingwick Moraine allowed waters of Glacial Lake Vermont (Fort Ann phase) to expand onto the Appalachian Piedmont of southeastern Québec and to merge with waters of Glacial Lake Memphremagog; glaciolacustrine water levels remained at the level of the Fort Ann phase for at least some time following construction of the Ulverton-Tingwick Moraine. The next lower series of shorelines are those formed during early Champlain Sea incursion.

(8) The Danville Varves, which contain a typical arctic freshwater ostracode fauna (**Candona subtriangulata**), together with other late-glacial varve series provide key additional evidence for regional glaciolacustrine water-bodies prior to Champlain Sea incursion. The presence and extent of these glacial lakes provide further evidence that the uplands of the

Asbestos-Valcourt region were essentially ice-free at the time of Champlain Sea incursion.

(9) The upper marine shorelines are also tilted upward to the northwest; the marine limit thus stands at altitudes ranging from 165 to 175 m ASL in the study area. By about 12 000 years BP (shell dates), marine waters had replaced glaciolacustrine waters in the Appalachian Piedmont of the Asbestos-Valcourt region. Champlain Sea incursion likely took place only after the Laurentide Ice Sheet had retreated from the edge of the Outer Appalachian Uplands in the vicinity of Warwick and Victoriaville. Offlap history of the Champlain Sea had already begun by about 11 500 years BP; by 10 500 years BP, marine waters had locally receded to about 80 m ASL and had thus withdrawn from this part of the Appalachian Piedmont.

7.2 Recommendations for future study

(1) This study proposes that Chaudière Till and its correlative, drift unit A, were essentially produced by an Appalachian glacier complex (except at the Rivière Noire section); this hypothesis should be further investigated in stratigraphic sequences of the Thetford-Mines area and of the middle and lower Chaudière River valley.

(2) Because this study found solid evidence contrary to the hypothesis of a late-glacial ice-flow reversal in the Asbestos region, the latter concept should be re-investigated in the Thetford-Mines region, particularly since there is at least a possibility that there may be two distinct episodes of northward ice-flow in that region and in other regions of the southern Quebec Appalachians.

(3) As stated earlier (see section 6.1.2), a new stratotype should be sought to designate glacial sediments that underlie the

Massawippi Formation: since the Ascot River sections constitute the type sections for major regional units and since "Johnville Till" is absent at its type section (Ascot River II), this new stratotype should be preferably located in the Sherbrooke region.

(4) The possibility that the Saint-Sylvestre moraine was emplaced by a glacial readvance, as suggested by Lortie (1976) and Shilts (1976b, 1981) in the former context of the Highland Front Morainic System, should be investigated since the relationships between the postulated ice-flow reversal and glaciolacustrine water bodies remains problematical or, at best, poorly documented in the lower and middle Chaudière River valley.

(5) Stratigraphic drilling should be carried out in the Asbestos-Valcourt region with at least the specific objective of finding out whether a southeastward (Laurentide) ice-flow episode took place during the early part of glacial phase A or whether it took place during an earlier, distinct glacial phase.

(6) Given the paucity of dateable organics in glaciolacustrine sediments of unit B and of the Gayhurst Formation, TL dating of these units should be at least attempted; however, there is a distinct possibility that the TL signal of these deep-water, mainly proximal sediments may not have been set back to "zero" at the time of deposition.

APPENDIX I

STRATIGRAPHIC SECTIONS

Sections are listed in the order in which they appear in text. Appendix I includes descriptions of the following sections:

- Section MP-79-18A (Norbestos)
- Section MP-79-18B (Norbestos)
- Section MP-79-18C (Norbestos)
- Section MP-79-9 (Rivière des Rosiers)
- Section MP-79-1 (Willow Brook)
- Section MP-79-1 (Chemin des Ecossais)
- Section MP-82-4 (Rivière Noire)
- Section MP-79-5 (Wotton)
- Section MP-79-15 (Tingwick)
- Section MP-79-17 (Notre-Dame-de-Ham)
- Section MP-80-2 (Bromptonville)
- Section MP-79-14 (Arthabasca)
- Section MP-82-1 (Melbourne)
- Section MP-79-10 (Rivière Danville)
- Section MP-79-16 (Rivière Landry)
- Section MP-79-13 (Warwick)
- Section MP-79-19 (Danville)
- Section MP-81-1 (Ascot River I)
- Section MP-82-3 (Ascot River II)

Unit	Thickness (m)	Depth of base (m)

Section MP-79-18 (Norbestos)

North side of abandonned open-pit asbestos mine (Norbestos mine); Warwick map-area (21 E/13); about 2.75 km northeast of Les Trois Lacs. UTM grid zone 19T: 278.70 E and 5077.50 N. Altitude: approx. 250 m.

(Because the slump cover was generally thick and because exposed sediments showed important lateral facies changes, three subsections were investigated and measured at most favorable locations, working toward the west end of the abandoned excavation. See Figure 4-2).

Subsection A

Drift unit C: **Lodgement till**. Compact, olive oxidized, fissile, pebbly, sandy silt diamicton. Sharp, conformable basal contact. Precambrian clasts common. Upper part (solum) removed.	1.8	1.8
Unit B: **Glaciolacustrine muds**. Gray and calcareous below 4 m; oxidized above that level. Turbidite bedding, consisting of A, D and E divisions, is common throughout unit. A-division layers range in thickness from 3 to 30 cm and consist of graded silt and silty sand containing granules and small pebbles; they are arranged in 5 overall thinning-and-fining-upward sequences. D- and E-division layers have a thickness between 1 and 3 cm and consist of clayey silt with abundant ice-rafted clasts. Uppermost 90 cm of unit consist of a massive diamicton bed grading upward into pebbly sand and sand layers.	7.2	9.0
Drift unit A: **Deformation till and lodgement till complex**. Very compact, gray and calcareous diamicton. Deformation till consists of stacked thrust-slices of glaciolacustrine muds (resembling those of unit B). Major shear planes between slices dip south. Axial planes of overturned and recumbent folds within slices also dip south while synthetic sets of small low-angle normal faults dip north (Plate 4-1). Contacts of lodgement till beds with intervening deformation till units are sharp and erosional. A clay-till wedge, striking N 100° and dipping about 75° north, is present within the upper-most lodgement till bed. Lowermost lodgement till unit contains some ultramafic clasts, but no Precambrian clasts were noted.	7.0	16.0
(Slumped sediments)	(>4.0)	(>20.0)

Unit	Thickness (m)	Depth of base (m)
	Subsection B	
Drift unit C (2 subunits):	2.7	2.7
1) **Supraglacial till complex** (0 - 1.1 m): Loose, oxidized, sandy to gravelly diamicton containing several thin lenses of plane-bedded gravelly sand. Crudely stratified unit. Contains some boulders. Precambrian clasts are common; no ultramafic clasts were seen.		
2) **Lodgement till** (1.1 - 2.7 m): Oxidized, olive, fissile, rather pebbly diamicton. Silty sand matrix shows distinct textural layering. Boulder zone occurs near middle of unit. Precambrian clasts are common; only one ultramafic clast was seen.		
Unit B: **Assemblage of glaciolacustrine turbidites and other mass flow sediments.** Seven overall sequences of variable thickness show fining-and-thinning-upward trends. Most sequences consist of a basal bed of massive matrix-supported diamicton (one of these (#2) is inversely graded), overlain by massive or plane-bedded gravelly sand layers and by plane-laminated or graded sand layers. A layer of imbricated gravel is present at the base of sequence #6. Basal contacts of sequences are sharp and occasionnally channelized (see Plate 4-3A). Sequence #5 consists of a 1 m-thick series of AD(E) turbidites with abundant ice-rafted clasts: the thickness of graded sand layers varies from 2 to 5 cm, and that of silt layers varies from 0.5 to 1.5 cm. Two small overturned folds were observed near the top of sequence #5: their axial planes strike N 26° and N 133° and dip 28° and 31°, respectively, toward west. The massive 2 m-thick diamicton at a depth of 7.8 m is considered a debris flow sediment. Overall unit resembles a subquatic mid-fan sequence. Unit is oxidized to a depth of 5.8 m.	10.1	12.8
Drift unit A: **Lodgement till.** Very compact, gray, calcareous, pebbly, sandy silt diamicton. Boulders in boulder zone (not a pavement) near top of unit have SSE-trending long axes. Ultramafic clasts are present, but no Precambrian clasts were noted.	6.2	19.0
(Slumped sediments)	(>1.0)	(>20.0)

Unit	Thickness (m)	Depth of base (m)
Subsection C		
(Removed sediments, including soil zone; thickness estimated)	(2.0)	(2.0)
Drift Unit C (2 subunits)	4.4	6.4
1) Supraglacial till complex (2.0 - 4.5 m): Loose, oxidized, sandy to gravelly diamicton. This matrix-supported diamict includes several lenses of plane-bedded sand and gravelly sand. Crudely stratified unit. Precambrian clasts are common; no ultramafic clasts were seen.		
2) Lodgement till (4.5 - 6.4 m): Olive to light olive gray, fissile, silty sand diamicton. Degree of oxidation and leaching decreases with depth; till is calcareous near base. Sandy lens at the level of boulders, near top of unit, is sheared toward the SE sector. Precambrian clasts are common while ultramafic clasts are very rare.		
Unit B: Glaciolacustrine sediments. Exposed unit consist of only two thick turbidite beds with ABDE divisions. Upper turbidite contains rip-up silt clasts and seems only slightly deformed near contact with overlying glacial unit; its basal contact is loaded.	1.2	7.6
Drift unit A: Lodgement till. Very compact, hard, gray, calcareous, sandy diamicton. Distinct shear planes are present throughout unit, particularly near top. Textural layering is associated with shear planes. Below boulder zone at a depth of 11.5 m, till is more stony and more sandy. Ultramafic clasts are common; a few "in situ" Precambrian clasts were noted.	7.8	15.6
(Slumped sediments)	(>4.4)	(>20.0)

Unit	Thickness (m)	Depth of base (m)

Section MP-79-9 (Rivière des Rosiers)

Left bank of Rivière des Rosiers, 3.4 km southwest (S 40° W) of 4-way intersection in Tingwick; Warwick map-area (21 E/13). UTM grid zone 19T: 269.25 E and 5082.25 N. Altitude: approx. 152 m.

(Vegetation covered slumped sediments; thickness of about 1.5 m)

Glaciolacustrine silt and clay: gray, non-calcareous DE turbidites; 1 to 3 cm-thick couplets; probably varves. — 1.0 — 1.0

Drift unit C (3 subunits): — 5.0 — 6.0

1) **Flow till (1.0 - 2.4 m)**: gray calcareous, sandy silt diamicton layers are interbedded with thin sand layers (lenses ?); diamicton-sand contacts are wavy and non-erosional.

2) **Lodgement till (2.4 - 5.5 m)**: dark gray, compact, fissile to massive, calcareous silty sand diamicton; upper half shows textural layering while lower half contains a few large up-sheared silt lenses (rising toward SE); a major shear plane forms basal contact of subunit.

3) **Lodgement till (5.5 - 6.0 m)**: brownish, compact, silty diamicton containing several pebble-size clasts of laminated silt and clay.

Drift unit A (2 subunits): — 6.6 — 12.6

1) **Stratified diamicton (6.0 - 8.6 m)**: this stratified diamicton and gravel complex consists of poorly sorted pebbly matrix-supported diamicton with numerous layers and lenses of pebbly sand. A 30 cm-thick bed of better sorted and rounded sandy gravel occurs at a depth of 7.5 m. Sediment is olive and slightly calcareous above the gravel bed; below, it is more oxidized, non-calcareous and buff.

2) **Lodgement till (8.6 - 12.6 m)**: very compact, fissile, calcareous, pebbly, sandy silt diamicton; textural layering present in upper 1.2 m; till is slightly oxidized (pale olive) in upper 1.2 m, but it is gray and strongly calcareous below that.

(Slumped sediments obscuring base of section) — (1.0) — (13.6)

Bedrock to river level. — (>0.4) — (>14.0)

Unit	Thickness (m)	Depth of base (m)

Section MP-76-1 (Willow Brook)

Right bank of Willow Brook, 6.8 km north of new bridge in Windsor; Richmond map-area (31 H/9). UTM grid zone 18T: 732.75 E and 5057.00 N. Altitude: approx. 198 m.

Drift unit C (2 subunits)	5.0	5.0
1) **Lodgement till (0 - 2.9 m)**: compact, fissile, silty sand diamicton; olive-gray and calcareous below 1.7 m; oxidized and leached of carbonates above 1.7 m; contains several ultramafic and Precambrian clasts.		
2) **Subglacial melt-out till (2.9 - 5.0 m)**: vaguely stratified, compact, gray, calcareous, pebbly, silty sand diamicton; contains a few sand lenses.		
Unit B: **Glaciolacustrine sediments.** Unit comprises four overall fining-and-thinning-upward sequences of subequal thickness. Four beds of gray, calcareous, massive, matrix-supported diamicton which lie at the base of individual sequences make up to 45% of the unit. Diamicton beds are overlain by plane-bedded or massive sandy gravel layers, and by plane-laminated, massive or graded sand layers. Graded silty sand layers occur in uppermost sequence where they are cut across by small thrust faults (strike N 072°; dip 8° N). Muddy facies (ADE and DE turbidites) with dropstones occur at a depth of 7.4 m. The overall sequence resembles a subaquatic mid-fan sequence.	6.8	11.8
Drift unit A: **Lodgement till.** Very compact, fissile, gray, calcareous, sandy silt diamicton. Several east-dipping shear planes are present in upper 40 cm. A few thin sandy lenses are also present and deformed by small overturned folds whose axial planes strike N 165° and dip 78° toward east. A conjugate set of vertical joints is visible in till near river level: main joints trend N 055° and secondary ones, N 095°. Several ultramafic clasts are present in this unit, but only one Precambrian clast was found.	>1.8	>13.6
(River level)		

Unit	Thickness (m)	Depth of base (m)

Section MP-79-1 (Chemin des Ecossais)

Roadcut on the south side of Chemin des Ecossais, about 150 m east of Transquébécoise highway (#55); Sherbrooke map-area (21 E/5). UTM grid zone 19T: 268.95 E and 5036.80 N. Altitude: approx. 206 m.

Glaciolacustrine sediments (3 subunits)	2.7	2.7
Laminated sand (0 - 1.8 m): Plane-laminated medium to fine sand; buff and oxidized; soil zone extends to ad depth of about 1 m below irregular top surface (postglacial gullying); considered a near-shore lake sediment.		
Pebbly sand (1.8 - 2.0 m): Poorly sorted matrix-supported pebbly sand; clast content increases toward top; oxidized. Unit may be a local lag deposit formed during a sudden (?) fall of glacial-lake level.		
Laminated silt and clay (2.0 - 2.7 m): Thin laminae of yellowish brown silt and clay; non-calcareous and oxidized; fine structures are not discernible, perhaps because of oxidation; considered a deep-water glacial-lake sediment.		
Drift unit C: **Lodgement till.** Compact, fissile, sandy silt diamicton; olive gray and calcareous at base; olive, non-calcareous and slightly oxidized above a depth of 4.0 m; contains several ultramafic clasts. At the west end of excavation, the bedrock surface rises and, where it is directly overlain by this till sheet, it bears striations trending between N 140° and N 150°.	2.0	4.7
Drift unit A: **Lodgement till.** Compact, olive, calcareous, sandy silt diamicton; bouldery zone from 5.2 to 5.5m; fissile above bouldery zone; sharp contact with base of overlying till unit. Where this till overlies bedrock, the polished bedrock surface bears two sets of striations; one set consists of fine striae trending between N 90° and N 115° which are crosscut by a few deeper striae trending N 140°.	2.0	6.7
Bedrock (slate) to road level.	>1.3	>8.0

Unit	Thickness (m)	Depth of base (m)

Section MP-82-4 (Rivière Noire)

Left bank of Rivière Noire, 1.7 km upstream of bridge north of Roxton-East; Richmond map-area (31 H/9). UTM grid zone 18T: 697.00 E and 5045.30 N. Altitude: approx. 155 m. (This section was previously reported by McDonald (1967b: section MS-65-85).

(Vegetation-covered slumped sediments)	(2.0)	(2.0)
Drift unit C: Lodgement till. Light yellowish brown, oxidized, fissile, pebbly, silty sand diamicton. Because of thick slump cover, top and base of unit were not exposed; however, McDonald (1967b: p. 143) observed "contorted sand lenses" and a "basal silt rich ... unit" containing "clasts of varved lake silts" in the basal 1.2 m of unit.	3.2	5.2
Unit B: Stratified sand. Light yellowish brown to light gray, medium- to fine-grained sand. Ripple-drift lamination is more common than climbing-ripple and horizontal lamination. Paleocurrent toward SE sector. Below a depth of 17 m, unit also contains several sandy silt layers. Lower 1.5 m of unit consists of cross-bedded coarse sand containing a few thin gravelly lenses; this material is stained with orange-red iron oxide. This unit is interpreted as subaquatic outwash sediments deposited in a glacial lake. Thrust faults dipping toward NW are present between depths of 6 m and 7 m; two measured faults strike N 018° and N 030° and dip 12° NW and 26° NW, respectively.	17.8	23.0
Drift unit A: Lodgement till. Compact, fissile, gray, calcareous, silty diamicton. Contains a few Precambrian clasts.	>1.5	>24.5
(River level)		

Unit	Thickness (m)	Depth of base (m)

Section MP-79-5 (Wotton)

Gravel pit on east side of highway #216, about 1.3 km southwest of bridge at Moulin-Samson (2.5 km due north of 4-way intersection in Wotton); Warwick map-area (21 E/13). UTM grid zone 19T: 281.40 E and 5070.90 N. Altitude: approx. 260 m.

(This section consists of three adjacent excavations; pits A and B are only a few tens of meters apart and are located on the east side of the road; Pit C is about 60 m west of the road; see Figure 4- ; the stratigraphic log of pit A is presented, along with a few notes on sediments exposed in adjacent pits).

Drift unit C (3 subunits): 4.6 4.6

1) **Lodgement till** (0 - 2.2 m): compact, friable, oxidized, yellowish brown, sandy diamicton. Till is not very pebbly, but contains several ultramafic clasts and a few Precambrian clasts. This till has a sharp basal contact. In pit B, basal contact is erosional and marked by a boulder zone; a 2 m-deep till wedge protrudes from the base of unit into the underlying sandy sediments; till wedge strikes N 020° and dips 75° toward SE.

2) **Subglacial allo-till** (2.2 - 3.4 m): sandy, substratified to massive diamicton containing several silt clasts and sand lenses, several of which are distinctly sheared. Several till facies were observed, the most common being subaquatic melt-out till.

3) **Deformation till** (3.4 - 4.6 m): Brecciated material consisting mainly of clasts of substratified diamicton and of stratified silty sand; subunit is a lens-shaped body not found in pits B and C.

Unit B: **Subaquatic outwash sediments**: >3.4 >8.0

Glaciolacustrine sediments consist of alternating layers of plane-and cross-laminated fine sand; ripple-drift and climbing ripple lamination are common. Water-escape structures (vertical pillars) were observed. Paleocurrent toward SE. In pit B, a large lens of massive fractured sand forms the top of the unit and is injected by the till wedge. Numerous thrust faults which dip toward NW occur throughout the unit in pits A and B. In pit C, sand is undeformed and grades downward into layers of graded silt and sand.

(Floor of gravel pit)

Unit	Thickness (m)	Depth of base (m)
Section MP-79-15 (Tingwick)		
Borrow pit on east side of country road leading from Tingwick to Chesterville, 5.1 km northeast of 4-way intersection in Tingwick; left flank of Rivière des Pins valley; Warwick map-area (21 E/13). UTM grid zone 19T: 274.70 E and 5088.90 N.. Altitude: approx. 215 m.		
(Removed solum; estimated thickness)	(0.7)	(0.7)
Drift unit C (2 subunits)	5.7	6.4
1) **Supraglacial melt-out till** (0.7 - 2.5 m): Loose, oxidized, yellowish brown, massive, sandy diamicton. Unit is crudely substratified, but contains almost no lenses of stratified sediments. Till contains several Precambrian clasts.		
2) **Lodgement till** (2.5 - 6.4 m): Very compact, fissile, brownish gray, calcareous, silty sand diamicton; contains several Precambrian clasts. A 60 cm-deep and 15 cm-wide till dike protrudes from till base into underlying sand. Till dike trends N 100° and dips 75° toward S; a coeval normal fault with a 2.5 cm throw has the same attitude as the till dike and is aligned with its north edge. A few other smaller till injections were observed at the base of this till sheet which has a sharp, erosional basal contact.		
Unit B: **Subaquatic outwash sediments:** Glaciolacustrine unit consists of plane-bedded and trough-cross-bedded medium sand and of ripple-drift-laminated fine sand. Silt layers are occasionnally present between cosets of cross-laminated fine sand.	2.6	9.0
(Slumped sediments: sediments similar to those of unit B were observed under slumped material to a depth of about 20 m.)	(>11.0)	(>20.0)

Unit	Thickness (m)	Depth of base (m)

Section MP-79-17 (Notre-Dame-de-Ham)

Borrow pit on east side of country road, about 2.2 km southwest (S 30° W) of 3-way intersection in Notre-Dame-de-Ham; Warwick map-area (21 E/13). UTM grid zone 19T: 286.65 E and 5085.05 N. Altitude: approx. 308 m.

Drift unit C: Lodgement till. Very compact, fissile, silty sand diamicton. Till is olive-gray and calcareous below 4.8 m, and olive and oxidized above that depth. Thin sand lenses are present at depths of 3.0 and 3.8 m. Lower 0.9 m of unit consists of a more sandy till which contains sheared lenses of glacio-lacustrine silt at its base and which is overlain by a 25 cm-thick zone containing sandy lenses.	5.9	5.9
Unit B: Glaciolacustrine sediments. Above a depth of 10.6 m, unit consists mainly of plane-bedded medium sand. A 70 cm-thick bed of rather sandy matrix-supported diamicton which contains a few flow structures and which shows overall grading occurs at a depth of 7.1 m; it is interpreted as a debris flow sediment. Interval between 10.6 and 12.6 m is slump-covered. Below a depth of 12.6 m, unit consists of graded sand and silt layers; thickness of single layers is about 2.5 cm.	8.7	14.6
(Slumped sediments to road level)	(>1.4)	(>16.0)

Unit	Thickness (m)	Depth of base (m)

Section MP-80-2 (Bromptonville)

Gravel pit on northeast side of country road, 3.7 km northeast (N 73° E) from north end of bridge in Bromptonville; Sherbrooke map-area (21 E/5). UTM grid zone 19T: 273.80 E and 5041.10 N. Altitude: approx. 240 m.

(This measured section (subsection A) is located at the northwest end of the gravel pit; however, units described below are exposed almost continuously along the 250 m-long, 8 to 10 m-high, northeast face of the gravel pit. Subsection A is one of six investigated sections; see Figure 4-17).

Drift unit C: (2 subunits)	4.5	4.5
1) Lodgement till (0 - 2.5 m): Fairly compact, fissile, massive, olive to olive gray, sandy silt diamicton; except for basal 0.5 m which is calcareous, unit is oxidized. Contains several Precambrian and ultramafic clasts. In most subsections (A, B, C, E), basal contact of unit is sharp and erosional; basal contact is sharp but conformable in subsections D and F where the lower part of the till contains several sand lenses. In subsection C, a small (40 cm-deep, 35 cm-wide), SE-dipping till wedge protrudes from the base of the till bed.		
2) Subglacial mlo-till (2.5 - 4.5 m): Compact, cobbly, massive to subtratified, olive gray diamicton. This boulder-bearing diamicton is locally clast-supported and contains a few gravel lenses. This unit pinches out toward southeast and is absent in other subsections. Sharp, erosional basal contact.		
Unit B: Subaquatic outwash sediments. Mainly cross- and plane-bedded sand and gravel. Locally contains large lenses of massive silty sand or massive sand (turbidites). Consists of plane- and cross-laminated sand in subsection F. Paleocurrent toward SE. (Subaquatic origin is also inferred from previous observations by the author; see section 4.3.2).	>3.5	>8.0
(Floor of gravel pit)		

Unit	Thickness (m)	Depth of base (m)

Section MP-79-14 (Arthabasca)

Borrow pit on east side of Highway #161, about 1.8 km south of main 4-way intersection in Arthabasca; Arthabasca map-area (21 L/4). UTM grid zone 19 T: 274.50 E and 5100.30 N. Altitude: approx. 185 m.

Drift unit C: (3 subunits)	>4.6	>4.6
1) **Lodgement till** (0 - 1.4 m): Compact, massive, oxidized, brown, matrix-dominated, sandy diamicton. Sharp basal contact. Contains many Precambrian clasts. Boulders are more abundant near base of subunit.		
2) **Stratified drift - flow till assemblage** (1.4 - 2.2 m): Consists mainly of sub-stratified, brown, oxidized, matrix-supported, sandy diamicton containing numerous slightly deformed lenses and pods of stratified sand. In other parts of the exposure, this subunit consists of stratified gravelly sand and sand containing lenses of diamicton.		
3) **Lodgement till** (2.2 - 4.6 m): Very compact, fissile, brown, slightly calcareous, matrix-dominated, silty sand diamicton. Upper 30 cm contain sandy stringers that rise toward SE. Contains several Precambrian clasts. Base of unit not exposed.		
(Gravel pit floor)		

Unit	Thickness (m)	Depth of base (m)

Section MP-82-1 (Melbourne)

Borrow pit on east side of Highway #143, 1.6 km northwest (N 50° W) of 4-way intersection in Melbourne; Richmond map-area (31 H/9). UTM grid zone 18 T: 720.90 E and 5060.75 N. Altitude: approx. 122 m.

(Sediments disturbed by heavy machinery)	(0.5)	(0.5)
Varves (2 distinct thinning-and-fining-upwards sequences are present)	6.5	7.0
Sequence #2 (0.5 - 2.4 m): Consists of 23 couplets whose thickness decreases from 15 cm at the base to 2 cm at the top (upper 20 cm could not counted and may contain another 10 to 15 couplets). Thickness of thinly laminated clay (winter) layers decreases from 3 cm at the base to 1.5 cm at the top. Summer layers contain trace fossils (Paschichnia: grazing trace) and consist of graded-to-laminated, calcareous, silty sand in lower 10 couplets and of thinly laminated, calcareous, silt in upper 13 couplets.		
Sequence #1 (2.4 - 7.0 m): Consists of 33 couplets whose thickness decreases from 1.1 m in basal varve to 2.5 cm in couplet #33. Thickness of thinly laminated clay (winter) layers decreases upwards only slightly, from 3 cm in the 1.1 m-thick basal varve to 2 cm in upper couplets; sandy summer layer of varve #1 consist of several Bouma sequences (paleocurrent toward SE); subsequent summer layers consist of graded-to-laminated, calcareous, silty sand grading upwards into thinly laminated calcareous silt.		
Ice-contact stratified drift: Mainly plane-bedded gravel (best exposed in a contiguous gravel pit); collapsed bedding due to melting of buried ice blocks.	>2.0	>9.0
(Floor of borrow pit)		

Unit	Thickness (m)	Depth of base (m)

Section MP-79-10 (Rivière Danville)

Right bank of Rivière Danville, 9 km due north of 4-way intersection in Saint-Claude; Dudswell map-area (21 E/12). UTM grid zone 19T: 268.45 E and 5069.30 N. Altitude: approx. 200 m.

Glaciolacustrine sediments (2 subunits):	5.0	5.0
1) **Laminated sand (0 - 2.8 m)**: Plane- and cross-laminated, oxidized, buff, fine sand; a few silt layers in basal meter of unit.		
2) **Varves (2.8 - 5.0 m)**: Couplets consist of 2 to 3 cm-thick graded silt layers overlain by thin (1 to 2 cm-thick) fine clay layers; thinning-upwards sequence; lower couplets contain multiple graded silt layers, some of which have thin sandy partings. Slightly oxidized, brownish gray, non-calcareous.		
Drift unit C: **Lodgement till.** Compact, dark gray calcareous, matrix-dominated silty sand diamicton. Contains a few ultramafic clasts and several Precambrian clasts.	>7.0	>12.0
(River level)		

Unit	Thickness (m)	Depth of base (m)

Section MP-79-16 (Rivière Landry)

Right bank of Rivière Landry, in a sharp bend (meander), 1.2 km northwest (N 27° W) of 4-way intersection in Danville; Drummondville map-area (31 H/16). UTM grid zone 18 T: 730.75 E and 5075.40 N. Altitude: approx. 122 m.

Regressive sand (Champlain Sea): Mainly plane- and cross-bedded sand; overall fining-upwards sequence starting with pebble and cobble gravel at base; sharp, erosional basal contact. Oxidized unit; soil developped in upper meter of unit.	2.0	2.0
Marine silt (Champlain Sea): Mainly plane-laminated, unctuous, clayey silt; thin fine sand partings between depths of 8 and 6 m; above 6 m, sandy partings gradually thicken to form 2 to 3 cm-thick layers that are interbedded with 4 to 7 cm-thick silt layers near the top of unit; coarsening-and-thickening-upwards sequence. Unit contains a few ice-rafted pebbles, cobbles and boulders. Oxidized above a depth of 4.5 m, but gray and calcareous below that. Above a depth of 7.5 m, unit contains sparse shells of Macoma balthica in growth position; a few displaced valves of Hiatella arctica were also found between depths of 6 and 4 m.	8.0	10.0
Glaciolacustrine (Danville) varves: Silt and clay varves consisting of 103 couplets whose average thickness decreases from about 25 cm near the base of unit to about 2.5 cm near top. This thinning-upwards trend is predominantly recorded within summer layers which consist mainly of plane-laminated, light gray, calcareous, slightly bioturbated silt; a few thick (30 cm or more), contorted summer layers are present in lower 3.5 m of unit. Very fine sand partings, which occur in summer layers throughout the unit, contain trace fossils, mainly grazing traces (Psecichnia) but also occasional crawling traces (Bapichnia); rare current lineations, trending NW-SE, also occur within these partings. Feeding structures (Fodinichnia) are present within laminated silt layers above a depth of 15.5 m. Trace fossils are absent within winter layers which consist of thinly laminated or faintly laminated, stiff, dark gray, non calcareous clay and whose thickness only decreases from about 4 cm near the base of unit to about 1.5 cm near the top. The contact with the overlying marine silt is marked by a 15 cm-thick transition zone where a few non-varved graded silt and clay layers pass upward to thinly laminated silt and sand layers and hence to thinly laminated silt.	>9.0	>19.0

(River level; varves extend at least another 70 cm below river level)

Unit	Thickness (m)	Depth of base (m)

Section MP-79-13 (Warwick)

Gravel pit on east side of Highway #116, about 1.2 km southwest (N 202°) of 4-way intersection in Warwick; Drummondville map-area (31 H/16). UTM grid zone 18T: 732.40 E and 5091.70 N. Altitude: 137 ± 1 m.

(This measured section (subsection A) is located on the west flank of a buried esker ridge; subsection A, which is one of several subsections that were investigated in this gravel pit, contains the most complete stratigraphic record; see Figure 4-31).

Regressive marine sand (2 subunits)	7.0	7.0
1) Deltaic topset beds (0 - 0.9 m): Trough-cross-bedded pebbly sand; tabular unit with a sharp, erosional basal contact; soil zone.		
2) Deltaic foreset beds (0.9 - 7.0 m): Sandy foresets inclined at an angle of 27° toward NW; gradational basal contact; non-fossiliferous.		
(This unit is indirectly dated by the ^{14}C age (10 780 ± 190 BP, UQ- 289) of a shallow-water marine fauna (Hiatella arctica, Macoma balthica, Balanus crenatus, Mytilus edulis, Mya truncata ovata, in order of decreasing abundance) collected in wave-reworked, regressive sand and gravel in an adjacent subsection. See Figure 4.31).		
Marine silt Coarsening-and-thickening-upwards sequence consisting of fossiliferous plane-laminated clayey silt grading upward into laminated silt with minor sandy partings. Contains sparse shells of Macoma balthica in growth position. Contains a few dropstones.	2.5	9.5
Resedimented marine gravel and sand Stratified matrix-supported silty gravel with thin sandy interbeds. Contains a slightly displaced marine fauna consisting of Hiatella arctica (valves commonly unbroken and closed) and Balanus crenatus (several specimens unbroken and still attached to pebbles). Sharp basal contact. Interpreted as slightly wave-reworked esker sediments. ^{14}C-dated 11 700 ± 170 BP (I-13 342).	0.3	9.8
Esker sediments Tabular sets or broad trough sets of cross- and plane-bedded pebble gravel and pebbly sand; non-fossiliferous. Unit is best exposed in other parts of the gravel pit.	>4.0	>13.0
(Gravel pit floor)		

Unit	Thickness (m)	Depth of base (m)

Section MP-79-19 (Danville)

Gravel pit on west side of Highway #116, approximately 0.6 km south of 4-way intersection in Danville; Drummondville map-area (31 H/16). UTM grid zone 18T: 731.30 E and 5073.70 N. Altitude: 153 ± 1 m. (Delta of Rivière Landry into the Champlain Sea).

Topset gravel: Trough-cross-bedded pebbly gravel; erosional basal contact. Soil zone.	1.0	1.0
Foreset sand: Sandy foresets inclined at a shallow angle (10°) toward N; minor ripple-laminated sand in the lower meter of unit. Base of unit is gradational with underlying silts and is extensively loaded (ball-and-pillow structures); this loaded unit contains a slightly displaced (valves attached and mostly closed; periostracum present) molluscan fauna (Macoma balthica), dated 11 370 ± 200 BP (UQ-290).	3.0	4.0
Bottomset silt and sand: Coarsening-and-thickening-upwards sequence consisting of alternating silt and fine sand layers (rhythmites). Silt layers are between 2 and 15 cm-thick and commonly contain burrow pits (Domichnia) that were likely made by Macoma balthica; sparse shells of Macoma balthica in growth position are present in silt layers. Sand layers reach a thickness of up to 15 cm in the upper part of unit, but their thickness decreases gradually downward; only sandy partings are present in the lower 2 m.	>8.0	>12.0

(Base of section; road level)

Unit	Thickness (m)	Depth of base (m)

Section MP-81-1 (Ascot River I)

Right bank of Ascot River, 3.4 km due west of 3-way intersection in Johnville and 6.2 km southeast (N 128°) of 4-way intersection in Lennoxville; Sherbrooke map-area (21 E/5). UTM grid zone 19 T: 281.05 E and 5023.35 N. Altitude: approx. 220 m.

(This section was designated by McDonald and Shilts (1971) as the type section for Lennoxville Till, Chaudière Till and Massawippi Formation and as a reference section for the Gayhurst Formation; the section was originally described in McDonald (1967a) where it was labelled M-64-3).

Fluvial gravel: Trough-cross-bedded gravel and sand; contains ultramafic and Precambrian clasts. Oxidized; soil zone in upper 90 cm.	2.5	2.5
Lacustrine sediments: Laminated clayey silt; a 20 cm-thick layer of massive sand is present at the base of unit. Gray and calcareous.	0.9	3.4
Lennoxville Till (2 subunits)	7.3	10.7

1) **Lodgement till (3.4 - 8.2 m)**: Compact, fissile, gray, calcareous, matrix-dominated, sandy silt diamicton. Upper 0.5 m slightly oxidized. Contains Precambrian and ultramafic clasts. Erosional basal contact.

2) **Lodgement till/local facies (8.2 - 10.7 m)**: Compact, gray to olive gray, calcareous, mainly matrix-dominated, diamicton; includes a 1 m-thick bouldery zone; lower meter of unit shows distinct textural layering and contains abundant sheared lenses of silt and sand that are presumably derived from the Gayhurst Formation. Except in bouldery zone, diamicton is matrix-dominated; matrix texture varies from clayey to sandy. Erosional basal contact.

(continued next page)

Unit	Thickness (m)	Depth of base (m)
MR-81-1 (continued)		
Gayhurst Formation (2 subunits)	6.7	17.4
1) Laminated sandy silt (10.7 - 12.6 m): Compact, plane-laminated sandy silt; coarsening upwards. Upper 70 cm are intensely deformed and contain contorted black lenses (disseminated sulfides?). Lower part of unit is also slightly oxidized (yellowish brown, slightly calcareous) and contains sparse pebbles (dropstones?). Base of unit consists of a 30 cm-thick layer of matrix-supported silty diamicton. Sharp basal contact. Lacustrine sediment.		
2) Laminated clayey silt (12.6 - 17.4 m): Compact, gray to olive gray, calcareous, laminated clayey silt; laminae are faintly graded; fining-upwards sequence. Upper 2.5 m contain several black organic stringers; convolute lamination in lower 1.5 m. Ice-rafted clasts (granules, small pebbles) are present throughout the unit. Lacustrine sediment.		
Chaudière Till: Compact to very compact, fissile, gray, calcareous, generally matrix-dominated, sandy silt diamicton. Unit is dark gray-brown immediately above Massawippi Formation and contains sheared lenses of silt and silty sand. Contains thin (10 - 20 cm) pebbly layers at depths of 20.8 and 31.2 m; boulder zones at depths of 23.2, 26.5 and 28.3 m. Light-gray granodiorite clasts are present throughout unit; no Precambrian clasts were found; only a few ultramafic clasts were found in upper 3 m.	16.3	33.7
Massawippi Formation: Compact, olive, non calcareous, laminated silt and sandy silt; vivianite present in organic-rich (disseminated plant fragments) sandy layers; oxidized along joints; minor thrust faults striking N 144° and dipping 28° toward NE. Plant material dated >54 000 BP (Y-1683; in McDonald, 1967a). Lacustrine sediment.	>1.8	>35.5
(River level: McDonald (1967a) reports that two boreholes penetrated another 3 m into Massawippi Fm prior to striking bedrock)		

Unit	Thickness (m)	Depth of base (m)

Section MP-82-3 (Ascot River II)

Left bank of Ascot River, about 200 m downstream from MP-81-1, Sherbrooke map-area (21 E/5). UTM grid zone 19T: 280.85 E and 5023.15 N. Altitude: approx. 195 m.

(This section was designated by McDonald and Shilts (1971) as the type section for Johnville Till and pre-Johnville sediments; this section was originally described by McDonald (1967a) where it was labelled M-64-49. As a result of a flood during the fall of 1982, the section became well exposed; 4 subsections were investigated; basic descriptions are given for subsection A, along with notes on subsections B, C and D.)

Fluvial sediments (2 subunits underlie a 5 m-high post-glacial fluvial terrace)	2.1	2.1
1) Sand and silt (0 – 1.5 m): Mainly plane-bedded sand and silt; commonly vaguely stratified; contains sparse pebbles; oxidized. Interpreted as a flood plain deposit.		
2) Cobble gravel (1.5 – 2.1 m): Crudely bedded, mainly clast-supported, cobble gravel; oxidized. Sharp, erosional basal contact. Interpreted as a channel lag deposit.		
Chaudière Till: Compact, fissile, olive gray to olive, non calcareous, matrix-supported, sandy silt diamicton. Contains a sheared lens (up to 30 cm-thick) of organic-bearing sandy silt (Massawippi Fm); sand laminae are oxidized at the surface of the exposure but not inwards. Below silt lens, diamicton is oxidized (bright red-orange) along fissility planes but is olive away from them; rusty coatings "intersect" pebbles; post-depositional groundwater oxidation. Directly overlies "oxidized" gravel in subsection C. Erosional basal contact.	2.6	4.7
Massawippi Formation: Compact, olive, non calcareous, laminated silt and fine sand; contains finely divided organics. Unit reaches a thickness of 1.3 m at west end of exposure (subsection D). Lacustrine sediment.	0.2	4.9
Oxidized fluvial gravel: Compact, cemented (mainly by bright red-orange oxide), clast-supported cobble gravel; imbrication dips toward east; locally, cement consists of black (Mn?) oxide. In subsection D, a bed of gray silty sand is overlain and underlain by "oxidized" gravel. Groundwater oxidation. Unit contains Precambrian clasts.	>0.8	>5.7
(River level: gravel unit extends at least another 60 m below river level)		

APPENDIX II

RESULTS OF TILL CLAST FABRIC MEASUREMENTS

The first part of Appendix I consists of contoured clast fabric stereograms (Figures A-1 through A-13). Field data (azimuth and plunge of clast A- and C-axes) were contoured with the help of a computer program written by Starkey (1970). The stereograms are grouped according to sections and units described in Appendix I.

The second part of this appendix consists of a listing of eigenvectors and eigenvalues (Table A-1) obtained by a computer program written by Mark (1973).

FT-29A NORBESTOS/79-18A- 1.4M (N=50)

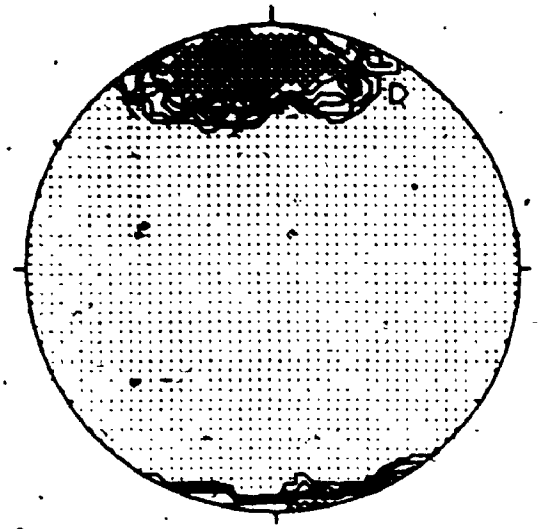

CONTOURED AT 1 2 3 4 5

POINTS PER 2.0 % AREA

FT-29C NORBESTOS/79-18A- 1.4M (N=38)

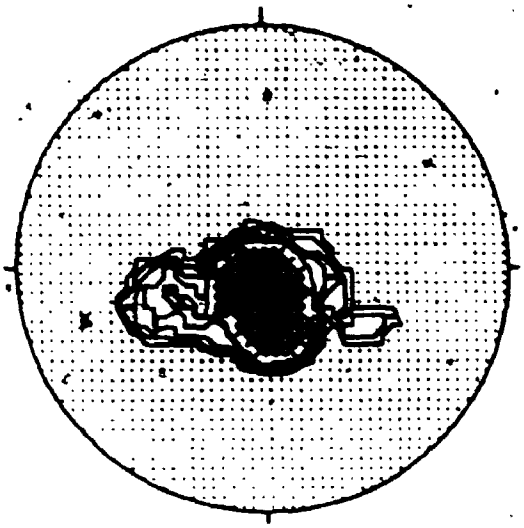

CONTOURED AT 1 2 3 4 5

POINTS PER 2.6 % AREA

FT-31A NORBESTOS/79-18B- 1.7M (N=50)

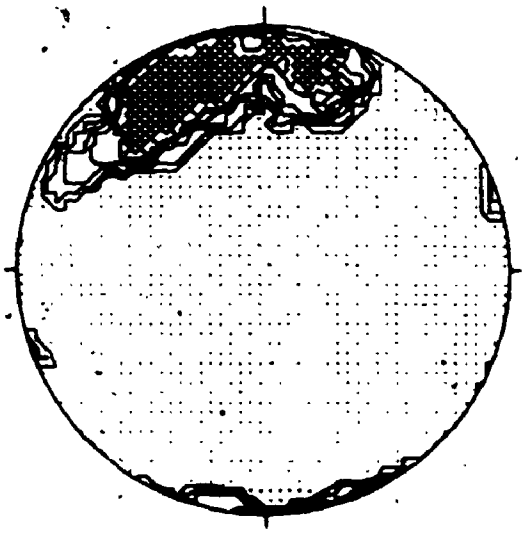

CONTOURED AT 1 2 3 4 5

POINTS PER 2.0 % AREA

FT-31C NORBESTOS/79-18B- 1.7M (N=35)

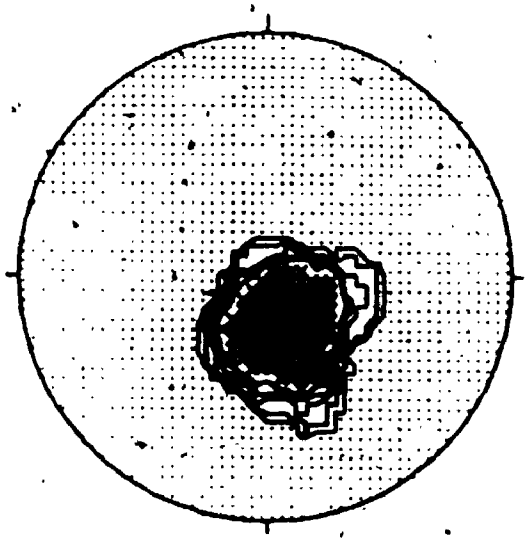

CONTOURED AT 1 2 3 4 5

POINTS PER 2.9 % AREA

Figure A-1: Contoured clast fabric stereograms, drift unit C, Norbestos section (MP-79-18). (continued next page)

FT-25A NORBESTOS/79-18C- 6.0M (N=50)

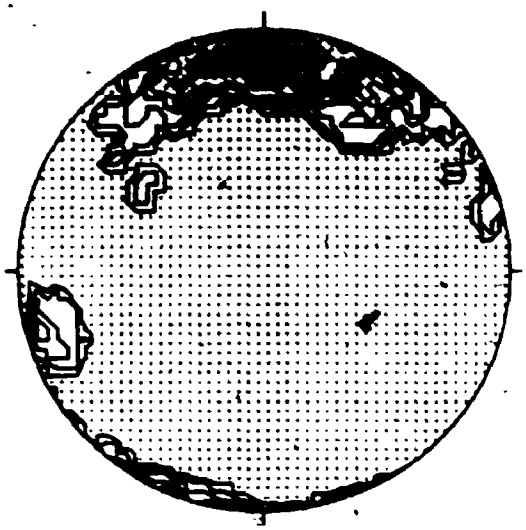

CONTOURED AT 1 2 3 4 5

POINTS PER 2.0 % AREA

FT-25C NORBESTOS/79-18C- 6.0M (N=29)

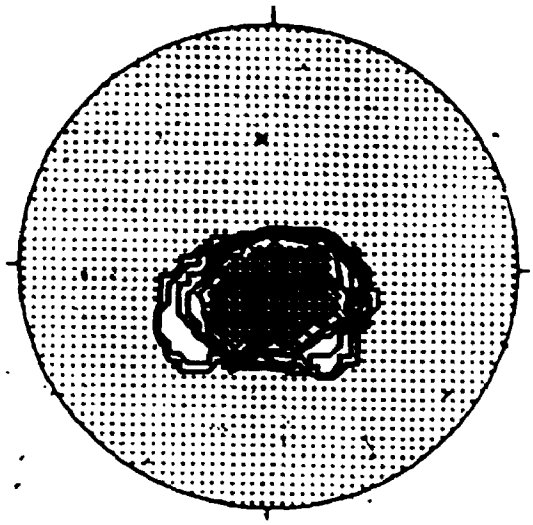

CONTOURED AT 1 2 3 4 5

POINTS PER 3.4 % AREA

Figure A-1 (continued)

FT-26A NORBESTOS/79-18B- 8.0M (N=25)

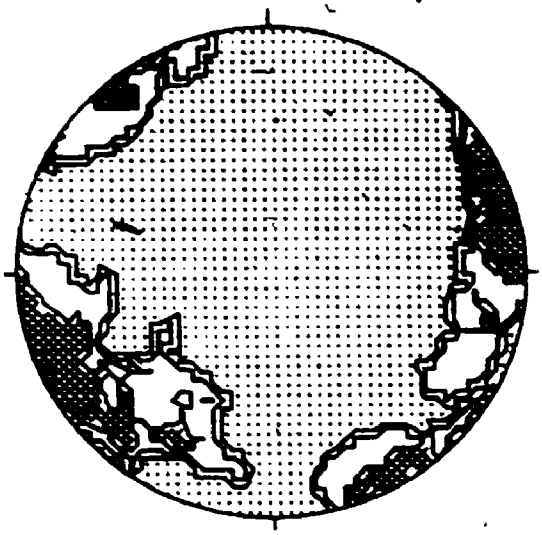

CONTOURED AT 1 2 3 POINTS PER 4.0 % AREA

FT-26C NORBESTOS/79-18B- 8.0M (N=20)

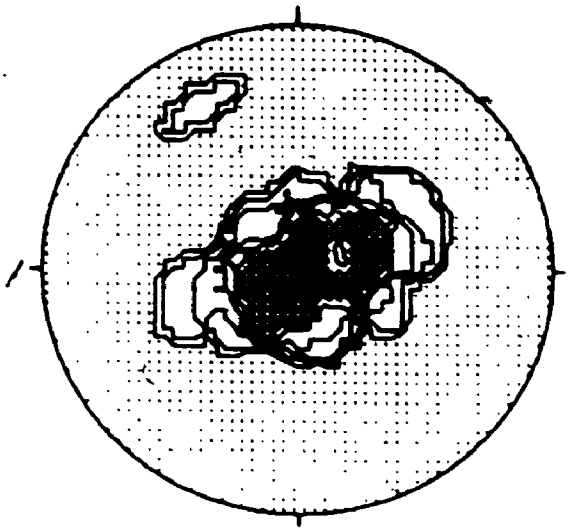

CONTOURED AT 1 2 3 4 5
POINTS PER 5.0 % AREA

FT-27A NORBESTOS/79-18B- 14.0M (N=50)

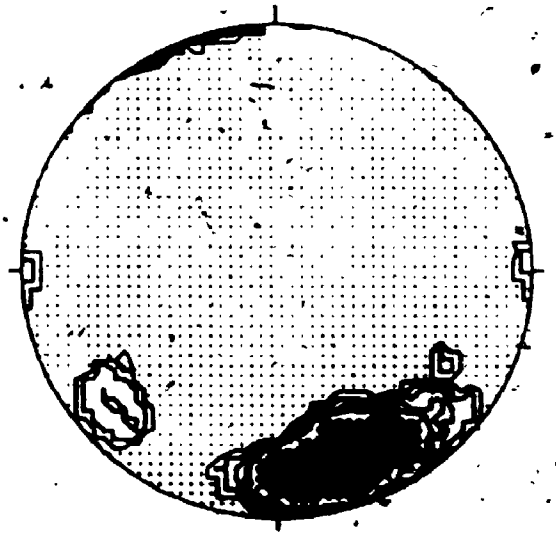

CONTOURED AT 1 2 3 4 5
POINTS PER 2.0 % AREA

FT-27C NORBESTOS/79-18B- 14.0M (N=35)

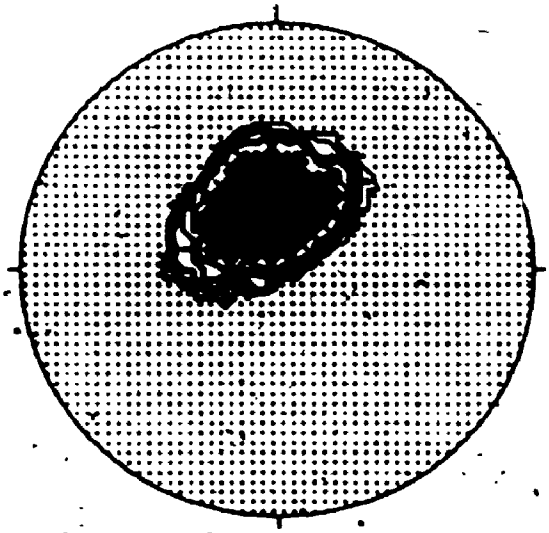

CONTOURED AT 1 2 3 4 5
POINTS PER 2.9 % AREA

Figure A-2: Contoured clast fabric stereograms, unit B and drift unit A, Norbestos subsection B (MP-79-18B).

FT-22A NORBESTOS/79-18C- 0.2M (N=50)

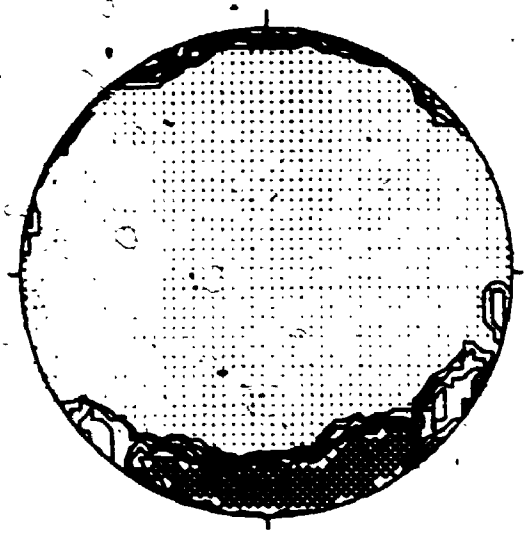

CONTOURED AT 1 2 3 4 5

POINTS PER 2.0 % AREA

FT-22C NORBESTOS/79-18C- 0.2M (N=38)

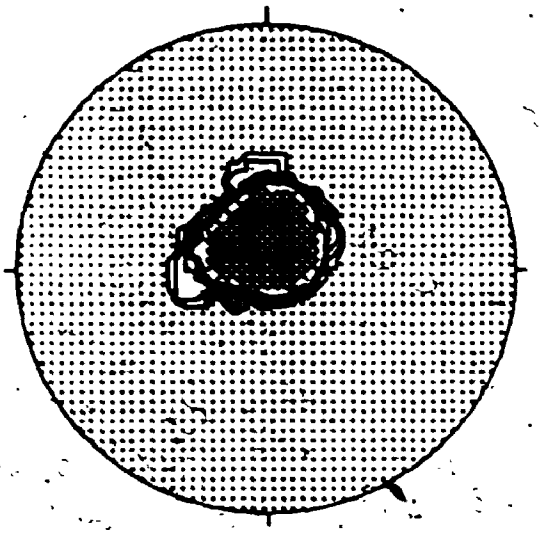

CONTOURED AT 1 2 3 4 5

POINTS PER 2.6 % AREA

FT-23A NORBESTOS/79-18C- 11.2M (N=50)

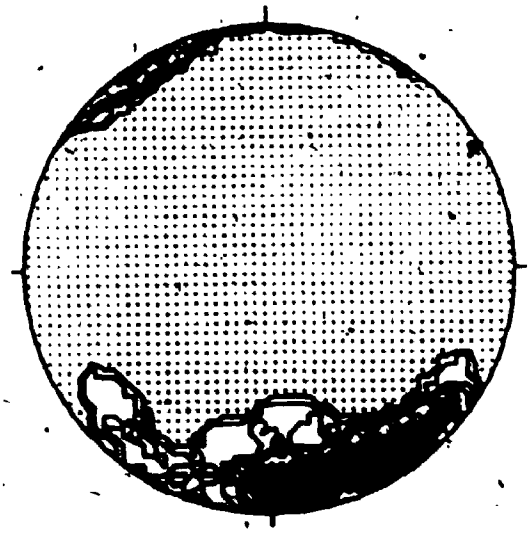

CONTOURED AT 1 2 3 4 5

POINTS PER 2.0 % AREA

FT-23C NORBESTOS/79-18C- 11.2M (N=37)

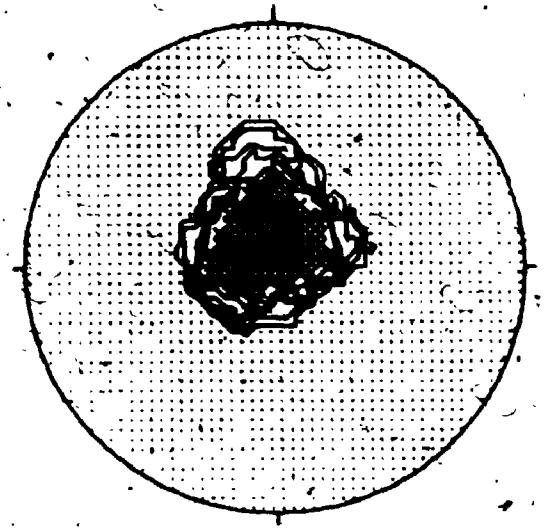

CONTOURED AT 1 2 3 4 5

POINTS PER 2.7 % AREA

Figure A-3: Contoured clast fabric stereograms; drift unit A, Norbestos subsection C (MP-79-18C). (continued next page)

FT-24A NORBESTOS/79-18C- 12.0M (N=50)

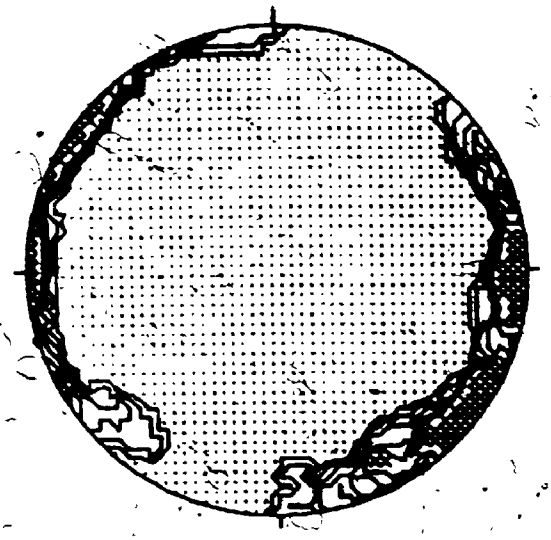

CONTOURED AT 1 2 3 4 5

POINTS PER 2.0 % AREA

FT-24C NORBESTOS/79-18C- 12.0M (N=34)

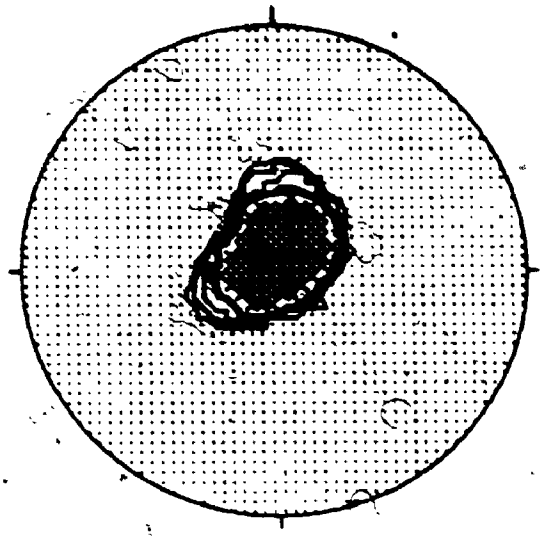

CONTOURED AT 1 2 3 4 5

POINTS PER 2.0 % AREA

FT-30A NORBESTOS/79-18C- 13.5M (N=50)

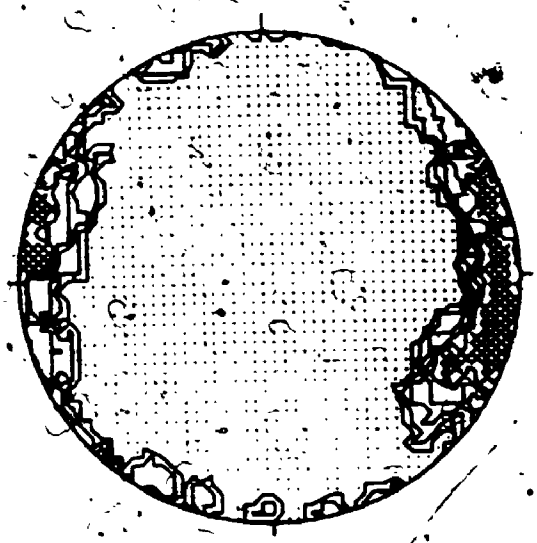

CONTOURED AT 1 2 3 4 5

POINTS PER 2.0 % AREA

FT-30C NORBESTOS/79-18C- 13.5M (N=30)

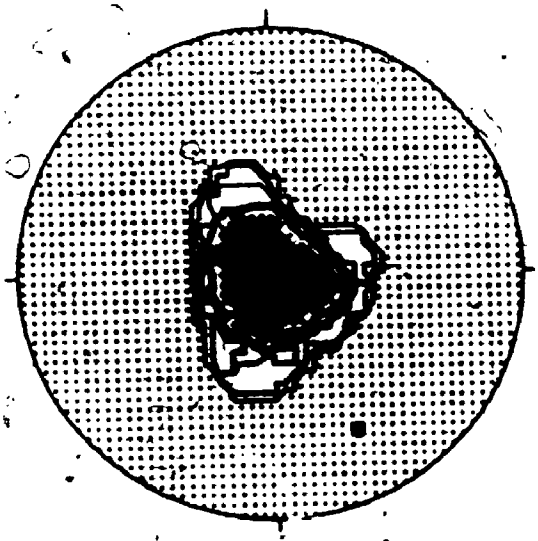

CONTOURED AT 1 2 3 4 5

POINTS PER 2.0 % AREA

Figure A-3 (continued)

FT-47A RIV-DES-ROSIERS/79-9+ 2.0M (N=50)

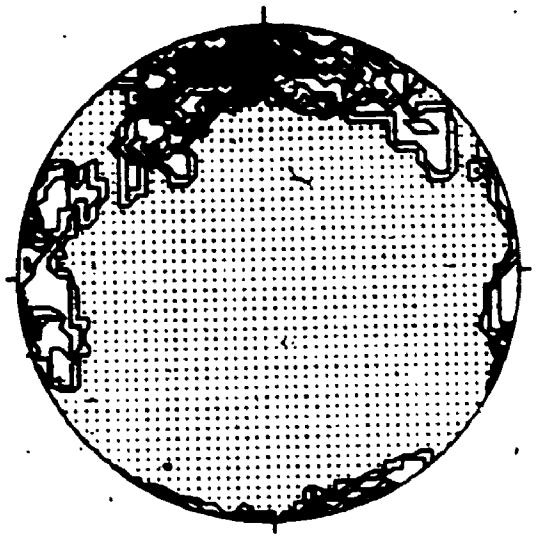

CONTOURED AT 1 2 3 4 5

POINTS PER 2.0 % AREA

FT-47C RIV-DES-ROSIERS/79-9+ 2.0M (N=46)

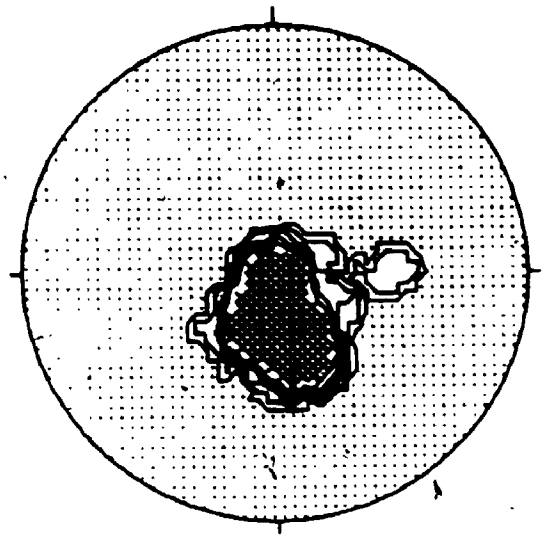

CONTOURED AT 1 2 3 4 5

POINTS PER 2.2 % AREA

FT-46A RIV-DES-ROSIERS/79-9+ 5.2M (N=50)

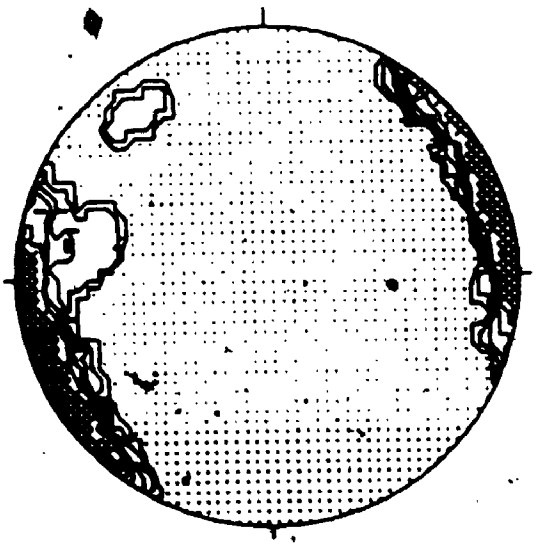

CONTOURED AT 1 2 3 4 5

POINTS PER 2.0 % AREA

FT-46C RIV-DES-ROSIERS/79-9+ 5.2M (N=38)

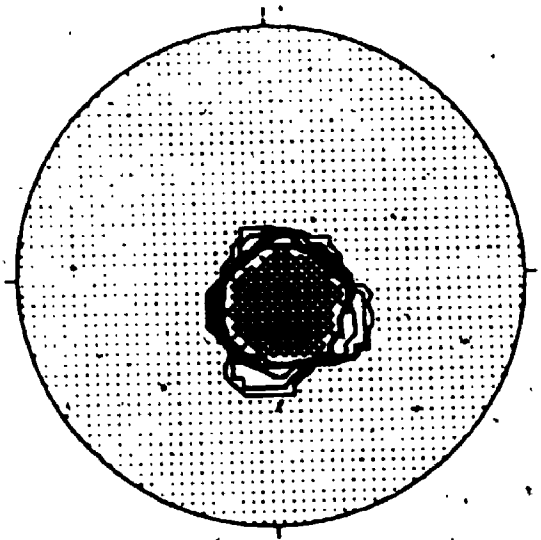

CONTOURED AT 1 2 3 4 5

POINTS PER 2.6 % AREA

Figure A-4: Contoured clast fabric stereograms, drift unit C, Rivière des Rosiers section (MP-79-9).

FT-45A RIV-DES-ROSIERS/79-9- 11.5M (N=50)

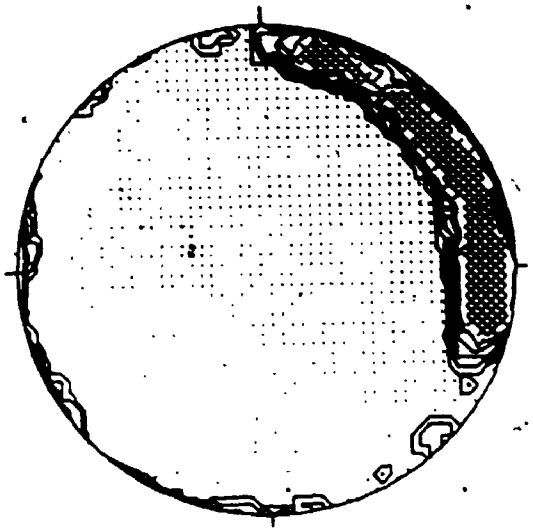

CONTOURED AT 1 2 3 4 5

POINTS PER 2.0 % AREA

FT-45C RIV-DES-ROSIERS/79-9- 11.8M (N=40)

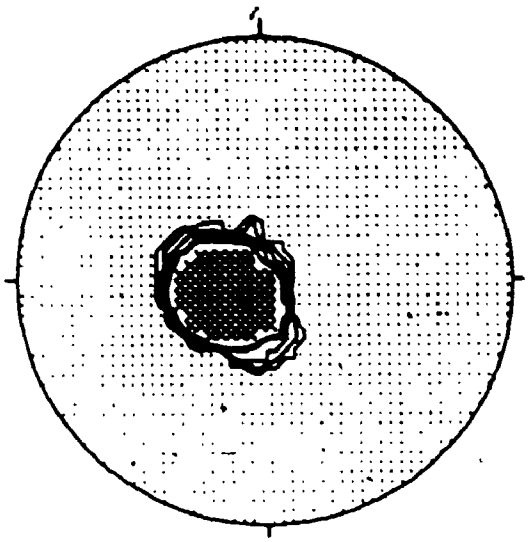

CONTOURED AT 1 2 3 4 5

POINTS PER 2.5 % AREA

FT-44A RIV-DES-ROSIERS/79-9- 9.4M (N=50)

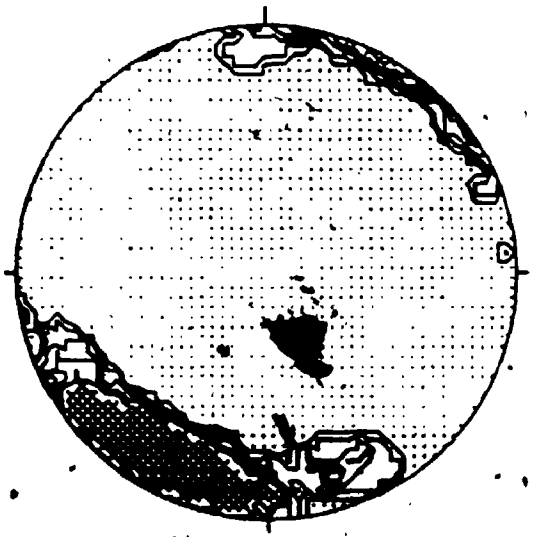

CONTOURED AT 1 2 3 4 5

POINTS PER 2.0 % AREA

FT-44C RIV-DES-ROSIERS/79-9- 9.4M (N=34)

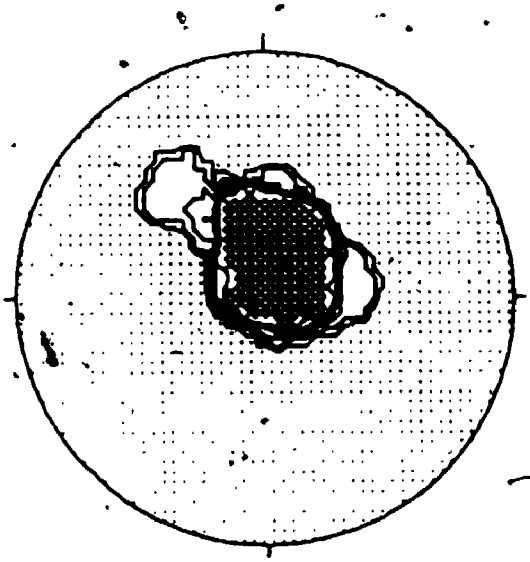

CONTOURED AT 1 2 3 4 5

POINTS PER 2.9 % AREA

Figure A-5: Contoured clast fabric stereograms, drift unit A, Rivière des Rosiers section (MP-79-9).

FT-16A WILLOW BR/MP-76-11 1.5M (N=50)

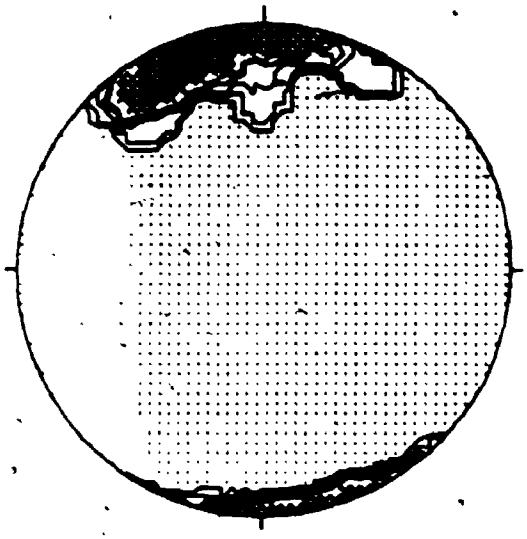

CONTOURED AT 1 2 3 4 5

POINTS PER 2.0 % AREA

FT-16C WILLOW BR/MP-76-11 1.5M (N=30)

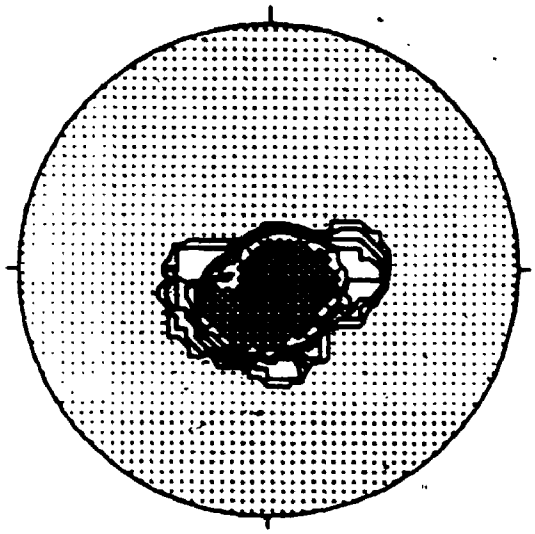

CONTOURED AT 1 2 3 4 5

POINTS PER 2.6 % AREA

FT-48A WILLOW BR / 76-1- 12.3M (N=50)

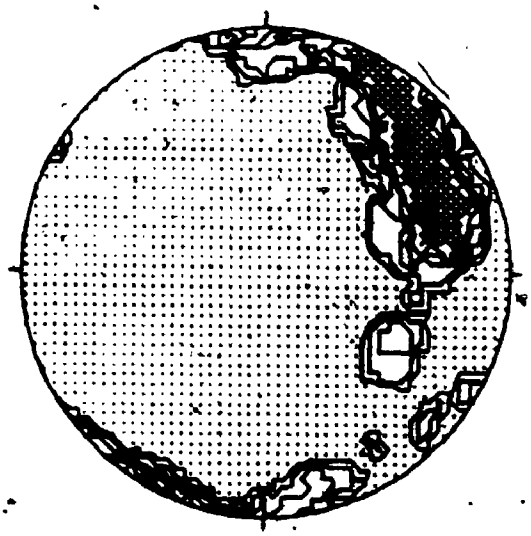

CONTOURED AT 1 2 3 4 5

POINTS PER 2.0 % AREA

FT-48C WILLOW BR / 76-1- 12.3M (N=29)

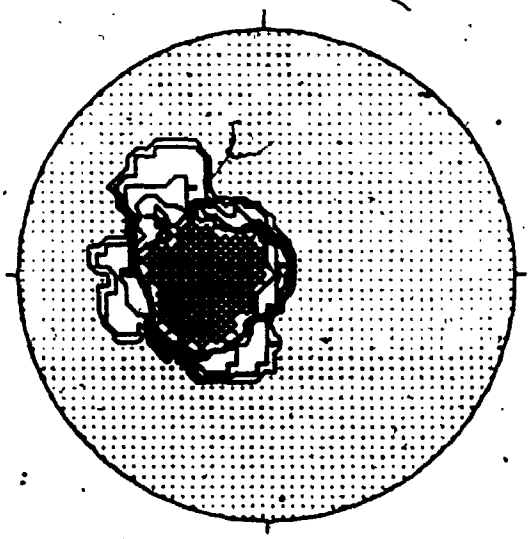

CONTOURED AT 1 2 3 4 5

POINTS PER 3.4 % AREA.

Figure A-6: Contoured clast fabric stereograms, drift units C and A, Willow Brook section (MP-76-1).

FT-20A SCOTCH RD/79-1- 3.7M (N=50)

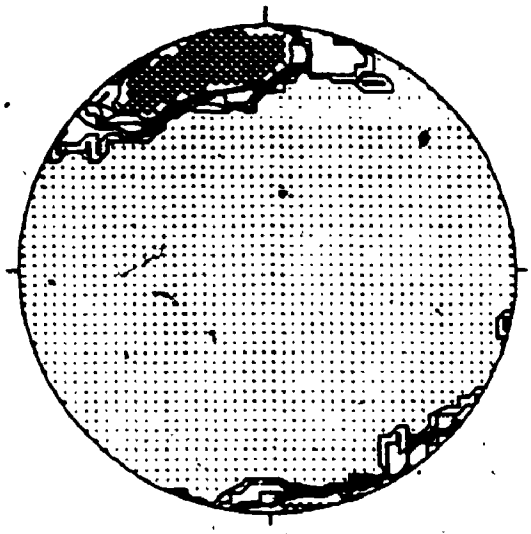

CONTOURED AT 1 2 3 4 5

POINTS PER 2.0 % AREA

FT-20C SCOTCH RD/79-1- 3.7M (N=41)

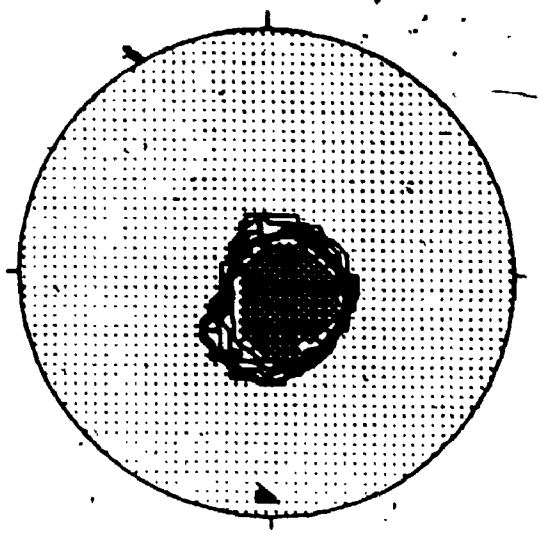

CONTOURED AT 1 2 3 4 5

POINTS PER 2.4 % AREA

FT-19A SCOTCH RD/79-1- 5.5M (N=50)

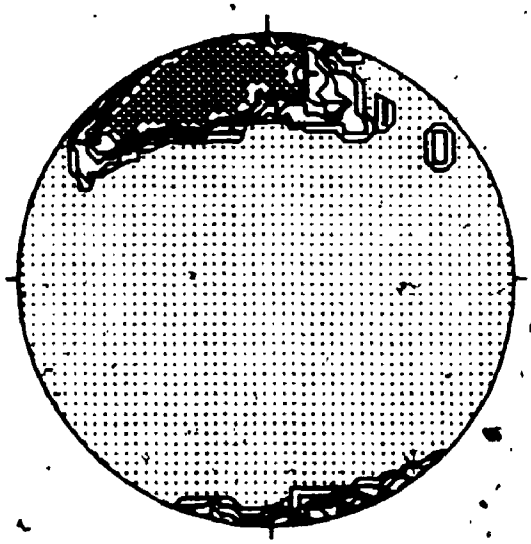

CONTOURED AT 1 2 3 4 5

POINTS PER 2.0 % AREA

FT-19C SCOTCH RD/79-1- 5.5M (N=47)

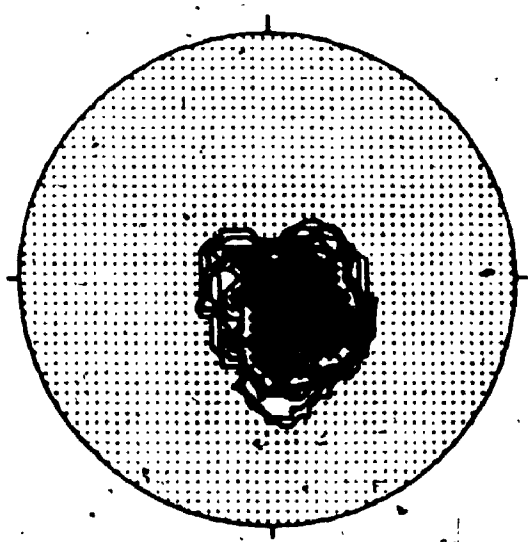

CONTOURED AT 1 2 3 4 5

POINTS PER 2.1 % AREA

Figure A-7: Contoured clast fabric stereograms, drift units C and A, Chemin des Ecossais section (MP-79-1).

FT-32A TINGWICK/79-15- 5.75M (N=50)

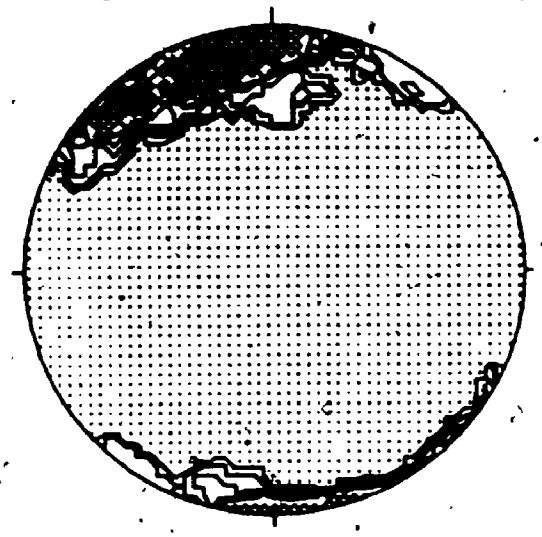

CONTOURED AT 1 2 3 4 5

POINTS PER 2.0 % AREA

FT-32C TINGWICK/79-15- 5.75M (N=43)

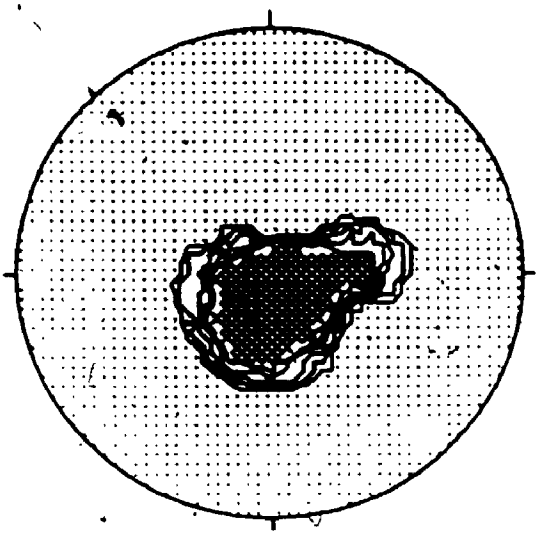

CONTOURED AT 1 2 3 4 5

POINTS PER 2.3 % AREA

FT-50A RIVIERE NOIRE/82-4: 23.4M (N=40)

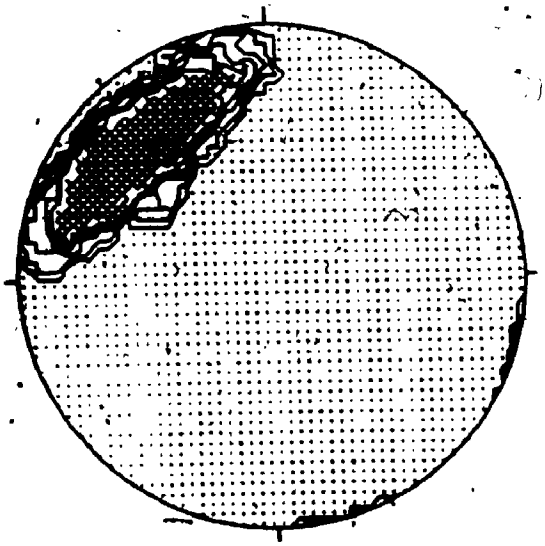

CONTOURED AT 1 2 3 4 5

POINTS PER 2.5 % AREA

FT-50C RIVIERE NOIRE/82-4: 23.4M (N=25)

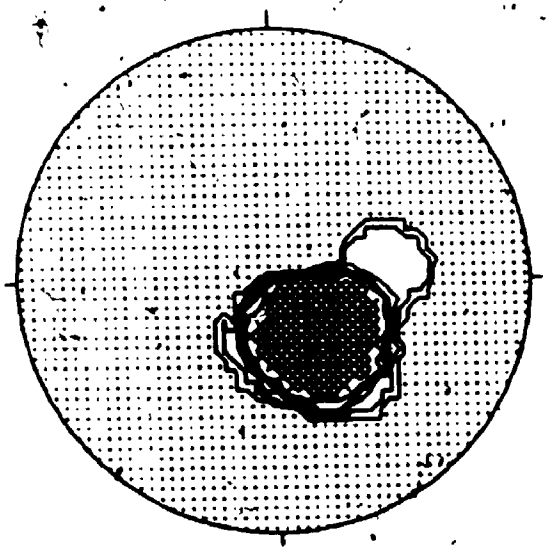

CONTOURED AT 1 2 3 4 5

POINTS PER 4.0 % AREA

Figure A-8: Contoured clast fabric stereograms, drift unit C (Tingwick / MP-79-15) and drift unit A (Rivière Noire /MP-82-4).

FT-21A WOTTON/79-5- 1.4-2.0M (N=50)

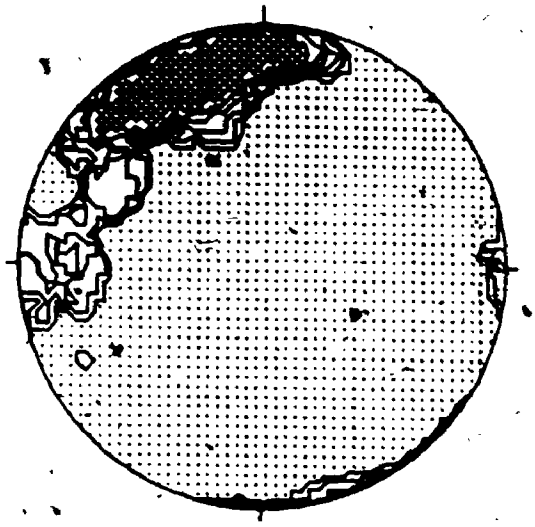

CONTOURED AT 1 2 3 4 5

POINTS PER 2.0 % AREA

FT-21C WOTTON/79-5- 1.4-2.0M (N=33)

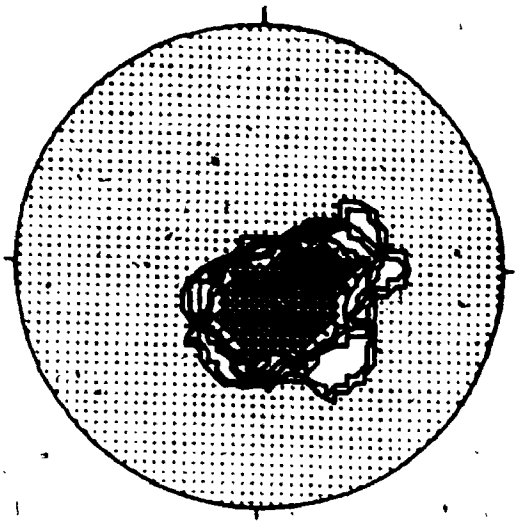

CONTOURED AT 1 2 3 4 5

POINTS PER 3.0 % AREA

WOTTON/79-5- POLES/THRUST FAULTS (N=40)

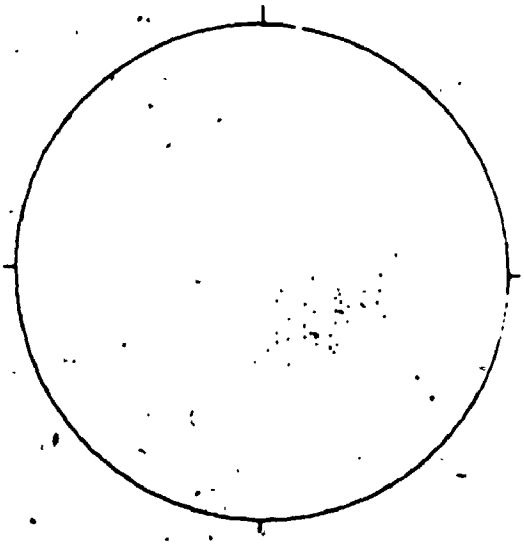

WOTTON/79-5- POLES/THRUST FAULTS (N=40)

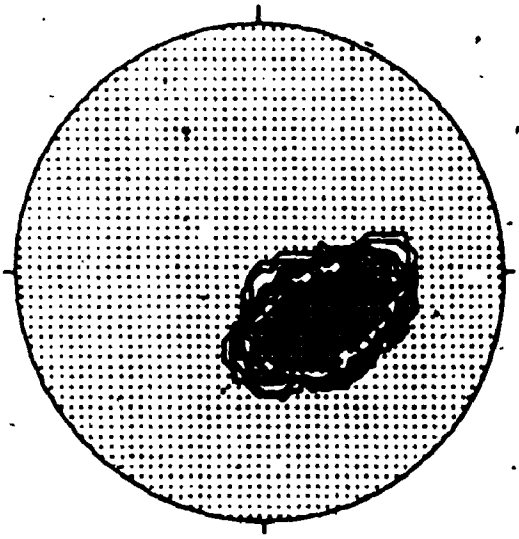

CONTOURED AT 1 2 3 4 5

POINTS PER 2.5 % AREA

Figure A-9: Contoured stereograms, till clast fabric (drift unit C) and subtill thrust faults, Wotton section (MP-79-5).

FT-34A N-D DE HAM/79-17- 2.6M (N=50)

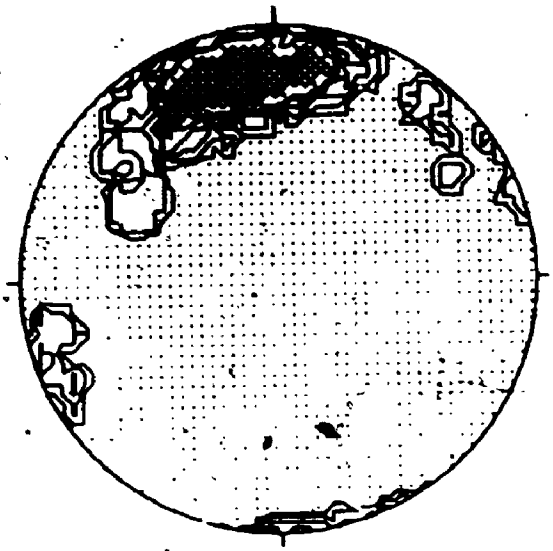

CONTOURED AT 1 2 3 4 5

POINTS PER 2.0 % AREA

FT-34C N-D DE HAM/79-17- 2.6M (N=34)

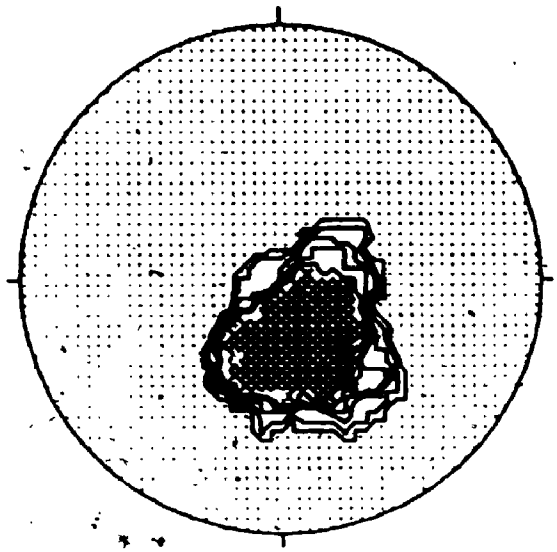

CONTOURED AT 1 2 3 4 5

POINTS PER 2.9 % AREA

FT-33A N-D DE HAM/79-17- 5.5M (N=50)

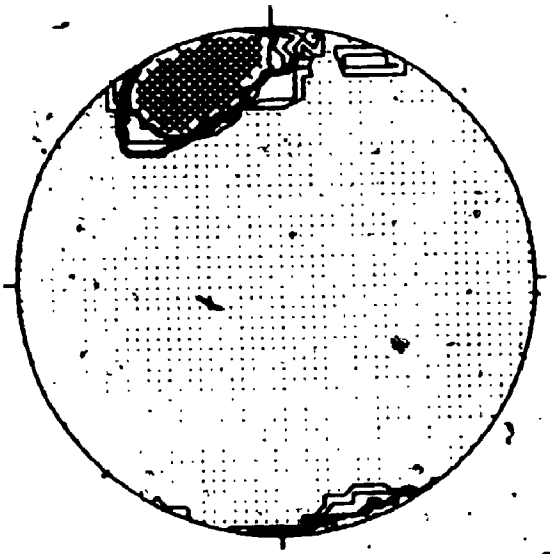

CONTOURED AT 1 2 3 4 5

POINTS PER 2.0 % AREA

FT-33C N-D DE HAM/79-17- 5.5M (N=38)

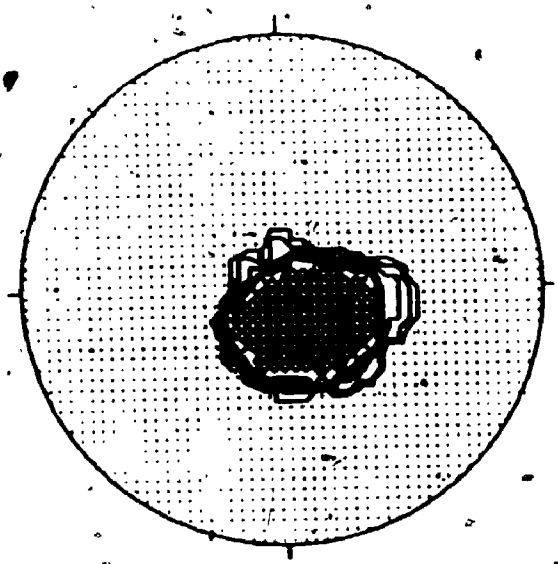

CONTOURED AT 1 2 3 4 5

POINTS PER 2.6 % AREA

Figure A-10: Contoured clast fabric stereograms, drift unit C, Notre-Dame-de-Ham section (MP-79-17).

FT-36A ARTHABASCA/79-14- 1.1M (N=50)

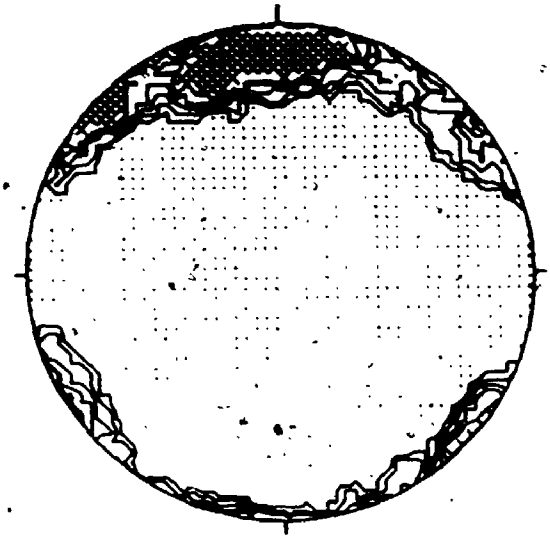

CONTOURED AT 1 2 3 4 5

POINTS PER 2.0 % AREA

FT-36C ARTHABASCA/79-14- 1.1M (N=31)

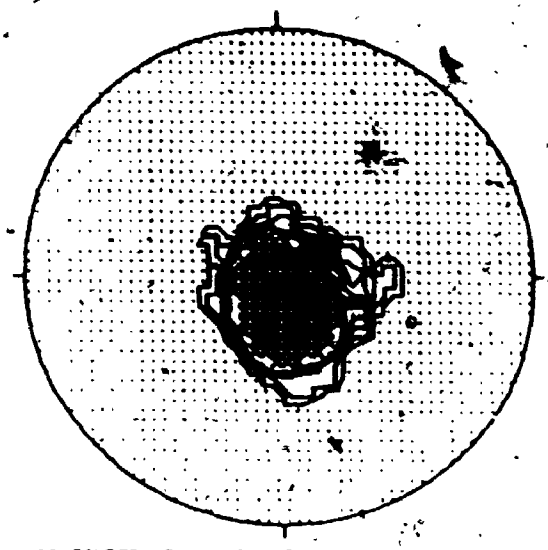

CONTOURED AT 1 2 3 4 5

POINTS PER 3.2 % AREA

FT-35A ARTHABASCA/79-14- 4.0M (N=50)

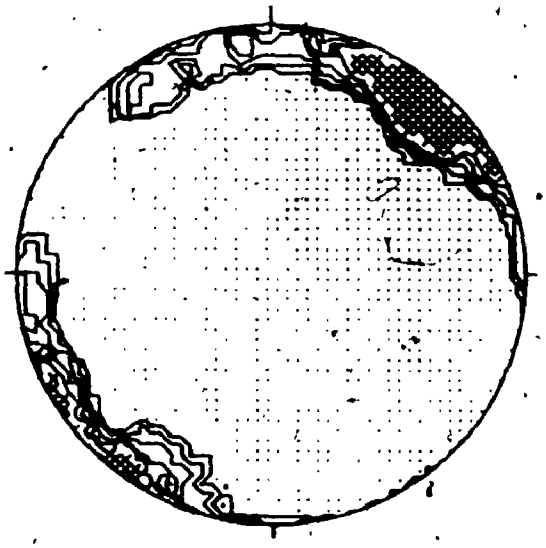

CONTOURED AT 1 2 3 4 5

POINTS PER 2.0 % AREA

FT-35C ARTHABASCA/79-14- 4.0M (N=36)

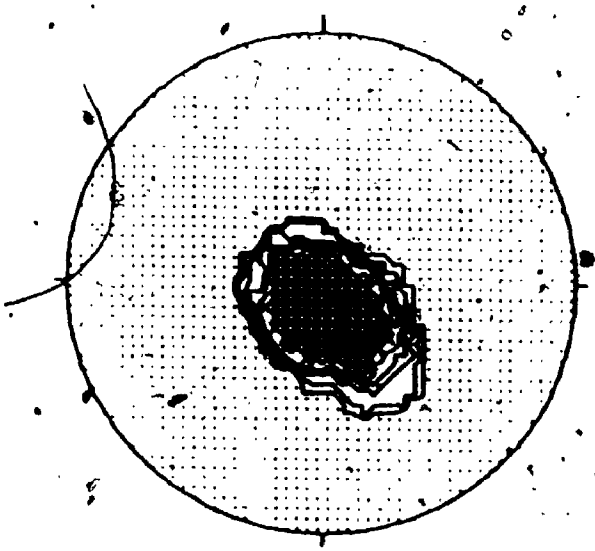

CONTOURED AT 1 2 3 4 5

POINTS PER 2.8 % AREA

Figure A-11: Contoured [illegible]st fabric stereograms, drift unit C, Arthabasca section ([illegible]79-14).

FT-43A ASCOT RIVER/81-1- 5.0M (N=50)

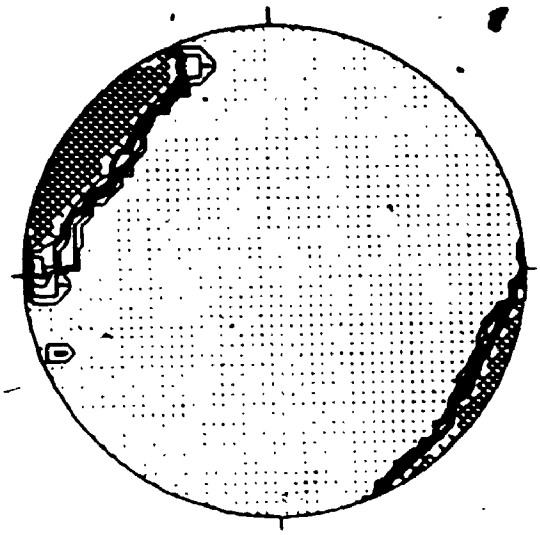

CONTOURED AT 1 2 3 4 5

POINTS PER 2.0 % AREA

FT-43C ASCOT RIVER/81-1- 5.0M (N=40)

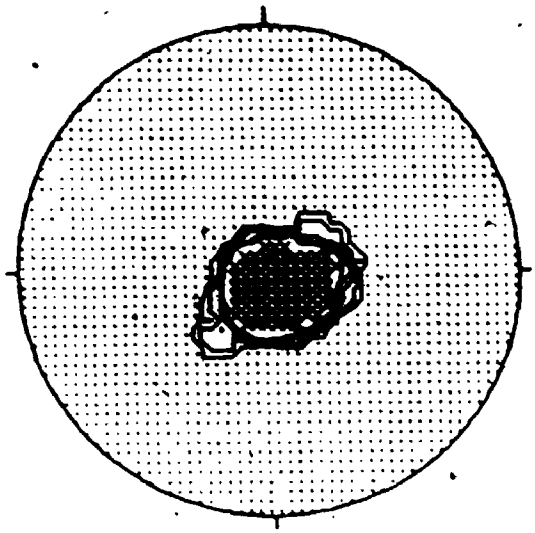

CONTOURED AT 1 2 3 4 5

POINTS PER 2.5 % AREA

FT-41A ASCOT RIVER/81-1- 8.3M (N=50)

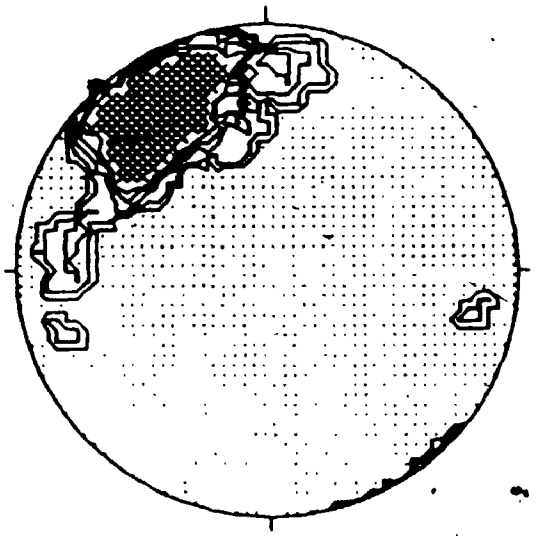

CONTOURED AT 1 2 3 4 5

POINTS PER 2.0 % AREA

FT-41C ASCOT RIVER/81-1- 8.3M (N=32)

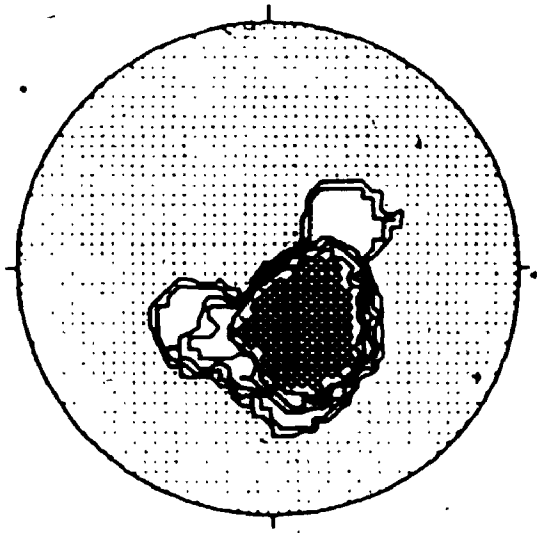

CONTOURED AT 1 2 3 4 5

POINTS PER 3.1 % AREA

Figure A-12: Contoured clast fabric stereograms, Lennoxville Till, Ascot River I section (MP-81-1).

FT-38A ASCOT RIVER/81-1+ 19.8M (N=50)

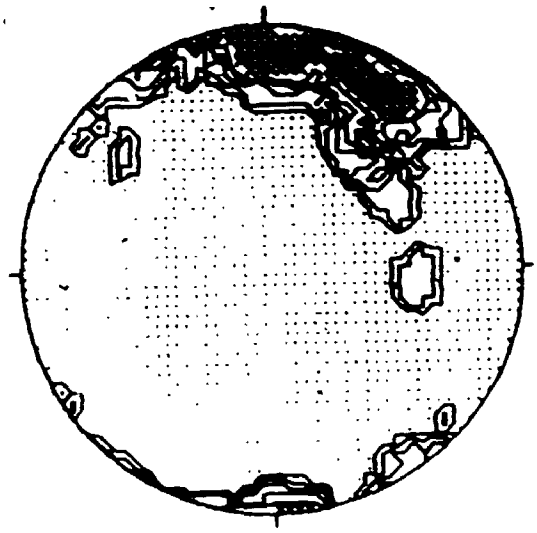

CONTOURED AT 1 2 3 4 5

POINTS PER 2.0 % AREA

FT-38C ASCOT RIVER/81-1+ 19.8M (N=35)

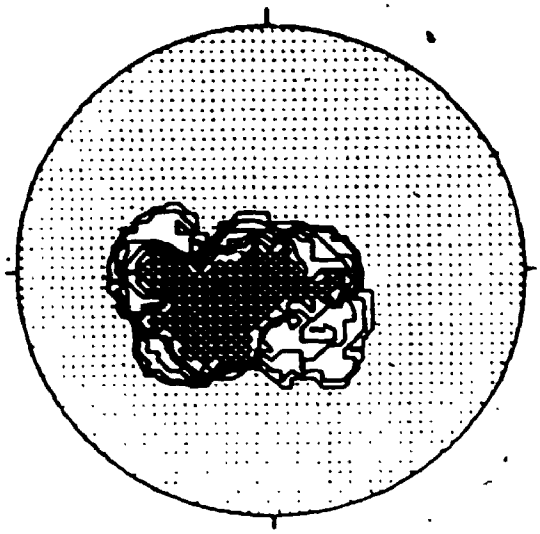

CONTOURED AT 1 2 3 4 5

POINTS PER 2.9 % AREA

FT-39A ASCOT RIVER/81-1+ 22.6M (N=50)

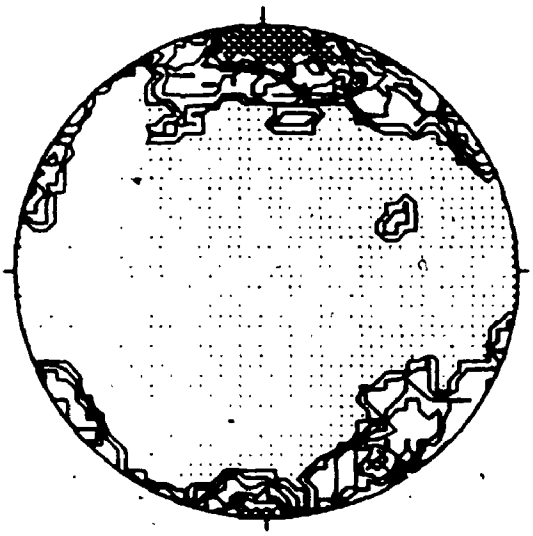

CONTOURED AT 1 2 3 4 5

POINTS PER 2.0 % AREA

FT-39C ASCOT RIVER/81-1+ 22.6M (N=40)

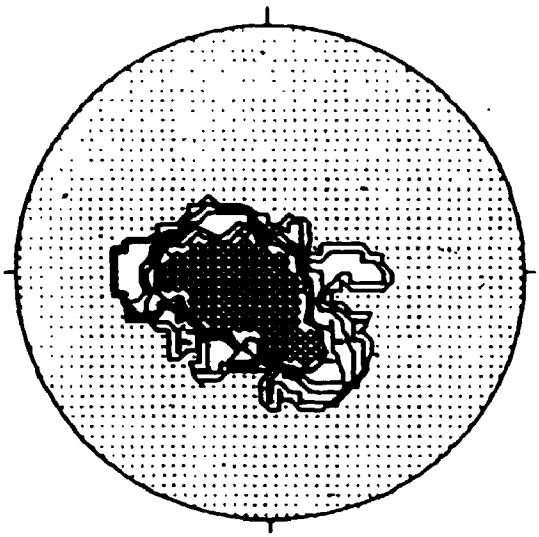

CONTOURED AT 1 2 3 4 5

POINTS PER 2.5 % AREA

Figure A-13: Contoured clast fabric stereograms, Chaudière Till, Ascot River I and II sections (MP-81-1 and MP-82-3). (continued next page)

FT-37A ASCOT RIVER/81-1+ 24.9M (N=50)

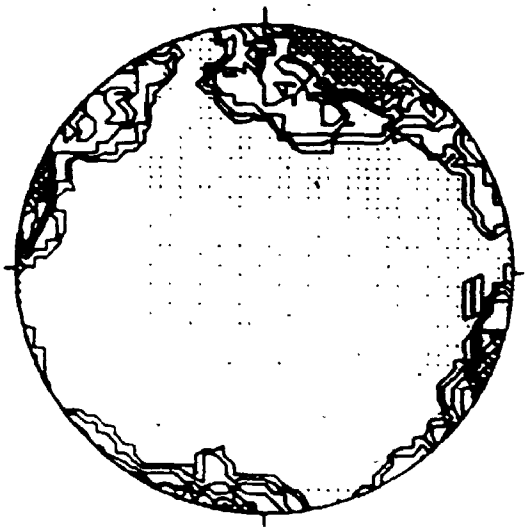

CONTOURED AT 1 2 3 4 5

POINTS PER 2.0 % AREA

FT-37C ASCOT RIVER/81-1+ 24.9M (N=96)

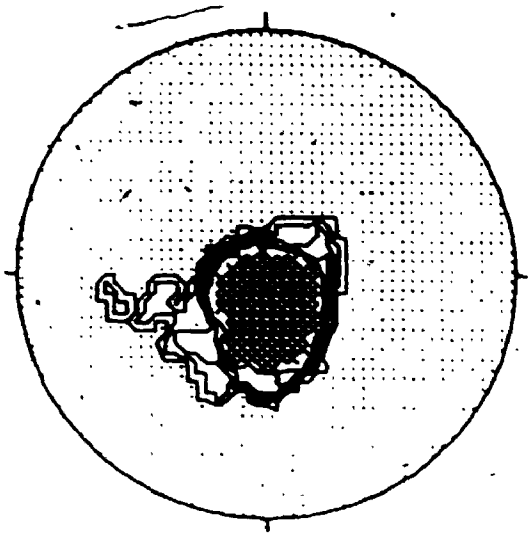

CONTOURED AT 1 2 3 4 5

POINTS PER 2.0 % AREA

FT-40A ASCOT RIVER/81-1+ 27.9M (N=50)

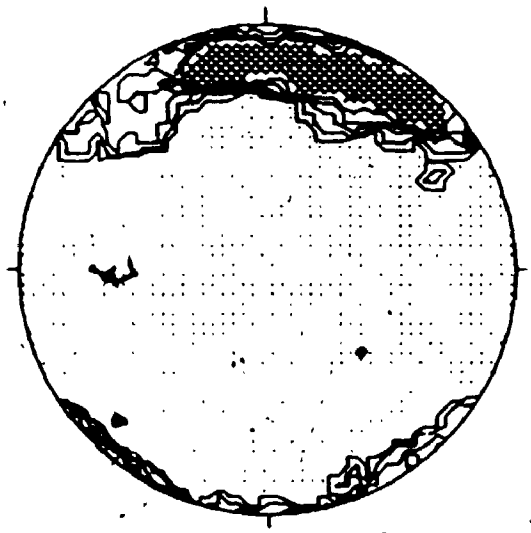

CONTOURED AT 1 2 3 4 5

POINTS PER 2.0 % AREA

FT-40C ASCOT RIVER/81-1+ 27.9M (N=37)

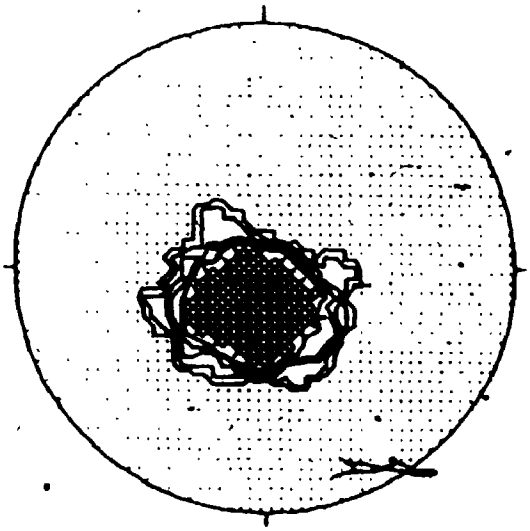

CONTOURED AT 1 2 3 4 5

POINTS PER 2.7 % AREA

Figure A-13 (continued next page)

FT-42A ASCOT RIVER/81-1- 33.3M (N=50)

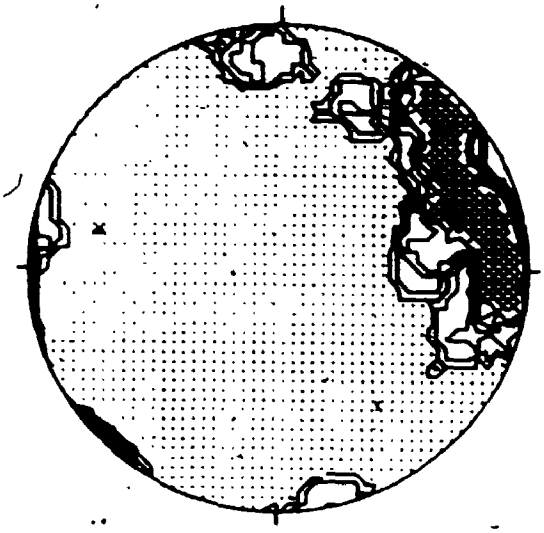

CONTOURED AT 1 2 3 4 5

POINTS PER 2.0 % AREA

FT-42C ASCOT RIVER/81-1- 33.3M (N=44)

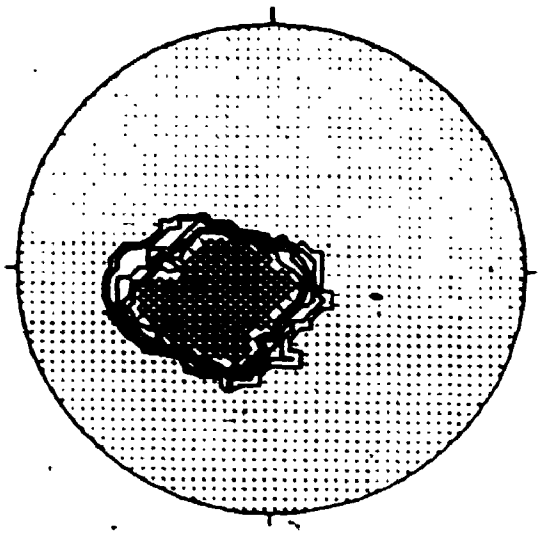

CONTOURED AT 1 2 3 4 5

POINTS PER 2.3 % AREA

FT-49A ASCOT RIVER II/82-3A 3.9M (N=50)

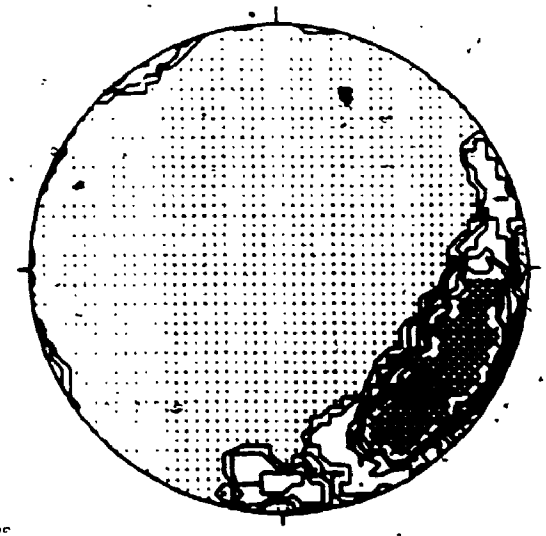

CONTOURED AT 1 2 3 4 5

POINTS PER 2.0 % AREA

FT-49C ASCOT RIVER II/82-3A 3.9M (N=39)

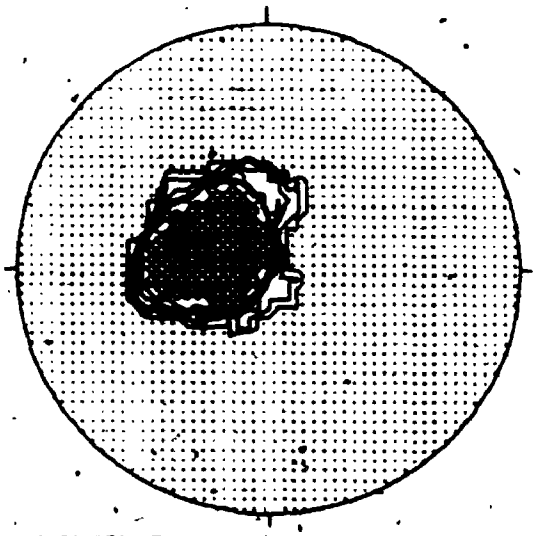

CONTOURED AT 1 2 3 4 5

POINTS PER 2.6 % AREA

Figure A-13 (continued)

TABLE A-1: Results of numerical analyses of clast fabric measurements

Sample			Azimuth	Plunge	S	θ
FT-16	A-axes (n=50)	V_1	345°	9°	0.90534	17.9°
		V_2	253°	1°	0.07699	73.9°
		V_3	156°	81°	0.01766	82.4°
	C-axes (n=38)	V_1	161°	81°	0.91338	17.1°
		V_2	251°	0°	0.06901	74.8°
		V_3	342°	9°	0.01760	82.4°
FT-19	A-axes (n=50)	V_1	347°	16°	0.85341	22.5°
		V_2	76°	2°	0.11722	70.0°
		V_3	176°	74°	0.02937	80.1°
	C-axes (n=47)	V_1	150°	74°	0.91648	16.8°
		V_2	264°	7°	0.04488	77.8°
		V_3	356°	14°	0.03864	78.7°
FT-20	A-axes (n=50)	V_1	343°	10°	0.87619	20.6°
		V_2	73°	5°	0.10470	71.1°
		V_3	192°	79°	0.01911	82.1°
	C-axes (n=41)	V_1	155°	80°	0.96055	11.5°
		V_2	12°	8°	0.02403	81.1°
		V_3	282°	6°	0.01542	82.9°
FT-21	A-axes (n=50)	V_1	332°	18°	0.74227	30.5°
		V_2	238°	8°	0.22951	61.4°
		V_3	127°	70°	0.02822	80.3°
	C-axes (n=33)	V_1	140°	74°	0.91855	16.6°
		V_2	244°	4°	0.05718	76.2°
		V_3	336°	16°	0.02427	81.0°
FT-22	A-axes (n=50)	V_1	170°	11°	0.78307	27.8°
		V_2	259°	0°	0.20782	62.9°
		V_3	351°	79°	0.00911	84.5°
	C-axes (n=38)	V_1	357°	80°	0.94261	13.9°
		V_2	104°	3°	0.03820	78.7°
		V_3	193°	9°	0.01918	82.0°

TABLE A-1: Results of numerical analyses of clast fabric measurements (continued)

Sample			Azimuth	Plunge	S	θ
FT-23	A-axes (n=50)	V_1	162°	12°	0.80670	26.1°
		V_2	253°	9°	0.17077	65.6°
		V_3	19°	75°	0.02253	81.4°
	C-axes (n=37)	V_1	350°	79°	0.91922	16.5°
		V_2	202°	9°	0.05816	76.0°
		V_3	112°	6°	0.02262	81.3°
FT-24	A-axes (n=50)	V_1	116°	5°	0.69334	33.6°
		V_2	205°	6°	0.29308	57.2°
		V_3	346°	83°	0.01358	83.3°
	C-axes (n=34)	V_1	6°	84°	0.94412	13.7°
		V_2	231°	4°	0.04347	78.0°
		V_3	141°	4°	0.01241	83.6°
FT-25	A-axes (n=50)	V_1	8°	16°	0.72983	31.3°
		V_2	276°	9°	0.23932	60.7°
		V_3	157°	72°	0.03085	79.9°
	C-axes (n=29)	V_1	168°	80°	0.91088	17.4°
		V_2	77°	0°	0.06998	74.7°
		V_3	348°	10°	0.01913	82.0°
FT-27	A-axes (n=50)	V_1	162°	20°	0.82302	24.9°
		V_2	253°	7°	0.15570	66.8°
		V_3	2°	69°	0.02128	81.6°
	C-axes (n=35)	V_1	352°	69°	0.90882	17.6°
		V_2	198°	19°	0.05381	76.6°
		V_3	106°	9°	0.03737	78.9°
FT-28	A-axes (n=25)	V_1	255°	9°	0.54477	42.4°
		V_2	168°	19°	0.36839	52.6°
		V_3	10°	69°	0.08684	72.9°
	C-axes (n=20)	V_1	38°	86°	0.78917	27.3°
		V_2	293°	1°	0.12083	69.7°
		V_3	202°	4°	0.09000	72.5°

TABLE A-1: Results of numerical analyses of clast fabric measurements (continued)

Sample			Azimuth	Plunge	S	θ
FT-29	A-axes (n=50)	V_1	357°	13°	0.89376	19.0°
		V_2	266°	1°	0.07910	74.7°
		V_3	174°	77°	0.02715	80.5°
	C-axes (n=38)	V_1	189°	79°	0.91851	16.6°
		V_2	96°	1°	0.06278	75.5°
		V_3	5°	11°	0.01871	82.1°
FT-30	A-axes (n=50)	V_1	97°	5°	0.71238	32.4°
		V_2	186°	0°	0.23791	60.8°
		V_3	282°	85°	0.04971	77.1°
	C-axes (n=30)	V_1	250°	88°	0.91109	17.3°
		V_2	144°	1°	0.05473	76.5°
		V_3	53°	2°	0.03418	79.3°
FT-31	A-axes (n=50)	V_1	345°	19°	0.80941	25.9°
		V_2	253°	2°	0.16485	66.4°
		V_3	157°	71°	0.02574	80.8°
	C-axes (n=35)	V_1	162°	72°	0.92415	16.0°
		V_2	58°	4°	0.04650	77.5°
		V_3	328°	18°	0.02935	80.1°
FT-32	A-axes (n=50)	V_1	347°	9°	0.84302	23.3°
		V_2	255°	5°	0.13277	68.6°
		V_3	138°	79°	0.02421	81.0°
	C-axes (n=43)	V_1	165°	81°	0.91970	16.5°
		V_2	65°	1°	0.05802	76.1°
		V_3	336°	9°	0.02228	81.4°
FT-33	A-axes (n=50)	V_1	344°	13°	0.94258	13.9°
		V_2	249°	14°	0.04005	78.5°
		V_3	115°	71°	0.01738	82.4°
	C-axes (n=38)	V_1	142°	78°	0.94820	13.2°
		V_2	259°	6°	0.03254	79.6°
		V_3	351°	11°	0.01926	82.0°

TABLE A-1: Results of numerical analyses of clast fabric measurements (continued)

Sample			Azimuth	Plunge	S	θ
FT-34	A-axes (n=50)	V_1	352°	21°	0.75136	29.9°
		V_2	258°	8°	0.21478	62.4°
		V_3	149°	68°	0.03387	79.4°
	C-axes (n=34)	V_1	160°	69°	0.89594	18.8°
		V_2	59°	4°	0.05398	76.6°
		V_3	328°	21°	0.05009	77.1°
FT-35	A-axes (n=50)	V_1	38°	5°	0.78804	27.4°
		V_2	308°	10°	0.18650	64.4°
		V_3	156°	79°	0.02546	80.8°
	C-axes (n=36)	V_1	167°	79°	0.92625	15.8°
		V_2	318°	10°	0.05686	76.2°
		V_3	48°	5°	0.01689	82.5°
FT-36	A-axes (n=50)	V_1	356°	11°	0.69674	33.4°
		V_2	85°	0°	0.28500	57.7°
		V_3	177°	79°	0.01826	82.2°
	C-axes (n=31)	V_1	161°	81°	0.94371	13.7°
		V_2	309°	7°	0.03197	79.7°
		V_3	38°	5°	0.02431	81.0°
FT-37	A-axes (n=50)	V_1	10°	12°	0.60209	39.1°
		V_2	101°	1°	0.35711	53.3°
		V_3	195°	78°	0.04080	78.3°
	C-axes (n=36)	V_1	191°	79°	0.87629	20.6°
		V_2	58°	8°	0.08971	52.6°
		V_3	328°	8°	0.03400	79.4°
FT-38	A-axes (n=50)	V_1	15°	16°	0.69752	33.4°
		V_2	110°	12°	0.24705	60.2°
		V_3	235°	70°	0.05543	76.4°
	C-axes (n=35)	V_1	231°	75°	0.87479	20.7°
		V_2	95°	11°	0.08675	72.9°
		V_3	1°	10°	0.03846	78.7°

TABLE A-1: Results of numerical analyses of clast fabric measurements (continued)

Sample			Azimuth	Plunge	S	θ
FT-39	A-axes (n=50)	V_1	359°	5°	0.63313	37.3°
		V_2	89°	12°	0.29289	57.2°
		V_3	245°	76°	0.07399	74.2°
	C-axes (n=40)	V_1	222°	78°	0.81926	25.2°
		V_2	107°	5°	0.12672	69.1°
		V_3	15°	10°	0.05402	76.6°
FT-40	A-axes (n=50)	V_1	10°	14°	0.72438	31.7°
		V_2	281°	1°	0.24576	60.3°
		V_3	184°	76°	0.02985	80.1°
	C-axes (n=37)	V_1	198°	77°	0.93604	14.6°
		V_2	98°	2°	0.03794	78.8°
		V_3	6°	13°	0.02603	80.7°
FT-41	A-axes (n=50)	V_1	326°	23°	0.80108	26.5°
		V_2	56°	2°	0.15983	66.4°
		V_3	151°	67°	0.03910	78.6°
	C-axes (n=32)	V_1	156°	69°	0.88520	19.8°
		V_2	52°	5°	0.08318	73.2°
		V_3	321°	20°	0.03162	79.8°
FT-42	A-axes (n=50)	V_1	70°	19°	0.71898	32.0°
		V_2	340°	4°	0.23890	60.7°
		V_3	239°	70°	0.04212	78.2°
	C-axes (n=44)	V_1	240°	71°	0.92387	16.0°
		V_2	91°	17°	0.04914	77.2°
		V_3	358°	9°	0.02699	80.5°
FT-43	A-axes (n=50)	V_1	305°	6°	0.88405	19.9°
		V_2	34°	5°	0.10293	71.3°
		V_3	162°	82°	0.01302	83.4°
	C-axes (n=40)	V_1	161°	83°	0.93491	14.8°
		V_2	16°	6°	0.04345	78.0°
		V_3	287°	4°	0.02164	81.5°

TABLE A-1: Results of numerical analyses of clast fabric measurements (continued)

Sample			Azimuth	Plunge	S	θ
FT-44	A-axes (n=50)	V_1	207°	12°	0.80273	26.4°
		V_2	116°	7°	0.16772	65.8°
		V_3	356°	76°	0.02955	80.1°
	C-axes (n=34)	V_1	9°	75°	0.92705	15.7°
		V_2	136°	9°	0.05500	76.4°
		V_3	227°	12°	0.01795	82.3°
FT-45	A-axes (n=50)	V_1	69°	13°	0.71754	32.1°
		V_2	340°	0°	0.27499	58.4°
		V_3	248°	77°	0.00747	85.9°
	C-axes (n=40)	V_1	249°	77°	0.97583	8.9°
		V_2	132°	6°	0.01576	82.8°
		V_3	39°	12°	0.00841	84.7°
FT-46	A-axes (n=50)	V_1	255°	3°	0.83878	23.7°
		V_2	347°	11°	0.13823	68.2°
		V_3	151°	78°	0.02300	81.3°
	C-axes (n=38)	V_1	158°	79°	0.96572	10.7°
		V_2	52°	3°	0.01886	82.1°
		V_3	323°	10°	0.01542	82.9°
FT-47	A-axes (n=50)	V_1	352°	17°	0.64835	36.4°
		V_2	260°	3°	0.32085	55.5°
		V_3	162°	73°	0.03080	79.9°
	C-axes (n=46)	V_1	173°	74°	0.92573	15.8°
		V_2	30°	13°	0.04172	78.2°
		V_3	299°	9°	0.03255	79.6°
FT-48	A-axes (n=50)	V_1	47°	19°	0.68449	34.2°
		V_2	145°	19°	0.28626	57.7°
		V_3	277°	62°	0.02925	80.2°
	C-axes (n=29)	V_1	267°	68°	0.90550	17.9°
		V_2	151°	10°	0.06315	75.4°
		V_3	57°	20°	0.03136	79.8°

TABLE A-1: Results of numerical analyses of clast fabric measurements (continued)

Sample			Azimuth	Plunge	S	θ
FT-49	A-axes (n=50)	V_1	126°	21°	0.76298	29.1°
		V_2	34°	2°	0.21311	62.5°
		V_3	299°	69°	0.02390	81.1°
	C-axes (n=39)	V_1	294°	70°	0.92256	16.2°
		V_2	99°	20°	0.04361	77.9°
		V_3	190°	5°	0.03383	79.4°
FT-50	A-axes (n=40)	V_1	318°	24°	0,82647	24.6°
		V_2	224°	6°	0.13544	68.4°
		V_3	121°	65°	0.03809	78.7°
	C-axes (n=25)	V_1	144°	66°	0.93330	15.0°
		V_2	240°	3°	0.04420	77.9°
		V_3	333°	23°	0.02249	81.4°
Poles to thrust faults (Section MP-79-5/n=40)		V_1	126°	63°	0.94353	13.7°
		V_2	239°	11°	0.04576	77.6°
		V_3	335°	24°	0.01071	84.1°

APPENDIX III

RESULTS OF SEDIMENTOLOGIC AND PETROLOGIC ANALYSES

Appendix III consists of Tables A-2, A-3 and A-4. Sand, silt and clay percentages as well as carbonate content are reported to the nearest 0.1% figure throughout this appendix; however, the accuracy of these analytical data are probably not better than to the nearest full percent and therefore, full percentage figures are used in text. Similarly, granulometric parameters (M_z, σ_I, Sk_I and K_G) are reported to the second decimal place in Tables A-2 and A-4; yet, the accuracy of these results is probably not better than to the first decimal place and consequently, one decimal place figures are used in text.

Limits utilized for particle size grades are those of the classical Udden-Wentworth scale:

Sand: 2.0 to 0.063 mm
Silt: 0.063 to 0.004 mm
Clay: less than 0.004 mm

Granulometric parameters were calculated using the following formulae (Folk and Ward, 1957):

$$M_z = \frac{\varphi_{16} + \varphi_{50} + \varphi_{84}}{3}$$

$$\sigma_I = \frac{\varphi_{84} - \varphi_{16}}{4} + \frac{\varphi_{95} - \varphi_5}{6.6}$$

$$Sk_I = \frac{\varphi_{16} + \varphi_{84} - 2\varphi_{50}}{2(\varphi_{84} - \varphi_{16})} + \frac{\varphi_5 + \varphi_{95} - 2\varphi_{50}}{2(\varphi_{95} - \varphi_5)}$$

$$K_G = \frac{\varphi_{95} - \varphi_5}{2.44(\varphi_{75} - \varphi_{25})}$$

Table A-2: Granulometric, heavy mineral, carbonate and trace element data of samples from stratigraphic sections.

SAMPLE #	UNIT*	COLOUR/ MUNSELL (dry)	GRANULOMETRY (-2.0 mm) SAND (%)	SILT (%)	CLAY (%)	M_z (φ)	σ_i (φ)	Sk_i	K_G	HEAVY MINERALS (0.250-0.125 mm) WEIGHT (%)	MAGNETIC (%)	CARBONATES (-0.063 mm) Dol. (%)	Calc. (%)	Total (%)	TRACE ELEMENTS (ppm) (-0.063 mm) Ni	Cr	Co	Cu	Pb	Zn
76-1-0	C	2.5Y 6/4	55.3	31.9	12.8	4.16	3.03	0.30	1.10	4.2	11.3	0.0	0.0	0.0	153	66	12	29	5	53
-1	C	5Y 6/2	53.9	38.1	8.0	4.01	2.58	0.16	1.01	4.1	11.4	0.9	0.4	1.3	134	40	15	26	10	47
-2	C	5Y 6/2	60.5	34.8	4.7	3.66	2.38	0.21	1.10	4.4	10.5	1.5	3.0	4.5	155	45	17	30	11	55
-3	C	5Y 6/2	71.5	25.0	3.5	3.13	2.08	0.20	1.52	4.1	14.7	1.3	3.2	4.7	144	48	12	22	11	43
-4	C	5Y 6/1	68.5	27.3	4.2	3.17	2.30	0.14	1.23	4.7	11.4	1.5	1.8	3.3	137	48	19	34	16	46
-5	C	5Y 6/1	68.8	27.0	4.2	3.23	2.23	0.24	1.20	4.4	9.4	1.5	2.2	3.7	131	50	17	23	12	44
-6	B	5Y 6/1	49.2	42.6	8.2	4.23	2.48	0.16	1.03	4.5	10.3	2.2	4.2	6.4	88	43	12	18	4	40
-7	B	5Y 6/1	66.9	28.9	4.2	3.18	2.33	0.14	1.14	4.7	10.4	2.4	2.5	4.9	88	37	10	14	4	32
-8	B	5Y 6/1	73.3	22.7	4.0	3.01	1.99	0.23	1.32	4.6	9.8	2.4	2.1	4.5	93	34	12	13	5	30
-9	B	5Y 6/1	61.7	34.5	3.8	3.58	2.11	0.22	1.15	3.9	11.3	2.0	2.1	4.1	127	48	12	20	13	42
-11	A	5Y 6/1	43.1	48.2	8.7	4.58	2.45	0.08	0.99	4.4	9.7	2.7	4.6	7.3	67	32	9	13	4	34
-10	A	5Y 6/1	43.1	49.4	7.5	4.51	2.34	0.06	0.98	4.3	10.2	2.7	4.6	7.3	62	26	8	18	4	33
79-1-2	/C	2.5Y 6/4	17.0	43.4	39.6	7.03	2.79	-0.10	0.79	---	---	0.0	0.0	0.0	63	43	16	33	12	80
-3	C	5Y 6/3	50.0	44.6	5.4	4.06	2.27	0.05	1.07	3.4	15.3	0.0	0.0	0.0	67	22	8	20	6	36
-4	C	5Y 6/3	45.2	46.6	8.2	4.44	2.50	0.07	0.99	3..	16..	0.0	0.0	0.0	78	27	8	18	8	41
-5	C	5Y 6/2	44.3	49.4	6.3	4.28	2.28	0.02	0.98	3.3	16.3	1.1	1.3	2.4	80	32	11	19	9	43
-6	A	5Y 6/3	42.1	39.6	18.3	4.80	3.29	0.06	0.88	3.3	6.2	0.9	1.3	2.2	36	26	15	27	17	80
-7	A	5Y 6/3	49.8	41.9	18.3	4.93	3.25	0.02	0.91	3.7	8.0	0.9	1.3	2.2	38	26	14	25	16	83
-8	A	5Y 6/3	48.0	42.6	9.4	4.04	2.94	0.02	1.01	3.3	9.0	1.1	1.3	2.4	37	25	10	19	12	36
79-5-1	C	2.5Y 6/4	71.3	24.5	4.2	3.24	2.04	0.43	1.14	4.2	8.4	0.0	0.0	0.0	74	15	10	13	4	32
-2	C	2.5Y 6/4	65.3	28.5	6.2	3.39	2.32	0.40	1.06	4.3	11.1	0.0	0.0	0.0	74	17	14	26	4	44
-3	C	2.5Y 6/4	73.4	22.6	4.0	2.97	2.03	0.32	1.11	4.7	13.0	0.0	0.0	0.0	37	16	12	22	5	49
-4	C	2.5Y 6/2	65.5	29.1	5.4	3.41	2.21	0.35	1.06	4.6	11.5	0.0	0.0	0.0	27	12	7	20	4	43
-5	C	2.5Y 6/2	69.5	23.5	7.0	3.51	2.24	0.53	1.14	4.9	8.9	0.0	0.0	0.0	31	14	8	18	3	43
-6	B	2.5Y 6/2	89.6	10.1	0.3	3.03	0.69	0.23	1.08	2.3	4.2	0.0	0.0	0.0	9	8	5	10	5	26

Table A-2 (continued)

SAMPLE #	UNIT*	COLOUR/ MUNSELL (dry)	GRANULOMETRY (-2.0 mm) SAND (%)	SILT (%)	CLAY (%)	M_z (φ)	σ_I (φ)	Sk_I	K_G	HEAVY MINERALS (0.250-0.125 mm) WEIGHT (%)	MAGNETIC (%)	CARBONATES (-0.063 mm) Dol. (%)	Calc. (%)	Total (%)	TRACE ELEMENTS (ppm) (-0.063 mm) Ni	Cr	Co	Cu	Pb	Zn
79-9-28	/C	5Y 6/1	1.7	57.1	41.2	7.94	2.68	0.33	0.95	---	---	0.0	0.0	0.0	30	34	11	18	15	68
-3	C	5Y 5/1	38.0	36.8	25.2	5.69	3.64	0.18	0.84	5.7	9.9	1.5	4.4	5.9	20	16	11	20	7	64
-4	C	5Y 5/1	45.0	35.2	19.8	4.96	3.41	0.26	0.90	5.3	9.7	2.2	3.5	5.7	18	12	10	18	8	54
-5	C	5Y 5/1	50.0	28.8	21.2	4.82	3.48	0.36	0.90	5.6	10.2	2.2	4.4	6.6	17	14	9	19	6	58
-6	C	5Y 5/1	55.1	24.9	20.0	4.68	3.77	0.46	1.20	5.6	9.5	2.4	6.7	9.1	18	13	9	17	7	48
-7	C	5Y 5/1	54.7	24.6	20.7	4.72	3.69	0.45	0.93	5.7	9.8	2.7	7.2	9.9	16	13	9	18	7	49
-8	C	5Y 5/1	53.5	27.5	19.0	4.64	3.58	0.43	1.04	5.5	10.3	2.9	8.1	11.0	18	13	8	16	6	45
-9	C	2.5Y 6/2	21.8	51.5	26.7	6.24	2.90	0.03	1.03	4.3	6.9	2.2	4.4	6.6	23	18	13	22	9	55
-10	A	5Y 6/4	46.2	42.5	11.3	4.46	2.86	0.10	0.92	4.2	9.3	0.7	0.2	0.9	22	16	13	26	9	80
-12	A	5Y 6/2	34.7	37.7	27.6	5.78	3.73	0.05	0.93	3.8	9.1	1.5	6.8	8.3	29	18	15	28	12	71
-13	A	5Y 6/3	38.9	35.1	26.0	5.47	3.92	0.17	0.90	3.4	12.8	1.5	2.5	4.0	33	18	17	34	12	82
-14	A	5Y 5/2	37.7	39.1	23.2	5.30	3.55	0.05	0.93	3.7	8.8	2.7	12.5	15.2	25	16	13	28	11	61
-15	A	5Y 5/1	32.8	41.0	26.2	5.80	3.59	0.06	0.97	3.5	7.7	3.2	12.4	15.6	21	16	9	21	10	50
79-10-78	/C	2.5Y 6/2	1.8	75.2	23.0	6.94	1.47	-0.20	1.18	---	---	0.0	0.0	0.0	24	20	10	19	6	70
-6	C	5Y 5/1	44.4	41.6	14.0	4.64	2.95	0.14	0.93	---	---	2.4	4.2	6.6	57	26	12	22	7	47
-5	C	5Y 5/1	52.5	30.9	16.6	4.51	3.38	0.37	1.03	5.0	9.3	1.8	7.1	8.9	44	27	11	19	5	47
-4	C	5Y 5/1	52.2	29.7	18.1	4.64	3.53	0.41	1.11	---	---	3.7	13.4	17.1	21	13	9	17	6	46
-3	C	5Y 5/1	52.2	28.5	19.3	4.76	3.68	0.42	1.07	---	---	3.1	12.6	15.7	34	21	9	16	7	45
-2	C	2.5Y 5/1	52.5	25.6	21.9	5.01	4.10	0.45	0.97	4.7	10.6	2.9	16.2	19.1	53	34	9	14	4	38
-1	C	2.5Y 5/1	55.5	25.0	19.5	4.74	3.76	0.48	1.11	---	---	2.6	17.4	20.0	24	16	7	13	7	39
79-14-6	C	10YR 5/3	87.8	10.9	1.3	2.21	1.46	0.24	1.18	7.3	12.6	0.0	0.0	0.0	8	9	5	11	4	24
-5	C	10YR 6/3	89.2	14.5	2.3	2.47	1.67	0.26	1.26	7.3	10.6	0.7	0.4	1.1	8	10	5	14	6	32
-4	C	10YR 5/3	83.2	14.4	2.4	2.47	1.69	0.30	1.34	8.5	11.3	0.0	0.4	0.4	10	10	5	16	6	36
-3	C	10YR 5/3	79.3	18.4	2.3	2.72	1.76	0.26	1.17	6.4	13.7	0.0	0.4	0.4	9	12	5	14	4	41
-2	C	10YR 5/3	76.0	20.4	3.6	2.94	1.94	0.32	1.23	7.1	13.2	0.0	0.4	0.4	11	13	6	15	5	45
-1	C	10YR 5/3	73.8	22.6	3.6	3.03	1.96	0.29	1.18	7.0	12.3	0.7	0.2	0.9	11	14	7	17	6	50

Table A-2 (continued)

SAMPLE #	UNIT*	COLOUR/ MUNSELL (dry)	GRANULOMETRY (-2.0 mm) SAND (%)	SILT (%)	CLAY (%)	M_z (φ)	σ_1 (φ)	Sk_1	K_G	HEAVY MINERALS (0.250-0.125 mm) WEIGHT (%)	MAGNETIC (%)	CARBONATES (-0.063 mm) Dol. (%)	Calc. (%)	Total (%)	TRACE ELEMENTS (ppm) (-0.063 mm) Ni	Cr	Co	Cu	Pb	Zn
79-15-10	C	2.5Y 6/4	61.7	24.4	13.9	3.88	3.17	0.50	1.07	4.9	9.9	0.0	0.0	0.0	19	13	10	18	8	55
-8	C	2.5Y 6/4	66.0	22.2	11.8	3.62	3.05	0.51	1.20	4.9	9.4	0.0	0.0	0.0	20	13	10	19	9	58
-9	C	2.5Y 6/4	62.0	26.2	11.8	3.82	2.94	0.44	0.95	4.9	10.1	0.0	0.0	0.0	23	12	12	22	8	64
-7	C	2.5Y 6/3	54.9	33.2	11.9	4.04	2.89	0.28	1.18	3.7	9.6	1.8	5.0	6.8	29	14	15	23	13	76
-6	C	2.5Y 6/3	55.0	34.2	10.8	4.02	2.82	0.27	1.09	4.4	10.3	1.8	5.0	6.8	25	14	12	21	11	70
-5	C	2.5Y 6/3	53.5	33.6	12.9	4.23	2.97	0.29	1.06	4.3	9.9	1.1	5.8	6.9	22	13	12	21	10	67
-4	C	2.5Y 6/3	53.5	32.5	14.0	4.32	3.04	0.31	1.02	4.6	8.9	1.3	4.7	6.0	21	12	11	20	9	64
-3	C	2.5Y 6/3	54.0	31.2	14.8	4.31	3.16	0.33	1.00	4.7	9.0	1.5	4.7	6.2	20	13	10	20	11	65
-1	B	2.5Y 6/2	95.9	1.9	2.2	2.29	0.69	0.20	1.18	7.4	5.7	1.3	5.5	6.8	14	9	8	13	7	38
-2	B	2.5Y 6/3	31.7	63.1	5.2	4.41	1.27	0.58	1.66	---	---	1.3	2.0	3.3	8	6	3	8	2	24
79-17-8	C	5Y 5/3	60.8	30.0	9.2	3.77	2.71	0.39	0.99	4.1	9.2	0.0	0.0	0.0	18	13	10	21	6	70
-7	C	5Y 6/3	56.0	36.4	7.6	4.00	2.48	0.26	0.93	3.5	8.7	0.0	0.0	0.0	15	14	9	18	6	72
-6	C	5Y 6/3	57.0	37.2	5.8	3.86	2.38	0.22	0.87	4.0	7.0	0.0	0.0	0.0	16	10	10	17	6	65
-5	C	5Y 6/2	61.5	34.8	3.7	3.59	2.17	0.23	0.94	3.8	6.0	0.0	0.0	0.0	14	9	9	14	5	59
-4	C	5Y 6/2	71.0	22.9	6.1	3.13	2.41	0.42	1.13	5.3	8.4	1.3	1.4	2.7	13	12	9	16	6	65
-3	C	5Y 6/2	67.2	27.2	5.6	3.36	2.32	0.38	1.03	4.9	7.6	1.3	1.4	2.7	15	10	9	15	6	61
-2	B	2.5Y 6/2	70.4	22.5	7.1	3.26	2.50	0.44	1.12	5.9	10.0	1.3	1.4	2.7	18	13	11	18	6	70
-1	B	2.5Y 6/2	85.3	9.7	4.9	2.31	1.84	0.40	2.01	5.5	7.8	0.9	0.6	1.5	18	13	11	18	5	70
79-18A-8	C	5Y 5/3	47.5	34.5	18.0	4.68	3.41	0.23	0.92	4.1	7.7	0.0	0.0	0.0	38	24	12	35	11	85
-5	C	5Y 5/3	55.0	33.8	11.2	4.10	2.92	0.26	0.93	4.2	9.3	0.0	0.0	0.0	36	23	13	32	13	75
-7	C	5Y 5/3	44.8	37.7	17.5	4.73	3.28	0.15	0.90	4.8	6.3	0.0	0.0	0.0	41	26	11	36	13	76
-6	C	5Y 5/3	55.2	33.3	11.5	4.00	3.03	0.24	0.90	4.1	9.0	0.0	0.0	010	35	20	13	33	12	75
-9	B	5Y 5/1	21.2	45.4	33.4	6.78	3.40	0.02	1.05	---	---	2.8	5.6	8.4	23	17	11	34	7	58
-4B	B	5Y 6/1	1.8	71.2	27.0	7.19	1.83	0.20	1.29	---	---	2.5	5.7	8.2	23	18	11	20	4	55
-4A	B	5Y 6/1	27.0	45.5	27.5	6.11	3.44	0.06	1.04	6.0	8.0	3.0	4.4	7.4	20	17	12	19	9	52

Table A-2 (continued)

SAMPLE #	UNIT*	COLOUR/ MUNSELL (dry)	GRANULOMETRY (-2.0 mm) SAND (%)	SILT (%)	CLAY (%)	M_z (φ)	σ_I (φ)	Sk_I	K_G	HEAVY MINERALS (0.250–0.125 mm) WEIGHT (%)	MAGNETIC (%)	CARBONATES (-0.063 mm) Dol. (%)	Calc. (%)	Total (%)	TRACE ELEMENTS (ppm) (-0.063 mm) Ni	Cr	Co	Cu	Pb	Zn
78-18A-3	A	5Y 6/1	38.3	45.6	16.1	5.07	3.07	0.17	1.15	5.0	6.9	3.0	4.2	7.2	20	14	11	18	7	53
-2	A	5Y 5/1	39.0	37.3	23.7	5.52	3.68	0.15	0.96	5.8	7.6	3.0	5.1	8.1	20	16	11	20	8	60
-1	A	5Y 5/1	46.0	37.0	17.0	4.81	3.42	0.23	1.04	5.3	7.0	2.7	4.2	6.9	32	20	13	23	7	60
79-18B-8	C	5Y 5/3	58.4	32.0	9.6	3.79	2.87	0.29	0.89	4.4	10.9	0.0	0.0	0.0	34	15	17	37	15	74
-6	C	5Y 5/3	58.4	31.0	10.6	3.76	2.96	0.28	0.96	4.2	10.5	0.0	0.0	0.0	35	16	14	34	37	60
-7	C	5Y 5/3	57.0	33.0	10.0	3.92	2.90	0.28	0.94	4.6	8.7	0.0	0.0	0.0	34	14	16	32	13	77
-9	B	5Y 5/3	62.5	28.1	9.4	3.56	2.94	0.33	1.03	5.7	8.9	0.7	0.6	1.3	60	24	13	36	16	71
-5	B	5Y 6/1	44.5	33.6	21.9	5.03	3.80	0.23	0.96	6.3	7.3	2.2	5.9	8.9	33	18	10	23	9	59
-4	A	5Y 6/1	51.1	31.9	17.0	4.48	3.37	0.29	0.92	5.7	7.0	2.7	5.4	8.1	24	14	9	20	6	54
-3	A	5Y 5/2	41.0	43.3	15.7	4.72	3.22	0.04	0.95	6.4	6.3	1.3	2.2	3.5	74	30	16	29	12	63
-2	A	5Y 5/2	40.8	44.1	15.1	4.73	3.21	-0.01	0.94	6.6	6.0	0.9	2.2	3.1	74	31	15	28	13	62
-1	A	5Y 5/2	38.0	46.9	15.1	4.79	3.13	0.00	0.98	6.2	5.9	0.9	2.2	3.1	71	28	17	27	12	58
79-18C-6	C	5Y 5/3	67.8	24.2	8.0	3.32	2.76	0.38	1.09	6.5	11.9	0.0	0.0	0.0	36	17	15	55	15	85
-5	C	5Y 6/2	47.2	41.0	11.8	4.38	2.85	0.13	0.91	5.5	9.9	0.0	0.0	0.0	31	22	15	36	11	77
-13	C	5Y 5/3	60.2	29.2	10.6	3.71	3.05	0.30	1.01	6.3	9.0	0.7	0.6	1.3	37	15	17	58	18	81
-12	C	5Y 6/2	61.0	30.5	8.5	3.56	2.82	0.25	0.99	4.3	10.7	1.8	5.2	7.0	27	15	12	27	11	66
-4	C	5Y 6/2	55.0	35.3	9.7	3.90	2.82	0.25	0.88	4.7	11.0	1.8	4.6	6.4	26	17	12	33	9	61
-11	C	5Y 6/2	61.0	30.5	8.5	3.60	2.74	0.27	0.98	4.7	10.1	1.8	5.2	7.0	28	14	11	28	11	65
-3	A	5Y 6/1	35.5	45.5	19.0	5.31	3.14	0.14	1.05	5.0	8.5	2.7	4.4	7.1	23	15	11	21	5	55
-10	A	5Y 5/1	30.0	46.0	24.0	5.82	3.07	0.07	0.94	5.7	6.6	2.8	5.8	8.6	23	16	11	21	7	60
-2	A	5Y 5/1	39.3	46.7	14.0	4.66	2.98	0.04	0.90	5.8	10.1	2.7	3.2	5.9	67	38	18	27	8	62
-9	A	5Y 5/1	44.3	47.9	7.8	4.30	2.68	-0.04	0.92	5.8	7.0	1.3	2.0	3.3	70	30	16	38	12	60
-1	A	5Y 5/1	51.5	40.2	8.3	3.96	2.91	0.06	1.02	5.8	9.2	2.5	3.0	5.5	65	28	17	29	9	55
-14	A	5Y 6/3	50.4	41.4	8.2	4.01	2.76	0.06	0.97	5.1	7.7	2.8	3.5	6.3	72	27	14	24	9	54

Table A-2 (continued)

SAMPLE #	UNIT*	COLOUR/ MUNSELL (dry)	GRANULOMETRY (-2.0 mm) SAND (%)	SILT (%)	CLAY (%)	M_z (φ)	σ_i (φ)	Sk_i	K_G	HEAVY MINERALS (0.250-0.125 mm) WEIGHT (%)	MAGNETIC (%)	CARBONATES (-0.063 mm) Dol. (%)	Calc. (%)	Total (%)	TRACE ELEMENTS (ppm) (-0.063 mm) Ni	Cr	Co	Cu	Pb	Zn
80-2-4	C	5Y 6/3	39.3	44.0	16.7	4.97	3.05	0.02	0.92	3.4	14.5	0.0	0.0	0.0	95	33	11	26	9	54
-3	C	5Y 5/3	46.8	41.0	12.2	4.41	2.87	0.09	0.97	3.2	10.8	0.0	0.0	0.0	61	25	11	25	11	52
-2	C	5Y 6/2	48.8	40.1	11.1	4.33	2.78	0.13	0.86	3.1	10.6	0.0	0.0	0.0	67	26	12	25	11	52
-1	C	5Y 6/2	48.8	40.1	11.1	4.29	2.88	0.11	0.98	3.2	11.0	1.3	2.7	4.0	67	26	12	25	10	58
81-1-14	/LT	5Y 6/1	0.1	74.7	25.2	6.76	1.75	-0.05	0.74	---	---	0.9	2.5	3.4	50	28	--	--	--	--
-13	LT	5Y 6/1	28.7	56.8	14.5	5.36	2.52	-0.03	0.96	3.0	10.8	0.9	1.1	2.0	65	32	--	--	--	--
-12	LT	5Y 5/1	29.5	52.2	18.3	5.40	2.91	-0.08	0.98	3.5	12.0	0.9	1.5	2.4	56	32	--	--	--	--
-11	LT	5Y 6/1	28.9	51.1	19.1	5.44	2.99	-0.09	0.97	4.6	9.7	1.8	2.7	4.5	44	28	--	--	--	--
-10	LT	5Y 6/1	28.4	49.4	22.2	5.68	3.08	-0.04	0.98	4.6	8.3	1.5	2.7	4.2	46	24	--	--	--	--
-9	LT	5Y 6/1	35.3	48.5	16.2	5.07	3.09	-0.09	0.94	4.5	8.9	1.3	2.7	4.0	46	24	--	--	--	--
-88	LT	5Y 6/2	47.5	45.0	9.3	4.26	2.85	0.04	1.06	4.5	9.9	0.9	2.5	3.4	45	22	--	--	--	--
-8	LT	5Y 6/2	57.5	33.2	9.3	3.84	2.86	0.22	1.03	5.0	9.9	1.3	2.5	3.8	42	23	--	--	--	--
-7	LT	5Y 6/1	14.0	48.5	40.2	7.39	3.22	0.12	0.95	2.9	9.5	1.1	2.0	3.1	46	24	--	--	--	--
-6	LT	5Y 5/1	37.2	40.3	22.5	5.54	3.28	0.26	1.00	[illegible]	6.3	[illegible]	1.5	2.6	39	19	--	--	--	--
-1	GP	5Y 6/2	48.0	49.7	2.3	1.05	1.05	0.28	1.68	0.8	2.2	0.0	0.0	0.0	24	12	--	--	--	--
-2	GP	2.5Y 6/4	27.4	71.2	1.4	0.89	0.89	0.16	1.83	---	---	0.7	0.8	1.5	21	10	--	--	--	--
-3	GP	5Y 6/2	1.4	83.6	15.0	1.06	1.06	0.14	1.25	---	---	0.9	1.5	2.4	56	24	--	--	--	--
-4	GP	5Y 6/1	4.8	80.2	15.0	6.69	1.39	0.01	1.36	---	---	1.1	2.0	3.1	44	22	--	--	--	--
-5	GP	5Y 6/1	15.0	77.2	7.8	5.69	1.66	0.02	1.03	2.6	4.7	1.8	2.0	3.8	26	14	--	--	--	--
-15	CT	5Y 6/1	24.2	59.3	16.5	5.56	2.78	-0.14	1.21	3.7	8.9	1.3	2.0	3.3	44	22	--	--	--	--
-16	CT	5Y 6/1	26.2	58.0	15.8	5.39	2.80	-0.11	1.18	3.5	9.7	1.3	2.0	3.3	44	20	--	--	--	--
-17	CT	5Y 5/1	26.0	52.8	21.2	5.72	3.12	0.05	1.19	3.1	7.8	0.9	1.8	2.7	49	22	--	--	--	--
-18	CT	5Y 5/1	29.8	52.0	18.2	5.39	3.16	0.01	1.19	3.3	8.3	1.3	2.8	4.1	44	23	--	--	--	--
-19	CT	5Y 5/1	40.4	45.8	13.8	4.80	3.00	0.13	1.12	3.0	6.4	1.3	2.2	3.5	46	19	--	--	--	--
-20	CT	5Y 5/1	42.0	41.0	17.0	4.73	3.44	0.08	1.03	3.2	7.0	1.3	2.5	3.8	54	20	--	--	--	--
-21	CT	5Y 5/1	30.6	49.2	20.2	5.47	3.23	0.04	1.13	3.5	9.1	1.1	2.2	3.3	47	20	--	--	--	--
-22	CT	5Y 5/1	21.5	56.1	22.4	6.04	2.76	0.03	1.12	2.6	6.2	0.9	1.8	2.7	43	22	--	--	--	--

Table A-2 (continued)

SAMPLE #	UNIT*	COLOUR/ MUNSELL (dry)	GRANULOMETRY (-2.0 mm) SAND (%)	SILT (%)	CLAY (%)	M_z (φ)	σ_I (φ)	Sk_I	K_G	HEAVY MINERALS (0.250-0.125 mm) WEIGHT (%)	MAGNETIC (%)	CARBONATES (-0.063 mm) Dol. (%)	Calc. (%)	Total (%)	TRACE ELEMENTS (ppm) (-0.063 mm) Ni	Cr	Co	Cu	Pb	Zn
81-1-23	CT	5Y 5/1	16.4	58.1	25.5	6.43	2.71	0.02	1.20	2.5	6.7	0.9	1.8	2.7	46	22	—	—	—	—
-24	CT	5Y 5/1	17.5	45.3	37.2	6.87	3.37	-0.06	1.16	3.5	5.6	0.9	2.0	2.9	59	28	—	—	—	—
-25	CT	5Y 5/1	24.5	45.3	30.2	6.20	3.46	-0.05	1.10	3.6	6.6	0.9	2.0	2.9	53	27	—	—	—	—
-26	CT	5Y 5/2	24.0	58.8	17.2	5.40	2.90	-0.10	1.25	3.3	10.0	0.9	1.1	2.0	44	26	—	—	—	—
-27	MP	5Y 5/3	3.4	90.8	5.8	5.28	1.13	0.39	1.21	---	---	0.9	0.6	1.5	16	12	—	—	—	—
-28	MP	5Y 5/2	3.5	84.3	12.2	6.02	1.63	0.25	1.09	---	---	0.9	0.6	1.5	23	18	—	—	—	—
-29	MP	5Y 5/2	47.1	46.6	6.3	4.52	1.66	0.42	1.43	1.2	2.6	1.3	0.8	2.1	21	17	—	—	—	—
82-4-1	C	2.5Y 6/4	56.0	32.0	12.0	4.29	2.79	0.40	1.61	---	---	0.0	0.0	0.0	16	18	—	—	—	—
-2	B	2.5Y 7/2	92.1	7.9	0.0	3.00	0.63	0.19	0.98	---	---	0.0	0.0	0.0	6	8	—	—	—	—
-3	B	2.5Y 6/4	29.0	67.6	3.4	4.51	0.98	0.34	1.42	---	---	0.0	0.0	0.0	9	6	—	—	—	—
-4	A	5Y 6/2	31.0	53.4	15.6	5.21	2.90	0.01	1.11	---	---	1.1	1.3	2.4	34	26	—	—	—	—

* A (drift unit A); B (unit B); C (drift unit C); /C (post-drift unit C); /LT (post-Lennoxville Till); LT (Lennoxville Till); GF (Gayburet Formation); CT (Chaudière Till); MP (Masawippi Formation).

Table A-3: Trace element and grain-size data of surface till samples.

SAMPLE #	NTS SHEET #	UTM COORD.	DEPTH (m)	CLASS*	TRACE ELEMENTS (ppm) (-0.063 mm)						GRAIN SIZE (-2.0 mm)		
					Ni	Cr	Co	Cu	Pb	Zn	% SAND	% SILT	% CLAY
78-01	21 E/12	19T878512	1.0	III	48	28	12	34	21	62	41.4	43.6	15.0
78-03	-	19T856508	1.5	III	67	36	16	30	20	67	38.8	38.4	22.8
78-05	-	19T229464	1.0	III	54	32	16	26	19	59	35.2	44.8	20.0
78-09	-	19T754484	1.2	III	66	37	18	35	21	63	43.6	39.1	17.3
78-10	-	19T751470	1.8	III	79	42	14	27	23	73	42.0	38.2	19.8
78-14	-	19T825446	1.0	III	67	37	16	32	20	67	44.5	41.3	14.2
78-15	-	19T845480	1.3	III	45	29	12	21	18	52	46.0	42.2	11.8
78-17	-	19T865523	2.7	III	72	29	18	30	20	70	49.7	40.0	10.3
78-18	-	19T902542	1.5	III	57	25	18	32	22	72	49.1	33.2	17.7
78-26	-	19T689460	1.2	III	111	55	19	26	20	59	40.0	42.1	17.9
78-28	-	19T702518	1.5	I	64	30	18	29	21	60	38.2	44.0	17.8
78-32	-	19T758539	0.9	III	79	42	18	33	20	65	48.8	31.6	19.6
78-34	-	19T710532	1.8	I	61	50	18	25	20	65	45.0	39.9	15.1
78-36	-	19T761548	1.0	III	77	50	19	32	22	82	41.2	35.2	23.6
78-37	-	19T825574	1.8	III	69	40	17	34	22	73	55.2	29.6	15.2
78-38	-	19T723506	1.5	III	60	35	19	38	25	66	38.5	41.5	20.0
78-39	-	19T713456	1.5	III	90	44	16	30	20	56	48.0	39.1	12.7
78-41	-	19T834489	1.8	I	48	25	15	19	17	53	43.8	42.3	13.9
78-42	-	19T854501	2.4	III	53	24	15	25	19	59	51.0	40.7	8.3
78-[illegible]	-	19T720538	1.8	III	64	37	15	38	21	68	43.5	42.0	14.5
78-[illegible]	-	19T773445	1.2	III	39	29	12	20	16	62	46.0	46.7	7.3
78-[illegible]	-	19T744425	0.9	III	91	45	15	30	20	62	41.2	42.1	16.7
78-46	-	19T735457	0.9	III	67	39	17	25	18	55	42.0	41.4	16.6
78-47	-	19T696472	1.0	III	100	48	16	26	16	63	41.8	43.5	14.7
78-49	-	19T792537	1.2	III	63	36	16	28	17	76	44.5	39.7	15.8
78-51	-	19T831516	1.2	III	65	40	13	32	20	60	39.4	40.8	19.8
78-53	-	19T796[illegible]	2.4	I	55	35	15	23	19	58	46.8	37.6	15.6
78-54	-	19T809[illegible]	0.9	III	67	36	18	29	18	69	40.4	35.8	23.8
78-56	-	19T826552	1.3	III	46	30	10	28	18	65	42.0	42.1	15.9
78-57	-	19T859558	0.9	III	59	32	15	32	21	63	46.2	35.4	18.4

Table A-3 (continued)

SAMPLE #	NTS SHEET #	UTM COORD.	DEPTH (m)	CLASS*	TRACE ELEMENTS (ppm) (-0.063 mm)						GRAIN SIZE (-2.0 mm)		
					Ni	Cr	Co	Cu	Pb	Zn	% SAND	% SILT	% CLAY
78-58	21 E/12	19T877583	1.2	I	67	28	17	25	20	58	49.5	41.3	9.2
78-60	"	19T758516	0.8	III	61	36	14	28	18	53	44.2	44.0	11.8
78-61	"	19T773492	1.0	III	62	36	16	28	20	57	43.6	38.2	18.0
78-62	"	19T778608	0.8	III	53	29	12	24	17	58	43.2	41.5	15.3
78-64	"	19T677632	1.4	I	64	34	16	26	20	55	49.7	35.4	14.9
78-68	"	19T701615	1.6	I	49	29	18	32	20	63	53.5	39.0	7.5
78-69	"	19T776580	1.0	III	52	32	14	27	18	63	35.0	47.0	18.0
78-70	"	19T768485	0.9	III	60	36	18	28	19	72	45.8	38.3	15.9
76-1-0	31 H/9	18T337570	1.5	III	153	66	12	29	5	53	55.3	31.9	12.8
78-71	"	18T335533	1.2	III	136	60	18	29	20	51	55.0	39.1	5.9
78-72	"	18T336549	0.7	III	195	100	28	47	29	70	59.7	30.1	10.2
78-73	"	18T321588	1.5	III	142	51	22	26	20	67	48.2	40.5	11.3
78-74	"	18T302594	0.6	III	92	46	14	25	14	48	58.3	38.9	2.8
78-75	"	18T286582	0.5	III	73	39	17	20	19	50	70.2	25.3	4.5
78-76	"	18T324629	1.3	III	136	69	20	32	18	63	53.2	38.2	8.6
78-77	"	18T321654	0.8	III	78	38	27	64	28	78	63.8	30.6	5.6
78-78	21 E/12	19T669654	1.7	III	59	24	14	26	17	55	69.3	27.4	3.3
78-79	"	19T760622	1.2	I	53	26	18	25	20	70	42.2	42.4	14.4
78-80	"	19T728667	1.3	III	61	34	16	36	20	65	47.3	37.7	15.0
78-81	"	19T702676	1.8	III	94	42	19	28	20	65	59.0	32.1	8.9
78-82	"	19T748651	1.0	III	53	33	18	32	21	63	52.0	38.8	9.2
78-83	"	19T767635	1.2	I	51	28	20	28	21	63	54.3	38.1	7.6
78-84	"	19T747560	1.0	III	48	22	13	30	5	59	50.1	39.8	10.1
78-89	31 H/9	18T328538	1.1	III	108	52	15	26	7	50	50.0	36.1	13.9
78-90	"	18T308552	1.0	III	165	61	18	36	11	55	53.4	33.5	13.1
78-91	21 E/12	19T674589	0.9	III	61	28	12	33	12	64	49.5	37.4	13.1
78-92	"	19T663598	1.0	I	112	37	16	28	6	52	63.3	29.7	7.0
78-93	"	19T669611	1.6	III	55	27	9	29	8	52	67.8	28.0	4.2
78-94	"	19T697622	1.1	II	38	23	12	32	7	63	54.0	34.9	11.1
78-98	"	19T723610	1.0	I	61	27	17	43	10	86	47.9	40.3	11.8

Table A-3 (continued)

SAMPLE #	NTS SHEET #	UTM COORD.	DEPTH (m)	CLASS*	TRACE ELEMENTS (ppm) (-0.063 mm)						GRAIN SIZE (-2.0 mm)		
					Ni	Cr	Co	Cu	Pb	Zn	% SAND	% SILT	% CLAY
78-100	21 E/12	19T699569	0.9	III	84	30	19	45	15	71	53.0	35.2	11.8
78-101	"	19T676564	0.8	III	148	48	19	34	12	69	42.0	36.2	21.8
78-102	"	19T687534	0.9	III	81	38	16	40	13	68	40.0	39.3	20.7
78-103	"	19T806664	2.0	III	63	27	11	36	8	73	55.2	35.8	9.0
78-105	"	19T892620	1.3	II	50	22	16	31	10	73	45.1	36.2	18.7
78-107	"	19T818615	1.3	II	57	22	17	35	10	80	45.5	38.1	16.4
78-110	"	19T795673	1.5	I	42	23	14	33	9	60	55.5	35.0	9.5
78-111	"	19T831606	1.2	I	45	20	12	25	7	60	54.0	36.0	10.0
78-112	"	19T709637	1.4	III	135	33	13	25	6	36	52.0	39.5	8.5
78-113	"	19T727656	1.1	III	37	24	9	20	7	46	54.2	32.8	13.0
78-115	"	19T839669	1.2	III	50	18	13	21	9	42	72.0	22.6	5.4
79-1-4	21 E/5	19T689368	3.6	III	78	27	8	18	8	41	45.2	46.6	8.2
79-109	21 E/13	19T679734	1.0	III	19	12	11	19	7	55	66.4	19.7	13.9
79-110	"	19T735706	1.6	III	27	17	11	26	7	53	51.5	31.8	16.7
79-111	31 H/8	18T342407	1.5	I	84	38	13	17	7	42	30.1	51.0	18.9
79-113	21 E/13	19T727722	1.5	I	48	25	15	31	11	68	47.0	39.5	13.5
79-114	"	19T728738	1.2	III	47	25	12	32	11	63	51.0	34.0	15.0
79-115	31 H/8	18T313396	1.0	III	92	50	10	14	5	29	54.0	38.2	7.8
79-118	21 E/12	19T677695	1.5	III	24	13	8	54	7	62	75.0	22.3	2.7
79-119	21 E/13	19T771872	1.1	III	21	12	12	26	9	62	77.4	18.1	4.5
79-120	"	19T758856	1.2	III	18	14	10	17	10	55	58.5	30.2	11.3
79-122	"	19T754818	1.6	III	25	14	10	31	13	72	67.9	26.2	6.2
79-123	"	19T754818	2.7	III	25	11	12	33	11	70	55.0	35.9	9.1
79-124	"	19T701883	1.5	II	15	12	7	20	7	45	66.1	25.0	8.9
79-126	"	19T782796	1.2	III	27	18	12	39	7	79	55.0	33.3	11.7
79-127	"	19T803758	1.2	III	32	19	13	29	8	64	59.8	28.3	11.9
79-128	"	19T797749	2.0	III	28	17	15	30	7	73	69.5	20.0	10.5
79-129	"	19T785710	1.2	III	59	29	13	35	7	61	53.8	30.7	15.5
79-130	21 E/12	19T842668	1.2	III	57	22	14	28	7	60	58.5	25.0	16.5
79-131	"	19T848689	1.8	III	46	18	11	23	5	59	55.5	34.6	9.9

Table A-3 (continued)

SAMPLE #	NTS SHEET #	UTM COORD.	DEPTH (m)	CLASS*	TRACE ELEMENTS (ppm) (-0.063 mm)						GRAIN SIZE (-2.0 mm)		
					Ni	Cr	Co	Cu	Pb	Zn	% SAND	% SILT	% CLAY
79-4-2	21 E/13	19T676738	2.1	III	11	8	7	13	2	36	75.5	20.3	4.2
79-5-1	"	19T814709	1.2	III	74	15	10	13	4	32	71.3	24.5	4.2
79-6-3	31 H/16	18T315720	2.0	II	26	28	14	27	7	76	29.0	42.4	28.6
79-7-2	21 E/13	19T772776	1.4	III	25	21	12	32	11	66	44.0	37.0	19.0
79-8-5	"	19T681757	1.2	III	37	22	14	38	8	58	52.0	35.9	12.1
79-9-6	"	19T693823	3.7	I	18	13	9	17	7	48	55.1	24.9	20.0
79-10-5	21 E/12	19T685693	6.5	I	44	27	11	19	5	47	52.5	30.9	16.6
79-12-2	21 E/13	19T742894	1.0	III	22	14	11	24	9	80	54.9	29.8	15.3
79-15-8	"	19T747889	1.5	III	20	13	10	19	9	58	66.0	22.2	11.8
79-17-8	"	19T867851	1.5	III	18	13	10	21	6	70	60.8	30.0	9.2
79-18C-13	"	19T785774	5.2	III	37	15	17	58	18	81	60.2	29.2	10.6
77-2-2	21 E/12	19T807632	2.0	III	58	18	11	25	7	58	53.0	36.2	10.8
80-2-4	21 E/5	19T738411	1.0	III	95	33	11	26	9	54	39.3	44.0	16.7
80-101	21 E/13	19T692754	1.5	III	63	20	10	30	9	67	51.2	34.9	13.9
80-102	"	19T704754	1.2	III	34	22	10	21	9	46	50.3	34.7	15.0
80-103	"	19T733763	1.3	III	60	26	12	32	10	65	48.0	37.0	15.0
80-105	"	19T712807	1.0	III	26	11	10	24	8	60	69.0	25.2	5.8
80-106	"	19T704784	1.5	III	85	18	22	67	19	87	60.0	29.8	10.2
80-107	31 H/9	18T282652	1.0	III	39	16	14	38	17	63	43.0	43.5	13.5
80-108	"	18T258602	2.0	III	38	10	14	28	9	43	70.9	27.1	2.0
80-109	"	18T306653	1.2	III	26	14	8	14	7	34	66.8	28.4	4.8
80-110	"	18T273611	1.2	III	38	18	11	25	9	66	50.0	39.1	10.9
80-111	"	18T241617	2.0	III	39	15	11	30	9	70	49.0	44.6	6.4
80-112	"	18T254645	1.0	III	32	17	9	21	7	46	54.7	34.4	10.9
80-113	"	18T268672	1.5	III	56	20	11	32	8	61	65.3	21.7	13.0
80-114	"	18T293701	1.2	III	31	19	9	25	8	52	52.2	31.7	16.1
80-117	21 E/12	19T782636	1.6	II	57	26	19	45	13	68	56.0	30.7	13.3
80-118	21 E/13	19T717710	1.5	II	29	14	9	18	8	50	60.1	31.5	8.4
80-119	21 E/12	19T726692	2.0	III	46	18	9	24	9	58	68.7	25.4	5.9
80-120	"	19T783682	1.0	III	58	26	13	27	9	64	50.0	39.0	11.0

Table A-3 (continued)

SAMPLE #	NTS SHEET #	UTM COORD.	DEPTH (m)	CLASS*	TRACE ELEMENTS (ppm) (-0.063 mm)						GRAIN SIZE (-2.0 mm)		
					Ni	Cr	Co	Cu	Pb	Zn	% SAND	% SILT	% CLAY
80-121	21 E/12	19T806694	1.5	III	42	22	7	29	8	62	55.2	37.4	7.4
80-122	-	19T833641	1.2	I	50	20	13	22	9	59	47.5	42.1	10.4
80-123	-	19T881633	1.2	III	68	24	13	32	14	75	58.0	31.6	10.4
80-124	-	19T865647	1.0	III	90	26	15	29	12	66	52.0	38.6	9.4
80-125	-	19T877666	1.6	III	40	22	11	21	7	70	43.1	44.6	12.3
80-126	-	19T929665	1.2	III	53	35	13	22	11	53	46.4	35.5	18.1
80-127	21 E/13	19T959715	1.0	III	113	38	15	38	14	74	44.5	35.4	20.1
80-128	-	19T944728	0.8	III	165	80	18	32	11	80	39.2	41.7	19.1
80-129	21 E/12	19T878687	1.0	III	36	22	9	21	7	57	58.0	31.8	10.2
80-130	21 E/13	19T868698	2.0	III	42	24	12	22	12	70	44.0	35.8	20.2
80-131	-	19T876711	1.2	III	83	39	17	39	18	81	40.9	36.5	22.6
80-132	-	19T923744	0.8	III	45	25	10	24	11	72	43.0	38.4	18.6
80-133	-	19T893743	0.7	III	74	34	12	27	12	76	39.1	42.4	18.5
80-134	-	19T829742	0.6	III	51	27	9	22	10	73	43.4	41.0	15.6
80-135	-	19T846741	1.2	III	63	28	7	23	8	61	52.8	35.9	11.3
80-136	-	19T882769	1.0	III	62	24	12	28	17	63	56.8	31.9	11.3
80-137	-	19T879812	1.2	III	31	16	8	29	12	73	52.4	34.7	12.9
80-138	-	19T801726	1.0	III	63	30	13	30	15	62	45.8	35.3	18.9
80-139	-	19T861770	0.8	III	46	22	12	31	17	75	39.7	40.3	20.0
80-140	-	19T904801	1.2	III	26	16	12	25	11	70	52.1	31.8	16.1
80-141	-	19T925788	1.2	III	50	26	9	16	7	45	40.0	49.8	10.2
80-142	31 H/9	18T328704	1.5	III	71	29	13	23	8	65	48.3	34.5	17.2
80-143	31 H/16	18T321709	1.2	III	54	25	12	27	11	65	64.0	28.1	7.9
80-146	21 E/12	19T677687	1.6	III	110	40	12	23	9	46	42.3	45.5	12.2
80-147	31 H/9	18T329487	4.0	III	120	38	11	14	5	46	43.9	48.3	7.8
80-149	-	18T304470	3.3	III	230	70	17	16	6	48	41.8	46.2	12.0
80-150	-	18T213502	1.3	III	96	33	15	25	8	56	48.1	38.8	13.3
80-151	-	18T182490	1.2	III	28	15	8	15	3	39	62.8	31.9	5.3
80-152	-	18T289532	2.0	III	180	40	11	11	4	31	42.4	45.6	12.0
80-154	-	18T293529	3.4	II	185	42	13	14	4	36	63.3	31.6	5.1

Table A-3 (continued)

SAMPLE #	NTS SHEET #	UTM COORD.	DEPTH (m)	CLASS*	TRACE ELEMENTS (ppm) (-0.063 mm)						GRAIN SIZE (-2.0 mm)		
					Ni	Cr	Co	Cu	Pb	Zn	% SAND	% SILT	% CLAY
80-155	31 H/19	18T274543	3.0	I	450	160	25	18	8	48	41.2	31.6	27.2
80-156	"	18T322501	1.2	III	275	95	18	16	6	47	46.0	38.9	15.1
80-157	"	18T216629	1.0	III	24	16	9	20	7	48	48.6	37.1	14.3
80-158	"	18T218672	1.3	III	16	11	5	12	6	32	37.5	49.9	12.6
80-159	"	18T238658	1.2	III	21	12	9	15	7	38	58.7	33.4	7.9
80-160	31 H/16	18T300718	1.2	III	60	19	12	30	11	58	64.0	27.3	8.7
80-161	"	18T276740	1.0	III	30	18	9	27	13	70	54.8	33.1	12.1
80-162	31 H/9	18T170452	1.0	III	46	29	10	22	8	53	58.4	31.2	10.4
80-163	31 H/8	18T276420	1.2	III	112	50	10	11	7	27	57.0	40.0	3.0
80-164	31 H/9	18T271435	1.3	III	71	31	9	16	9	51	40.5	50.5	9.0
80-165	31 H/9	18T286453	1.5	III	265	36	15	17	9	50	40.2	46.3	13.5
80-166	31 H/16	18T257791	1.4	III	18	13	7	19	8	52	58.7	28.3	13.0
80-167	"	18T273781	1.4	III	26	19	10	30	11	70	55.3	32.1	12.6
82-101	31 H/9	18T228574	1.5	II	21	13	--	--	--	--	55.1	38.9	6.0
82-102	"	18T207594	1.5	III	47	20	--	—	—	—	59.3	32.8	7.9
82-104	21 E/12	19T928628	1.2	III	72	20	—	—	--	—	45.3	33.1	21.6
82-105	"	19T966685	1.0	I	77	30	—	—	—	—	40.3	38.1	21.6
82-106	"	19T953671	1.0	III	65	30	—	—	—	--	37.8	47.2	15.0
82-107	"	19T915612	1.4	III	66	22	—	--	--	—	43.5	41.0	15.5
82-108	"	19T936586	1.5	III	64	22	—	—	—	—	44.0	36.8	19.2
82-109	"	19T941565	1.2	III	60	17	--	--	--	—	45.8	36.5	17.7
82-110	"	19T953618	1.4	III	63	24	—	--	—	—	44.0	37.1	18.9
82-111	"	19T969604	1.0	III	57	20	--	--	--	—	41.6	38.7	19.7
82-112	"	19T978660	0.9	III	22	10	—	—	--	—	50.5	33.5	16.0
82-113	21 E/13	19T976705	1.0	III	79	42	--	--	—	—	41.5	39.0	19.5
82-114	"	19T982728	0.9	III	170	58	—	--	—	—	37.0	42.7	20.3
82-115	"	19T995756	2.5	I	126	46	--	--	—	—	42.7	46.8	10.5
82-116	"	19T972789	1.2	III	47	17	--	—	--	—	47.8	37.5	14.7
82-117	"	19T983802	0.8	III	42	19	--	--	--	—	42.0	39.2	18.8
82-118	"	19T937761	1.2	III	40	20	--	—	—	--	55.7	36.0	8.3

Table A-3 (continued)

SAMPLE #	NTS SHEET #	UTM COORD.	DEPTH (m)	CLASS*	TRACE ELEMENTS (ppm) (-0.063 mm)						GRAIN SIZE (-2.0 mm)		
					Ni	Cr	Co	Cu	Bb	Zn	% SAND	% SILT	% CLAY
82-119	21 E/13	19T903719	0.6	III	101	31	--	--	--	--	50.0	38.2	11.8
82-121	"	19T907759	1.2	III	44	23	--	--	--	--	53.8	33.7	12.5
82-126	21 E/5	19T726397	0.8	III	76	46	--	--	--	--	40.0	43.2	16.8
82-127	21 E/12	19T697426	1.0	III	128	43	--	--	--	--	42.2	43.2	14.6
82-128	21 E/5	19T681403	1.0	III	62	34	--	--	--	--	42.8	42.5	14.7
82-129	"	19T667369	1.8	II	95	30	--	--	--	--	58.0	38.3	3.7
82-130	31 H/8	18T311376	1.5	III	106	37	--	--	--	--	76.0	19.9	4.1
82-131	"	18T323368	1.2	III	79	30	--	--	--	--	44.0	48.9	7.1
82-132	"	18T307367	1.2	III	83	32	--	--	--	--	42.5	46.2	11.3
82-133	"	18T293366	1.0	III	63	36	--	--	--	--	33.7	52.7	13.6
82-134	"	18T277367	0.8	III	77	53	--	--	--	--	37.3	51.8	10.9
82-135	"	18T256395	1.0	III	251	65	--	--	--	--	46.3	40.7	13.0
82-136	"	18T313415	1.5	III	198	65	--	--	--	--	43.6	43.7	12.7
82-137	21 E/12	19T660431	1.2	III	89	30	--	--	--	--	40.0	46.5	13.5
82-138	21 H/9	18T321451	0.9	III	165	59	--	--	--	--	40.6	43.7	15.7
82-139	"	18T250461	1.2	III	59	33	--	--	--	--	48.0	41.1	10.9
82-140	"	18T262450	1.0	III	56	24	--	--	--	--	50.8	44.4	4.8
82-141	"	18T274462	1.0	II	88	34	--	--	--	--	47.2	45.6	7.2
82-142	"	18T262471	0.8	III	132	47	--	--	--	--	61.8	32.4	5.8
82-143	"	18T286477	1.4	III	255	68	--	--	--	--	44.7	40.5	14.8
82-144	"	18T269489	0.9	III	194	63	--	--	--	--	35.2	46.2	18.6
82-145	"	18T249495	1.2	I	210	78	--	--	--	--	45.6	45.1	9.3
82-146	"	18T235510	1.1	III	70	30	--	--	--	--	38.8	45.5	15.7
82-147	"	18T227547	1.6	III	107	32	--	--	--	--	43.2	48.0	8.8

* I (fresh, calcareous till), II (slightly oxidized, calcareous till), III (oxidized till); all samples below solum.

Table A-4: Grain size, carbonates and organic matter, Rivière Landry section.

SAMPLE #	UNIT	GRANULOMETRY SAND (%)	SILT (%)	CLAY (%)	Md (φ)	M_z (φ)	σ_I (φ)	Sk_I	K_G	CARBONATES (-0.063 mm) Dol. (%)	Calc. (%)	Total (%)	ORGANIC MATTER (-0.063 mm) (%)
79-16-1	Marine silt	6.1	71.0	22.9	6.33	6.61	2.18	0.25	1.03	1.2	0.4	1.6	0.29
-2	" "	6.9	62.6	30.5	6.70	6.91	2.44	0.17	0.95	2.2	3.6	5.8	0.45
-3	" "	0.1	64.7	35.0	7.20	7.48	2.27	0.27	1.01	2.8	2.8	5.6	0.45
-4	" "	0.[illegible]	62.4	36.8	6.93	7.58	2.18	0.45	0.99	2.3	3.3	5.6	0.56
79-16-5W*	Danville Varves	0.2	7.8	92.0	10.33	10.34	1.63	-0.02	1.07	1.4	2.3	3.7	0.89
-5S	" "	0.1	19.7	80.2	9.06	9.05	1.39	-0.11	1.27	1.4	2.5	3.9	0.60
-6	" "	0.1	20.9	79.0	9.60	9.58	1.96	-0.004	0.99	2.1	8.1	10.2	0.97
-7W	" "	0.1	10.6	89.3	11.00	11.00	2.41	-0.03	1.07	0.8	0.3	1.1	0.93
-7S	" "	0.2	55.8	44.0	7.80	8.04	1.67	0.25	1.08	2.4	3.7	6.1	0.58
-8W	" "	0.0	10.6	89.4	9.33	9.30	0.78	-0.31	1.89	1.5	1.4	2.9	0.83
-8S	" "	0.2	78.3	21.5	7.10	7.08	1.31	0.02	1.11	3.1	7.4	10.5	0.51

* W and S at the end of sample number designate winter and summer layers, respectively.

APPENDIX IV

STRANDLINE FEATURES OF LATE WISCONSINAN WATER BODIES

Table A-5: Elevation of strandline features related to the Sherbrooke phase of Glacial Lake Memphrémagog

FEATURE #	*ELEVATION (m ASL) AND ERROR	DEPARTURE (m) FROM SHERBROOKE PHASE ISOBASES*	METHOD OF MEASUREMENT	FEATURE	LOCALITY	REFERENCE
1	249 +/- 2	-1	Altimeter	Floor of spillway	Lac Nick, Qc	McDonald, 1967 (Fig. 14: #7)
2	233 +/- 4	-1	Map contours	Delta (fluvial)	Ayer's Cliff, Qc	McDonald, 1967 (Fig. 14: #15)
3	248 +/- 2	0	Altimeter (X of 2 measurements)	Delta (fluvial)	Castle Brook, Qc	McDonald, 1967 (Fig. 14: #8 and #10)
4	249 +/- 2	0	Altimeter	Delta (ice-contact)	Cherry River, Qc	McDonald, 1967 (Fig. 14: #6)
5	249 +/- 2	-1	Altimeter	Delta (ice-contact)	Cherry River, Qc	McDonald, 1967 (Fig. 14: #5)
(6)	246 +/- 3	N.A.	Altimeter	Delta (ice-contact)	Cherry River, Qc	McDonald, 1967 (Fig. 14: #4)
7	255 +/- 2	-1	Altimeter	Terrace	St-Denis-de-Brompton, Qc	McDonald, 1967 (Fig. 14: #3)
8	259 +/- 4	0	Map contours	Wave-cut terrace	Côte St-Joseph, Qc	Parent, this study
(9)	254 +/- 2	N.A.	Altimeter	Delta (fluvial)	Lac Brompton, Qc	McDonald, 1967 (Fig. 14: #2)
10	273 +/- 2	+1	Spot elevation	Ice-contact lake terrace	St-François-Xavier-de-Brompton, Qc	Parent, this study (replaces McDonald, 1967, Fig. 14: #1)
11	240 +/- 4	0	Map contours	Delta (ice-contact)	North Hatley, Qc	Parent, this study
12	233 +/- 2	-1	Altimeter	Delta (fluvial)	Waterville, Qc	McDonald, 1967 (Fig. 14: #14)
13	248 +/- 2	+3	Altimeter	Delta (ice-contact)	Ascot Corner, Qc	McDonald, 1967 (Fig. 14: #9)
14	244 +/- 2	+3	Altimeter	Delta (ice-contact)	Brookbury, Qc	Parent, this study

Table A-5 (continued)

15	242 +/- 2	0	Altimeter,	Delta (ice-contact)	Bishopton, Qc	Parent, this study
16	254 +/- 2	0	Altimeter	Beach gravel	Mont Carrier, Qc	Parent, this study
17	255 +/- 2	-1	Altimeter	Beach gravel	Windsor, Qc	Parent, this study
18	251 +/- 4	-1	Map contours	Delta (fluvial)	Ruisseau Niquette, Qc	Parent, this study
(19)	262 +/- 2	N.A.	Altimeter	Delta (ice-contact)	St-Claude, Qc	Parent, this study
20	267 +/- 4	0	Map contours	Delta (ice-contact)	Wotton, Qc	Parent, this study
21	240 +/- 4	+1	Map contours	Delta (ice-contact)	Bury, Qc	Parent, this study

* Elevation of feature minus elevation of isobase; mean departure = 0.1 m (s.d. = 1.3).

( ) These features were not used for constructing isobases.

N.A. Not applicable.

Table A-6: Elevation of strandline features related to the Fort Ann phase of Glacial Lake Vermont

FEATURE #	ELEVATION (m ASL) AND ERROR	DEPARTURE (m) FROM FORT ANN ISOBASES*	METHOD OF MEASUREMENT	FEATURE	LOCALITY	REFERENCE
1-A	227 +/- 2	-1	Altimeter	Delta (ice-contact)	Tingwick, Qc	Parent, this study
1-B	229 +/- 4	0	Map contours	Ice-contact lake terrace	Tingwick, Qc	Parent, this study
2-A	226 +/- 2	+3	Altimeter	Delta (ice-contac)	Tingwick, Qc	Parent, this study
2-B	221 +/- 4	+6	Map contours	Delta (fluvial)	Moulin Samson, Qc	Parent, this study
3	226 +/- 1	+1	Spot elevation	Delta (ice-contact)	Colline Elliott, Qc	Parent, this study
4	221 +/- 4	+3.5	Map contours	Beach sediments	Pinnacle Shipton, Qc	Parent, this study
(5)	225 +/- 2	N.A.	Altimeter	Beach sediments	Chevrefils, Qc	Parent, this study
6	210 +/- 4	-3	Map contours	Beach sediments	St-Claude, Qc	Parent, this study
(7)	225 +/- 2	N.A.	Altimeter	Beach sediments	Perkins Corner, Qc	Parent, this study
8	206 +/- 4	-1	Map contours	Delta (fluvial)	Riv. Watopéka, Qc	Parent, this study
9	202 +/- 4	-4	Map contours	Delta (fluvial)	Riv. Stoke, Qc	Parent, this study
(10)	216 +/- 2	N.A.	Altimeter	Wave-cut terrace	Mont-Carrier, Qc	Parent, this study
11	229 +/- 4	-3	Map contours	Delta (fluvial)	Denison Mills, Qc	Parent, this study
12	214 +/- 2	-6	Altimeter	Wave-cut terrace	Richmond, Qc	McDonald, 1967 (Fig. 14: #18)
13	213 +/- 2	-6	Altimeter	Delta (fluvial)	Kingsbury, Qc	McDonald, 1967 (Fig. 14: #19)
14	227 +/- 2	-5	Altimeter	Delta (ice-contact)	Dalling, Qc	McDonald, 1967 (Fig. 14: #16)
15	229 +/- 2	-3	Altimeter	Wave-cut terrace	Dalling, Qc	Parent, this study
16	229 +/- 4	0	Map contours	Delta (fluvial)	Valcourt, Qc	Parent, this study

Table A-6 (continued)

17	220 +/- 2	-15	Altimeter	Delta (ice-contact)	Béthanie, Qc	McDonald, 1967 (Fig. 14: #17)
18	209 +/- 4	0	Map contours	Wave-cut terrace	Petit Lac St-François, Qc	Parent, this study
19	229 +/- 4	-1	Map contours	Littoral boulders	Martin Corner, Qc	Doiron, 1981
20	217 +/- 4	-2	Map contours	Delta (fluvial)	Lawrenceville, Qc	Parent, this study
(21)	206 +/- 2	N.A.	Altimeter	Wave-cut terrace	Bromptonville, Qc	McDonald, 1967 (Fig. 14: #20)
(22)	210 +/- 2	N.A.	Altimeter	Beach sediments	Chemin Duvernay, Qc	Parent, this study
23	195 +/- 2	-5	Altimeter	Delta (fluvial)	Key Brook, Qc	McDonald, 1967 (Fig. 14: #22)
(24)	203 +/- 2	N.A.	Altimeter	Beach sediments	Lennoxville, Qc	McDonald, 1967 (Fig. 14: #21)
(25)	**200 +/- 4	N.A.	Map contours	Delta (fluvial)	Huntingville, Qc	McDonald, 1967 (Fig. 14: #23)
26	192 +/- 2	+1	Altimeter	Delta (fluvial)	Capelton, Qc	McDonald, 1967 (Fig. 14: #24)
27	190 +/- 2	0	Altimeter	Wave-cut terrace	Ayer's Cliff, Qc	Boissonneault et al., 1981 (p. 29)
28	229 +/- 4	-7	Map contours	Wave-cut terrace	St-Joachim-de-Shefford, Qc	Parent, this study
29	223 +/- 4	-12	Map contours	Beach sediments	Savage Mills, Qc	Prichonnet, 1982a (Fig. 29-6)
30	229 +/- 4	-4	Map contours	Wave-cut terrace	Mont Shefford, Qc	Parent, this study (also Doiron, 1981)
31	224 +/- 4	0	Map contours	Wave-cut terrace	Pine Mountain, Qc	Parent, this study
32	216 +/- 4	-4	Map contours	Delta (ice-contact)	Brome Centre, Qc	Prichonnet et al., 1982
33	213 +/- 4	-1	Map contours	Delta (fluvial)	Brome, Qc	Prichonnet et al., 1982

Table A-6 (continued)

34	213 +/- 4	0	Map contours	Delta (fluvial)	Sutton Junction, Qc	Prichonnet et al., 1982
35	219 +/- 4	+3	Map contours	Beach ridges	Farnham Corners, Qc	Prichonnet, 1982b (Fig. 3)
36	215 +/- 4	0	Map contours	Beach ridges	Lac Selby, Qc	Prichonnet, 1982b (Fig. 3)
37	210 +/- 4	+1	Map contours	Delta (fluvial)	Alva, Qc	Prichonnet et al., 1982
38	200 +/- 4	0	Map contours	Delta (fluvial)	Dunkib, Qc	Dubé, 1983, p. 106
39	187 +/- 4	-11	Map contours	Terrace (fluvial?)	Manseonville, Qc	Parrott and Stone, 1972 (Fig. 1: #31)
40	191 +/- 4	-11	Map contours	Terrace (fluvial?)	Travor Road, Qc	Parrott and Stone, 1972 (Fig. 1: #34)
41	203 +/- 4	-2	Map contours	Terrace (fluvial?)	Potton Springs, Qc	Parrott and Stone, 1972 (Fig. 1: #39)
42	186 +/- 4	-9	Map contours	Littoral terrace	Troy, Vt	Parrott and Stone, 1972 (Fig. 1: #28)
43	198 +/- 3	-3	Map contours	Delta-terrace	East Richford, Vt	Parrott and Stone, 1972 (Fig. 1: #29)
44	186 +/- 3	-12	Map contours	Delta, terrace	East Berkshire, Vt	Parrott and Stone, 1972 (Fig. 1: #27)
45	183 +/- 3	-11	Map contours	Terrace (fluvial?)	Montgomery, Vt	Parrott and Stone, 1972 (Fig. 1: #26)
46	186 +/- 3	-6	Map contours	Terrace (fluvial?)	Montgomery Center, Vt	Parrott and Stone, 1972 (Fig. 1: #25)
47	183 +/- 3	-12	Map contours	Beach sediments	West Enosburg, Vt	Parrott and Stone, 1972 (Fig. 1: #23)
48	183 +/- 3	-12	Map contours	Beach	Bellevue Hill, Vt	Wagner, 1972 (Fig. 1: F-32)
49	186 +/- 3	-1	Map contours	Delta (ice-contact)	Buck Hill, Vt	Wagner, 1972 (Fig. 1: F-31)

Table A-6 (continued)

50	174 +/- 3	-10	Map contours	Delta	Binghamville, Vt	Wagner, 1972 (Fig. 1: P-30)
51	168 +/- 3	-12	Map contours	Delta	Cambridge, Vt	Wagner, 1972 (Fig. 1: P-28)
52	162 +/- 3	-18	Map contours	Delta	Fairfax, Vt	Wagner, 1972 (Fig. 1: P-26)
53	171 +/- 3	-14	Map contours	Beach	Arrowhead Mountain, Vt	Wagner, 1972 (Fig. 1: P-29)
54	180	-2	Leveling	Beaches	Peru, NY	Chapman, 1937 (Fig. 15: #23)
55	182	-4	Leveling	Beach	Schuyler Falls, NY	Chapman, 1937 (Fig. 15: #24)
56	183	-6	Leveling	Beach	Beckwith School, NY	Chapman, 1937 (Fig. 15: #25)
57	190	-3	Leveling	Beaches	Morrisonville, NY	Chapman, 1937 (Fig. 15: #26)
58	192	-2	Leveling	Delta	Morrisonville, NY	Chapman, 1937 (Fig. 15: #27)
59	197	0	Leveling	Beaches	West Beekmantown, NY	Chapman, 1937 (Fig. 15: #28)
60	198	0	Leveling	Littoral terrace	West Beekmantown, NY	Chapman, 1937 (Fig. 15: #29)
61	203	+2	Leveling	Beaches	Shelter's Corners, NY	Chapman, 1937 (Fig. 15: #30)
62	206	+1	Leveling	Beaches	Cobblestone Hill, NY	Chapman, 1937 (Fig. 15: #31)
63	210	0	Leveling	Beach	Pine Ridge, NY	Chapman, 1937 (Fig. 15: #32)
64	215	+1	Leveling	Beaches	Bear Pond, NY	Chapman, 1937 (Fig. 15: #34)

Table A-6 (continued)

65	222	+3	Leveling	Beaches	Cannon Corners, NY	Chapman, 1937 (Fig. 15: #35)
66	223	0	Map contours	Beaches	Cannon Corners Road, NY	Denny, 1974 (Fig. 6)
67	226.5 +/- 1.5	-1	Map contours	Beach	Maritana, Qc	Clark and Karrow, 1984 (Fig. 2: #18)
68	220.5 +/- 1.5	-1	Map contours	Beach	Earlville, NY	Clark and Karrow, 1984, (Fig. 2: #17)
69	214.5 +/- 1.5	0	Map contours	Beach	Burke Center, NY	Clark and Karrow, 1984, (Fig. 2: #16
70	208.5 +/- 1.5	-1	Map contours	Beach	Malone, NY	Clark and Karrow, 1984, (Fig. 2: #15)
71	205.5 +/- 1.5	+1	Map contours	Beach	East Dickinson, NY	Clark and Karrow, 1984, (Fig. 2: #14)

* Elevation of feature minus elevation of isobase. Mean departure = -3.4 m (s.d. = 5.1); when features from the Vermont-Missisquoi region (#39 through #53) are excluded, mean departure falls to -1.6 m (s.d. = 3.5).

** Recent map (1:20 000) shows several spot elevations at 200 m on extensive flat surface.

( ) These features are assigned to a transitional water-plane (Figure 5-10) and were not used for constructing isobases shown in Figures 5-12 and 5-13.

N.A. Not applicable.

Table A-7: Elevation of strandline features defining the marine limit

FEATURE #	ELEVATION (m ASL) AND ERROR	DEPARTURE (m) FROM MARINE LIMIT ISOLINES*	METHOD OF MEASUREMENT	FEATURE	LOCALITY	REFERENCE
1	161.5 +/- 1.5	-6	Map contours	Beach	Maritana, Qc	Clark and Karrow, 1984 (Fig. 2: #41)
2	160	-4	Leveling	Beaches	Covey Hill, Qc	Chapman, 1937 (Fig. 15: #57)
3	164	+3	Leveling	Beaches	English River, NY	Chapman, 1937 (Fig. 15: #56)
4	162	+4	Leveling	Beaches	Cannon Corners, NY	Chapman, 1937 (Fig. 15: #55)
5	157	+1	Leveling	Delta	North Branch, NY	Chapman, 1937 (Fig. 15: #54)
6	152	-1	Leveling	Beach	Woods Falls, NY	Chapman, 1937 (Fig. 15: #53)
7	148	-2	Leveling	Beaches	Sciota, NY	Chapman, 1937 (Fig. 15: #52)
8	142	0	Leveling	Beaches	West Chasy, NY	Chapman, 1937 (Fig. 15: #51)
9	138	0	Leveling	Beaches	West Beekmantown, NY	Chapman, 1937 (Fig. 15: #50)
10	131	-1.5	Leveling	Beaches	West Beekmantown, NY	Chapman, 1937 (Fig. 15: #49)
11	130	-1.5	Leveling	Delta	Morrisonville, NY	Chapman, 1937 (Fig. 15: #48)
12	123	-5	Leveling	Terrace	Schuyler Falls, NY	Chapman, 1937 (Fig. 15: #47)
13	121	-5	Leveling	Beaches	Schuyler Falls, NY	Chapman, 1937 (Fig. 15: #46)
14	122	-3	Leveling	Delta	Schuyler Falls, NY	Chapman, 1937 (Fig. 15: #45)

Table A-7 (continued)

15	110	-7	Leveling	Delta	Milton, Vt	Chapman, 1937 (Fig. 16: #22)
16	120	0	Leveling	Delta	East Georgia, Vt	Chapman, 1937 (Fig. 16: #24)
17	119 +/- 3	-12	Map contours	Beach	St. Albans, Vt	Wagner, 1972 (Fig. 1: S-55)
18	134	-1	Leveling	Terrace	St. Albans, Vt	Chapman, 1937 (Fig. 16: #25)
19	119 +/- 3	-11	Map contours	Delta	Fairfield Station, Vt	Wagner, 1972 (Fig. 1: S-60)
20	125 +/- 3	-10	Map contours	Delta	Sheldon, Vt	Wagner, 1972 (Fig. 1: S-66)
21	119 +/- 3	-15	Map contours	Delta	South Franklin, Vt	Wagner, 1972 (Fig. 1: S-69)
22	137 +/- 3	-4	Map contours	Delta	East Franklin, Vt	Wagner, 1972 (Fig. 1: S-87)
23	149 +/- 4	0	Map contours	Delta	Prelighsburg, Qc	Wagner, 1972 (Fig. 1: S-88)
24	155	+1	Leveling	Beach	Dunham, Qc	Chapman, 1937 (Fig. 16: #26)
25	158	+3	Leveling	Beach	Oak Hill, Qc	Chapman, 1937 (Fig. 16: #27)
26	171	0	Leveling	Beach	Granby, Qc	Chapman, 1937 (Fig. 16: #28)
27	175	-3	Leveling (?)	Terrace	Mont Yamaska, Qc	Goldthwait, 1911 (in Brown Macpherson, 1967)
28	168	-4	Leveling	Terrace	Ste-Prudentienne, Qc	Chapman, 1937 (Fig. 16: #29)
29	171 +/- 4	-2	Map contours	Terrace	Ste-Prudentienne, Qc	Parent, this study

Table A-7 (continued)

30	175 +/- 2	0	Altimeter	Beach	South Durham, Qc	Parent, this study
31	176 +/- 2	+2	Altimeter	Wave-cut terrace	South Durham, Qc	Parent, this study
32	175 +/- 4	+2	Map contours	Beach sediments	L'Avenir, Qc	Parent, this study
33	170 +/- 2	0	Altimeter	Wave-cut terrace	Trenholm, Qc	Parent, this study
34	171 +/- 2	-2	Altimeter	Beach gravel	Mareuil, Qc	Parent, this study
35	164 +/- 2	-8	Altimeter	Beach	Mont Proulx, Qc	Parent, this study
36	165 +/- 2	0	Altimeter	Wave-cut terrace	Danville, Qc	Parent, this study
37	**164 +/- 2	-9	Altimeter	Beach gravel	Ste-Elizabeth-de-Warwick, Qc	Parent, this study
38	174 +/- 2	+2	Altimeter	Delta	Warwick, Qc	Parent, this study
39	172.5 +/- 2	-2.5	Altimeter	Delta	Mont St-Michel, Qc	Parent, this study
40	175 +/- 2	0	Altimeter	Terrace	Norbertville, Qc	Parent, this study
(41)	191 +/- 4	N.A.	Map contours	Wave-cut terrace	Laurierville, Qc	Parent, this study
(42)	191 +/- 4	N.A.	Map contours	Beach sediments	Laurierville, Qc	Parent, this study
(43)	183 +/- 4	N.A.	Map contours	Delta	Rectory Hill, Qc	Parent, this study (also Dubé, 1971)
(44)	181	N.A.	Unknown	Beach	Mont St-Hilaire, Qc	Brown Macpherson, 1967: Table 1
(45)	188	N.A.	Unknown	Highest marine shells	Mont Royal, Qc	Stanfield, 1915 (in Brown Macpherson, 1967: Table 1)

* Elevation of feature minus elevation of isoline; mean departure = -2.5 m (s.d. = 4.4).

** A sand blanket of either eolian or littoral origin extends up to 179 m ASL.

( ) These features were not used for constructing isolines shown in Figure 5-14.

N.A. Not applicable.

REFERENCES

Anderson, T.W., Mott, R.J. and Delorme, L.D., 1985, Evidence for a pre-Champlain Sea glacial lake phase in Ottawa valley, Ontario, and its implications: Currents Research Part A, Geol. Surv. Can., Paper 85-1A, 239-245.

Anderson, T.W. and Stephens, M.A., 1972, Tests for randomness of directions against equatorial and bimodal alternatives: Biometrika, 59, 613-621.

Andrews, J.T. and Smith, D.I., 1970, Till fabric analysis: methodology and local and regional variability (with particular reference to the North Yorkshire cliffs): Quat. Jour. Geol. Soc. London, 125, 503-542.

Antevs, E., 1925, Retreat of the last ice sheet in eastern Canada: Geol. Surv. Can., Memoir 146, 142 p.

Ashley, G.M., 1975, Rhythmic sedimentation in Glacial Lake Hitchcock, Massachusetts-Connecticut: in: Jopling, A.V. and McDonald, B.C. (eds), Glaciofluvial and glaciolacustrine sedimentation, Soc. Econ. Paleont. Mineral., Spec. Publ. no 23, p. 304-320.

ASTM, 1972, Standard method for particle-size analysis of soils: Philadelphia, PA, American Society for Testing and Materials, Annual Book of Standards D422-63, p. 112-122.

Avramtchev, L., 1985, Carte géologique du Québec: Québec, Min. de l'Energie et des Ressources, DV-84-02.

Avramtchev, L., Biron, S., Vallières, A., Skidmore, W.D. and St-Julien, P., 1985, Carte minérale des Appalaches du Québec: Québec, Min. de l'Energie et des Ressources, MB-85-24.

Banerjee, I., 1973, Sedimentology of Pleistocene glacial varves in Ontario, Canada: Geol. Surv. Can., Bull. 226, Part A, 1-44.

Banerjee, I. and McDonald, B.C., 1975, Nature of esker sedimentation: in: Jopling, A.V. and McDonald, B.C. (eds), Glaciofluvial and glaciolacustrine sedimentation, Soc. Econ. Paleont. Mineral., Spec. Publ. no 23, p. 132-154.

Blatt, H., Middleton, G. and Murray, R., 1980, Origin of sedimentary rocks, 2nd ed: Englewood Cliffs, N.J., Prentice-Hall Inc., 782 p.

Boissonnault, P. et Gwyn, Q.H.J., 1983, L'évolution du lac proglaciaire Memphrémagog, sud du Québec, Géogr. phys. Quat., 37, 197-204.

Borns, H.W.Jr. and Calkin, P.E., 1977, Quaternary glaciation, west-central Maine: Geol. Soc. America Bull., 88, 1773-1784.

Bostock, H.S., 1970, Physiographic regions of Canada: Geol. Surv. Can., Map 1254 A.

Boulton, G.S., 1968, Flow tills and related deposits on some Vestspitsbergen glaciers: Journal of Glaciology, 7(51), 391-412.

Boulton, G.S., 1970a, On the origin and transport of englacial debris in Svalbard glaciers: Journal of Glaciology, 9(56), 213-229.

Boulton, G.S., 1970b, On the deposition of subglacial and melt-out tills at the margins of certain Svalbard glaciers: Journal of Glaciology, 9(56), 231-245.

Boulton, G.S., 1971, Till genesis and fabric in Svalbard: in: Goldthwait, R.P. (ed.), Till, a Symposium, Ohio State University Press, p. 41-72.

Boulton, G.S., 1972, The role of thermal régime in glacial sedimentation: in: Price, R.J. and Sugden, D.E. (eds), Polar geomorphology, Inst. Brit. Geogr, Spec. Publ. no 4, p. 1-19.

Boulton, G.S., 1976, The origin of glacially fluted surfaces—Observations and theory: Journal of Glaciology, 17(76), 287-309.

Boulton, G.S., 1978, Boulder shapes and grain-size distributions of debris as indicators of transport paths through a glacier and till genesis: Sedimentology, 25, 773-799.

Cady, W.M., 1960, Stratigraphic and geotectonic relationships in northern Vermont and southern Quebec: Geol. Soc. America Bull., 71, 531-576.

Cady, W.M., 1969, Regional tectonic synthesis of northwestern New England and adjacent Quebec: Geol. Soc. America, Memoir 120, 181 p.

Caron, A., 1983a, Région d'Arthabasca (SE): Québec, Min. de l'Energie et des Ressources, DP-83-07.

Caron, A., 1983b, Région de Warwick (NE): Québec, Min. de l'Energie et des Ressources, DP-83-21.

Carver, R.E., 1971, Heavy mineral separation: in: Carver, R.E. (ed.), Procedures in sedimentary petrology, New York, Wiley-Interscience, p. 427-452.

Chalmers, R., 1898, Surface geology and auriferous deposits of southeastern Quebec: Geol. Surv. Can., Annual Report, vol. 10, part J, 160 p.

Chapman, D.H., 1937, Late-glacial and postglacial history of the Champlain Valley: Am. Jour. Sci., 34(200), 89-124.

Charbonneau, J.-M., 1980, Région de Sutton (W): Québec, Min. de l'Energie et des Ressources, DPV-681, 89 p.

Charbonneau, J.-M., 1981, Géologie du Groupe d'Oak Hill entre Saint-Sylvestre et St-Jacques-de-Leeds: Québec, Min. de l'Energie et des Ressources, DPV-790, 32 p.

Chauvin, L., 1979a, Dépôts meubles de la région de Thetford-Mines - Victoriaville: Québec, Min. des Rich. nat., DPV-622, 20 p.

Chauvin, L., 1979b, Géologie des dépôts meubles dans la région d'Asbestos-Disraëli: Québec, Min. de l'Energie et des Ressources, DPV-716, 13 p.

Chauvin, L., Martineau, G. and La Salle, P., 1985, Deglaciation of the Lower St. Lawrence region, Québec: Geol. Soc. America, Special Paper 197, p. 111-123.

Clark, J.A., Farrell, W.E. and Peltier, W.R., 1978, Global changes in postglacial sea level: a numerical calculation: Quatern. Res., 9(3), 265-287.

Clark, P. and Karrow, P.F., 1984, Late Pleistocene water bodies in the St. Lawrence Lowland, New York and regional correlations: Geol. Soc. America Bull., 95, 805-813.

Clark, T.H., 1964a, Région d'Upton: Québec, Min. des Rich. nat., RG-100, 39 p.

Clark, T.H., 1964b, Région de Saint-Hyacinthe (moitié ouest): Québec, Min. des Rich. nat., RG-101, 148 p.

Clark, T.H., 1964c, Région de Yamaska-Aston: Québec, Min. des Rich. nat., RG-102, 208 p.

Clark, T.H., 1977, Région de Granby (W): Québec, Min. des Rich. nat., RG-177, 109 p.

Clark, T.H. et Globensky, Y., 1973, Portneuf et parties de St-Raymond et de Lyster: Québec, Min. des Rich. nat., RG-148, 110 p.

Clark, T.H. et Globensky, Y., 1976, Région de Bécancour: Québec, Min. des Rich. nat., RG-165, 66 p.

Clément, P. and de Kimpe, C.R., 1977, Geomorphological conditions of gabbro weathering at Mount Megantic, Québec: Can. J. Earth Sci., 14, 2262-2273.

Clément, P. et Parent, M., 1977, Contribution à l'étude de la déglaciation wisconsinienne dans le centre des Cantons de l'Est, Québec: Géogr. phys. Quat., 31(3-4), 217-228.

Clément, P. et Poulin, A., 1975, La fossilisation des réseaux de vallées aux environs de Sherbrooke, Québec: Rev. Géogr. Montr., 29, 167-171.

Cloutier, M., 1982, Géologie et géomorphologie quaternaires de la région de Cowansville-Knowlton-Sutton, Québec: Unpublished M.Sc. thesis, Université du Québec à Montréal, 143 p.

Cooke, H.C., 1937, Thetford-Mines, Disraëli and eastern half of Warwick map-areas, Québec: Geol. Surv. Can., Memoir 211, 176 p.

Cooke, H.C., 1950, Geology of a southwestern part of the Eastern Townships of Quebec: Geol. Surv. Can., Memoir 257, 142 p.

Cronin, T.M., 1977a, Champlain Sea foraminifera and ostracoda: a systematic and paleoecological synthesis: Géogr. phys. Quat., 31(1-2), 107-122.

Cronin, T.M., 1977b, Late-Wisconsin marine environments of the Champlain Valley (New York, Quebec): Quatern. Res., 7(2), 238-253.

Cronin, T.M., 1979a, Foraminifer and ostracode species diversity in the Pleistocene Champlain Sea of the St. Lawrence Lowlands: Journal of Paleontology, 53(2), 233-244.

Cronin, T.M., 1979b, Late Pleistocene benthic foraminifers from the St. Lawrence Lowlands: Journal of Paleontology, 53(4), 781-814.

Curray, J.R., 1956, The analysis of two-dimensional orientation data: Jour. of Geology, 64, 117-131.

Davis, R.B. and Jacobson, G.L.Jr., 1985, Late glacial and early Holocene landscapes in northern New England and adjacent areas of Canada: Quatern. Res., 23, 341-368.

Denny, C.S., 1974, Pleistocene geology of the northeast Adirondack region, New York: U.S.G.S., Prof. Paper 786, 50 p.

de Römer, H.S., 1980, Région de Baie Fitch-Lac Massawippi: Québec, Min. de l'Energie et des Ressources, RG-196, 59 p.

de Römer, H.S., 1981, Géologie de la partie sud des monts Stoke: Québec, Min. de l'Energie et des Ressources, DPV-822, 31 p.

de Römer, H.S., 1984, Géologie de la partie nord des monts Stoke: Québec: Min. de l'Energie et des Ressources, ET 82-02, 32 p.

Dionne, J.-C., 1972, Le Quaternaire de la région de Rivière-du-Loup/Trois-Pistoles, côte sud du Saint-Laurent: Environnement Canada, Centre Rech. For. Laurentides, Rapport Q-F-X-27, 95 p.

Doiron, A., 1981, Les dépôts quaternaires de la région de Granby-Waterloo, Québec - Cartographie, sédimentologie et stratigraphie: Unpublished M.Sc. thesis, Université du Québec à Montréal, 198 p.

Dreimanis, A., 1962, Quantitative gasometric determination of calcite and dolomite by using Chittick apparatus: Jour. Sediment. Petrol., 32, 520-529.

Dreimanis, A., 1969, Selection of genetically significant parameters for investigation of tills: Zesz. Nauk. UAM, Geografia 8, 15-19.

Dreimanis, A., 1976, Tills: their origin and properties: in: Legget, R.F. (ed.), Glacial Till, Roy. Soc. Canada, Spec. Publ. no. 12, p. 11-49.

Dreimanis, A., 1983, Quaternary glacial deposits: implications for the interpretation of Proterozic glacial deposits: Geol. Soc. America, Memoir 161, 299-307.

Dubé, C., 1983, Géomorphologie quaternaire et déglaciation à l'ouest du lac Memphrémagog: Unpublished M.Sc. thesis, Université de Sherbrooke, 138 p.

Dubé, J.C., 1971, Géologie des dépôts meubles, région de Lyster: Québec, Min. des Rich. nat., R.P. 596, 12 p.

Dubois, J.-M., 1974, Proposition de régions physiographiques pour les Cantons de l'Est: un apport à la classification de Bostock: Geoscope, 5(2), 13-46.

Dyck, W., Fyles, J.G. and Blake, W., Jr., 1965, Geological Survey of Canada radiocarbon dates IV: Geol. Surv. Can., Paper 65-4, 23 p.

Elson, J.A., 1961, The geology of tills: in: Penner, E. and Butler, J. (eds), Proceedings of 14th Canadian Soil Mechanics Conference: National Res. Council Can., Associate Comm. Soil and Snow Mech., Techn. Mem., 69, 5-36.

Elson, J.A., 1962, Pleistocene geology between Montreal and Covey Hill: in: Clark, T.H. (ed.), Guide book, New England Intercollegiate Geological Conference, 54th annual meeting, p. 61-66.

Elson, J.A., 1969a, Radiocarbon dates, Mya arenaria phase of the Champlain Sea: Can. J. Earth Sci., 6, 367-372.

Elson, J.A., 1969b, Late Quaternary marine submergence of Quebec: Rev. Géogr. Montr., 23(3), 247-258.

Elson, J.A., 1981, Deformation till: INQUA Commission on genesis and lithology of Quaternary deposits, Work group no. 1, Circular no. 20, Appendix, 4 p.

Flint, R.F., 1971, Glacial and Quaternary geology: New York, J. Wiley and Sons, 892 p.

Folk, R.L. and Ward, W.C., 1957, Brazos River Bar: a study in the significance of grain size parameters: Jour. Sediment. Petrol., 27, 3-26.

Frey, R.W. and Pemberton, S.G., 1984, Trace fossil facies models: in: Walker, R.G. (ed.), Facies models, 2nd ed., Geoscience Canada, Reprint series 1, p. 189-207.

Gadd, N.R., 1964, Surficial geology, Beauceville map-area, Québec: Geol. Surv. Can., Paper 64-12, 3 p.

Gadd, N.R., 1971, Pleistocene geology of the Central St. Lawrence Lowland: Geol. Surv. Can., Memoir 359, 153 p.

Gadd, N.R., 1976, Quaternary stratigraphy in southern Quebec: in: Mahaney, W.C. (ed.), Quaternary stratigraphy of North America, Dowden, Hutchinson and Ross Inc., Stroudsburg, Penn., p. 37-50.

Gadd, N.R., 1978, Surficial geology of Saint-Sylvestre map-area, Quebec: Geol. Surv. Can., Paper 77-16, 9 p.

Gadd, N.R., 1980, Late-glacial regional ice-flow patterns in eastern Ontario: Can. J. Earth Sci., 17, 1439-1453.

Gadd, N.R., 1983, Notes on the deglaciation of southeastern Quebec: Current Research Part B, Geol. Surv. Can., Paper 83-1B, 403-412.

Gadd, N.R., McDonald, B.C. and Shilts, W.W., 1972a, Deglaciation of southern Quebec: Geol. Surv. Can., Paper 71-47, 19 p. (including Map 10-1971).

Gadd, N.R., La Salle, P., Dionne, J.-C., Shilts, W.W. and McDonald, B.C., 1972b, Quaternary geology and geomorphology, southern Quebec: 24th Intern. Geol. Congress (Montreal, 1972), Field Excursion A44/C44, 70 p.

Gauthier, R.C., 1975, Déglaciation d'un secteur des rivières Chaudière et Etchemin, Québec: Unpublished M.Sc. thesis, McGill University, 180 p.

Genes, A.N., Newman, W.A. and Brewer, T.B., 1981, Late Wisconsinan glaciation models of northern Maine and adjacent Canada: Quatern. Res., 16, 48-65.

Globensky, Y., 1978, Région de Drummondville: Québec, Min. des Rich. nat., RG-192, 107 p.

Harron, G.A., 1976, Métallogénèse des gîtes de sulfure des Cantons de l'Est: Québec, Min. Rich. nat., Et.-spéc. no 27, 42 p.

Hébert, Y., 1982, Géologie du complexe ophiolitique de Thetford Mines: Unpublished Ph.D. thesis, Université Laval.

Hillaire-Marcel, C., 1977, Les isotopes du carbone et de l'oxygène dans les mers post-glaciaires du Québec: Géogr. phys. Quat., 31(1-2), 81-106.

Hillaire-Marcel, C., 1979, Les mers post-glaciaires du Québec: quelques aspects: Thèse de Doctorat d'Etat ès Sciences Naturelles, Univ. Pierre et Marie Curie, Paris, 2 vols.

Hillaire-Marcel, C., 1980, Les faunes des mers post-glaciaires du Québec: quelques considérations paléo-écologiques: Géogr. phys. Quat., 34(1), 3-59.

Hillaire-Marcel, C. and Occhietti, S., 1980, Chronology, paleogeography and paleoclimatic significance of late and post-glacial events in eastern Canada: Z. Geomorph., 24(4), 373-392.

Hodgson, R.A. (undated), Precision altimeter survey procedures (3rd edition): Los Angeles, American Paulin System, 58 p.

Humlum, O., 1978, A large till wedge in Denmark: implication for the subglacial thermal regime: Bull. Geol. Soc. Denmark, 27, 63-71.

Koteff, C. and Pessl, F. Jr., 1985, Till stratigraphy in New Hampshire: Correlations with adjacent New England and Quebec: Geol. Soc. America, Special Paper 197, p. 1-12.

Lamarche, R.Y., 1971, Northward moving ice in the Thetford Mines area of southern Quebec: Am. Jour. Sci., 271, 383-388.

Lamarche, R.Y., 1973, Géologie du complexe ophiolitique d'Asbestos, Cantons de l'Est: Québec, Min. Rich. nat., GM-28558, 9 p.

Lamarche, R.Y., 1974, Southeastward, northward and westward ice movement in the Asbestos area of southern Quebec: Geol. Soc. America Bull., 85, 465-470.

Lamothe, M., 1984, Le Quaternaire de la région de Pierreville, Basses-Terres du Saint-Laurent: in: Le Quaternaire du Québec méridional - aspects stratigraphiques et géomorphologiques: AQQUA, 5e Congrès (Sherbrooke, 1984), Livret-guide d'excursion, p. 26-38 (republished as: Bulletin de recherche, Département de géographie, Univ. de Sherbrooke, nos 77-78, p. 31-44).

Lamothe, M., 1985, Lithostratigraphy and geochronology of the Quaternary deposits of the Pierreville and St-Pierre Les Becquets areas, Quebec: Unpublished Ph.D. thesis, University of Western Ontario, 227 p.

Lamothe, M., Hillaire-Marcel, C. et Pagé, P., 1983, Découverte de concrétions calcaires striées dans le till de Gentilly, basses-terres du Saint-Laurent, Québec: Can. J. Earth, Sci., 20, 500-505.

La Salle, P., 1981, Géologie des dépôts meubles de la région de Saint-Jean - Lachine: Québec, Min. de l'Energie et des Ressources, DPV-780, 13 p.

La Salle, P., 1984, Quaternary stratigraphy of Quebec: A review: in: Fulton (ed.), Quaternary stratigraphy of Canada - A Canadian contribution to IGCP Project 24:. Geol. Surv. Can., Paper 84-10, 155-171.

La Salle, P., Martineau, G. et Chauvin, L., 1977a, Dépôts morainiques et stries glaciaires dans la région de Beauce-Monts Notre-Dame-Parc des Laurentides: Québec, Min. Rich. nat., DPV-515, 22 p.

La Salle, P., Martineau, G. et Chauvin, L., 1977b, Morphologie, stratigraphie et déglaciation dans la région de Beauce, Monts Notre-Dame et Parc des Laurentides: Québec, Min. des Rich. nat., DPV-516, 74 p.

La Salle, P., de Kimpe, C.R. and Laverdière, M.R., 1985, Sub-till saprolites in southeastern Québec and adjacent New England: Erosional, stratigraphic and climatic significance: Geol. Soc. America, Special Paper 197, p. 13-20.

La Salle, P., Matthews, J.V.Jr. and Mott, R., 1986, Stratigraphy and paleoenvironmental conditions from a section near Bethanie, Quebec, Canada: AMQUA, Program and Abstracts (9th biennial meeting, Champaign, Illinois, June 1986), p. 144.

Laurent, R., 1980, Environment of formation, evolution and emplacement of the Appalachian ophiolites from Québec: in: Ophiolites (Proceedings of the International Ophiolite Symposium, Cyprus, 1979), Cyprus Geol. Surv. Dept (Nicosia), 172-181.

Lawson, D.E., 1979, Sedimentological analysis of the western terminus of the Matanuska Glacier, Alaska: U.S. Army Corps of Engineers, Cold Regions Research and Engineering Lab. Report 79-9, 122 p.

Lee, H.A., 1962, Surficial Geology of Rivière-du-Loup-Trois-Rivières area, Quebec: Geol. Surv. Can., Paper 61-32, 2 p.

Lindsay, J.F., 1970, Clast fabric of till and its development: Jour. Sediment. Petrol., 40, 629-641.

Lord, C.S., 1938, Mégantic Sheet (west half), Frontenac County, Québec: Geol. Surv. Can., Map 379A.

Lortie, G., 1975, Direction d'écoulement des glaciers du Pléistocène des Cantons de l'Est, Québec: Geol. Surv. Can., Paper 75-1A, 415-416.

Lortie, G., 1976, Les écoulements glaciaires wisconsiniens dans les Cantons de l'Est et la Beauce, Québec: Unpublished M.Sc. thesis, McGill University, 219 p.

Lowdon, J.A. and Blake, W.Jr., 1970, Geological Survey of Canada radiocarbon dates IX and X: Geol. Surv. Can., Paper 70-2 (part B), 46-85.

Lowdon, J.A. and Blake, W.Jr., 1973, Geological Survey of Canada radiocarbon dates XIII: Geol. Surv. Can., Paper 73-7, 61 p.

Lowdon, J.A. and Blake, W.Jr., 1976, Geological Survey of Canada radiocarbon dates XVI: Geol. Surv. Can., Paper 76-7, 21 p.

Lowdon, J.A. and Blake, W.Jr., 1979, Geological Survey of Canada radiocarbon dates XIX: Geol. Surv. Can., Paper 79-7, 58 p.

Lowell, T.V., 1985, Late Wisconsin ice-flow reversal and deglaciation, northwestern Maine: Geol. Soc. America, Special Paper 197, 71-83.

Lowell, T.V., Decker, D.A. and Calkin, P.E., 1986, Quaternary stratigraphy in northwestern Maine: a progress report: Géogr. phys. Quat., 40, 71-84.

Lowell, T.V. and Kite, J.S., 1986, Glaciation style of northwestern Maine: Maine Geol. Surv., Bull. 37, 53-68.

Macpherson, J.B., 1967, Raised shorelines and drainage evolution in the Montreal Lowland: Cahiers de géographie de Québec, 11(23), 343-360.

Mark, D.M., 1973, Analysis of axial orientation data, including till fabrics: Geol. Soc. America Bull., 84, 1369-1374.

Mark, D.M., 1974, On the interpretation of till fabrics: Geology, 2, 101-104.

Marleau, R.-A., 1968, Région de Woburn/Mégantic-est/Armstrong: Québec, Min. des Rich. nat., RG-131, 60 p.

McDonald, B.C., 1966, Surficial geology, Richmond-Dudswell, Quebec: Geol. Surv. Can., Map 4-1966.

McDonald, B.C., 1967a, Pleistocene events and chronology in the Appalachian region of southeastern Quebec, Canada: Unpublished Ph.D. thesis, Yale University, 161 p.

McDonald, B.C., 1967b, Surficial geology, Sherbrooke-Orford-Memphrémagog, Québec: Geol. Surv. Can., Map 5-1966.

McDonald, B.C., 1968, Deglaciation and differential postglacial rebound in the Appalachian region of southeastern Quebec: Jour. of Geology, 76, 664-677.

McDonald, B.C., 1969, Surficial geology of La Patrie-Sherbrooke area, Quebec, including Eaton River watershed: Geol. Surv. Can., Paper 67-52, 21 p.

McDonald, B.C., 1971, Late Quaternary stratigraphy and deglaciation in eastern Canada: in: Turekian, K.K. (ed.), The Late Cenozoic glacial ages: New Haven, Yale University Press, p. 331-353.

McDonald, B.C. and Shilts, W.W., 1971, Quaternary stratigraphy and events in southeastern Quebec: Geol. Soc. America Bull., 82, 683-698.

McDonald, B.C. and Shilts, W.W., 1975, Interpretation of faults in glaciofluvial sediments: in: Jopling, A.V. and McDonald, B.C. (eds), Glaciofluvial and glaciolacustrine sedimentation, Soc. Econ. Paleont. Mineral., Spec. Publ. no 23, p. 123-131.

McKeague, J.A. (ed.), 1978, Manuel de méthodes d'échantillonnage et d'analyse des sols (2ème édition): Soc. Canadienne de la Science du Sol, 250 p.

Menzies, J., 1979, The mechanics of drumlin formation with particular reference to the change in pore-water content of the till: Journal of Glaciology, 22(87), 373-384.

Middleton, G.V. and Hampton, M.A., 1976, Subaqueous sediment transport and deposition by sediment gravity flows: in: Stanley, D.J. and Swift, D.J.P. (eds), Marine sediment transport and environmental management: New York, J. Wiley and Sons, p. 197-212.

Milliman, J.D. and Emery, K.O., 1968, Sea levels during the past 35 000 years: Science, 162, 1121-1122.

Mills, H.H., 1977, Differentiation of glacier environments by sediment characteristics: Athabasca Glacier, Alberta, Canada: Jour. Sediment. Petrol., 47, 728-737.

Mills, H.H., 1978, Some characteristics of glacial sediments on Mount Rainier, Washington: Jour. Sediment. Petrol., 48, 1345-1356.

Mörner, N.-A., 1972, The first report on till wedges in Europe and Late Weichselian ice flows over southern Sweden: Geol. För. i Stockholm Förh., 94, 581-587.

Mörner, N.-A., 1973, A new find of till wedges in Nova Scotia, Canada: Geol. För. i Stockholm Förh., 95, 272-273.

Mott, R.J., 1977, Late-Pleistocene and Holocene palynology in southeastern Québec: Géogr. phys. Quat., 31(1-2), 139-149.

Occhietti, S., 1977, Stratigraphie du Wisconsinien de la région de Trois-Rivières-Shawinigan, Québec: Géogr. phys. Quat., 31(3-4), 307-322.

Occhietti, S., 1980, Le Quaternaire de la région de Trois-Rivières-Shawinigan. Contribution à la paléogéographie de la vallée moyenne du Saint-Laurent et corrélations stratigraphiques: Paléo-Québec, 10, 218 p.

Occhietti, S., 1982, Synthèse lithostratigraphique et paléoenvironnements du Quaternaire au Québec méridional. Hypothèse d'un centre d'englacement wisconsinien au Nouveau-Québec: Géogr. phys. Quat., 36(1-2), 15-49.

Osberg, P.H., 1965, Structural geology of the Knowlton-Richmond area, Québec: Geol. Soc. America Bull., 76, 233-250.

Pardi, R., 1977, Queens College radiocarbon measurements II: Radiocarbon, 19(2), 237-244.

Parent, M., 1977, Déglaciation dans la région d'Asbestos: nouvelles observations: Annales de l'ACFAS, 44(1), 92 (abstract).

Parent, M., 1978, Géomorphologie quaternaire de la région de Stoke-Watopéka, Québec: Unpublished M.Sc. thesis, Université de Sherbrooke, 206 p.

Parent, M., 1984a, Le Quaternaire de la région d'Asbestos-Valcourt: aspects stratigraphiques: in: Le Quaternaire du Québec méridional - aspects stratigraphiques et géomorphologiques: AQQUA, 5e Congrès (Sherbrooke, 1984), Livret-guide d'excursion, p. 2-25 (republished as: Bulletin de recherche, Département de géographie, Univ. de Sherbrooke, nos 77-78, p. 2-30).

Parent, M., 1984b, Stratigraphie quaternaire des Appalaches du Québec méridional: la coupe-type de la rivière Ascot: in: Le Quaternaire du Québec méridional - aspects stratigraphiques et géomorphologiques: AQQUA, 5e Congrès (Sherbrooke, 1984), Livret-guide d'excursion, p. 39-46 (republished as: Bulletin de recherche, Département de géographie, Univ. de Sherbrooke, nos 77-78, p. 45-54).

Parent, M., 1984c, Notes on the deglaciation of southeastern Quebec: Discussion: Current Research Part B, Geol. Surv. Can., Paper 84-1B, 395-397.

Parent, M., 1984d, Les épisodes glaciolacustres et l'invasion marine sur la bordure des Appalaches, région de Victoriaville-Valcourt, Québec: Annales de l'ACFAS, 51, 146 (abstract).

Parent, M., Dubois, J.M.M., Bail, P., Larocque, A. et Larocque, G., 1985, Paléogéographie du Québec méridional entre le 12 500 et 8 000 and BP: Recherches amérindiennes au Québec, 15(1-2), 17-37.

Parrott, W.B. and Stone, B.D., 1972, Standline features and Late Pleistocene chronology of northwest Vermont: in: Doolan, B. and Stanley, R.S. (eds), Guidebook for field trips in Vermont, New England Intercollegiate Geological Conference, 64th Ann. Meet., p. 359-376.

Prest, V.K. and Hode-Keyser, J., 1977, Geology and engineering characteristics of surficial deposits, Montreal Island and vicinity, Québec: Geol. Surv. Can., Paper 75-27, 29 p.

Prichonnet, G., 1982a, Quelques données nouvelles sur les dépôts quaternaires du Wisconsinien et de l'Holocène dans le piedmont appalachian, Granby, Québec: Current Research Part B, Geol. Surv. Can., Paper 82-1B, 225-238.

Prichonnet, G., 1982b, Résultats préliminaires sur la géologie quaternaire de la région de Cowansville, Québec: Current Research Part B, Geol. Surv. Can., Paper 82-1B, 297-300.

Prichonnet, G., 1984, Dépôts quaternaires de la région de Granby, Québec (31 H/7): Comm. géol. Canada, Etude 83-30, 8 p.

Prichonnet, G., Cloutier, M. et Doiron, A., 1982, Données récentes lithostratigraphiques: Nouveaux concepts sur la déglaciation wisconsinienne en bordure des Appalaches au sud du Québec: ACFAS (50e Congrès, UQAM, mai 1982), Livret-guide d'excursion, 49 p.

Prichonnet, G., Doiron, A. et Cloutier, M., 1982, Le mode de retrait glaciaire tardiwisconsinien sur la bordure appalachienne au sud du Québec: Géogr. phys. Quat., 36(1-2).

Richard, P.J.H., 1977, Végétation tardiglaciaire au Québec méridional et implications paléogéographiques: Géogr. phys. Quat., 31(1-2), 161-176.

Richard, P.J.H., 1978, Histoire tardiglaciaire et postglaciaire de la végétation au mont Shefford, Québec: Géogr. phys. Quat., 32, 81-93.

Richard, P.J.H., 1985, Couvert végétal et paléoenvironnements du Québec entre 12 000 et 8 000 ans bP: Recherches amérindiennes au Québec, 15(1-2), 39-56.

Richard, S.H., 1974, Surficial geology mapping: Ottawa-Hull area (parts of 31 F,G): Current Research Part B, Geol. Surv. Can., Paper 74-1B, 218-219.

Richard, S.H., 1975, Surficial geology mapping: Ottawa Valley Lowlands (Parts of 31 G, B, F): Current Research Part B, Geol. Surv. Can., Paper 75-1B, 113-117.

Rust, B.R., 1977, Mass flow deposits in a Quaternary succession near Ottawa, Canada: diagnostic criteria for subaqueous outwash: Can. J. Earth Sci., 14, 175-184.

Rust, B.R. and Romanelli, R., 1975, Late Quaternary subaqueous outwash deposits near Ottawa, Canada: in: Jopling, A.V. et McDonald, B.C. (eds), Glaciofluvial and glaciolacustrine sedimentation, Soc. Econ. Paleont. Mineral., Spec. Publ. no 23, p. 177-192.

Samson, C., Barrette, L., La Salle, P. and Fortier, J., 1977, Quebec radiocarbon measurements I: Radiocarbon, 19(1), 96-100.

Scheidegger, A.E., 1965, On the statistics of the orientation of bedding planes, grain axes, and similar sedimentological data: U.S. Geol. Surv., Prof. Paper 525-C, 164-167.

Seilacher, A., 1964, Biogenic sedimentary structures: in: Imbrie, J. and Newell, N.D. (eds), Approaches to paleoecology, New York, John Wiley, p. 296-316.

Shilts, W.W., 1970, Pleistocene geology of the Lac-Mégantic region, Southern Québec, Canada: Unpublished Ph.D. thesis, Syracuse University, 154 p.

Shilts, W.W., 1973a, Glacial dispersal of rocks, minerals and trace elements in Wisconsinan till, southeastern Quebec, Canada Geol. Soc. America, Memoir 136, 189-219.

Shilts, W.W., 1973b, Till indicator train formed by glacial transport of nickel and other ultrabasic components: a model for drift prospecting: Geol. Surv. Can., Paper 73-1A, 213-218.

Shilts, W.W., 1975, Principles of geochemical exploration for sulphide deposits using shallow samples of glacial drift: Can. Min. and Metal. Bull., 18, 114-121.

Shilts, W.W., 1976a, Glacial till and mineral exploration: in: Legget, R.F. (ed.), Glacial Till, Roy. Soc. Canada, Spec. Publ. no 12, p. 205-224.

Shilts, W.W., 1976b, Glacial events in southern Quebec, northern New England; a reappraisal: Geol. Soc. America, Abstracts with Programs, 8(2), 267 (abstract).

Shilts, W.W., 1978, Detailed sedimentological study of till sheets in a stratigraphic section, Samson River, Quebec: Geol. Surv. Can., Bull. 285, 30 p.

Shilts, W.W., 1981, Surficial geology of the Lac Mégantic area, Québec: Geol. Surv. Can., Memoir 397, 102 p.

Shilts, W.W., 1982, The Highland Front Moraine Complex: in: La Salle, P., David, P.P. et Bouchard, M.A. (eds), Guidebook of the 45th Annual Meeting of the Friends of the Pleistocene, Drummondville-Saint-Hyacinthe, Québec, Canada; Montréal, Université de Montréal, p. 47-51.

Shilts, W.W. and Smith, S.L., 1986, Stratigraphic setting of buried gold-bearing sediments, Beauceville area, Quebec: Current Research Part B, Geol. Surv. Can., Paper 86-1B, 271-278.

Siegel, F.R., 1974, Applied geochemistry: New York, John Wiley and Sons, 346 p.

Spiker, E., Kelly, L. and Rubin, M., 1978, US Geological Survey radiocarbon dates XIII: Radiocarbon, 20(1), 139-156.

Starkey, J., 1970, A computer programme to prepare orientation diagrams: in: Paulitsch, P. (ed.), Experimental and natural rock deformation: New York, Springer-Verlag, p. 51-74.

Starkey, J., 1977, The contouring of orientation data represented in spherical projection: Can. J. Earth Sci., 14, 268-277.

Stewart, D.P. and MacClintock, P., 1969, The surficial geology and Pleistocene history of Vermont: Vermont Geological Survey, Bull. no 31, 251 p.

Stewart, R.A., 1982, Glacial and glaciolacustrine sedimentation in Lake Maumee III near Port Stanley, southwestern Ontario: Unpublished Ph.D. thesis, University of Western Ontario, 350 p.

St-Julien, P., 1970, Région d'Orford-Sherbrooke: Québec, Min. des Rich. nat., carte 1619.

St-Julien, P. and Hubert, C., 1975, Evolution of the Taconian orogen in the Quebec Appalachians: Am. Jour. Sci., 275-A, 337-362.

St-Julien, P., Hubert, C., Skidmore, B. and Béland, J., 1972, Appalachian structure and stratigraphy, Quebec: 24th International Geol. Congress (Montreal, 1972), Guidebook A56/C56, 99 p.

Terasmae, J. and Lasalle, P., 1968, Notes on late-glacial palynology and geochronology at St. Hilaire, Quebec: Can. J. Earth Sci., 5, 249-257.

Thomas, R.H., 1977, Calving bay dynamics and ice sheet retreat up the St. Lawrence Valley System: Géogr. phys. Quat., 31(3-4), 347-356.

Wagner, F.J.E., 1970, Faunas of the Pleistocene Champlain Sea: Geol. Surv. Can., Bull. 181, 104 p.

Wagner, W.P., 1972, Ice margin and water levels in northwest Vermont: in: Doolan, B. and Stanley, R.S. (eds), Guidebook for field trips in Vermont, New England Intercollegiate Geological Conference, 64th Ann. Meet., p. 319-342.

Walcott, R.I., 1970, Isostatic response to loading the crust in Canada: Can. J. Earth Sci., 7, 716-727.

Walcott, R.I., 1972, Late Quaternary vertical movements in Eastern North America: quantitative evidence of glacio-isostatic rebound: Rev. Geophys. Space Phys., 10, 849-884.

Walcott, R.I., 1973, Structure of the Earth from glacio-isostatic rebound: Ann. Rev. Earth Planet. Sciences, 1, 15-37.

Walker, R.G., 1984, Turbidites and associated coarse clastic deposits: in: Walker, R.G. (ed.), Facies models, 2nd ed., Geoscience Canada, Reprint Series 1, p. 171-188.

Warren, B. et Bouchard, M., 1976, Carte des dépôts meubles, Drummondville (31 H/16): Québec, Min. des Rich. nat., DPV-437.

Watson, G.S., 1966, The statistics of orientation data: Jour. of Geology, 74, 786-797.

Williams, H. and St-Julien, P., 1982, The Baie Verte-Brompton line: Early Paleozoic continent - ocean interface in the Canadian Appalachians: in: St-Julien, P. and Béland, J. (eds), Major structural zones and faults of the Northern Appalachians, Geol. Assoc. Canada, Special Paper 24, p. 177-207.

Woodcock, N.H., 1977, Specification of fabric shapes using an eigenvalue method: Geol. Soc. America Bull., 88, 1231-1236.

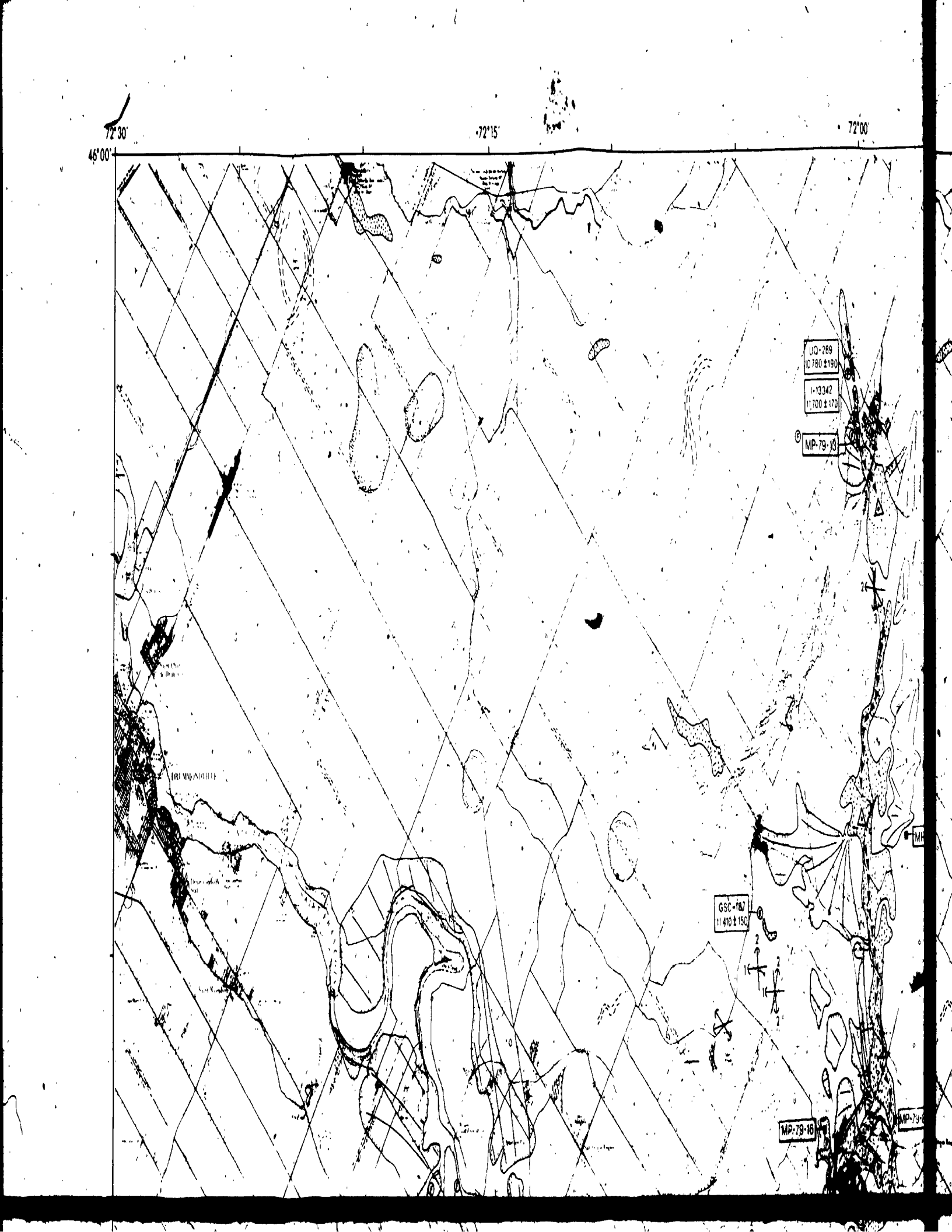
72°30'
72°15'
72°00'
46°00'
UQ-289
10 780 ± 190
I-13342
11 700 ± 170
MP-79-13
GSC-187
11 410 ± 150
MP-79-16

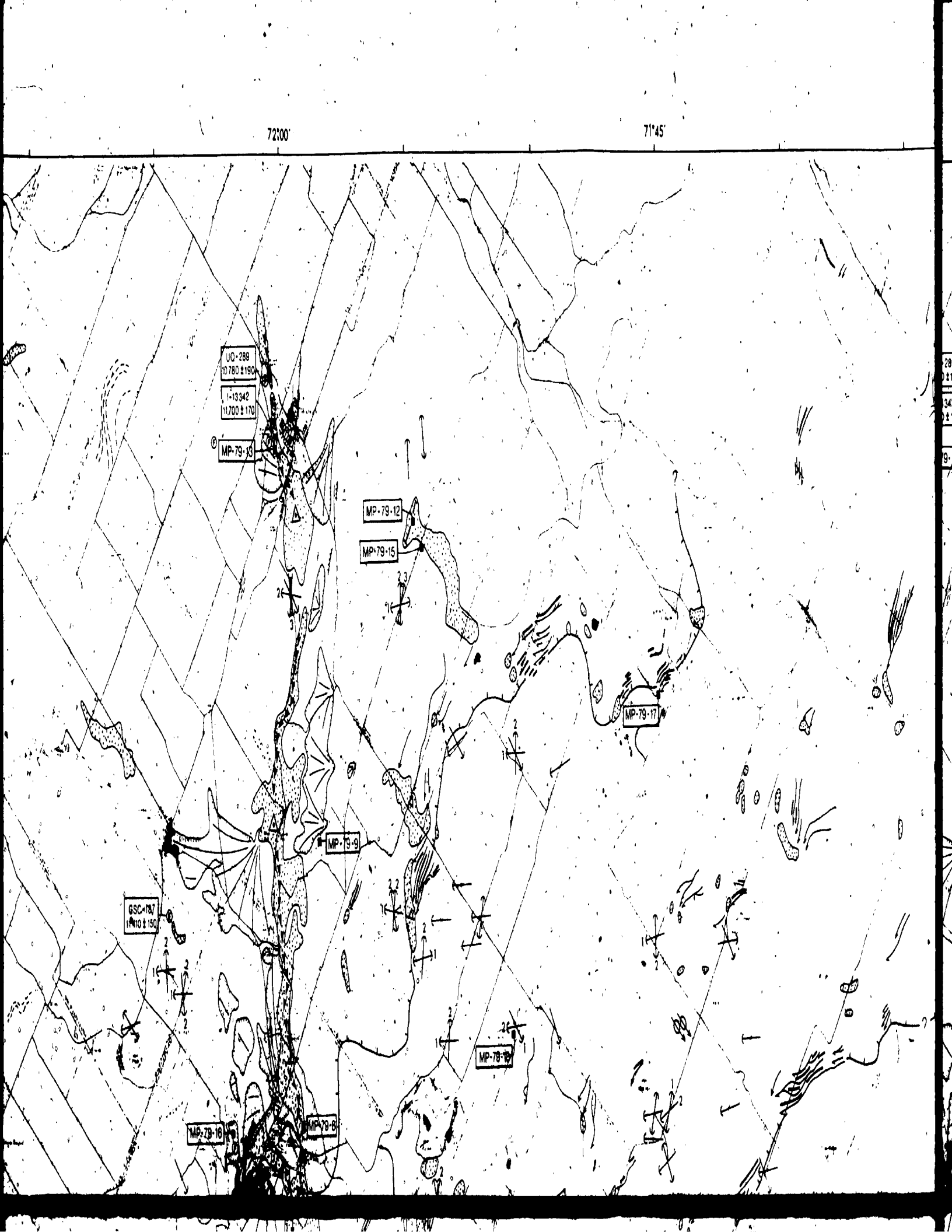
72°00'
71°45'
UO-289
10 780 ± 190
I-13342
11 700 ± 170
MP-79-13
MP-79-12
MP-79-15
MP-79-17
MP-79-9
GSC-187
MP-78-19
MP-79-16
MP-79-8

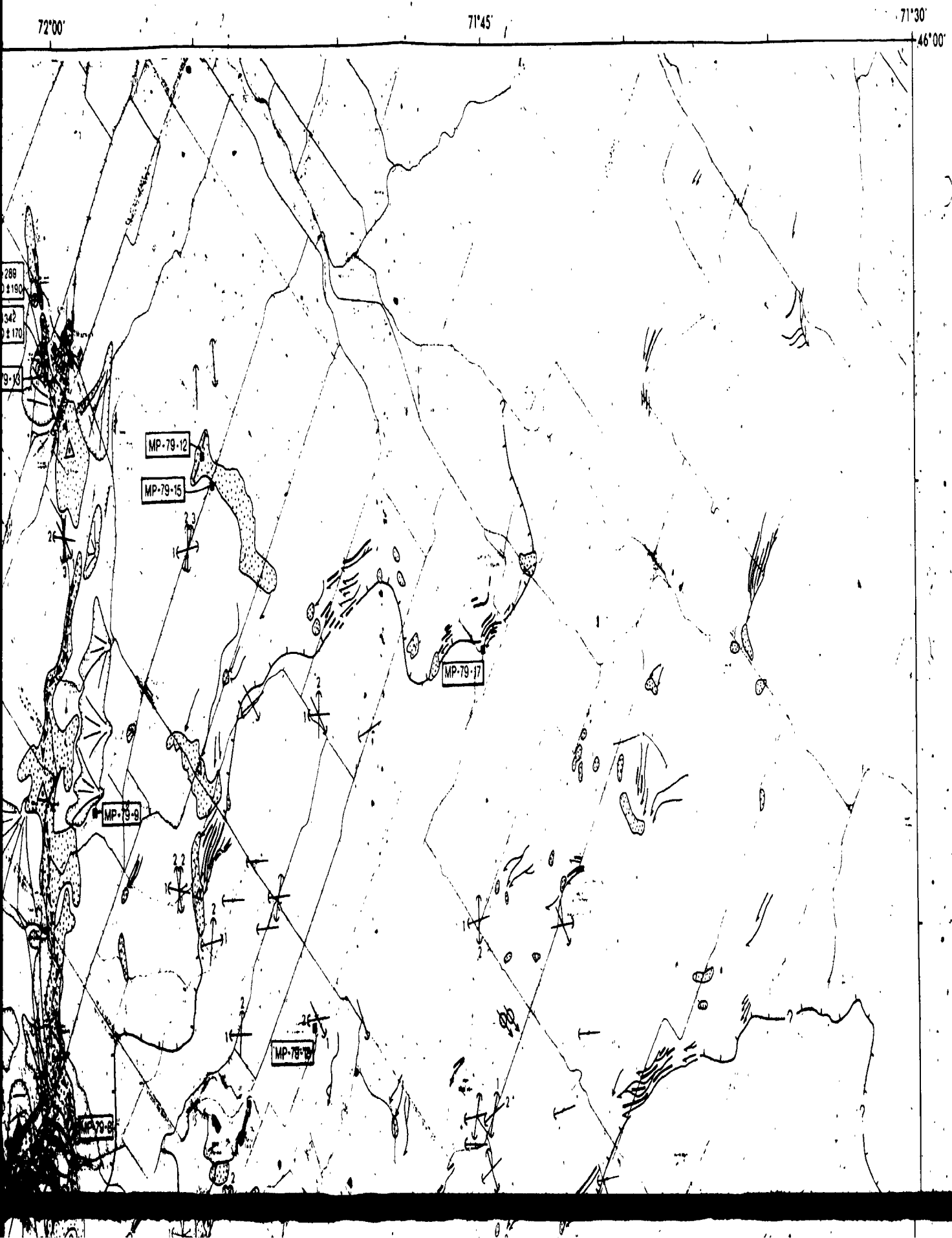
72°00'
71°45'
71°30'
46°00'
MP-79-12
MP-79-15
MP-79-17
MP-79-9
MP-78-19

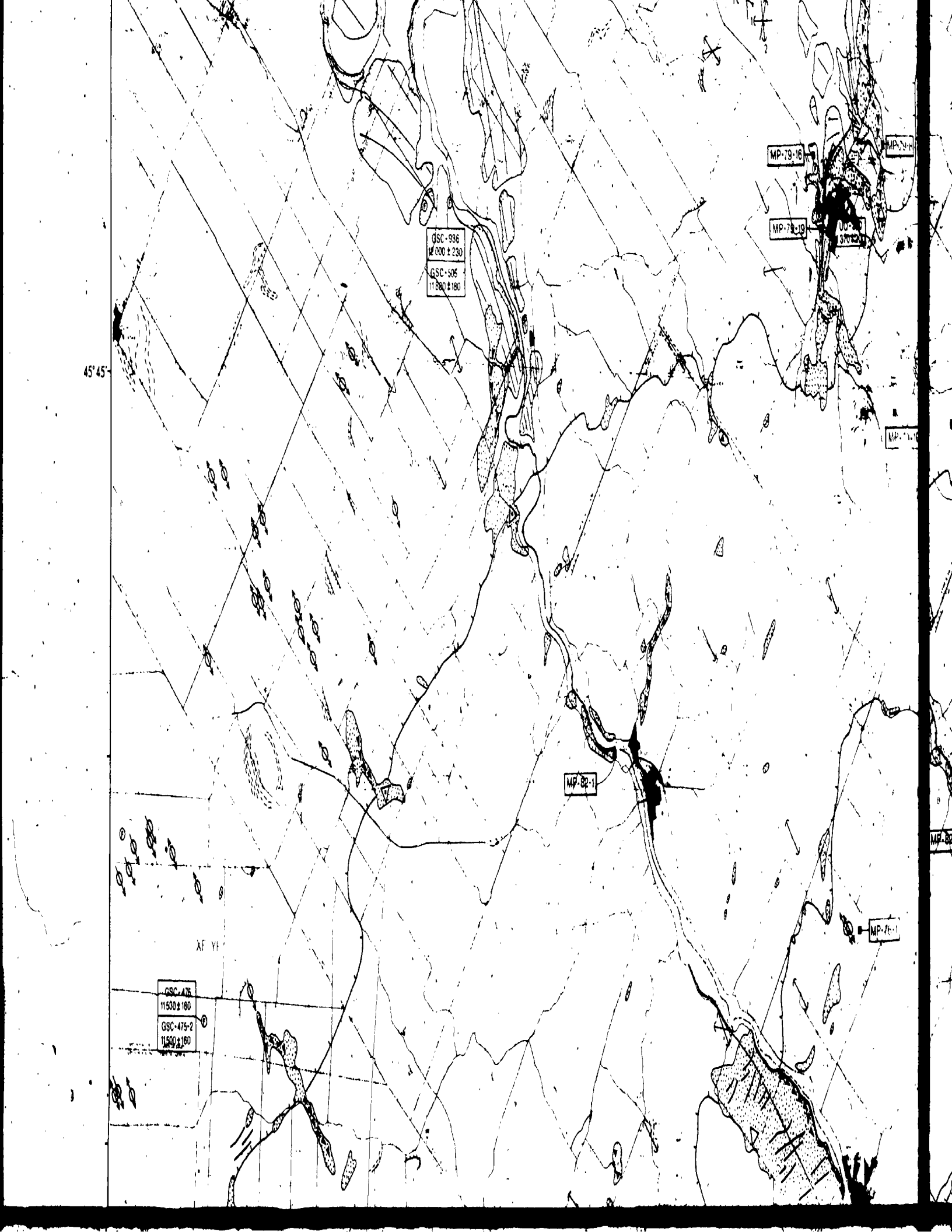
45°45'
GSC-936
GSC-505
11 880 ± 180
MP-79-16
MP-80-1
GSC-475
11 530 ± 160
GSC-475-2
11 500 ± 160

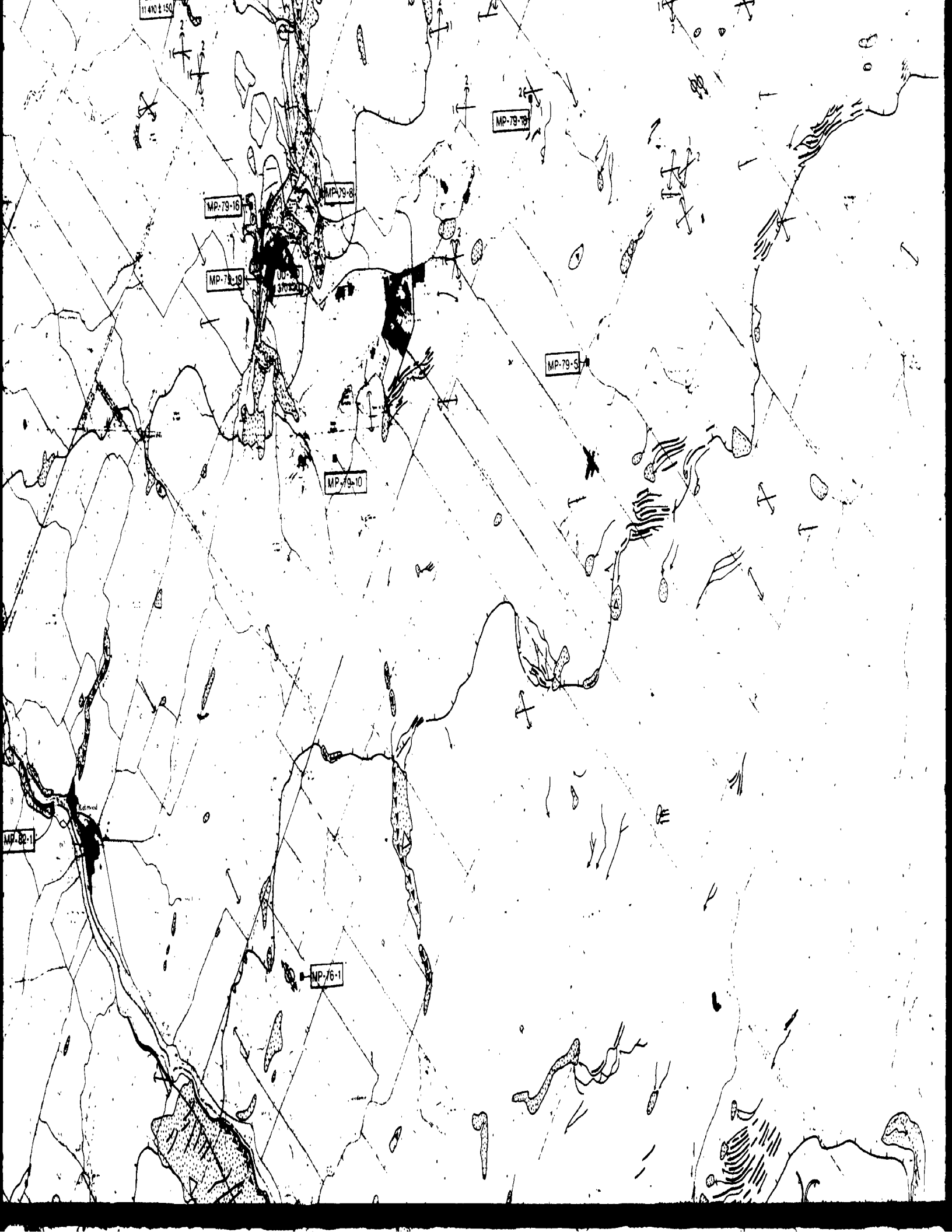
MP-79-16
MP-79-8
MP-79-19
MP-79-5
MP-79-10
MP-82-1
MP-76-1

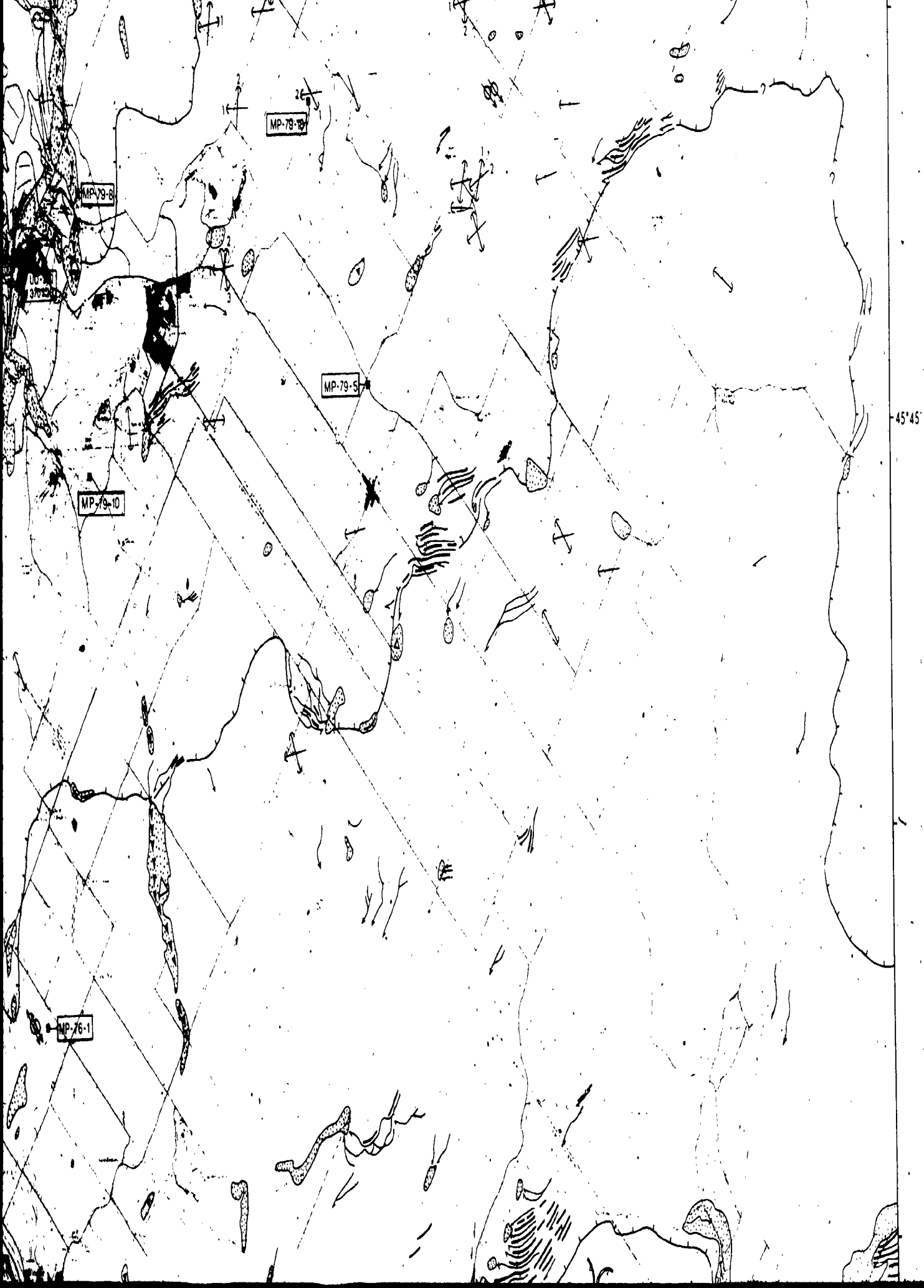
MP-79-8
MP-79-5
MP-79-10
MP-76-1
45°45'

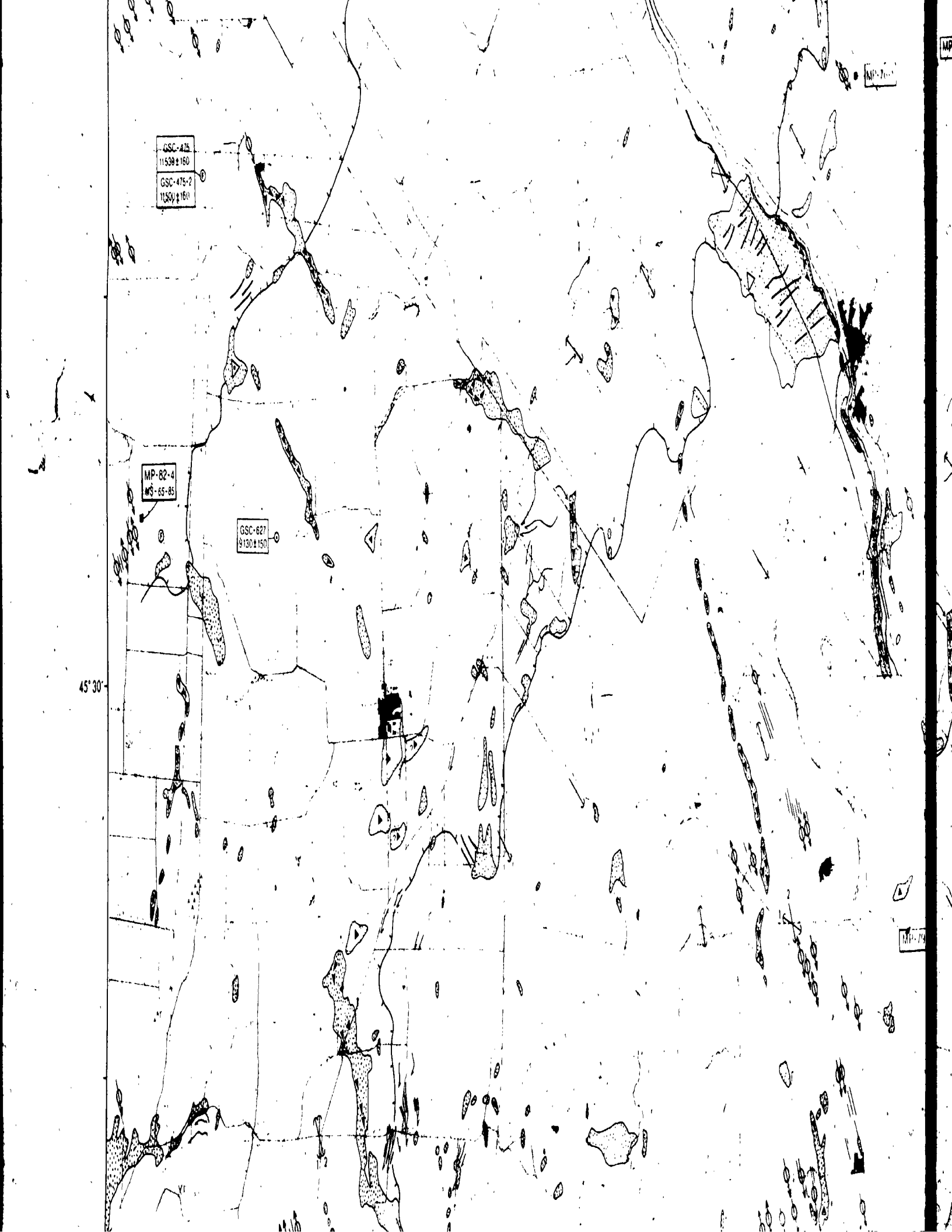
GSC-475
11539±160
GSC-475-2
11500±160
MP-82-4
MS-65-85
GSC-627
9130±150
45°30'

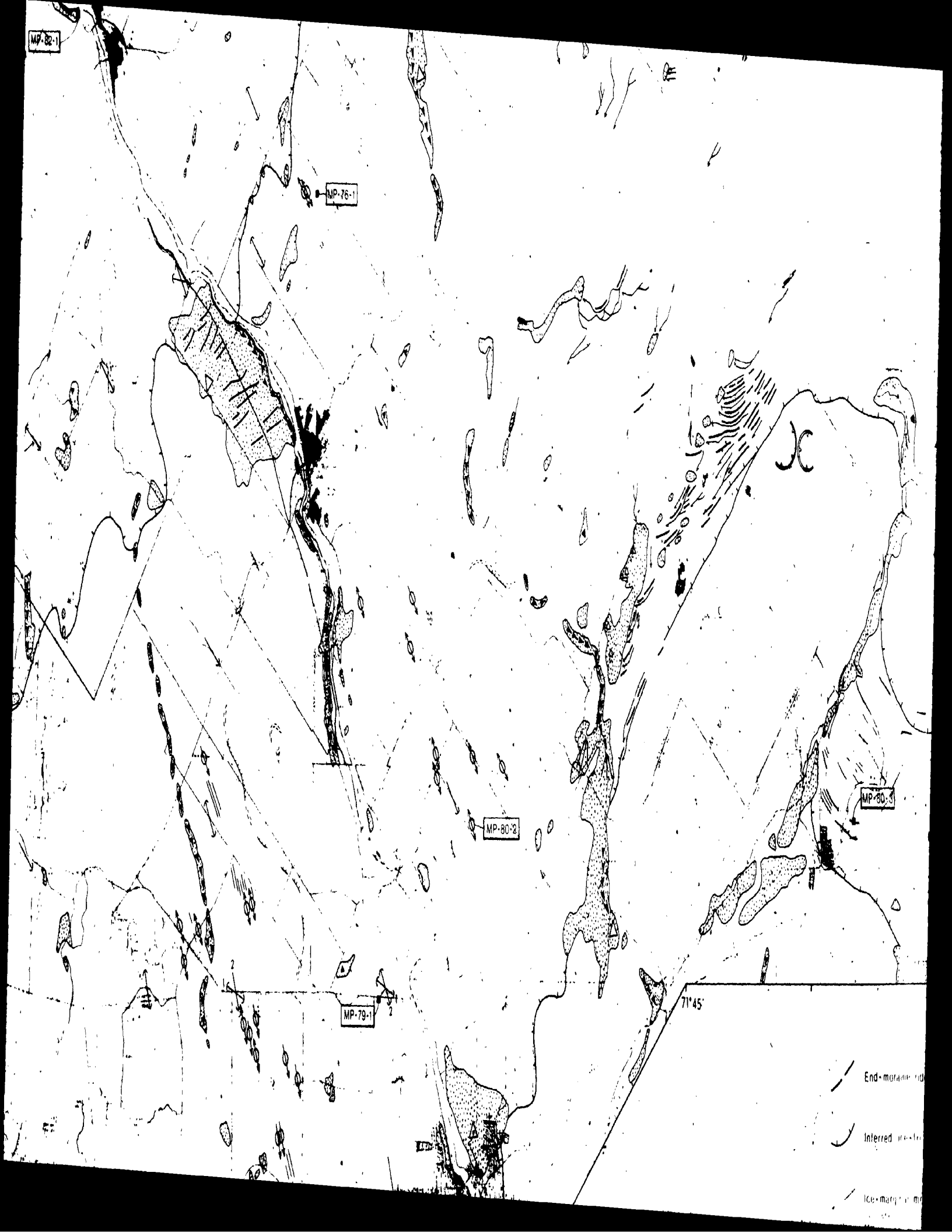
MP-82-1
MP-76-1
MP-80-2
MP-80-3
MP-79-1
71°45'
End-moraine
Inferred
Ice-margin

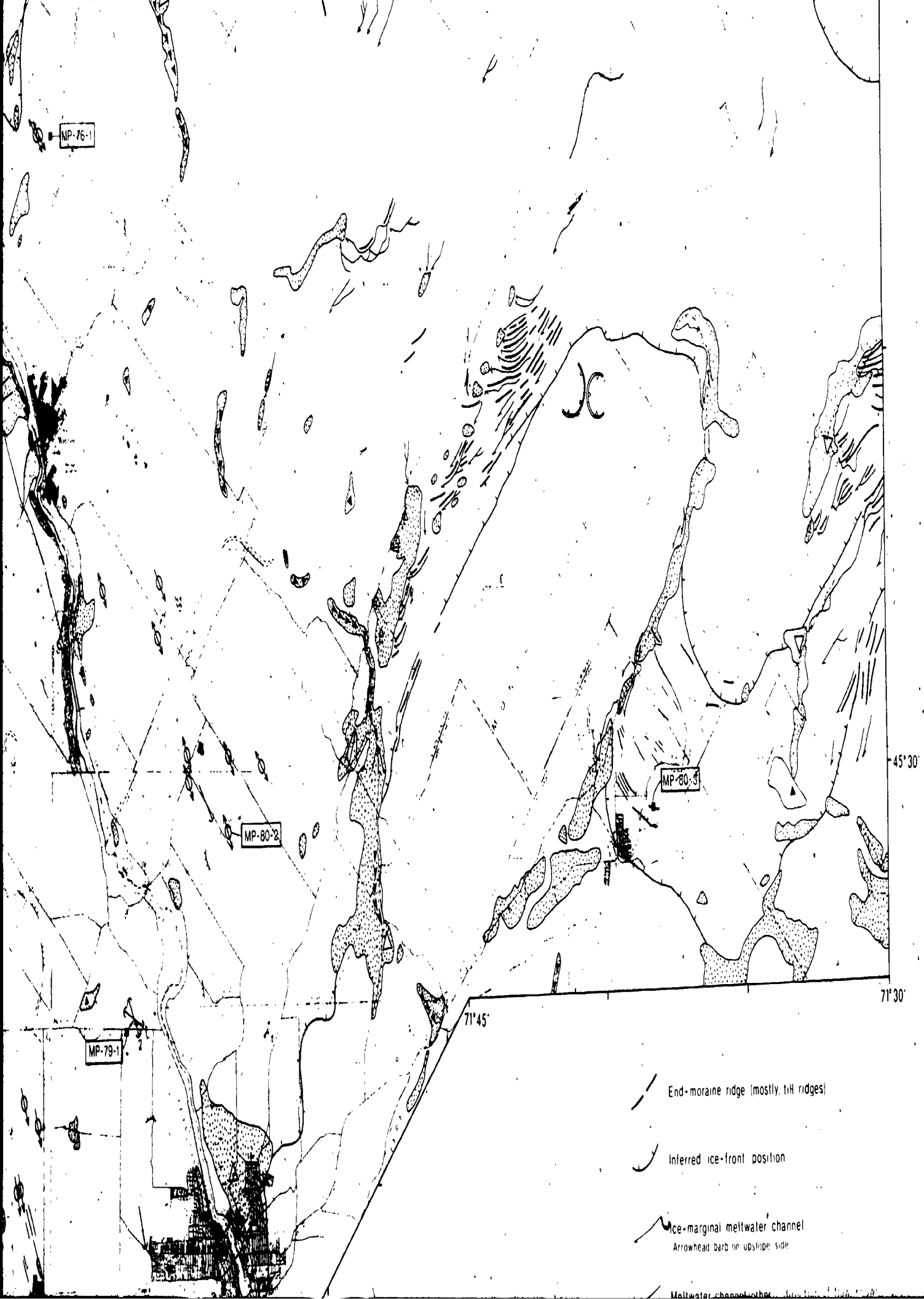
MP-76-1
MP-80-2
MP-80-3
MP-79-1
45°30'
71°30'
71°45'
End-moraine ridge (mostly, thin ridges)
Inferred ice-front position
Ice-marginal meltwater channel
Arrowhead barb on upslope side
Meltwater channel other

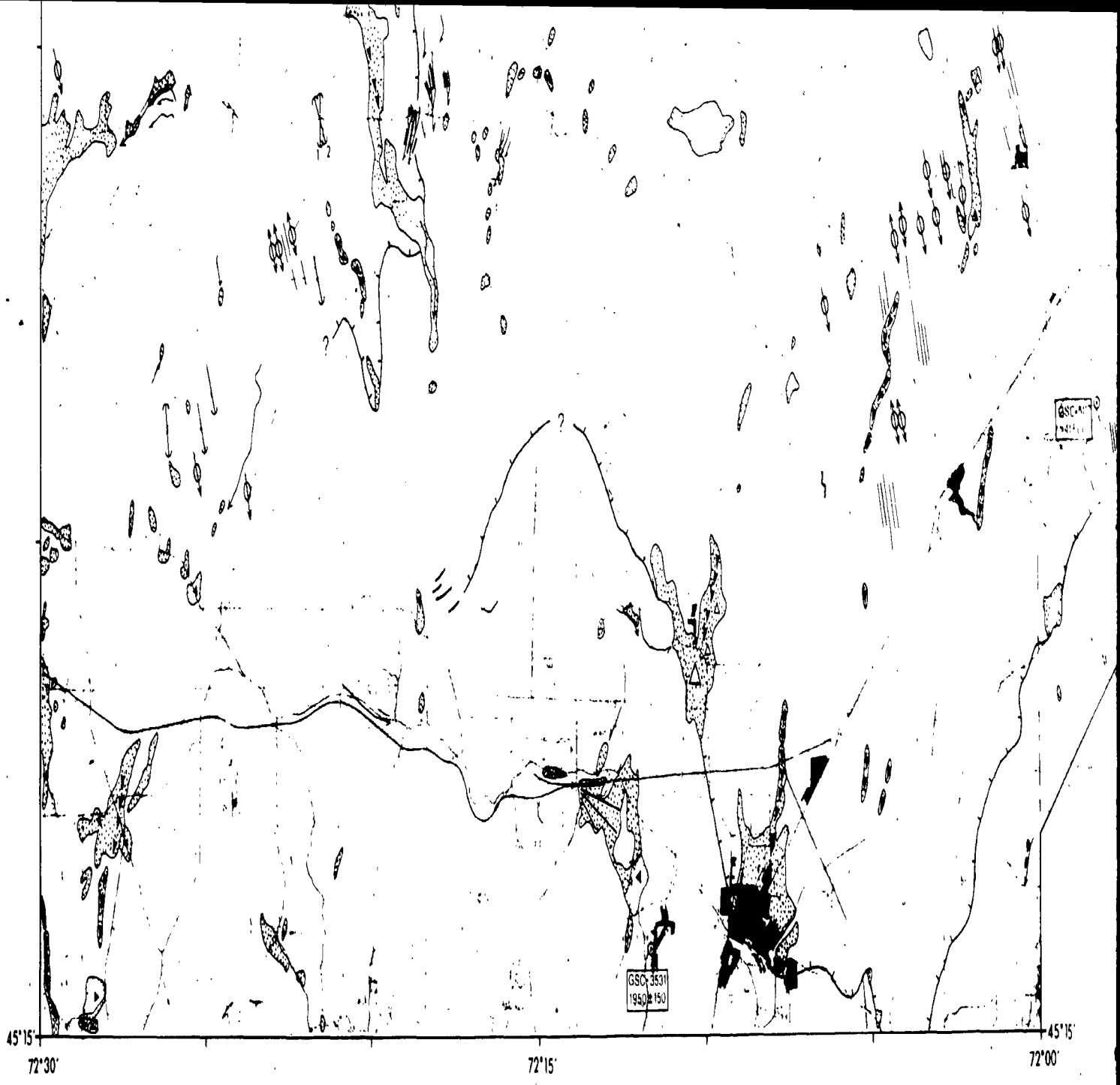

Michel PARENT
(1985)

WISCONSINAN GLACIAL AND DEGLACIAL FEATURES.

Figure 3-1

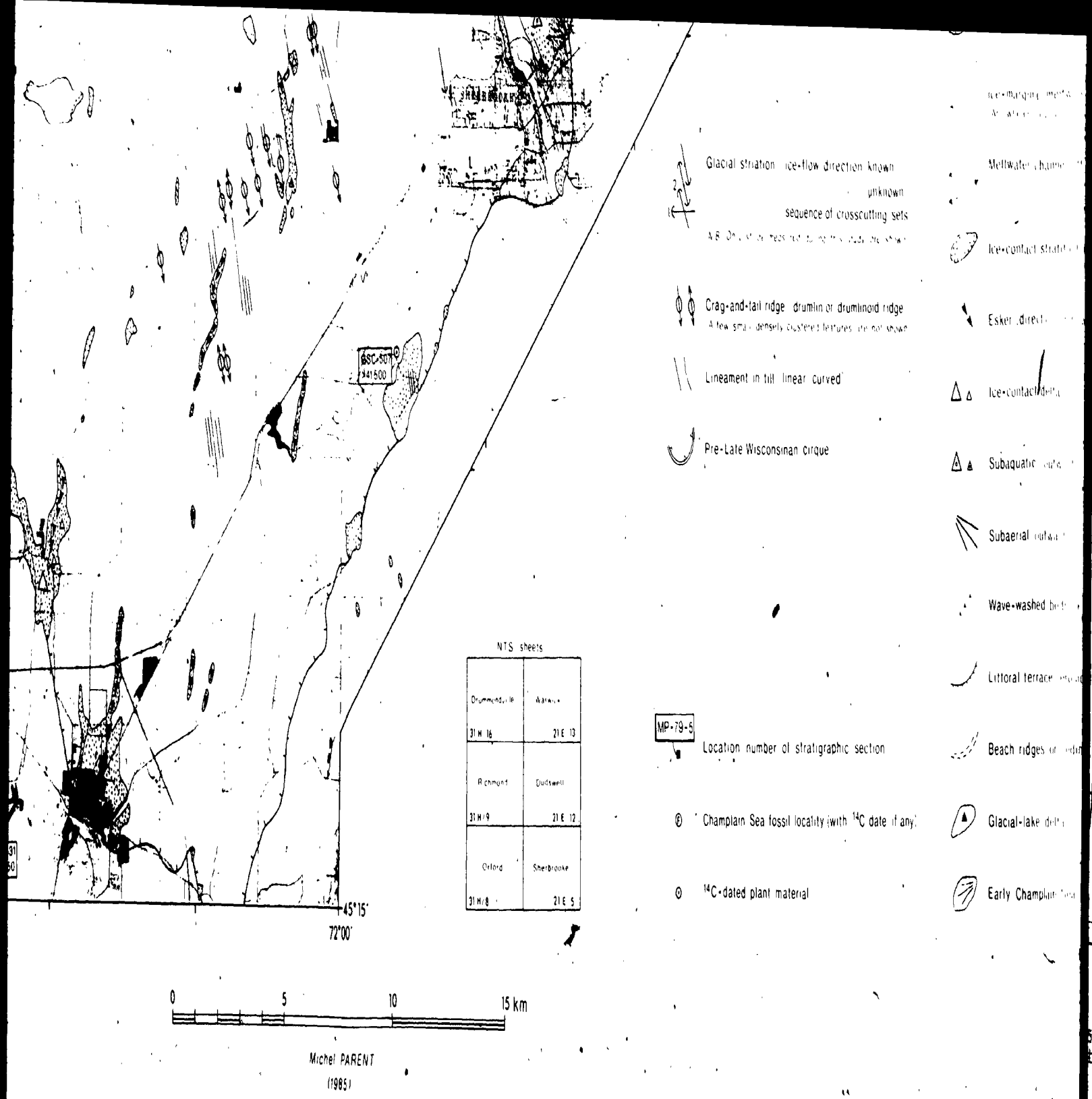

GLACIAL AND DEGLACIAL FEATURES, ASBESTOS-VALCOURT REGION (SE QUÉBEC)

Figure 3-1

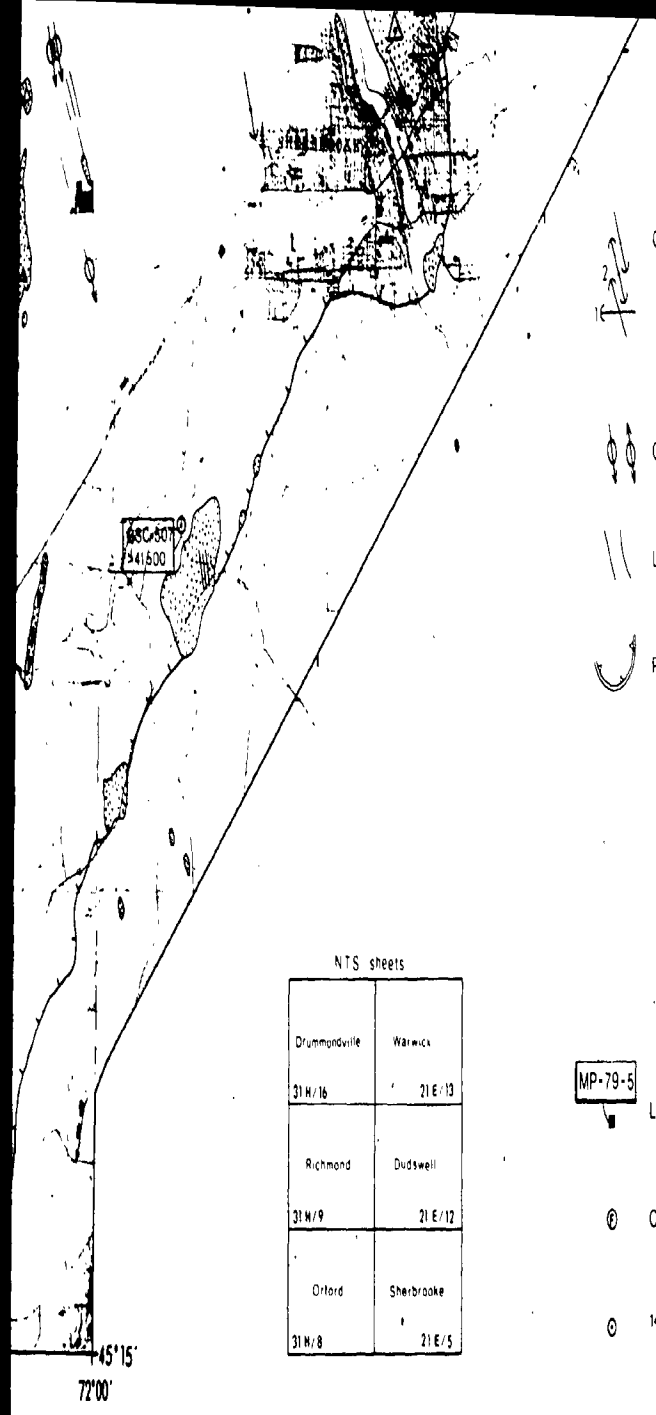

NTS sheets

Drummondville 31H/16	Warwick 21E/13
Richmond 31H/9	Dudswell 21E/12
Orford 31H/8	Sherbrooke 21E/5

Glacial striation ice-flow direction known
unknown
sequence of crosscutting sets
NB On, striae measured along this study, are shown

Crag-and-tail ridge drumlin or drumlinoid ridge
A few small densely clustered features are not shown

Lineament in till linear curved

Pre-Late Wisconsinan cirque

MP-79-5 Location, number of stratigraphic section

Champlain Sea fossil locality (with ^{14}C date if any)

^{14}C-dated plant material

Ice-marginal meltwater channel

Meltwater channel other direction of flow known
unknown

Ice-contact stratified drift includes some patches of

Esker direction of flow known or inferred

Ice-contact delta glaciolacustrine

Subaquatic outwash

Subaerial outwash

Wave-washed bedrock

Littoral terrace erosional

Beach ridges or sediments

Glacial-lake delta

Early Champlain Sea delta (above ~115 m ASL)

10 15 km

Michel PARENT
(1985)

FEATURES, ASBESTOS-VALCOURT REGION (SE QUÉBEC)

Figure 3-1